NON-CANONICAL PATHWAYS OF HIF1-ALPHA REGULATION IN OVARIAN CANCER: IMPLICATIONS FOR TUMOR ANGIOGENESIS AND METASTASIS

A DISSERTATION

SUBMITTED TO THE FACULTY OF THE GRADUATE SCHOOL OF

THE UNVERSITY OF MINNEOSTA

BY

HEMANT PRAKASH JOSHI

IN PARTIAL FULFILLMENT OF THE REQUIREMENTS FOR THE

DEGREE OF DOCTOR IN PHILOSOPHY

ADVISOR: SUNDARAM RAMAKRISHNAN

OCTOBER 2011

Acknowledgements

I am grateful to my advisor, Dr. Sundaram Ramakrishnan, for his support and tutelage over the last five years. Patient, understanding and helpful, Ramki, with his wealth of experience and expertise in the field, guided my progression from naïve student to seasoned researcher. I am truly indebted to him and consider him to be an exceptional mentor and role model.

I must also express my gratitude to Dr. Indira Subramanian. From my first day in the lab through my last, Indira has helped me with nearly all facets of my graduate school career. She has indulged my scientific curiosities, tolerated my incessant questioning and provided that sense of humor and levity that makes work enjoyable. Without her assistance, this work would not have been at all possible. I thank Dr. Goutam Ghosh, also a Research Associate in our lab, as well. As my bench-mate, Goutam was forced to interact with me more often than he probably liked, but he always was willing to lend an ear and offer helpful advice. Finally, Dr. Yawu Jing has been an essential contributor this work and the work of our lab.

I would also like to thank my committee members: my committee chair, Dr. Yan Zeng, and Drs. Sundaram Ramakrishnan, Peter Bitterman, Hiroshi Hiasa and Kirill Martemyanov, for their suggestions and thoughtful criticisms that helped shape this work.

Finally, I would like to thank my family and friends for their support. It's been a long, strange – and arduous and sometimes frustrating – trip, but these folks helped me keep it all in perspective and realize that, in the end, the journey has been a fulfilling one.

This work is dedicated to my parents and grandparents.

Abstract

The high rates of mortality associated with epithelial ovarian cancer (EOC) are a direct consequence of its metastatic nature. Activation of angiogenesis is a significant factor in generation of metastases and is contingent upon the cellular response to hypoxia within the tumor microenvironment. Hypoxia-inducible factor 1 (HIF1) is a transcription factor composed of HIF1α and HIF1β subunits and is the master regulator of the hypoxic response. Hypoxia and HIF1 are therefore critical mediators of tumor angiogenesis and metastasis. Regulation of HIF1 is primarily at the level of protein. In normoxia, the HIF1α subunit is hydroxylated via an oxygen- and iron-dependent mechanism and targeted for destruction. In hypoxia, low oxygen levels preclude hydroxylation and HIF1α is stabilized, allowing for its association with constitutively expressed HIF1β to form bioactive HIF1.

We have identified two novel mechanisms of HIF1α regulation that are oxygen-responsive in EOC cells (EOCCs). The first involves dynamins, a class of proteins involved in endocytic processes such as transferrin/iron uptake. Exposing EOCCs to hypoxic conditions results in lower levels of dynamin 2. Impairment of dynamin 2 activity in normoxia causes accumulation of HIF1α protein due to a rapid decrease in intracellular iron levels and HIF1α polyubiquitination. Treatment with a form of iron that is not dependent on dynamins for endocytosis reverses this effect. Conversely, overexpression of dynamin 2 in hypoxia results in suppression of HIF1α protein levels.

A second novel mechanism of HIF1α control involves microRNAs (miRNAs), ~22 nucleotide, non-coding RNA molecules that repress translation of target mRNAs by binding their 3' untranslated regions (UTRs). Using microarray and qPCR analysis, we found that exposing EOCCs to hypoxia reduced levels of miR-199a-1, a miRNA that is located in an intron within the dynamin 2 gene and is predicted *in silico* to target the HIF1α 3' UTR. We further demonstrated that miR-199a-1 directly targets the HIF1α 3' UTR and overexpression of miR-199a-1 suppresses HIF1α protein levels and HIF1-driven gene expression. Moreover, cells stably overexpressing miR-199a-1 exhibit marked defects in migratory ability. We corroborated these findings *in vivo* by overexpressing miR-199a-1 in a mouse model of metastatic EOC and found significant reductions in tumor vessel density and tumor burden.

Together, these findings provide insight into non-canonical, dynamin-dependent and miRNA-based mechanisms of HIF1 regulation that may have important implications in the progression of EOC.

Table of Contents

List of Figures

List of Tables

Abbreviations

aa: amino acids

AKT: protein kinase B

AMF: autocrine motility factor

ANG1: angiopoietin-1

ANGPTL4: angiopoeitin-related protein 4

ARD1: acetyltransferase arrest-defective 1

ARNT: aryl hydrocarbon receptor nuclear translocator (HIF1β)

ATP: adenosine triphosphate

Bcl-2: B-cell lymphoma 2

bHLH: basic helix-loop-helix

β-APN: beta-aminoproprionitrile

CA 125: cancer/carbohydrate antigen 125

CBP: CREB-binding protein

cPHD: collagen prolyl hydroxylase

CTC: circulating tumor cells

CTGF: connective tissue growth factor

CTSD: cathepsin D

CUL2: cullin-2

CXCR: chemokine receptor, type CXC

DGCR8: DiGeorge syndrome critical region gene 8

DLK1: protein delta homolog 1

Dmn: dynamin

DNA: deoxyribonucleic acid

DUSP1: dual specificity protein phosphatase 1

Dyn: dynamin

EC: endothelial cell

ECM: extracellular matric

ELGN B/C: elongin B/C

EMT: epithelial-mesenchymal transition

EOC: epithelial ovarian cancer

EOCC: epithelial ovarian cancer cell

EPO: erythropoietin

ERK: extracellular-signal-regulated kinase

FACS: fluorescence-activated cell sorting

Fc: fragment crystallizable region

FGF: fibroblast growth factor

FIH: factor inhibiting HIF1α

GAP: GTPase-activating proteins

GI: gastrointestinal

GLUT: glucose transporter type

GED: GTPase effector domain

GFP: green fluorescent protein

GTP: guanine triphosphate

HBSS: Hanks' buffered saline solution

Hg: mercury

HGF: hepatocyte growth factor

HGFR: MET/c-met/hepatocyte growth factor receptor

HIF: hypoxia-inducible factor

HRE : hypoxia response element

ID2: inhibitor of differentiation 2

IGF2: insulin-like growth factor 2

IgG: immunoglobulin G

IL: interleukin

IP: intraperitoneal

ITGA5: integrin, alpha 5

IV: intravenous

JMY: junction mediating and regulatory protein

MAPK: mitogen activated protein kinase

MCP1: monocyte chemoattractant protein

MET: c-met/hepatocyte growth factor receptor (HGFR)

miRNA: microRNA

miRNP: micro-ribonucleoprotein

mm: millimeters

MMP: matrix metalloproteinases

mTOR: mammalian target of rapamycin

NIP3:BCL2/adenovirus E1B 19kDa interacting protein

NIX:BCL2/adenovirus E1B 19kDa interacting protein 3-like

NOS: nitric oxide synthase

NRP: neuropilin

Oct4: octamer binding transcription factor 4

ODDD: oxygen-dependent degradation doman

OPN: osteopontin

ORF: open reading frame

p300: E1A binding protein p300

PACT: protein kinase, interferon-inducible double stranded RNA dependent activator

PAS: PER-ARNT-SIM

PBS: phosphate buffered saline

PCR: polymerase chain reaction

PH: pleckstrin homology

PHD: prolyl hydroxylase

PLD: pegylated liposomal doxorubicin

PDGF: platelet-derived growth factor

PlGF: placental growth factor

pO_2: partial pressure of oxygen

PRD: proline-rich domain

PVDF: Polyvinylidene fluoride

qPCR: quantitative polymerase chain reaction

RAS: rat sarcoma

Rb: retinoblastoma

RBC: red blood cell

RBX: ring box, E3 ubiquitin protein ligase

RCC: renal cell carcinoma

RISC: RNA-induced silencing complex

RNA: ribonucleic acid

ROS: reactive oxygen species

SD: standard deviation

SDF: stromal cell-derived factor

SDS-PAGE: sodium dodecyl sulfate polyacrylamide gel eletrophoresis

SE: standard error

shRNA: short hairpin RNA

TAD: transactivation domain

TCF3: transcription factor 3

TGF: transforming growth factor

TKI: tyrosine kinase inhibitor

TRBP: TAR (HIV-1) RNA binding protein 2

TRKB: neurotrophic tyrosine kinase, receptor, type 2

Ub: ubiquitin

uM: micromolar

uPAI: urokinase-type plasminogen activator inhibitor

uPAR: urokinase receptor

US: ultrasound

UTR: untranslated region

VDA: vascular disrupting agents

VEGF: vascular endothelial growth factor

VEGFR: vascular endothelial growth factor receptor

VHL: von-Hippel Lindau protein

WNT: wingless-type MMTV integration site family

ZEB: zinc finger E-box binding homeobox 1

CHAPTER I:

BACKGROUND

Ovarian Cancer

Statistics

Ovarian cancer is the leading cause of death among gynecological malignancies: in 2010, over 13,000 women in the United States succumbed to the disease and over 15,000 are predicted to die as a result of ovarian cancer in 2011 [1, 2]. Though ovarian cancer comprises only three percent of total new cancer cases, ranking as the ninth most commonly diagnosed cancer in women, it is the fifth most common cause of cancer-related deaths. Every year, an estimated 21,550 women are diagnosed with the disease in the U.S. alone, corresponding to an overall lifetime risk of 1.8 percent [1, 3]. The one-year survival rate for patients diagnosed with ovarian cancer is approximately 75 percent and the five-year survival rate is less than 50 percent. Importantly, about half of women diagnosed with ovarian cancer are over the age of 60 and therefore significant comorbidities often complicate strategies for treatment and recovery [1].

Pathophysiology

Types of ovarian cancer

Three main types of ovarian tumors exist and each is named based on the cell from which it originates. Germ cell tumors, which account for approximately 2 to 5 percent of ovarian malignancies, are mostly benign and include teratomas, endodermal

sinus tumors and choriocarcinomas. These usually affect younger women and have a relatively high five-year survival rate of 90 percent. Stromal tumors comprise about 2-5 percent of ovarian cancers. These types of tumors can be either benign (thecomas, fibromas) or malignant (granulosa cell tumors, Sertoli-Leydig cell tumors), but most types are responsive to therapy and long-term survival rates are 75 percent [1]. The vast majority of ovarian cancers (~90 percent) are of epithelial origin, and among this population of tumors, 85-90 percent are malignant [1, 4]. Because epithelial ovarian cancers (EOCs) are the most abundant and lethal form of ovarian malignancies, the work presented in this thesis focuses on this particular subtype of ovarian tumor.

Ovarian cancer tumorigenesis

EOCs, like most solid tumors, begin as single- to low multi-cell neoplasms that rapidly grow to about 1 mm^3 in size [5-7]. At this stage in the nascent tumor's development, a rate-limiting exigency is incurred. Having grown so quickly, thereby exhausting the local blood supply, the tumor must adapt to the oxygen deficit it now faces. To address this hypoxic challenge, ovarian tumor cells effect a number of cellular and physiological changes that alter both the tumor microenvironment and the host as a whole. Chief among these processes include: shunting energy to critical cellular functions to cope with the decreased resources available; relying on glycolosis and anaerobic respiration to circumvent hypoxia and continue to supply, albeit less efficiently, cellular fuel in the form of ATP; stimulating red blood cell synthesis to increase oxygen delivery to the tumor; secreting activators of angiogenesis, such as vascular endothelial growth factor (VEGF) to restore sufficient blood flow to the microenvironment; and inducing

tumor cell motility, reorganizing tumor-microenvironment interactions and deconstructing surrounding normal tissue to promote tumor cell migration to normoxic, resource-rich areas [8-11].

Each of these various cellular adaptations to hypoxia rely completely, or at least in part, on hypoxia-inducible factor 1 (HIF1), the master regulator and integrator of the cellular hypoxic response. Activation of HIF1 in ovarian cancer cells is of grave consequence because of the molecule's critical role in promoting two of the hypoxic responses outlined above in particular: angiogenesis and cell motility and migration Figure 1). Angiogenesis provides the fertile network of vessels to sustain EOC growth within and through the ovarian capsule. Meanwhile, ovarian tumor cells are primed for detachment and dissemination to distal sites. EOC cells (EOCCs) take advantage of this

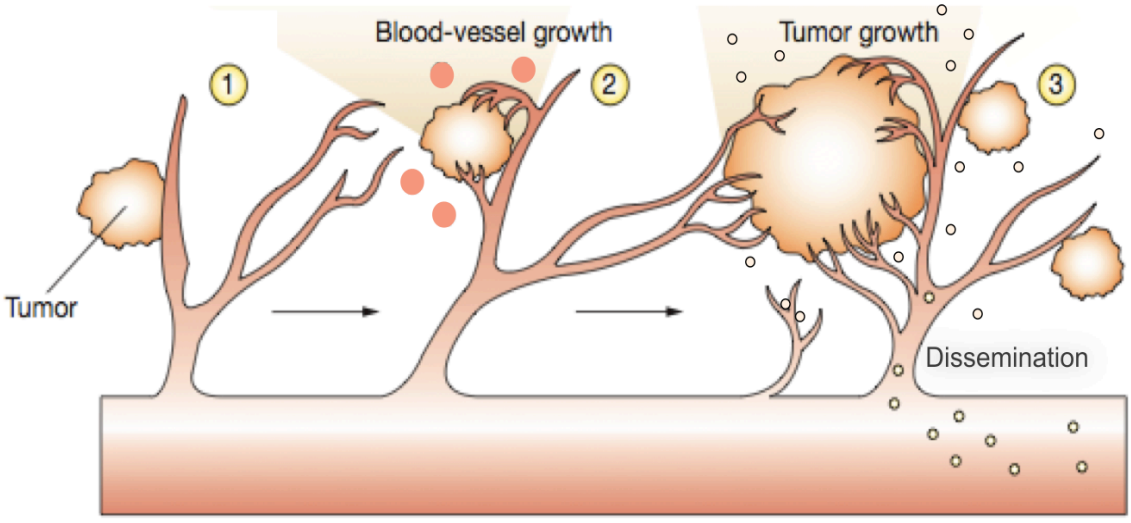

Figure 1: Early EOC tumorigenesis. (1) A nascent tumor grows rapidly to about 1 mm^3 in size, only to exhaust the local blood supply and create a hypoxic microenvironment. (2) Tumor cells, by activating the master regulator of the hypoxic response, HIF1, secrete pro-angiogenic factors (red circles), which promote formation of vasculature and increase oxygen delivery. (3) Increased oxygen allows the tumor to grow further, and tumor cells, primed for detachment and migration by the actions of HIF1, extravasate into the now robust vessel network and exfoliate into the peritoneal space, leading to metastases in the pelvis, abdomen and beyond. Adapted by permission from MacMillan Publishers Ltd: [12].

HIF1-induced duality to readily extravasate into the now abundant nearby vasculature and lymphatics and spread throughout the body via the blood [13]. Alternatively, and more commonly, EOCCs can opt for a more lethal route and exfoliate from the ovary directly into the peritoneal space, the largest cavity in the body with about 2 m^2 in surface area, to seed sites in the pelvis, stomach, bowel and omentum, and more distal locations such as the liver, diaphragm and pleura [14] (Figure 2). EOCs that have achieved these latter stages of metastasis are notoriously difficult to treat and have five-year survival rates of less than 30 percent [1].

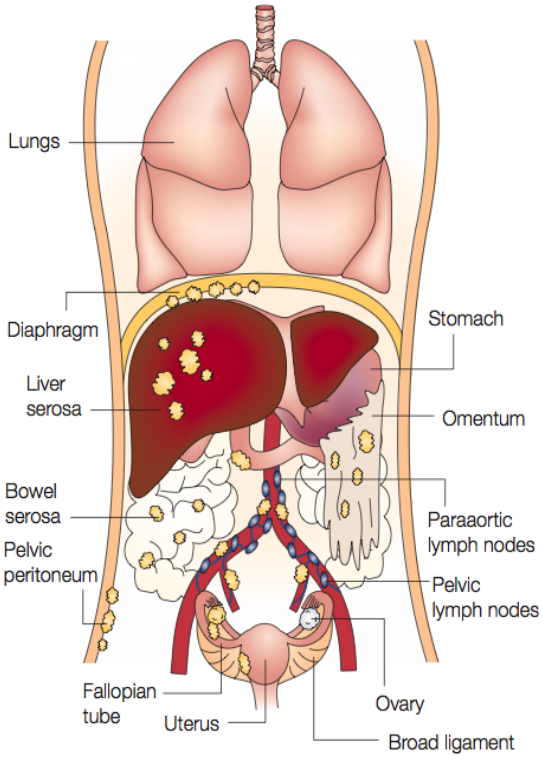

Figure 2: Typical sites of ovarian cancer metastasis. Reprinted by permission from MacMillan Publishers Ltd: [15].

Standard of care

Staging of ovarian cancer

Mainstay treatment of ovarian cancer is based upon the stage of the disease, which is determined at primary surgery. The staging system devised by the International Federation of Gynecology and Obstetrics (FIGO) is described in Table 1. Tumors that are diagnosed at FIGO stages I-IIA (only about 20 percent of cases) are usually treatable with

Table 1: FIGO staging system for ovarian cancer.

Stage I: limited to ovaries
• IA: one ovary; no ascites; no tumor on external surface; capsule intact
• IB: two ovaries; no ascites; no tumor on external surface; capsule intact
• IC: IA or IB with either surface tumor, ruptured capsule, ascites or peritoneal washings with malignant cells
Stage II: pelvic extension
• IIA: involvement of uterus and/or tubes
• IIB: involvement of other pelvic tissues
• IIC: IIA or IIB with factors as in IC
Stage III: peritoneal implants outside pelvis and/or positive retroperitoneal or inguinal nodes
• IIIA: grossly limited to true pelvis; negative nodes; microscopic seeding of abdominal peritoneum
• IIIB: implants of abdominal peritoneum 2 cm or less; node negative
• IIIC: abdominal implants greater than 2 cm and/or positive retroperitoneal or inguinal nodes
Stage IV: distant metastases; positive pleural effusion

Adapted from [20] with permission.

surgery, though recurrences afflict 25 percent of patients treated in this manner [16]. Adjuvant chemotherapy is indicated for some of these patients, specifically, those with stage IC or worse disease, those with clear-cell histology or poorly/moderately differentiated tumors, or those who have undergone "non-optimal" surgery [17]. Patients with advanced disease (FIGO stages IIB-IV) normally undergo maximal surgical debulking with systemic based chemotherapy. Five-year survival rates for these patients are about 20 and 30 percent for stages III and IV, respectively [18, 19].

First-line treatments for ovarian cancer

The particular chemotherapeutics used in treatment of ovarian cancer following surgical debulking are usually platinum-based (with carboplatin favored over cisplatin due to ease of delivery and a more favorable toxicity profile) and often combined with paclitaxel. Delivery of the drugs is usually performed intravenously (IV), and although some evidence [21-23] has shown increased efficacy of intraperitoneal (IP) therapy, especially for optimally debulked stage IIIC EOCs, based on the fact that this method delivery is associated with higher levels of complications such as catheter issues, nausea, abdominal pain and neurotoxicity, in most countries chemotherapy is delivered IV. Doses

of chemoagents are given based on patient surface area are usually delivered IV over a period of hours every three weeks for six cycles [17].

Other drugs have been investigated to determine if triplet therapy (carboplatin-paclitaxel-Drug X) could improve progression free survival and overall survival. Thus far, studies testing triplet therapy with drugs such as gemcitabine, doxorubicin, topotecan, and epirubicin have generally been disappointing, failing to show increased efficacy compared to the standard carboplatin-paclitaxel combination therapy [17]. Alternatively, other studies have evaluated replacing paclitaxel with agents such as docetaxel or pegylated liposomal doxorubicin (PLD); the former strategy [24] has shown little improvement (though better side-effect profiles) over standard care while the latter has shown some promise [25]. Studies investigating different schedules of administration, such as "dose-dense" administration of paclitaxel, also seem to show benefit over standard regimens [26].

Novel therapies for ovarian cancer

While the standard carboplatin-paclitaxel therapy is effective in achieving response rates near 80 percent, approximately 70 percent of patients develop recurrence of the disease, with patients in stages III and IV experiencing recurrence rates approaching more than 90 percent [1]. Accordingly, a majority of patients die of recurrent disease [17]. Treatment of recurrent disease depends on the platinum-sensitivity of the tumor, which is determined by the period of time between completion of initial therapy and relapse. Patients with platinum-sensitive disease (relapse after more than 12 months) are given carboplatin with paclitaxel, gemcitabine, or PLD. Partially sensitive

(relapse between 6-12 months) and platinum refractory or resistant patients are often treated with novel agents and are the first to be enrolled in clinical trials of experimental drugs[17]. Among the most studied and promising new compounds in the treatment of ovarian cancer is the monoclonal antibody to VEGF, bevacizumab, which employs an anti-angiogenic strategy to treat the angiogenesis-dependent disease. Recent studies of bevacizumab have shown efficacy both as a first-line drug in combination with carboplatin and paclitaxel for advanced ovarian cancer [27, 28] and as a treatment for recurrent ovarian cancer [29, 30]. Other anti-angiogenic therapies under evaluation include the VEGF Trap, aflibercept, which contains the Fc portion of human IgG1 fused to the extracellular ligand-binding domains of VEGF receptors (VEGFRs) -1 and -2 to form a potent VEGF-binding decoy. Tyrosine kinase inhibitors (TKIs) such as cediranib, sorafenib, and sunitinib, inhibit VEGFR activity rather than inactivate VEGF and comprise another category of potential anti-angiogenic strategies being studied to treat ovarian cancer. VEGF Trap and TKIs are currently in Phase I and II clinical trials [7]. Drugs that disrupt existing vasculature – in contrast to those that prevent formation of new vessels – are also under investigation. These vascular disrupting agents (VDAs) have shown great promise in animal models and various compounds in this category are in Phase I clinical trials.

Quality of life

Acknowledging the high mortality rates associated with ovarian cancer is merely a small part of the daunting burden a patient diagnosed with the disease must endure.

And, indeed, understanding the specific biological processes of ovarian cancer and the minutiae of current mainstays of ovarian cancer treatment is, in the grand scheme of the disease, of little relevance to a patient, who must solve the more important problem of how to live her everyday life as normally as possible. Thus it is also important to consider, when discussing the pressing need for new strategies to combat ovarian cancer, the hardships and issues that have direct and constant ramifications for patients with ovarian cancer.

Diagnosis of ovarian cancer

The traditional symptoms of ovarian cancer may include weight loss, early satiety, frequent urination, menstrual irregularities, bloating, ascites, fatigue and pelvic and/or abdominal pain [4, 31]. This constellation of symptoms is hardly specific to ovarian cancer, of course, and is one of the reasons early detection of the disease is exceedingly difficult. In fact, when first presented to a physician, these symptoms are usually ascribed to a variety of other, more common disorders such as irritable bowel syndrome, gastritis, dietary factors, urinary tract infections, stress or depression [32]. As such, ovarian cancer is nearly always diagnosed incidentally during routine physicals or evaluation of non-gynecological issues [19]. While screening methods to diagnose the disease at early stages do exist, they suffer from poor specificity and sensitivity. An ovarian cancer symptom index has been developed [33] but is still being validated. Serum marker cancer/carbohydrate antigen 125 (CA 125), the most extensively studied ovarian cancer biomarker, is used to evaluate clinical response to treatment, but is only sensitive enough to detect 50 percent of stage I cases [34, 35] and demonstrates false positive

results for a number of benign gynecological and even non-gynecological causes at rates of up to 30 percent [36, 37]. Imaging, particularly transvaginal ultrasound (US), is valuable in promoting diagnosis at early stages of the disease, but is only routinely ordered if ovarian cancer is already suspected. Screening methods using CA 125 and transvaginal US together may paradoxically be more harmful than helpful, because as a screening method, it detects no more ovarian cancer cases than does normal medical care, and false positives can lead to unnecessary interventions that actually increase morbidity and mortality [38]. To be sure, the lack of effective screening and early detection methods of ovarian cancer remains a glaring weakness in efforts to combat this disease.

Treatment of ovarian cancer

The most tragic consequence of this inability to detect early stage ovarian cancer is that when a woman is first diagnosed, there is a 70-80 percent likelihood that the disease is already in its advanced stages, infiltrating and destroying involved tissues to cause multi-organ dysfunction – which her physician will then tell her equates to a five-year survival rate of about 30 percent [1, 19]. Compounding this crushing diagnosis is the realization that treatment of the disease is a dangerous process fraught with its own risk and potential for disability and death. Surgery, so often "the last resort" in the minds of many patients when it comes to illness, is, conversely, the first line of therapy for ovarian cancer [39]. The risks inherent to surgery are as plentiful as they are deadly. Typical side effects that may occur with any major surgery include weakness, postoperative pain, nausea and vomiting, fistulas, blood clots and wound infections. Complications specific to ovarian cancer debulking include urination and defecation difficulties, premature

menopause or infertility, vaginal, rectal or bladder prolapse, perforation of the bowel, and long-term effects such as osteoporosis and heart disease due to estrogen loss [40]. Recovery from surgery can take days and may leave the patient with residual symptoms for months or even years.

Unfortunately for the typical patient, treatment has only just begun. For once the surgical hurdle is overcome, she likely then faces 18 weeks of chemotherapy, which rears its own medley of debilitating side effects. Neutropenia, anemia, myelosuppression, neurotoxicity, ototoxicity, nephrotoxicity, gastrointestinal toxicity, neuropathy, arthralgia, myalgia, alopecia, sexual dysfunction, loss of taste and appetite, bowel and bladder incontinence, nausea and vomiting, diarrhea, edema, inability to sleep, weakness, headache, confusion and restricted mobility are a few of the possible consequences of treatment with platinum and paclitaxel [31, 41]. Several of these side effects persist long-term, requiring the patient to make major modifications to her life to cope. Indeed, while the disease itself takes a profound physical toll on a patient, the surgical and adjuvant chemotherapy treatments for the disease carry their own demons as well.

Other sources of stress for ovarian cancer patients

Beyond the physical torments from which an ovarian cancer patient suffers, there are countless other stressors. Psychological problems such as anxiety, depression, marital and relationship issues are common among women with ovarian cancer. In fact, one-fifth of patients are clinically depressed while another one-third suffer from anxiety issues [42]. These psychological issues derive not just from contemplating one's well-being and mortality as a result of a grave diagnosis, but also from reflecting on how treatment could

affect normal life. “Will I be strong enough to be self-reliant?” “Will I have the energy to care for my children/grandchildren?” “Will my partner still find me attractive?” are all questions a patient may find herself asking about life during and after treatment. As highlighted by these examples, social concerns add another dimension of stress and contribute to psychological issues as well. Serious illnesses like ovarian cancer challenge even strong family and friend networks and disrupt arrangement of care, balancing of family needs with treatment needs, roles and responsibilities, and togetherness, thereby confounding social support that provides tangible, beneficial effects for patients [43, 44]. Economics also play an important role in a cancer patient’s struggle with disease [45]. Treatment of ovarian cancer requires both significant monetary resources as well as time away from work. In the U.S., health insurance benefits are usually linked to employment, and as such, diseases such as ovarian cancer can strain access to healthcare. While some recently-enacted legislation prevents employers and insurers from denying coverage to cancer patients, issues still remain within the system that leave unprotected patients vulnerable to huge healthcare costs and the anxieties that accompany them [31].

A dire need for novel ovarian cancer therapies

Clearly, there is a dearth of effective methods to detect and treat ovarian cancer. That 70-80 percent of women are already suffering from advanced stages of the disease at the time of diagnosis should be unacceptable to healthcare professionals. Moreover, the side effect profiles of first-line adjuvant chemotherapy regimens beg the question: is it worth extending a patient’s life for a few months or years if during that time she is

miserable, suffering physically, mentally, emotionally, and psychologically not only due to the disease itself but the treatment as well? After all, extending life for the sake of extending life, without concern for quality of life, is far from the ultimate objective of healthcare. It is therefore incumbent upon us, as healthcare professions and researchers in the biomedical fields, to strive to investigate novel treatments that address both the severity of ovarian cancer as well as the fragility of the human body. Achieving this delicate balance should be the overall goal of all research strategies that aim to combat this deadly disease.

Hypoxia

Definition of hypoxia

Hypoxia has been described in myriad ways. Qualitatively, it is "a decrease in available oxygen reaching the tissues of the body" [46], "low levels of oxygen in tissues" [47] or, more simply, "a low oxygen condition" [48] or "suboptimal oxygen concentration" [49]. What defines "a decrease," "low" or "suboptimal" has been variously characterized as well. Quantitatively, oxygen partial pressures (pO_2s) of less than 20 [50], 19 [51], 10 [52, 53] and 2.5 [54-56] mm Hg in tissue all denote a state of "hypoxia," according to different studies. This wide range of values is primarily due to the fact that "normoxic" oxygen partial pressures vary by tissue. For example, while the normal pO_2 of skeletal muscle is 20-30 mm Hg [57], that of brain is much higher, between 45 and 65 mm Hg [58]. Within a particular tissue, as well, there may be a significant variation in what defines "normoxic." In the liver, pO_2s reach 95-105 mm Hg along the hepatic artery and fall to 30-40 mm Hg at sites near sinusoids and the central vein [46]. With regard to cancer, pO_2 in the tumor microenvironment has been measured to be as low as 1-10 mm Hg [59]. However, as is the case with different tissues, pO_2 varies between different types of tumors also. Thus it is difficult to provide a general and accurate description of "hypoxia." For the purposes of this work, however, hypoxia will be defined as "low oxygen levels compared to what is normal for the given, healthy tissue."

Physiologic hypoxia

Hypoxia may occur under normal physiological circumstances for a number of reasons. During embryogenesis, for example, the optimum pO_2 is between 23 and 38 mm Hg, a hypoxic range that promotes tubulogenesis, vasculogenesis, angiogenesis and even organogenesis in the rapidly developing fetus [60, 61]. In fact, if pO_2s approach normoxic levels, there is a greater likelihood of heart, kidney and lung defects [60, 62, 63]. In the adult, as well, hypoxia can play a necessary physiological role. During exercise, localized hypoxia in muscles causes a switch from aerobic to anaerobic metabolism. In persons who are experiencing high altitudes for the first time, hypoxia plays a role in effecting both short-term changes, such as increased heart rate, rate and volume of breaths and catecholamine release, as well as long-term adaptations, including increased mitochondrial density, glycolysis, hemoglobin levels, and red blood cell (RBC) count [64]. Certainly, there is a clear beneficial role for hypoxia under certain physiological conditions.

Tumor hypoxia

In addition to its role in normal physiology, hypoxia is involved in many pathophysiological processes such as ischemic disease, diabetes, atherosclerosis, inflammatory disorders, chronic obstructive pulmonary disease and cancer. Hypoxic states in these diseases can often play a beneficial role; for example, the development of

collateral vasculature to maintain oxygen delivery to the myocardium in patients with coronary artery disease is hypoxia-dependent. In the context of cancer, however, hypoxia has a deleterious effect, as it drives a number of processes that allow a tumor to survive, thrive and metastasize. Because hypoxia directly contributes to the lethality of cancers, it is an important consideration for new therapeutic strategies.

Pathogenesis of tumor hypoxia

Cancer cells demonstrate remarkable proliferative ability that allows a budding tumor mass to expand exponentially. As a result, a nascent solid tumor, such as an EOC, grows at a rate that rapidly outpaces the ability of local vasculature to supply sufficient levels of oxygen, since the diffusion limit of oxygen from a vessel to tissue is approximately 150 uM [65, 66]. A tumor mass that expands to ~1 mm^3 is therefore at great risk of starving itself as a result of the chronic hypoxic state (termed *diffusion*-limited hypoxia) it has created by growing so robustly (Figure 3) [5-7]. At this point in its development, the cancer has reached a critical juncture and to survive, tumor cells must initiate some mechanism to save themselves. This rescue process, effected primarily by the master regulator and integrator or the cellular response to low oxygen levels, HIF1, results in a number of changes in cell behavior. Perhaps most significant among these adaptations is the modification of cell metabolism to utilize more energy-efficient pathways and the activation of angiogenesis, the growth of new vessels from existing vasculature. By decreasing oxygen demand and enhancing supply, tumor cells are able to survive in their hypoxic microenvironment. Even as a growing cancer enacts these measures, however, it is important to note that the newly formed vasculature is irregular,

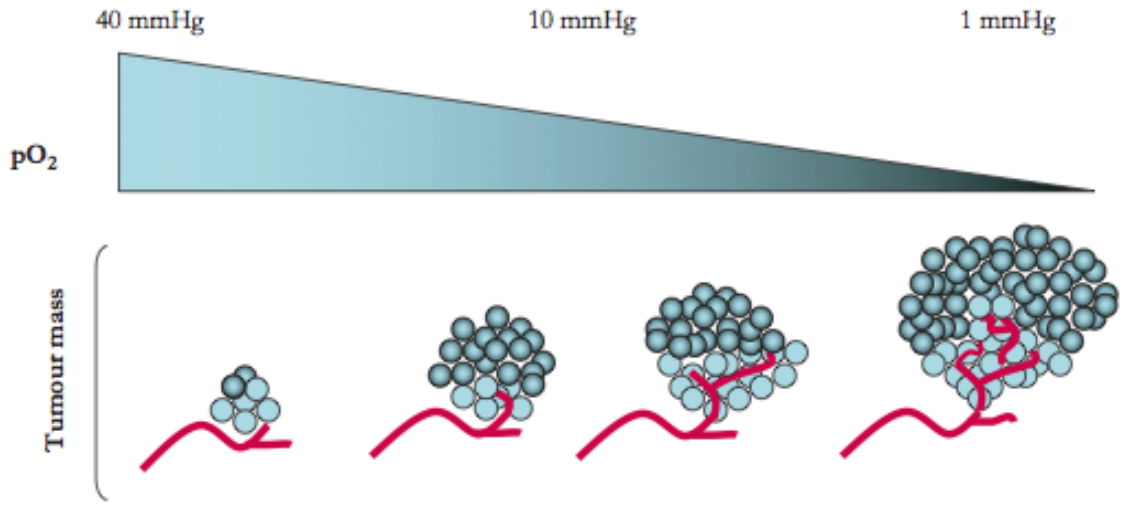

Figure 3: Pathogenesis of tumor hypoxia. As a nascent tumor rapidly expands, it quickly outpaces available vascular supply. As a result, pO_2 in the tumor microenvironment falls to hypoxic levels. Tumor cells respond to this low oxygen state by activating HIF1, which enacts a host of changes, primarily by decreasing oxygen demand through reorganization of cell metabolism and by increasing oxygen supply by activating angiogenesis. Adapted with permission from [47].

haphazardly organized, leaky and lacking complete endothelial lining [66, 67]. Consequently, while the tumor may have satiated its need for oxygen in the short term, acute hypoxic states (*perfusion*-limited hypoxia) may persist heterogeneously in various regions of the tumor microenvironment. This results in a feed-forward loop of sorts in which, despite the increased angiogenesis initiated at a tumor volume of ~1 mm^3, states of hypoxia remain scattered throughout the tumor and even more angiogenesis is propagated [46]. Other forms of tumor hypoxia, caused by treatment or defects in blood flow, for example, are more rare (see Table 2).

Role of hypoxia in malignancy and resistance

Though hypoxia is a serious threat to all cell types and can cell death, in general it confers tumor cells with several growth advantages. For instance, hypoxia contributes to

Table 2: Causative factors of tumor hypoxia.

Perfusion-limited hypoxia ("acute hypoxia")[a]
• Abnormal structure of microvessels
• Abnormal function of microvessels
• Transient flow stasis (ischemia)
Anemic hypoxia
• Tumor-associated anemia
• Therapy-induced anemia
Hypoxemic hypoxia
• Plasma flow only
• Microvessels arising from venous side
Diffusion-limited hypoxia ("chronic hypoxia")[a]
• Enlarged diffusion distances (rarefaction of vascular bed, expansion of interstitial space)
• Adverse diffusion geometry
Toxic hypoxia
• HbCO formation (in heavy smokers)

With kind permission from Springer Science: [75].

tumor cell survival by activating a number of growth factors and potentiating important survival pathways [68]. Moreover, by initiating changes in cell metabolism, hypoxia enhances the Warburg Effect, the dependence of tumor cells on glycolytic pathways over normal oxidative mechanisms, which has been associated with tumor progression [69]. As briefly described earlier, hypoxia also promotes angiogenesis, a process that is critical to the establishment of primary tumors and metastasis. Increased telomerase activity, spurred by low levels of oxygen, contributes to the immortalization of tumor cells in hypoxia [70]. Another effect of hypoxia on cancer is the acidification of tumor cells, primarily as a result of the shift from aerobic to anaerobic metabolism, which results in lactic acid accumulation. Cancer cells adapt to acidification by increasing proton efflux via upregulation of Na^+/H^+ exchangers and by activating carbonic anhydrases, enzymes that help cells maintain a more alkaline intracellular pH with resulting acidification of the extracellular environment [71-73]. Hypoxic and acidic environments also impair immune cell function [74]. In these ways, hypoxia protects tumor cells in acidic and low-oxygen environments, allowing them to survive in otherwise inhospitable locations.

In addition to increasing tumor cell survival, hypoxia creates and selects tumor cells with higher rates of mutation, thereby promoting a more malignant phenotype. Induction of DNA breaks and chromosomal rearrangements, amplification of certain

genes and DNA sequences, and inhibition of DNA repair mechanisms have all been associated with hypoxia, perhaps as a result of superoxide radicals and other reactive oxygen species (ROS) whose levels are commonly elevated in low-oxygen states [68, 76, 77]. In fact, cells cultured under hypoxic conditions have shown a nearly four-fold increase in the number of point mutations over cells grown in normoxia [78]. Hypoxia has also been shown to amplify p53-mutant populations, a process of clonal selection that favors apoptosis-resistant cells, thus enriching tumors with a more aggressive cell phenotype [69, 79, 80]. Moreover, in neuroblastoma, breast and other cancer models, hypoxia was found to induce dedifferentiation and development of stem-cell like features, such as the epithelial-mesenchymal transition (EMT), all of which compound the aggressive phenotype already selected for by low oxygen states [81, 82]. Cells that are more invasive, exhibit higher metastatic potential and suppress immune reactivity are also among those whose numbers are increased by hypoxia [83-85].

Finally, hypoxia imparts tumors with the ability to resist cancer treatment. While the exact mechanisms of such resistance remain unclear, it is thought that radiotherapy, which relies on the generation of free oxygen radicals to induce cytotoxicity, is rendered three-fold less effective in hypoxic areas because there is little free oxygen to convert to radical form [68, 75]. Alternatively, hypoxia may activate protective factors, such as heat shock proteins, that insulate tumor cells from the effects of radiotherapy. Furthermore, apoptotic-resistant cells, like those selected for by hypoxic states, have shown high rates of radioresistance. Hypoxic conditions also render chemotherapy less effective, most likely because of issues related to diffusion (distance from vessels to tissue) and perfusion (disfigured and ineffective vasculature). In addition, the same issues that plague

radiotherapy in hypoxic areas – inability to generate free radicals, activation of protective proteins and diminished apoptotic potential – play a role in chemoresistance in areas of low oxygenation [59, 75]. As a result of these limitations, it is increasingly common for tumors to be "normoxialized" to correct for hypoxic tumors by giving hemoglobin-rich blood transfusions, erythopoietin (EPO) or nitroimidazoles prior to radio- and chemotherapy [86-88].

Clinical implications

Clinical studies have shown impressive correlations between the degree of hypoxia in tumors and cancer growth and metastasis and patient morbidity and mortality. In cervical cancers, hypoxic tumors, defined as $pO_2 < 10$ mm Hg and measured using needle electrodes, result in a significant decrease in progression-free and overall survival (Figure 4) [90]. The prognosis of head and neck cancers, as well, seem to be dependent

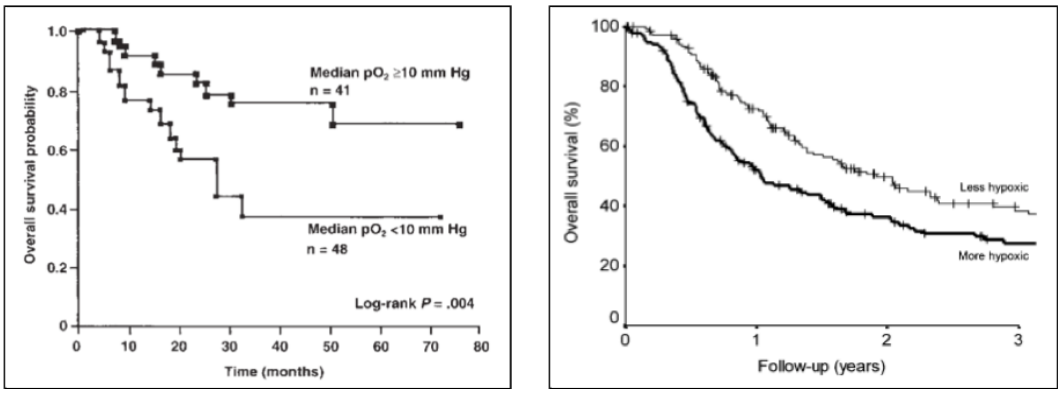

Figure 4: Effect of hypoxia on overall survival. Left panel: Kaplan-Meier plot of 89 cervical cancer patients treated with surgery and radiotherapy. With kind permission from Springer Science: [75]. Right panel: Kaplan-Meier plot of 397 patients with advanced head and neck cancer treated with radio- or radio- and chemotherapy (P= 0.006). Reprinted with permission from [89].

on intratumoral hypoxia (pO_2 < 2.5 mm Hg, Figure 4) [89]. Clinical investigations of the role of hypoxia in soft tissue sarcomas and breast cancer have also demonstrated the adverse impact of low oxygenation on metastatic potential and disease-free survival [51, 91]. One benefit to the development of hypoxic areas in tumors is that drugs designed to be active only in hypoxic areas – "bioreductive drugs" – can enhance the specificity of cancer treatments. Several of these are currently in preclinical and clinical trials [9, 92].

Hypoxia-inducible factor 1

The significant majority of the cellular response to low oxygen levels in mammals is mediated by the ubiquitously expressed transcription factor HIF1 [93]. As such, it is often described as the master regulator and integrator of the hypoxic response. HIF1 is an exceptionally important molecule both in normal physiology – HIF1 knockout mice die at embryonic day 10 [47] and HIF1 plays an essential role in wound healing – as well as the pathophysiology of many diseases. Nearly all of the previously described effects of hypoxia on tumor cells are driven by HIF1-based mechanisms, however, making HIF1 an attractive target for cancer treatments.

Structure of HIF1

HIF1 is a heterodimer composed of two members of basic helix-loop-helix (bHLH)/PER-ARNT-SIM (PAS) family of DNA binding proteins, HIF1α and HIF1β (Figure 5). The bHLH domains and PAS motifs, of which there are two per subunit, PAS-A and PAS-B, are necessary for heterodimer formation and DNA binding [94]. In

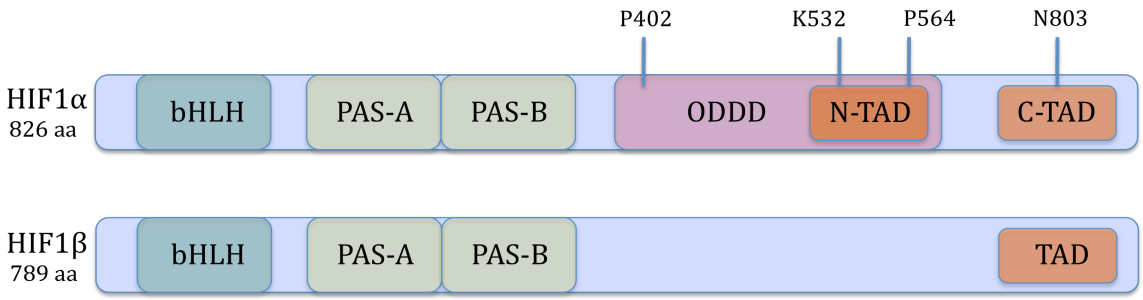

Figure 5: Domain structures of HIF1α and HIF1β. Each contains a bHLH domain and two PAS motifs. HIF1α additionally has an ODDD and two TADs. HIF1β only has one TAD. Four sites (three within the ODDD and one within the C-TAD) on HIF1α determine protein stability and activity.

addition, HIF1β (also called aryl hydrocarbon receptor nuclear translocator, ARNT) contains one transactivation domain (TAD), while HIF1α bears two, designated N-TAD (N-terminal) and C-TAD (C-terminal). The TADs are important for DNA binding specificity and recognition of hypoxia response elements (HREs), a DNA binding motif (sequence: 5'-RCGTG-3') in the promoter or enhancer regions of over 70 known (and, likely, many more unknown) target genes transactivated by HIF1 [95]. The C-TAD of HIF1α in particular is critical for HIF1 function as it interacts with co-activators such as CBP/p300 and other histone acetyltransferases/deacetylases and target gene-specific factors such as HNF4, Smad3 and C/EBPα that increase the transcription factor's activity significantly [96]. Perhaps the most unique element of HIF1α structure is the oxygen-dependent degradation domain (ODDD) that mediates oxygen-regulated protein stability (discussed below).

Regulation of HIF1

The two subunits of HIF1 are differentially regulated. HIF1β is constitutively expressed at all levels of synthesis, from transcription through translation, and its activity

is not affected by variations in oxygen levels [97, 98]. The predominant form of HIF1α (there are multiple splice variants), on the other hand, is regulated by multiple mechanisms that allow cells to fine-tune levels of the protein as conditions demand. Transcription of HIF1α, like that of its binding partner HIF1β, is constitutive and translation of HIF1α mRNA is regulated through the PI3/AKT/mTOR and MAPK/ERK pathways [99-101]. The most significant regulatory mechanisms are at the protein level, however, and HIF1α undergoes a number of post-translational modifications that determine its stability and activity [94, 102, 103]. Foremost among these is the prolyl hydroxylase (PHD)-based hydroxylation of two proline residues (402 and 564, indicated in Figure 5) in the ODDD [104-106]. PHDs are a family of 2-oxoglutarate-dependent dioxygenases with three members, PHD1, PHD2 and PHD3; PHD2 is the most active and plays the most significant role in HIF1α regulation [107, 108]. Hydroxylation by PHDs is an oxygen-, iron- and ascorbate-dependent process, and in normoxia, HIF1α is readily tagged with -OH groups on prolines 402 and 564 (Figure 6) [109]. Hydroxylated HIF1α is recognized and bound by von Hippel Lindau (VHL) ubiquitin E3 ligase complex (VCB-CUL2 E3 ligase complex), composed of VHL, cullin-2 (CUL2), elongins B and C (ELGN B/C) and ring box protein 1 (RBX1) [110]. The interaction of HIF1α with the VCB-CUL2 E3 ligase complex results in polyubiquitination of HIF1α and the ubiquinated protein is targeted for destruction by the 26S proteosome [111]. This process is remarkably efficient and under normoxic conditions, HIF1α protein is rapidly degraded shortly after translation. As a result, the half life of HIF1α is less than five minutes in optimally oxygenated tissue [112]. Under hypoxic conditions, however, PHD

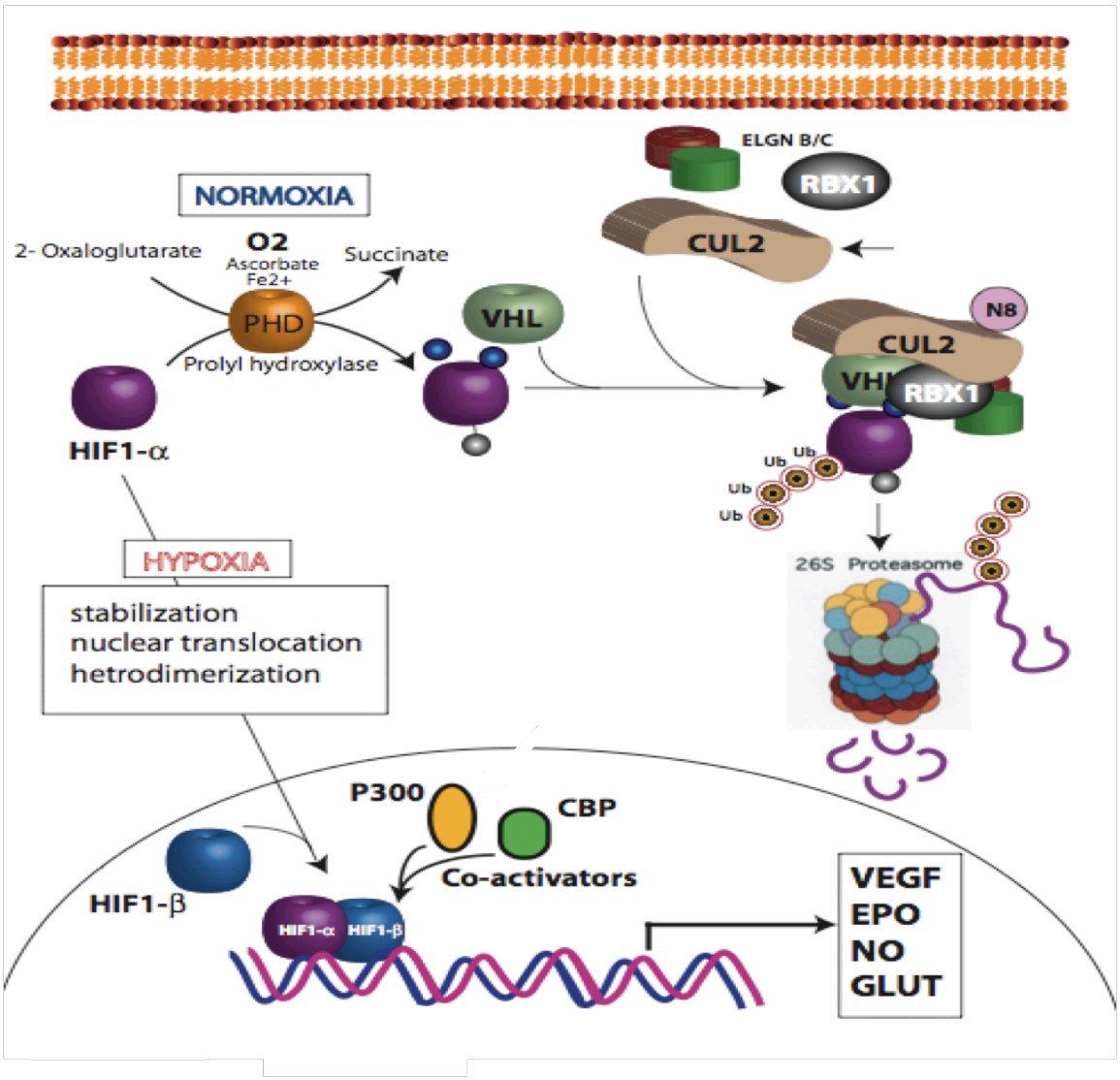

Figure 6: Regulation of HIF1α. In normoxic conditions, sufficient levels of oxygen allow PHD to hydroxylate HIF1α at proline residues 402 and 565. Hydroxylated HIF1α is recognized by VHL, which associates with scaffolding protein CUL2, RBX1, ELGN B/C to form the VCB-CUL2-E3 ligase complex. Interaction with this complex results in HIF1α polyubiquitination, leading to its degradation by the 28S proteasome. In hypoxia, low levels of oxygen prohibit PHD activity and HIF1α remains stable in the cytoplasm. After translocating to the nucleus, HIF1α binds HIF1β to form HIF1 and by interacting with co-activators such as CBP/p300, HIF1 transactivates target genes such as VEGF, EPO, NOS and GLUT 1/3. Courtesy of S. Ramakrishnan.

is unable to perform its hydroxylation function due to a lack of oxygen and HIF1α remains stable. HIF1α then translocates to the nucleus where it heterodimerizes with

HIF1β to form HIF1 and bind HREs of target genes and potentiate transcription [11].

Though PHD-based hydroxylation constitutes the predominant mechanism of HIF1α regulation, a second post-translational modification may also play a role in stability of the protein. As denoted in Figure 5, the HIF1α ODDD contains a lysine residue at amino acid 532. This site can by acetylated by the acetyl-transferase arrest-defective-1 (ARD1) in an oxygen-independent reaction. Acetylation of K532 enhances the association of HIF1α with the VCB-CUL2 E3 ligase complex, thereby leading to increased degradation of HIF1α [113]. Though ARD1 activity is not affected by oxygenation status, mRNA and protein levels of ARD1 decrease under hypoxic conditions, which would result in less acetylated HIF1α in hypoxia compared to normoxia [11, 113]. This mechanism of HIF1α regulation has been challenged, however, and remains controversial, as other studies were unable to confirm ARD1's ability to directly acetylate HIF1α [114-117]. Nevertheless, recent work has shown that ARD1 and deacetylase inhibitors reduce angiogenesis and tumor growth, perhaps via a HIF1-dependent mechanism [118, 119].

Whereas PHD and ARD1 affect the stability of HIF1α, factor inhibiting HIF1 (FIH) alters activity of the transcription factor. FIH exerts this influence by hydroxylating the asparagine residue at amino acid 803. Hydroxylation by FIH at this site, located within the co-activator recruiting C-TAD of HIF1α (Figure 5), impedes HIF1-CBP/p300 interaction, thus reducing HIF1's ability to bind DNA and transactivate target genes [96, 120, 121]. FIH activity, which is dependent on the same cofactors as PHDs, namely, oxygen, iron, ascorbate and 2-oxaloglutarate, is reduced under hypoxic conditions, and as

such, in low oxygen states, inhibition of HIF1α-CBP/p300 interaction in relieved to allow HIF-mediated transactivation [122]. Thus FIH-based hydroxylation provides a second layer of oxygen-dependent regulation of HIF1α.

Additional post-translational modifications of HIF1α regulate its activity as well. Phosphorylation of HIF1α by mitogen-activated protein kinase (MAPK) elements p42/p44 and p38 seems to enhance HIF1-mediated transactivation, perhaps by increasing HIF1α-HIF1β affinity [123, 124]. Similarly, S-nitrosation of HIF1α has been shown to increase its transactivation ability by increasing HIF1α-CBP/p300 interaction [125]. SUMOylation of HIF1α, on the other hand, has a repressive effect, decreasing HIF1α transactivation [126].

Other factors also play a role in HIF1α regulation, though to a lesser extent than those described previously. For example, inhibitors of histone deacetylases promote VHL- and ubiquitin-independent proteosomal degradation of HIF1α by interfering with heat shock proteins (HSPs) 70 and 90, which stabilize HIF1α during protein maturation [114]. Cytokines, growth factors and environmental factors, such as ROS and metal ions, have also been shown to affect HIF1α levels. These regulators are outlined in Table 3.

Role of HIF1 in tumorigenesis and metastasis

As described above, hypoxic conditions in the tumor microenvironment have severe consequences for patient morbidity and mortality. Importantly, nearly all of the advantages conferred by hypoxia to tumor growth and metastasis are mediated either directly or indirectly by HIF1 (Table 4). For example, HIF1 directly amplifies levels of

Table 3: Cytokine, growth factor and environmental regulators of HIF1α.

Regulator	Function/Pathway Involved	Consequence	Reference
Nickel (Ni^{2+})	Decreases cellular Fe level	Increased HIF-1α	Davidson et al., 2005
	Inhibits PHDs		
	Down-regulates the expression of FIH-1 and ARD1		Ke et al., 2005
	Depletes intracellular ascorbate		Salnikow et al., 2004
	PI3K/Akt		Li et al., 2004
Cobalt (Co^{2+})	Replaces Fe	Increased HIF-1α	Yuan et al., 2003
	Down-regulates the expression of FIH-1 and ARD1		Ke et al., 2005
	Depletes intracellular ascorbate		Salnikow et al., 2004
	PI3K	Increased HIF-1α	Gao et al., 2004
Arsenite	ROS		Duyndam et al., 2001
	p38 MAPK		Duyndam et al., 2003
Chromium	p38 MAPK, ROS	Increased HIF-1α	Gao et al., 2004
	PI3K/Akt, ROS	Increased HIF-1α	Gao et al., 2002
Vanadate	AMP-activated protein kinase (AMPK)		Hwang et al., 2004
Desferrioxamine (DFO)	Fe chelator	Increased HIF-1α	Wang and Semenza, 1993
Insulin Interleukin-1 (IL-1)	PI3K	Increased HIF-1α	Stiehl et al., 2002
Insulin-like growth factor (IGF)-1, IGF-2	ROS	Increased HIF-1α	Feldser et al., 1999
Fetal calf serum	ROS	Increased HIF-1α	Richard et al., 2000
Angiotensin II (Ang II)	ROS	Increased HIF-1α	Gorlach et al., 2001
Thrombin, Platelet-derived growth factor (PDGF)			
Nitric oxide (NO)	MAPK, PI3K	Increased HIF-1α	Kasuno et al., 2004
	Inhibits PHDs		Metzen et al., 2003b
Nitric oxide (NO) under hypoxia	Inhibits mitochondrial O_2 consumption	Decreased HIF-1α	Hagen et al., 2003
	Increases intracellular Fe and PHDs activity		Callapina et al., 2005
TGF-α	ROS	Increased HIF-1α translocation and activity	Haddad and Land, 2001
		Increased DNA binding	Hellwig-Burgel et al., 1999

Reprinted with permission from the American Society for Pharmacology and Experimental Therapeutics. From [11].

growth factors such as insulin-like growth factor-2 (IGF2) and transforming growth factor alpha (TGFα), activating signaling pathways that lead to cell survival and proliferation as well as increasing HIF1α expression itself to establish a feed-forward loop [127-129]. Similarly, the increased efficiency of anaerobic metabolism is driven by HIF1's transactivation of genes involved in glucose uptake (GLUT 1 and 3) and glycolysis (genes encoding nearly all the enzymes of the glycolytic pathway) [130, 131]. Interestingly, some products of glycolytic metabolism, namely pyruvate and lactate, have been shown to induce HIF1α accumulation even under normoxia, thus completing another positive feedback loop [11, 132].

Tumor angiogenesis is profoundly stimulated by HIF1, which is the main trigger of the "angiogenic switch" activated by tumors in hypoxia (see the section on angiogenesis below) [133]. HIF1 directly upregulates the gene encoding the most potent

Table 4: Partial list of genes regulated by HIF1.

Function	Gene (abbreviation)	Reference
Erythropoiesis/ iron metabolism	Erythropoietin (EPO)	Semenza et al., 1991
	Transferrin (Tf)	Rolfs et al., 1997
	Transferrin receptor (Tfr)	Bianchi et al., 1999
	Ceruloplasmin	Lok and Ponka, 1999
Angiogenesis	Vascular endothelial growth factor (VEGF)	Levy et al., 1995
	Endocrine-gland-derived VEGF (EG-VEGF)	LeCouter et al., 2001
	Leptin (LEP)	Grosfeld et al., 2002
	Transforming growth factor-β3 (TGF-β3)	Scheid et al., 2002
Vascular tone	Nitric oxide synthase (NOS2)	Melillo et al., 1995
	Heme oxygenase 1	Lee et al., 1997
	Endothelin 1 (ET1)	Hu et al., 1998
	Adrenomedulin (ADM)	Nguyen and Claycomb, 1999
	α_{1B}-Adrenergic receptor	Eckhart et al., 1997
Matrix metabolism	Matrix metalloproteinases (MMPs)	Ben-Yosef et al., 2002
	Plasminogen activator receptors and inhibitors (PAIs)	Kietzmann et al., 1999
	Collagen prolyl hydroxylase	Takahashi et al., 2000
Glucose metabolism	Adenylate kinase-3	O'Rourke et al., 1996
	Aldolase-A,C (ALDA,C)	Semenza et al., 1996
	Carbonic anhydrase-9	Wykoff et al., 2000
	Enolase-1 (ENO1)	Semenza et al., 1996
	Glucose transporter-1,3 (GLU1,3)	Chen et al., 2001
	Glyceraldehyde phosphate dehydrogenase (GAPDH)	Graven et al., 1999
	Hexokinase 1,2 (HK1,2)	Mathupala et al., 2001
	Lactate dehydrogenase-A (LDHA)	Semenza et al., 1996
	Pyruvate kinase M (PKM)	Semenza et al., 1994
	Phosphofructokinase L (PFKL)	Semenza et al., 1994
	Phosphoglycerate kinase 1 (PGK1)	Semenza et al., 1994
	6-phosphofructo-2-kinase/gructose-2,6-bisphosphate-3 (PFKFB3)	Minchenko et al., 2002
Cell proliferation/survival	Insulin-like growth factor-2 (IGF2)	Feldser et al., 1999
	Transforming growth factor-α (TGF- α)	Krishnamachary et al., 2003
	Adrenomedullin (ADM)	Cormier-Regard et al., 1998
Apoptosis	Bcl-2/adenovirus EIB 19kD-interacting protein 3 (BNip3)	Carrero et al., 2000
	Nip3-like protein X (NIX)	Bruick, 2000

Reprinted with permission from the American Society for Pharmacology and Experimental Therapeutics. From [11].

endothelial cell mitogen, VEGF [134], and the gene for transforming growth factor beta (TGFβ) [135], and indirectly upregulates fibroblast growth factor (FGF), angiopoietin-1 (ANG1) and placental growth factor (PlGF) [136], all important facilitators of angiogenesis. HIF1 also promotes angiogenesis by reorganizing stroma within the tumor microenvironment to facilitate formation of new vasculature. Levels of fibronectin, matrix metalloproteinases (MMPs), collagen prolyl hydroxylase (cPHD) and urokinase plasminogen activator receptors (uPAR)/inhibitors (uPAIs), increased by HIF1, all contribute to extra cellular matrix (ECM) deconstruction and angiogenesis in this manner [129, 137-139]. By potentiating the actions of NOTCH, a signaling molecule that maintains vessel homeostasis and regulates EC proliferation and migration, HIF1 may provide yet another stimulus for vessel growth [140, 141].

HIF1 further amplifies these pro-angiogenic effects by activating factors that promote vasodilation. Levels of nitric oxide synthase (NOS) [142], heme oxygenase 1 [143], adrenomedulin (ADM) [144] and α_{1B}-adrenergic receptors [145] are all heightened by HIF1, increasing the carrying capacity of vessels delivering blood to the tumor microenvironment. In addition to augmenting blood flow to a tumor by increasing vasculature and vasodilation, HIF1 also enhances oxygen delivery. HIF1 transactivates the gene for erythropoietin [146], as well as the genes encoding transferrin, transferrin receptor and ferroxidase, which increase iron uptake and availability, allowing for increased heme production [147-150]. Both of these HIF1-driven actions result in accelerated erythrocyte production thereby increasing delivery of oxygen to a tumor.

Another critical role of HIF1 in enhancing the lethality of cancers is its propagation of factors that increase tumor cell motility and metastasis. HIF1 directly upregulates expression of genes encoding lysyl oxidase (LOX) and lysyl oxidase-like 2 (LOX2), enzymes belonging to a family of amine oxidases that cross link collagen and elastin in (ECM) [151]. LOX family members increase Snail, suppress E-cadherin expression and potentiate focal adhesion kinase (FAK) activity [152-155]. HIF-driven expression of LOX promotes tumor cell detachment from the ECM and enhances tumor cell motility via these mechanisms, effecting elements of the epithelial-mesenchymal transition (EMT) that is a hallmark of malignant tumors [152, 156]. This role for HIF1-driven LOX expression and consequent increased metastatic potential of tumors is well established [154]. Studies of breast, melanoma and pancreatic cancer cells line *in vitro*, for example, showed marked inhibition of invasivity upon inhibition of LOX and LOX2 by shRNA or small molecules such as β-aminoproprionitrile (β-APN) [157, 158].

Inhibition of LOX and LOX2 by β-APN or antibodies to LOX family members also results in suppression of HIF1-mediated invasion and metastasis *in vivo* in breast cancer models [154, 159]. Clinical data corroborate these findings: in a retrospective study of 295 breast cancer patients, elevated hypoxia markers correlated with increased LOX levels and shorter metastasis-free and overall survival [160], while a prospective study of 91 head and neck cancer patients showed a similarly strong association between hypoxia, LOX and increased patient morbidity and mortality [161]. This link between hypoxia, LOX and tumor invasion and metastasis is therefore an important one in the context of malignancy and is summarized in Figure 7.

HIF1 promotes tumor cell motility and metastasis through several other mechanisms as well. While some of the EMT observed in hypoxia is borne through the HIF1-LOX relationship as described above, HIF1 directly upregulates other repressors of E-cadherin that contribute to the malignant phenotype as well. These include TWIST [162], TCF3, ZEB1 and ZEB2 [163]. Additionally, the same process HIF1 activates to break down stroma in the tumor microenviroment to promote angiogenesis – through factors such as MMPs, uPARs/uPAIs and cPHD – plays a significant role in the ability of tumor cells to translocate beyond the primary tumor [11, 47, 129]. By disrupting normal tissue homeostasis and deconstructing basement membranes, these HIF1-activated enzymes allow tumor cells to traverse ECM, intravasate into vessels and spread to distal sites. Similar furtherance of metastatic potential is achieved by HIF1-driven overexpression of the met oncogene (MET), a receptor that renders tumor cells more responsive to hepatocyte growth factor (HGF) – a ligand that is also upregulated in hypoxia – contributing to increased ECM degradation, cell dissociation and tumor cell

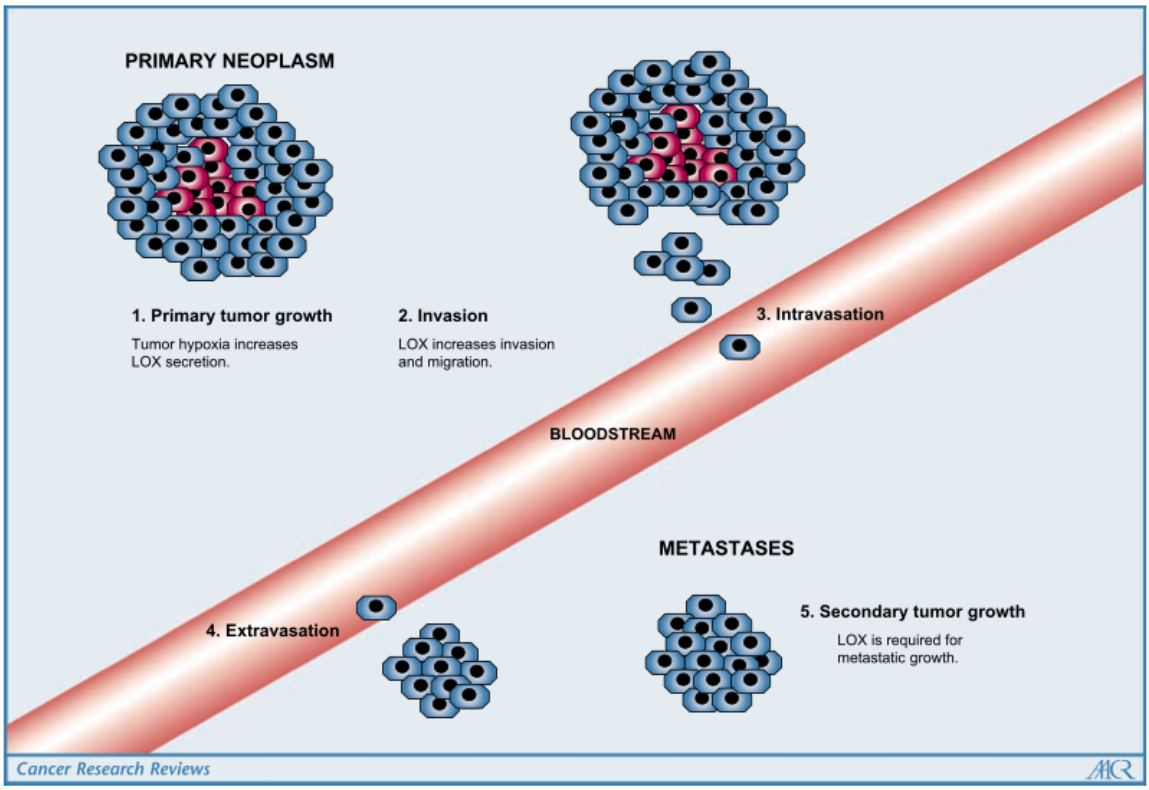

Figure 7: Role of the LOX family of amine oxidases in hypoxia-driven cancer metastasis. (1) A primary tumor with hypoxic areas (in red) activates HIF1, which directly upregulates LOX and LOX2. (2) LOX members promote tumor cell detachment, invasion and migration. (3) Tumor cells intravasate into nearby vessels, the growth of which has also been stimulated by HIF1-based mechanisms. (4) Tumor cells extravasate into tissue at distal sites. (5) Tumor cells colonize new areas. LOX members also play a role in preparing these new sites for tumor growth (see below). Reprinted from [156] with permission.

escape to secondary sites [83]. Autocrine motility factor (AMF), a cytokine secreted by tumors, is overexpressed in hypoxia via HIF1 and also contributes to increased migration through autocrine and paracrine signaling [164].

HIF1 not only primes cancer cells for detachment and facilitates their invasion into areas surrounding the primary tumor, but it also plays a role in tumor cell homing to distal sites and tumor development once cells have reached these new areas. Chemokine receptor CXCR4, for example, is induced by HIF1 and aids in metastatic homing of EOC tumor cells from the ovary to organs that express its cognate ligand, SDF1 [165]. HIF1-

regulated LOX, in addition to promoting tumor cell detachment, seems to prepare sites for detached cells to colonize – thereby establishing a "premetastatic niche" – through recruitment of $CD11b^+$ myeloid cells [166]. By conferring tumor cells the ability to survive in both hypoxic and acidic microenvironments, HIF1 also increases the number of potential sites cancers can seed, providing yet another metastatic advantage to cells that have activated this powerful transcription factor [9].

Finally, recent studies have also implicated HIF1 in several other malignancy-promoting processes. Increased levels of Oct4 have been associated with HIF1, suggesting a role for the transcription factor in fostering a stem cell-like phenotype [167, 168]. Similarly, HIF1 has also been shown to increase dedifferentiation by increasing expression of the differentiation inhibitor ID2 [169] and potentiating NOTCH signaling [140, 141]. Downregulation of DNA repair enzymes MSH2 and MSH6 [170, 171] and activation of multidrug resistance transporters ABCB1 and ABCG2 by HIF1 simultaneously make tumor cells more malignant and less sensitive to conventional treatments [172-174]. Together, these HIF1-driven changes in tumor cell phenotype mark grave developments in the progression on cancers, to be sure.

It is important to note that HIF1 also has a paradoxical role in inducing tumor cell apoptosis in addition to its aforementioned tumorigenic and pro-metastatic roles. By reducing levels of anti-apoptotic proteins such as Bcl-2 or increasing levels of pro-apoptotic factors such as p53, NIX and NIP3, for example, HIF1 is able to trigger suicide in cells [11, 68]. It is not known whether there is a hypoxic threshold at which HIF1 switches from being cytoprotective to apoptotic. Overall, however, as elucidated in this section, HIF1 provides tumor cells with several distinct and significant advantages.

HIF1 as a therapeutic target

It is difficult to overstate the tremendous role HIF1 plays in malignancy (Table 5). Nearly all of the hypoxia-driven adaptations that solid tumors undertake – activation of proliferative pathways, shifts in metabolism, angiogenesis, erythropoiesis, metastasis – to survive in and thrive beyond their low oxygen environments are HIF1-mediated. Indeed, HIF1 is such a crucial molecule that its dysregulation results in highly metastatic disease, as evidenced by the fact that loss of VHL in renal cell carcinoma (RCC) leads to unmitigated HIF1α accumulation and the formation of highly vascularized and metastatic tumors [47]. Targeting HIF1 in cancer therapy is therefore an obvious strategy. The majority of these approaches have focused on reducing HIF1α protein levels. Agents in this category include those that inhibit the mTOR pathway, topoisomerase activity, cyclin-dependent kinases, microtubule assembly, histone deacetylases or heat shock proteins, for example. Other potential treatments target HIF1 binding to DNA or transactivation activity to reduce the molecule's

Table 5: Clinical implications of HIF1α overexpression in human cancers.

Cancer	Association[a]
Bladder	Mortality, MVD[b], tumor grade, TTP
Brain	Mortality, MVD, tumor grade
Breast	Mortality, MVD, tumor grade, metastasis
Cervix (uterus)	Mortality, MVD, radiation resistance
Colon	Invasion, metastasis, MVD
Endometrium (uterus)	Mortality, MVD
Esophagus	MVD, venous invasion, PDT response[c]
Head and neck	Survival
Head and neck	Mortality (HIF-2α), MVD
Liver	Venous invasion, MVD
Lung (NSCLC)	Survival, apoptosis
Lung (NSCLC)	Mortality
Oropharynx	Mortality, radiation resistance
Ovary	Mortality[d], MVD
Pancreas	Metastasis, MVD, TNM stage
Skin (melanoma)	Mortality (HIF-2α)
Stomach (GIST)	Mortality, metastasis, MVD

[a]HIF1α association unless HIF2α is indicated

[b]Abbreviations: MVD, microvessel density; TTP, time to progression; MVD (DCIS), microvessel density in ductal carcinoma *in situ*; PDT, photodynamic therapy; GIST, gastrointestinal stromal cell tumor; NSCLC, non-small-cell lung carcinoma; TNM, tumor-node-metastasis

[c]Tumors overexpressing HIF1α and BCL2

[d]Tumors overexpressing HIF1α and mutant p53

Reprinted from [175] with permission.

tumorigenic and pro-metastatic properties. One drug, GL331, is uniquely designed to suppress HIF1α mRNA levels [175].

Though dozens of HIF1-targeting drugs are being evaluated as cancer treatments, few have been investigated in appropriate *in vivo* models, let alone clinical trials, in the context of hypoxia. Indeed, although HIF1 is an attractive therapeutic target because it is intimately involved in so many processes inherent to the development of tumor malignancy, researchers must also be cognizant that HIF1 is also essential to many physiological processes and beneficial in certain pathophysiological contexts. Moreover, most of the drugs that have been shown to suppress HIF1 expression are not HIF1-specific; topotecan and digoxin, for example, affect a number of other cellular functions, and therefore must be used with caution in the context of targeting hypoxia in solid tumors [9]. Interestingly, HIF1 does bear some pro-apoptotic characteristics and it is possible that mitigating HIF1's role may actually have unintended consequences that may actually promote malignancy. Thus if HIF1-targeting drugs are to be used in a clinical setting, it will be important to establish the appropriate framework and role of such therapy, as well as proper consideration of combination therapies [175].

HIF2α and HIF3α

Though HIF1α is the major determinant of the hypoxic response in most cell types, HIF2α plays a role as well. HIF2α is structurally related to HIF1α, bearing bHLH and PAS motifs as well as two TAD domains and sharing 48 percent amino acid sequence homology with HIF1α. Accordingly, it functions similarly by heterodimerizing

with HIF1β to bind HREs and transactivate certain genes. In contrast to HIF1α, which is expressed ubiquitously, however, HIF2α expression is predominantly in the lung, endothelium and carotid body [176, 177]. Interestingly, HIF1α promotes angiogenesis while HIF2α mediates vascular maintenance [178]. In cancers, both HIF1α and HIF2α have been found to contribute to an aggressive phenotype [129, 179]; nevertheless, they seem to have different roles in this context. In MCF-7 breast cancer cells, for example, HIF1α was primarily responsible for transactivation of the VEGF and IGF genes. In RCC cells, in which VHL function is impaired, however, HIF2α was found to drive VEGF expression as well as other genes canonically regulated by HIF1α. Moreover, in MCF7 cells, knocking down either HIF1α or HIF2α results in a compensatory increase in the other [180]. Together, these data suggest an important, albeit tissue-specific, secondary role for HIF2α in the hypoxic response.

Compared to HIF1α and HIF2α, HIF3α has not been extensively studied. Like HIF2α, HIF3α expression seems to be limited to certain tissue types [11]. There are multiple HIF3α splice variants, at least two of which, HIF3α2 and HIF3α4, act as negative regulators of HIF1α in a dominant-negative fashion [181-184]. HIF3α isoforms, like HIF1α and HIF2α, are regulated and targeted for degradation in an oxygen-dependent matter by VHL, but their precise roles in the overall hypoxic response is as of yet unclear [185].

Angiogenesis

Angiogenesis is the formation of new blood vessels from existing vasculature. This process is distinct from the related vasculogenesis, in which vessels are formed *de novo* from progenitor cells, and other mechanisms of vessel formation such as intussusception, vessel co-option, vascular mimicry and tumor cell to endothelial cell differentiation (Figure 8) [186, 187]. In 1971, Judah Folkmann published his seminal work on the critical role of angiogenesis in the progression of solid tumors [6]. Since then, angiogenesis has been implicated in tumorigenesis and metastasis and increased patient morbidity and mortality. Thus although essential for embryogenesis and tissue growth and regeneration, angiogenesis has a nefarious role in the progression of metastatic disease. As such, anti-angiogenic therapies to treat cancer constitute a significant area of research interest.

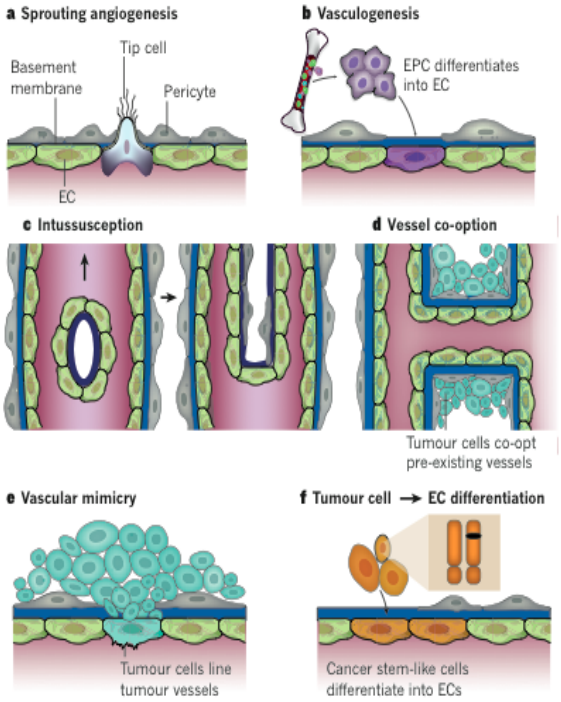

Figure 8: Mechanisms of new vessel formation. (a) Sprouting angiogenesis, the extension and branching of new vasculature from existing vessels; (b) Vasculogenesis, the creation of new vessels *de novo* from circulating bone marrow-derived and/or resident endothelial progenitor cells; (c) Intussusception, the splitting of existing vessels to form new ones; (d) Vessel co-option, the expansion of tumors to surround and utilize existing vasculature; (e) Vascular mimicry, the formation of vessel-like structures by tumor cells; (f) Tumor cell to endothelial cell differentiation; the maturation of dedifferentiated tumor cells into EC to form vessels. Reprinted by permission from MacMillan Publishers Ltd: [186].

Mechanisms of angiogenesis

Vessel structure and activity in angiogenesis

The endothelium is a specialized form of mesenchymal tissue that serves as the interface between circulating blood in the lumen and the rest of the vessel wall. This surface, which forms the interior lining of the entire vascular system, is composed of endothelial cells (ECs) connected by junctional molecules such as VE-cadherin and claudins. Surrounding ECs are pericytes, connective tissue cells of marginal differentiation that ensheath most vessel types. Between ECs and pericytes is a common basement membrane that is maintained by both cell types. These three elements comprise the most basic vessel structure [186]. Some vessels also contain a layer of smooth muscle outside the pericyte layer; together, the pericyte/smooth muscle layer is termed the mural layer and mural cells refer to pericytes or smooth muscle cells.

ECs have a remarkable lifespan; at any given time in healthy adult vessels, only 0.01 percent of ECs are undergoing mitosis and physiologic replacement of endothelium is a process that takes years [188, 189]. Nevertheless, the endothelium has a remarkable ability to abandon this quiescent state to effect robust vascular reorganization and proliferation in a matter of hours – if induced by the appropriate stimuli [187]. In most cases, these stimuli take the form of changing conditions within the endothelium microenvironment. In particular, oxygenation status is the most important determinant of EC activity. As such, EC have a remarkable oxygen sensing system that is anchored by HIF1. In response to low oxygen states, which can result from a number of processes – rapid tumor growth, for example – HIF1 is activated in EC and signaling molecules,

namely, VEGF, angiopoietins and FGFs, are upregulated and secreted to bind to receptors on the surface of ECs. In addition to this autocrine mechanism, other cells, such as tumor, inflammatory and stromal cells, secrete growth factors in hypoxic conditions to stimulate angiogenesis in a paracrine manner [186, 187].

When receptors in a quiescent vessel bind secreted growth factors, pericytes and ECs become activated to loosen cell-cell junctions and detach from the basement membrane of vessel wall via matrix remodeling [190]. This process results in vasodilation and increased vessel permeability, which allows plasma proteins such as fibronectin and fibrinogen to extravasate and form ECM. This new source of matrix serves as a fertile source of angiogenic factors like VEGF and FGFs as well as a scaffold onto which ECs migrate. A few endothelial cells, so-called tip cells, lead a path along the newly secreted ECM in the direction of neovascularization while stalk cells – ECs that follow tip cells – begin dividing to elongate the nascent vessel. Tip cells take advantage of their filopodia and follow guidance signals to maintain proper directionality whereas stalk cells coordinate amongst themselves spatial information to provide coherent tube formation [191]. Myeloid cells aid in bridging and fusing one neovessel to another to initiate blood flow, which is required to prevent vessel regression. To complete maturation, the vessel must return to its quiescent state. This is achieved by inhibiting ECM degradation, recruiting pericytes, depositing basement membrane and restituting of cell-cell junctions [186, 192]. This process, and the specific factors involved in each step, is summarized in Figure 9.

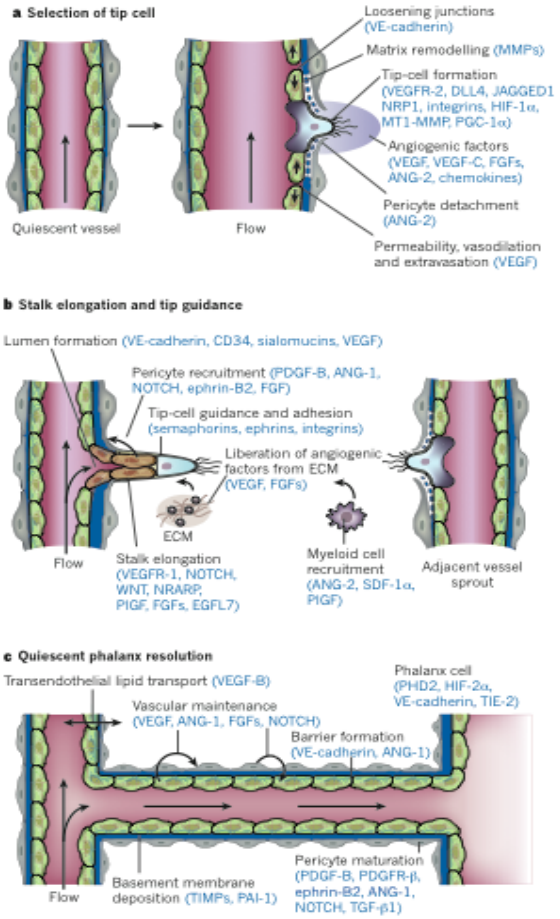

Figure 9: Mechanisms and factors involved in angiogenesis. (a) Stimulation by angiogenic factors causes vasodilation, degradation of ECM and basement membrane and pericyte and EC detachment. Plasma proteins extravasate and form new ECM. ECs begin migration along nascent ECM; these leading cells become tip cells. (b) Tip cells follow guidance signals and continue migration along ECM as lagging stalk cells proliferate, form tubular structures and begin recruitment of pericytes. Myeloid cells aid in fusion of nascent vessels by secreting angiogenic factors or freeing them from the ECM (c) Lumen formation allows blood flow, which is necessary to maintain patency and prevent vessel regression. Cell-cell and cell-ECM junctions are reestablished, pericytes and recruited and ECs return to their quiescent, phalanx state. Reprinted by permission from MacMillan Publishers Ltd: [186].

Factors involved in angiogenesis

Dozens of growth factors, adhesion molecules, proteases and chemokines are involved in fine-tuning the formation of new vasculature. The most important of these factors is discussed here and summarized in Table 6.

VEGF: VEGF is a family (VEGF-A through -D and placenta growth factor, PlGF) of growth factors whose roles are largely similar. VEGF-A (also known as, simply, "VEGF") is the main member and exerts the majority of its pro-angiogenic effects by binding VEGF receptor-2 (VEGFR2) and coreceptors neuropilins 1 and 2 (NRP1 and NRP2) [193-195]. Knockout of VEGF or VEGFR2 results in complete loss of vascular development and even heterozygous knockout is embryonic lethal in mice [196]. VEGF's most important roles are as an EC-specific survival factor and potent mitogen. By

Table 6: Major angiogenic factors and their roles in angiogenesis.

Ligand–receptor	Putative role in physiological angiogenesis
VEGF–VEGFR1 and VEGF–VEGFR2	Induce proliferation, sprouting and tube formation of endothelial cells; increase vascular permeability; suppress apoptosis for vessel stabilization; upregulate PDGFβ for mural cell recruitment
VEGFC–VEGFR3–NRP2	Lymphatic development
Notch pathway	Negative feedback for VEGF-mediated vessel sprouting and participates in vessel fate determination (arterial compared with venous)
Ephrin-B2–EPHB4	Arterial compared with venous endothelial cell specialization determination; guides vessel branching
PDGF-BB–PDGFRβ	Promotes migration, recruitment and proliferation of mural cells
ANGPT1–TIE2	Faciliates EC–matrix and EC–mural cell interaction for vessel stabilization; suppresses EC apoptosis
ANGPT2–TIE2	Induces EC apoptosis in absence of VEGF; participates in lymphatic patterning
TGFβ1–TGFβRII	Promotes ECM and protease production; promotes differentiation of fibroblasts to myofibroblasts and mesenchymal cells to mural cells

Reprinted by permission from MacMillan Publishers Ltd: [199].

providing tip cells with a gradient to follow during vessel extension, VEGF functions as a guide for vessel directionality [197]. VEGF also controls several vessel properties, such as helping to maintain vascular homeostasis and controlling vasodilation. VEGF also increases expression and activity of tissue remodeling factors such as uPAR and metalloproteases that are necessary for angiogenesis (see below) [198].

Other growth factors: These include PDGF, FGFs, angiopoietins, TGFβ and several others. The main role of the PDGF family is to recruit mural cells to complete maturation of newly formed vasculature. FGFs are important in vessel maintenance during EC quiescence as well as stimulation of other pro-angiogenic molecules during phases of EC activation. Angiopoietin-1 (ANG1) maintains EC quiescence, cell-cell junctions and basement membrane deposition, with an overall effect of promoting EC survival and vessel homeostasis and maturity. Angiopoietin-2 (ANG2), on the other hand, antagonizes ANG1, enhancing EC and pericyte detachment and vessel sprouting. Both are necessary for angiogenesis, though at different stages in the process[186]. TGFβ is responsible for several aspects of vessel maturation, such as

development of ECM and the recruitment of pericytes [199]. Some of these and other growth factors share redundant roles with VEGF; PDGF and IGF1, for example, are potent mitogens, but are not specific to EC, however, and induce fibroblast proliferation as well [198].

NOTCH and WNT pathway: NOTCH signaling plays an important role in maintaining order during migration of ECs to form new vasculature. By decreasing the sensitivity of stalk cells to VEGF, NOTCH ensures that tip cells lead EC movement in the desired direction of vessel growth and that large numbers of EC do not simply rush towards angiogenic stimuli [197]. In addition, NOTCH helps in determining whether a new vessel will be of arterial or venous nature. While NOTCH signaling aids in maturation and maintaining homeostasis during vessel quiescence, it also activates WNT in stalk cells to stimulate proliferation, thereby playing dual, almost oppositional, roles in angiogenesis [186, 200].

Proteases and integrins/junctional molecules: One of the major steps in angiogenesis is breakdown and reorganization of ECM and basement membrane. MMPs, uPAs and cPHDs are some of the enzymes that help degrade ECM and basement membrane to allow pericyte and EC detachment and movement in the early stages of angiogenesis. In addition, proteases like MMPs free angiogenic factors embedded in ECM, providing directional cues for tip cells [201]. In contrast, integrins and junctional molecules play a largely antagonistic role to that of proteases. Integrins mediate EC adhesion to ECM and basement membrane and help to anchor ECs during quiescence and vessel maturation. By virtue of their bidirectional signaling abilities, integrins also allow ECs to act as hubs that coordinate EC, pericyte, ECM and basement membrane behavior

during EC detachment and migration, including tip cell sprouting. Junctional molecules such as connexins have a similar function, promoting cell-cell communication that is crucial for organized migration. VE-cadherin, claudins and other junctional molecules help maintain tight junctions during vessel quiescence and maturation. VE-cadherin also helps tip cells make new contacts at the leading edge of vessel sprouts [186].

Guidance signals: Tip cells traverse ECM to form new vessels with the aid of factors such as ephrins and semaphorins. These navigational landmarks, either cell-bound (ephrins) or cell-bound and secreted (semaphorins) bind EC surface receptors to influence filopodia extention and confer ECs the ability to explore their microenvironment and migrate appropriately. Like NOTCH, ephrins also participate in determination of vessel fate (arterial versus venous) and have an additional role in recruiting mural and progenitor cells during angiogenesis [184, 197]. That cells deficient in ephrin- or semaphorin- mediated signaling demonstrate marked vascular defects underscores their importance. Interestingly, ephrin levels increase in tumors treated with VEGF inhibitors, suggesting a role in resistance to anti-angiogenic drugs [186, 199, 202].

Physiologic angiogenesis

Angiogenesis is important for several physiological processes. For example, while a large part of embryonic development depends on vasculogenesis, angiogenesis is required in parallel to sustain elaborate oxygen-consuming processes such as organogenesis, which is associated with generation of large hypoxic areas in rapidly growing tissue [199]. Angiogenesis also plays a significant role normal wound repair. In

response to injury, both platelets and inflammatory cells, which are recruited to the wound site, secrete VEGF to reorganize and revascularize damaged tissue [192]. Finally, angiogenesis is also crucial in the context of the female reproductive cycle. Build up and maintenance of the corpus luteum in the ovary and the endometrium in the uterus, in particular, during the proliferative and secretory phases of the menstrual cycle require significant vascularization to sustain adequate oxygen and nutrient perfusion. In addition, because hormonal signaling is critical in determining the fate of various tissues within the ovary and uterus every cycle, the establishment of adequate vasculature is required for delivery of steroids from their sites of synthesis to their sites of action [203]. In these ways and others, angiogenesis functions as a necessary component of normal physiology.

Angiogenesis in cancer

Like the development of hypoxic states in tissues, angiogenesis has a role in both physiology and pathophysiology. In many cases, angiogenesis has a beneficial effect in the pathophysiologic context, such as development of collateral vasculature in patients with atherosclerosis or in wound repair (a physiologic or pathophysiologic process, depending on one's view). In cancers, however, angiogenesis – again, like most other hypoxia-driven processes – has a significant and detrimental overall effect on patient morbidity and mortality. This is largely because the formation of new vasculature in solid cancers sustains tumor growth and sets the foundation for invasion and metastasis of malignant cells beyond the primary tumor site. The mechanisms and implications of tumor angiogenesis are described here.

The angiogenic switch

The classical model of tumor angiogenesis posits that during nascent tumor development, pro-angiogenic factors – VEGF, MMPs and other agents discussed earlier – and anti-angiogenic factors – angiostatin, endostatin and others – are in balance with each other to maintain vessel quiescence. At a certain point during its rapid growth, usually around 1 mm^3 in volume, the avascular tumor reaches a critical hypoxic state requiring the immediate activation of rescue measures to ensure viability [5-7]. As described previously, the primary regulator of this response is HIF1. Among its many roles in orchestrating adaptations to low oxygen levels is HIF1's significant contribution to triggering the "angiogenic switch" (Figure 10) – the disruption of the balance responsible for vessel quiescence to induce angiogenesis. Through the direct and indirect activation and coordination of the many mediators of angiogenesis highlighted earlier, HIF1 tilts the scale in favor of pro-angiogenic factors and the elaborate process of vessel sprouting and branching proceeds. Coupled with other angiogenesis-inducing stimuli, such as activation of oncogenes or mutation of tumor suppressors, activation of HIF1 by the tumor thus addresses the ever-increasing oxygen demands of the expanding malignancy [192].

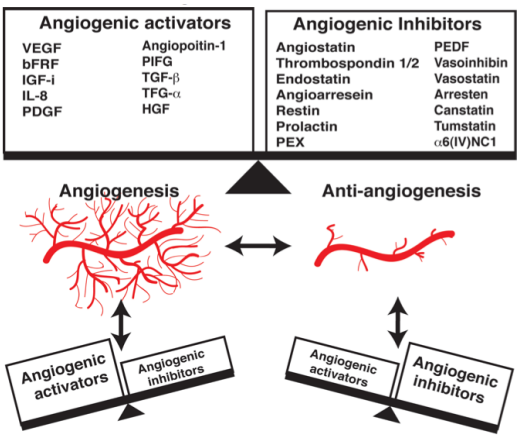

Figure 10: Activation of the angiogenic switch. During vessel quiescence (top), a balance exists between pro- and anti-angiogenic factors that inhibits further vascular proliferation. Tilting the balance towards pro-angiogenic molecules (bottom left), by stabilization of HIF1 under hypoxia, for instance, activates the angiogenic switch, leading to vessel branching and sprouting. From [204].

Angiogenesis, tumor progression and metastasis

Activation of the angiogenic switch occurs early in cancer development, even in premalignant stages, and is often cited as the rate-limiting step in tumorigenesis [5, 6, 187]. Angiogenesis can also be initiated in dormant primary or metastatic tumors, leading to activation or spread of disease in healthy individuals or patients who are thought to have been cured [187, 205]. Progression of the process, at whatever stage, usually results in rapid tumor vascularization. Importantly, however, these nascent vessels are structurally and functionally distinct from vessels borne of physiologic angiogenesis (Figure 11) [74]. In particular, tumor vessels tend to demonstrate increased vasodilation, permeability and irregularities of the endothelium, basement membrane and mural layers. Tumor vasculature is also more tortuous, arbitrarily branched and otherwise disorganized, bearing a mish-mash of characteristics associated with capillaries, arteries and venules as opposed to one specific vessel type [192]. Finally, tumor cells are often integrated into the walls of vessels, a hybrid form of vascular mimicry [206, 207]. Many of these irregularities, it is believed, are due to the fact that ECs stimulated by tumor-secreted VEGF, that is, in a paracrine fashion, react much differently than when stimulated by autocrine VEGF [208].

As a consequence of these defects, tumors that have activated the angiogenic switch reside in a unique milieu. The structural defects of tumor vasculature, combined with the high interstitial pressures created by increased vessel leakiness, cause significant maldistribution of blood flow and resources transported through the vasculature [199]. Accordingly, oxygen, nutrients, immune cells and, in patients being treatment with chemotherapy, anti-cancer drugs are hetereogenously delivered to various regions of the

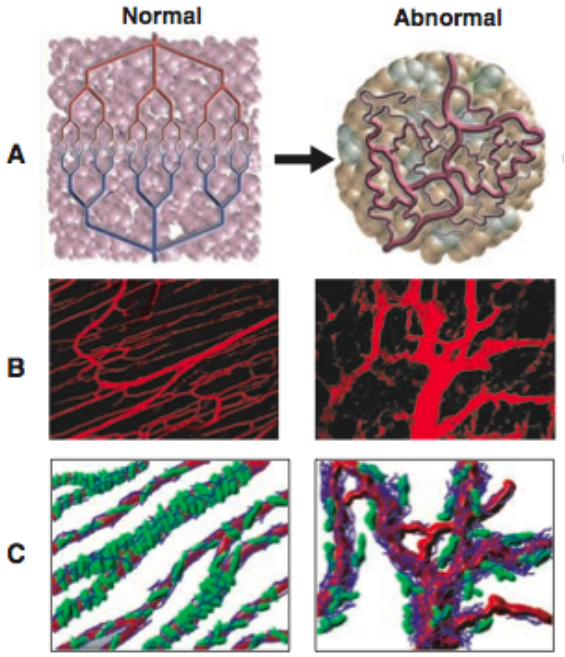

Figure 11: Physiologic versus tumor vasculature. (A) Normal vessels are organized, arranged with clear branch points and bear distinct characteristics of artery, vein or capillary. In contrast, tumor vasculature is convoluted, arbitrarily branched and demonstrates an amalgam of arterial, venous and capillary features. (B) Compared to normal vasculature, tumor vessels are irregular, dilated and more permeable. (C) Normal vessels are sheathed in pericytes (green) and basement membrane (blue) evenly and consistently, while in tumor vasculature pericytes are scattered and loosely bound and basement membrane is of heterogeneous thickness. Adapted from [74] with permission.

tumor. The resulting environment is both hypoxic and acidic, factors that, as described earlier, select for hardier, radio- and chemo-resistant and more malignant cells. Moreover, increased interstitial pressures and vascular fenestrations promote tumor cell escape from the primary tumor site into vasculature [74, 186]. Tumor angiogenesis, therefore, not only promotes selection of the most lethal tumor cells within a cancer, it also facilitates their distribution to distal sites. In this way, tumor angiogenesis enables tumors to survive, thrive and metastasize, and its activation by HIF1 does not portend well for patient morbidity and mortality.

Angiogenesis as a therapeutic target

Because of its widespread and severe deleterious consequences in the progression of malignancy, tumor angiogenesis has been a focus of anti-cancer therapies. Two seemingly contradictory approaches in particular have been of great interest. The first aims to starve tumors of blood flow by inhibiting activation of the angiogenic switch or

limiting the growth of new vasculature after angiogenesis has already been initiated. VEGF, overexpressed in the majority of solid tumors, is an attractive target because of its critical roles in various steps of angiogenesis. Drugs that target this potent growth factor include antibody to VEGF (bevacizumab), VEGF trap (aflibercept) and various agents (sorafenib, sunitinib) that inhibit tyrosine kinases that relay VEGF-, PDGF- and other growth factor- mediated signaling. Another class of drugs, termed vascular disrupting agents, targets preexisting vasculature in contrast to preventing formation of new vessels. Drugs such as these, which employ anti-vascular strategies, were briefly discussed in the section on novel therapies for ovarian cancer.

There are drawbacks to this approach, however. For example, it is possible that by starving a tumor of oxygen supply, anti-angiogenic drugs select for populations of cells that require lower levels of oxygen, which have been associated with a more malignant phenotype [9, 70, 192]. Alternatively, cells within hypoxic microenvironments induced by VEGF downregulation may shift to other growth factor-mediated pathways, such as PDGFs or FGFs, to promote angiogenesis [186]. Indeed, resistance to bevacizumab has become an issue, likely through both of these mechanisms [27, 209]. In addition, decreasing perfusion of tumors by targeting vasculature means that drugs that are dependent on vasculature for delivery to tumors, namely, chemotherapeutics, may have less of an effect as distribution is impaired [192]. However, because tumor vasculature is already so irregular and tortuous, the effect of decreased tumor vascularity on drug delivery may be negligible [210].

To address these limitations of anti-angiogenic therapy, another strategy to manipulate tumor vasculature has been developed. This approach focuses on

"normalizing" vasculature, that is, transforming tumor vessels so that they are more like those formed during physiologic angiogenesis. The concept behind vessel normalization is that vessels will distribute blood – and anti-cancer drugs – more uniformly to all regions of target tissues if they are more reflective of normal angiogenesis compared to tumor angiogenesis. In a sense, vessel normalization can be considered a pro-angiogenic strategy, as it aims to promote physiologic angiogenesis [7, 186]. Indeed, vessel normalization at least partially ameliorates tumor hypoxia [74].

In fact, there is overlap between the two aforementioned strategies. As it turns out, some anti-angiogenic strategies, such as VEGF blockade, not only decrease vessel density, but also seem to normalize vasculature – at certain doses and schedules. This latter caveat highlights the importance of coordinating combination therapies to maximize therapeutic benefit. The challenge, then, is to dose and schedule anti-angiogenic treatments and chemotherapies in a manner that takes advantage of the former's vessel normalization abilities as well as its inhibitory effects on vessel growth such that the cytotoxic potential of chemotherapeutics can be fully realized [74, 199, 209].

Metastasis

The initial stimulus for activation of the angiogenic switch in tumors is predominantly hypoxia-based and HIF1-driven. Nevertheless, the end result is a convoluted and haphazard response that, while transiently addressing low oxygenation issues, does not solve them completely. As such, the tumor microenvironment still bears persistent areas of hypoxia. In response to these adverse growth conditions, cancers develop a biological contingency plan of sorts. By conferring cells the ability to metastasize to distal sites, tumors are able to overcome the potential of starvation at the primary tumor site to survive and continue proliferation unchecked, albeit at a new location. This transformation from solitary tumor to metastatic disease requires several stages of development (Figure 12). These requisites can be organized into four fundamental processes: clonal selection, detachment and invasion, dissemination and colonization. Importantly, each of these steps is modulated by HIF1 and hypoxia-dependent mechanisms [9].

Clonal Selection

Metastatic tumor cells bear many genotypic characteristics that distinguish them from more benign types. While changes in genomic DNA were once believed to be strictly in the realm of advanced disease, it is now accepted that genomic instability is a hallmark of nascent tumor development [211]. In particular, these pre-malignant cells

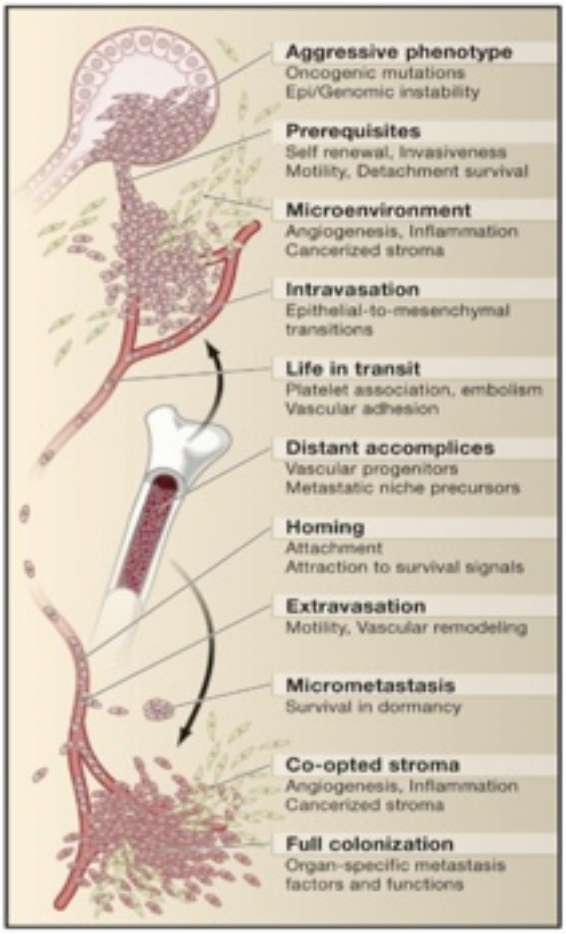

Figure 12: Stages of metastatic progression. Cell-intrinsic and microenvironmental pressures select for cells demonstrating an aggressive phenotype and certain prerequisite traits. These cells are primed for detachment, invasion and intravasation. In circulation, CTCs face hemodynamic forces and immune attack, which they can overcome by clumping via platelet activation. Recruitment of hematopoietic and progenitor and myeloid cells prepares sites of metastasis for CTC implantation while homing signals guide CTCs to the premetastatic niche. Extravasation at these prepared metastatic sites does not ensure macrometastasis development; micrometastases need to activate angiogenesis and enter the cell cycle for further growth. Completion of all these steps results in malignant disease. Reprinted from [211] with permission.

have increased DNA mutations, chromosomal rearrangements and epigenetic alterations. This includes constitutive activation of proto-oncogenes such as RAS [212] and mutations or inactivation of tumor suppressor genes such as Rb [213]. Alternatively, inhibition of genetic repair mechanisms [214], telomere dysfunction [215] or epigenetic plasticity resulting in changes in chromatin remodeling [216] also drive the accretion of DNA abnormalities. Finally, the ability of a cancer cell to "self-renew" – essentially, act as a tumor stem cell – is an important prerequisite for malignancy. Oct4, Wnt, Hedgehog and NOTCH signaling have all been implicated in this process [167, 168, 217, 218].

Within a growing tumor, only a handful of cells may accumulate enough of these "hits" to the genome to render a malignant disposition. Amplification of

this minority is therefore a crucial step in progression of metastatic disease. Several pressures shape this selective process and must be surmounted for a tumor to achieve metastatic potential [219]. These include cell-intrinsic mechanisms, such as activation of growth inhibitory, apoptotic and senescence pathways, and environmental factors, including chemical (e.g. build up of ROS), physical (e.g. basement membrane) and biological (e.g. immune and inflammatory response) [211]. These selective pressures are summarized in Figure 13. Principal among these forces is the development of hypoxia within the tumor microenvironment. As described above, low oxygen states promote generation and selection of genetically unstable, dedifferentiated/stem cell-like, and hypoxia-, low pH-, apoptosis-, immune-, radio- and chemo-resistant cell populations. Many, if not most of these adaptations are driven by HIF1 (see pages 26-32).

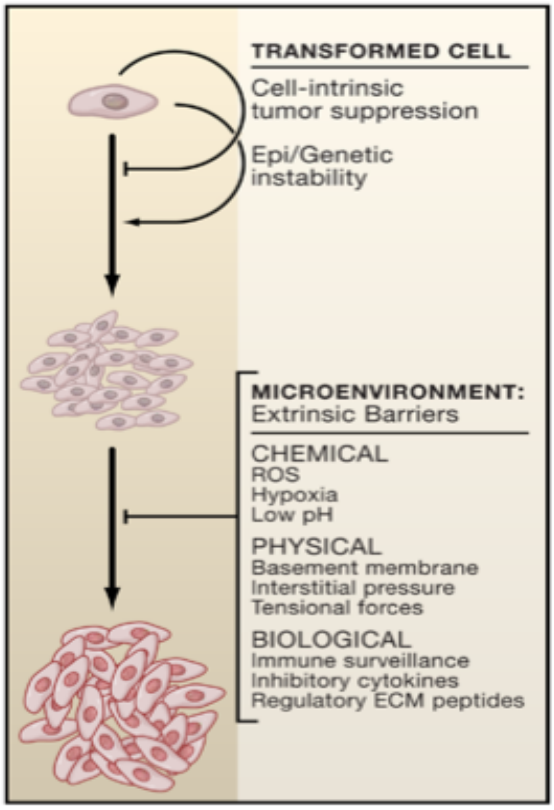

Figure 13: Constraints that drive selection of the metastatic phenotype. Cells face cell-intrinsic pressures, such as DNA repair machinery, that inhibit the aberrant proliferation seen in cancers. Overcoming these obstacles by induction of genomic instability or epigenetic modulation defines a tumor cell. The microenvironment also plays a role in selecting cells with metastatic potential. Only certain cell populations within the tumor can survive the chemical, physical and biological insults exampled here. Activation of certain factors, such as HIF1, provide protection from these pressures and those subpopulations of cells that have found a way to resist, overcome, or co-opt these threats become primed for metastasis. Reprinted from [211] with permission.

Detachment and invasion

Establishment of a sizable genotypically dysregulated tumor cell population is the first phase in progression of malignant disease. Many of the genetic aberrations amassed during pre-malignancy play important roles throughout the metastatic process. Indeed, activation of certain genes and repression of others have significant consequences for tumor cell detachment and invasion.

The epithelial-mesenchymal transition

The epithelial-mesenchymal transition (EMT) is a fundamental step in the progression of malignant disease and refers to the overt transformation seen in cancer cells as they dedifferentiate from cells with epithelial qualities to those of a more stem cell-like, mesenchymal character [220]. Though EMT plays a necessary role in embryogenesis, in the context of cancer it increases tumor cell metastatic potential by causing loss of cell-cell and cell-matrix adhesive qualities and reorganization of cytoskeleton, both of which ultimately promote a more motile phenotype [221]. These changes are driven by several mechanisms, of which the repression of E-cadherin and synchronous upregulation of N-cadeherin seems to be the most significant. E-cadherin is the main component of epithelial-epithelial adherens junctions and contributes to maintenance of epithelial integrity and polarity [222, 223]. In contrast, N-cadherin promotes epithelial-mesenchymal junctions and increases cytoskeletal remodeling with an overall effect of promoting tumor cell motility [224]. Transcription factors TWIST, Snail, Slug, TCF3, ZEB1 and ZEB2 directly repress E-cadherin expression and

potentiators of these factors, like HIF1, which increases TWIST, TCF3, and ZEB1/2, and the HIF1-driven LOX, which increases Snail activity, are therefore also major stimuli for EMT and tumor cell detachment [9, 153, 162, 163]. TWIST has also been shown to increase N-cadherin levels [225, 226]; however, thorough understanding of the mechanisms of N-cadherin regulation during EMT is lacking [223].

Other important catalysts of EMT are hepatocyte growth factor (HGF) and its cognate receptor, met oncogene (MET), which together suppress E-cadherin via multiple pathways including PI3/AKT and ERK/Snail [227]. Additionally, HGF/MET activate focal adhesion kinase (FAK), an enzyme primarily regulated by integrins, cell surface receptors that mediate cell-ECM interaction, that activates a cascade of pathways promoting cell survival and detachment from ECM [228, 229]. Of note, both HGF and MET are increased in hypoxia (MET directly by HIF1) and FAK activity is enhanced independently by LOX and TGFβ, levels of which are, in turn, both augmented by HIF1 [83, 154, 156, 166].

E- and N-cadherins function as mediators of cell-cell adhesion by virtue of their anchoring to the actin cytoskeleton, a rapidly assembling and disassembling determinant of cell architecture. Thus changes in cadherin expression not only affect intercellular processes, but intracellular events as well. In conjunction with other actin-regulating molecules, such as p120-catenin, for example, N-cadherin modulates actin remodeling by altering Rho-GTPase activity [223, 230, 231]. During EMT, Rho-GTPases, which are responsible for integrating and transmitting signals from chemokines and growth factor receptors to maintain actin cytoskeleton equilibrium, activate relatively static actin structures to become more dynamic [232, 233]. The result of this change is essentially

three-fold. First, actin-based membrane ruffling remodels the cytoplasm, introduces direction-of-movement cell polarity and deposits a fine mesh of actin filaments for lamellipodia extension [234]. Second, lamellipodia, flat, sheet-like protrusions formed by extending and branching actin filaments, provide a leading edge for cell movement. Finally, three-dimensional, actin-based structures termed invadopodia (the transformed cell version of podosomes) form to promote degradation of and movement into the ECM [223]. Again, HIF1 seems to have role in this metastasis-promoting process; a recent study showed that HIF1 transactivates the gene for junction-mediating and regulatory protein (JMY), an actin-nucleating protein that enhances tumor cell motility under hypoxia [235]. In these ways, EMT promotes actin remodeling with a corresponding enhancement of cell motility. With the decreased cell-cell and cell-ECM interactions also observed during EMT, increased cell motility provides tumor cells with sufficient impetus to mobilize from a primary tumor and begin its journey through the metastatic process. Reprising its role as a significant promoter of cancer lethality, HIF1 is a critical in effecting both the cell-cell/cell-ECM detachment and cell motility facets of EMT.

The role of dynamins

One of the many important classes of molecules that modulate EMT and cell motility is the dynamin family. Dynamins (Dnms or Dyns) take three major forms (Dnm1, Dnm2 and Dnm3) and multiple related forms (dynamin-like proteins, DLP/DRP). Expression of the dynamins vary by tissue; Dnm1 is found in neuronal cells, Dnm2 is ubiquitously expressed and Dnm3 is limited to the brain, lung and testes [236]. Dynamins are large, ~100 kDa proteins composed of five domains. The GTPase domain

at the N-terminal promotes hydrolysis of GTP to GDP and confers dynamins the ability to constrict. This is important as dynamins form polymeric collars around clathrin-coated endocytic vesicles and GTPase activation allows dynamins to pinch invaginations off the membrane (Figure 13). The pleckstrin homology (PH) domain binds phosphoinositides that enhance GTPase activity of dynamins [237]. The GTPase effector domain (GED) further promotes dynamin GTPase activity by acting as an internal GTPase-activating protein (GAP) [238]. The C-terminus of dynamins bears the proline-rich domain (PRD), which is important for interaction with various endocytic adapter proteins, lipid scaffolding/recruiting proteins, FAK, microtubules and actin-regulating elements [239-243]. The so-called "middle" domain of dynamins is of unknown function [236].

As a crucial player in clathrin-mediated endocytosis, dynamins regulate many functions. Cell attachment via cadherin uptake, iron regulation via transferrin/transferrin receptor uptake, neurotransmission via synaptic vesicle uptake, cell metabolism via glucose transporter GLUT4 uptake and other receptor-mediated endocytic processes are all dyamin-dependent [244-246]. Inhibition of dynamin by a dominant negative mutant, K44A-dynamin or the small molecule dynasore, impairs dynamin's endocytic function and suppresses E-cadherin [223, 247, 248] and transferrin/iron uptake [249], for example, tightening cell-cell and cell-ECM junctions and reducing intracellular stores of iron, respectively. Beyond clathrin-coated endocytosis, dynamins are also important for caveolar endocytosis and some forms of macropinocytosis [250].

In addition to its role in EMT by promoting cadherin uptake, dynamins are also intimately involved in several aspects of cell motility. By virtue of its ability to form polymeric scaffolds, associate with cytoskeletal elements such as actin and microtubules

and exert mechanical torsion by constricting, dynamin is vitally important to membrane ruffling, lamellipodia extension and invadopodia/podosome formation (Figure 14). By localizing at lamellipodial extensions, dynamins also serve in maintaining proper cell polarity and directionality of cell migration by regulating uptake of growth factors, such as EGF of PDGF, that mediate the cell navigation process [251]. Moreover, dynamins have been shown to associate with FAKs and promote focal adhesion disassembly, thereby contributing to another EMT-inducing process [236]. Inhibition of dynamin results in a host of detachment and motility dysfunctions, highlighting the importance of dynamins in endocytic processes, cell detachment and cell motility [236, 249].

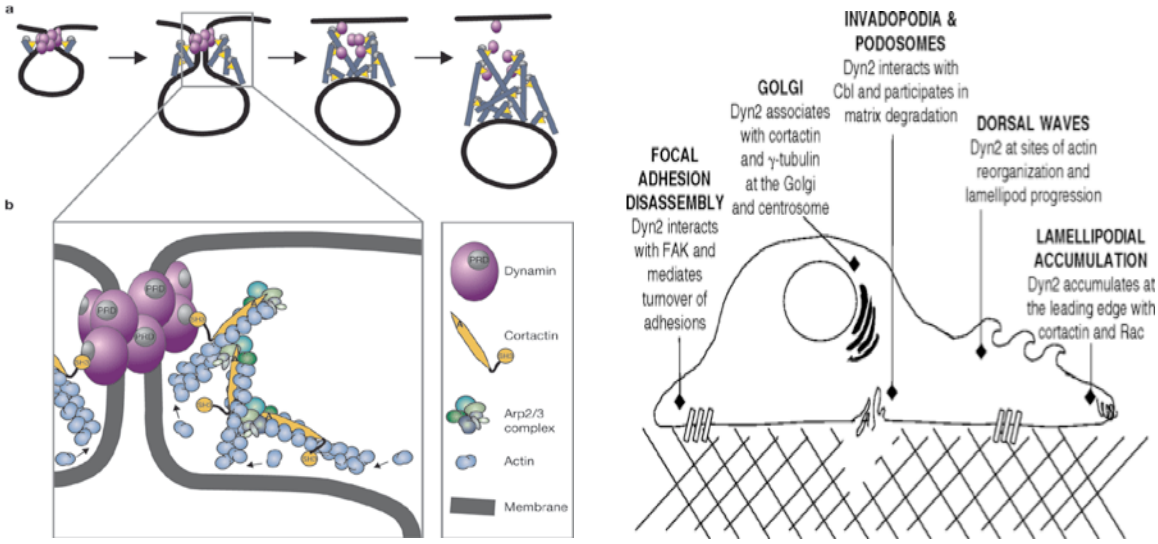

Figure 14: Functions of dynamins. **Left:** (a) Dynamins associate with various elements, including actin and actin-regulating proteins, such as cortactin and Arp2/3, to promote scission of a budding vesicle from the plasma membrane. Via this mechanism, dynamins regulate a host of endocytic processes including cadherin and transferrin/iron uptake (b) Enlargement of (a) showing interaction of dynamins with actin/cortactin/Arp2/3 via the PRD domain. Reprinted by permission from MacMillan Publishers Ltd: [252]. **Right:** Dynamins are involved in many aspects of cell adhesion and motility beyond its role in cadherin uptake. These include removal of focal adhesions, interaction with the cytoskeleton at the Golgi and centrosome, formation of invadopodia/podosomes, activation of membrane ruffling and lamellipodia accumulation, where it is also important in uptake of growth factors for intracellular signaling that determines directionality of movement. Reprinted from [236] with permission.

Invasion

A tumor cell that has detached from other cells and the ECM and has also adopted a motile phenotype still faces several constraints to movement, and at the invasion stage of metastasis, the tumor microenvironment still plays an important role. Specifically, basement membrane, comprised of glycoproteins and proteoglycans, and ECM, made of collagens and elastins, and other stromal elements create tough physical barriers that must be degraded for any appreciable cell migration. Destruction of the basement membrane and reorganization of the ECM depends on expression of many genes, several of which are activated during EMT, and include LOX, MMPs, uPARs/uPAIs and cPHD and other proteolytic factors. Certain extracellular proteases have a secondary action as they create bioactive peptides as a consequence of basement membrane and ECM cleavage. These byproducts modulate a host of processes including angiogenesis and tumor cell survival, proliferation, migration, invasion and metastasis [211]. As described in the section on hypoxia, expression of basement membrane and ECM degradation machinery are to a great extent regulated by HIF1 [129].

In addition to serving as an obstacle to tumor cell migration, tumor stroma has a unique function as a promoter of invasion and metastasis. Fibroblasts, circulating endothelial progenitor cells and immune and inflammatory cells have all been found to contribute to the metastatic potential of cancer cells within the tumor microenvironment [211]. For instance, fibroblasts in breast cancer stroma secrete SDF1, a ligand that increases the proliferative and migratory abilities of tumor cells by interacting with its receptor CXCR4, expression of which is increased by HIF1 [253]. Macrophages, for example, are recruited to necrotic and hypoxic areas of tumors and secrete high levels of

HIF1-driven VEGF, HGF and MMPs, which contribute to tumor cell migration, invasion and metastasis. As such, the appearance of macrophages within the tumor microenvironment corresponds with worsening disease [254]. Thus while tumor stroma is a barrier to tumor cell migration, mainly due to physical obstacles it poses in the form of basement membrane and ECM, it also aids tumor cell invasion to an extent [211, 220].

Dissemination

Invasion of cancer cells through tumor stroma into surrounding tissue marks a grave milestone in progression of the disease. Once a cancer has achieved this extent of migration, metastatic disease is likely inevitable. This is especially the case for ovarian cancers, as EOCCs that have penetrated the ovarian capsule are now free to exfoliate directly into the peritoneal space, the cavity with the largest surface area in the body [14]. As described previously, seeding of various organs within the peritoneal cavity is usually a death sentence for ovarian cancer patients.

Intravasation

In other solid tumors, however, additional hurdles remain for tumor cells to reach distal sites. The rate-limiting step in this process is the ability of tumor cells to intravasate into nearby vessels. By this point in a nascent tumor's growth, the angiogenic switch has likely already been activated, providing a robust, albeit disorganized, network of vasculature. MMPs and other proteases secreted by tumor cells, especially those having undergone EMT, break down the disorganized ECM and basement surrounding tumor

vasculature. High interstitial pressures, caused by the leakiness of malformed tumor vessels, meanwhile drive movement of tumor cells into permeable vessels for distribution throughout the body (see pages 45-46) [74]. In addition to metastasizing via blood vessels, tumor cells also intravasate into the lymphatic circulation, often colonizing regional lymph nodes before eventually entering the hematogenous circulation [211].

Circulation and extravasation

Once within the circulation, tumor cells still face variety of challenges such as immune cells and shear stress forces, for example. Recent evidence shows that circulating tumor cells (CTCs) may use platelets to clump together and form hardier structures that can resist inflammatory processes mediated by immune cells and physical hemodynamic forces [211]. Indeed, as has been clinically observed for over a century, cancer patients often exhibit hypercoagulable conditions [255]. Anoikis, cell death that is caused by lack of structural support, is another peril that CTCs must face. Expression of factors such as TrkB, which suppresses the effect of anoikis on cells and suppression of alpha-5 integrin (ITGA5), which sensitizes cells to anoikis, are two ways that tumor cells surive without a stormal platform [256-258]. Regulation of both of these factors is hypoxia-dependent. The clonal selection process described earlier also favors those cells that are already resistant to many types of stress and thus the dangers associated with transport may be minimal, especially if the travel time from primary tumor to a capillary bed at the site of metastasis is on the order of minutes, as has been shown to be the case in humans [211].

The signals that cue and promote CTC extravasation are largely unknown. It is thought that VEGF, which, in addition to promoting angiogenesis and vasodilation, also

increases vascular permeability, may be secreted by CTCs near sites of extravasation [259]. By activating Src kinases, VEGF degrades EC junctions, allowing CTCs to escape circulation. The observation that metastasis was diminished in mouse knockouts of Src favors this hypothesis [260]. Basement membrane and ECM degradation via MMPs and other proteases are thought to complete the extravasation process and promote CTC entry into surrounding tissue [9]. Many of the proteins involved in extravasation – VEGF, MMPs, ANGPTL4, for example – are regulated by HIF1.

Homing and the premetastatic niche

While some tumor circulating cells merely extravasate at random sites along their journey though the vasculature, it seems that most cells selectively exit the blood at predetermined locations. Indeed, Stephen Paget's 1889 hypothesis, formed after extensive study of breast cancer metastasis patterns, that tumor "seeds" will only grow in the appropriate microenvironment "soils" [261] has been shown to hold up under modern scrutiny; circulatory patterns fail to adequately predict preferred sites of metastasis, meaning that another mechanism is involved [262]. This concept was further confirmed serendipitously by a 1984 study that diverted peritoneal fluid of ovarian cancer patients to the jugular vein with aim of ameliorating the pain and pressure of malignant ascites. The procedure resulted in dissemination of millions of metastatic EOCCs into the circulation of patients for more than two years. Remarkably, however, the procedure did not result in widespread metastasis and metastases that did form were largely dormant [211, 263].

From these findings and other studies it became clear that two processes are at work that determine sites of circulating tumor cell extravasation. First, there seems to be

a homing mechanism that guides CTCs to specific sites. This has proven to be the case for breast cancer cells that home to lung tissue, a process that is driven by the affinity of the adhesion receptor metadherin, expressed on circulating breast cancer cells, for an as-of-yet unidentified ligand expressed specifically on lung capillary endothelial cells [264]. Similarly, expression of CXCR4 receptor in renal cell carcinoma [265], ovarian cancer [266], breast cancer [267] and non-small cell lung cancer [268] guides tumor cells to target organs that express SDF1, CXCR4's cognate ligand. The second process that determines site of extravasation involves establishment of a "pre-metastatic" niche that is serves as a fertile implantation cite for CTCs. This model postulates that hematopoietic progenitor cells are activated from the bone marrow by signals secreted by primary tumor cells. These recruited hematopoietic progenitor cells then home to and precondition metastatic sites [211, 269]. Myeloid cells may also be drawn to metastatic sites in a similar manner to support creation of the premetastatic niche [166]. As has been the case for nearly all the phases of metastasis described thus far, HIF1 once again has a hand in both of these mechanisms. HIF1 promotes CXCR4 expression to promote tumor cell homing and drives VEGF expression, which is necessary for recruitment of hematopoietic progenitor cells [269, 270], as well as LOX expression, which is responsible for homing of myeloid cells [166].

Colonization

Upon extravasation at a distal site, tumor cells still face a harsh microenvironment, despite any establishment of a premetastatic niche. One of the main

challenges faced by tumor cells at this juncture is a lack of adequate blood supply to feed growth of the extravasated cells. This results in a hypoxic microenvironment similar to that seen in the primary tumor and as a result, many micrometastases maintain long periods of dormancy [211]. Nevertheless, tumor cells that have experienced hypoxic stresses in the primary tumor and underwent appropriate adaptive changes at that stage may fare better at their new locations as they are better able to cope with a hostile microenvironment and transform it into a more habitable one [9]. Indeed, induction of angiogenesis, by recruitment of circulating and bone marrow-derived endothelial cells, for example, can wake dormant tumors from their slumber and promote rapid macrometastatic growth [271]. Of course, as is the case with anything angiogenesis-related, HIF1 has a large role in development of vasculature at sites of metastasis [9].

On the other hand, angiogenesis alone cannot revive micrometastases from dormancy, since disseminated tumor cells have been demonstrated to remain dormant even in areas of adequate blood perfusion. Of significance, these cells remained in cell cycle arrest, and as a result, were refractory to adjuvant chemotherapy [272]. In certain cancer types, cells that were extracted from dormant tumors showed proliferative potential *in vitro* [273, 274]. This finding was corroborated the results of other studies that showed that patients with dormant tumors composed of cells that could reinitiate the cell cycle suffered increased rates of morbidity and mortality compared to those with dormant tumors bearing cells that were unable to reenter the cell cycle [274]. Taken together, these data suggest that Paget's "seed and soil" hypothesis may be the most significant determinant of micro- to macro- metastatic transformation [9, 211].

HIF1 and metastasis

The vital role of HIF1 in metastasis has been highlighted above in each step. Figure 15 summarizes this important relationship and the mediators that connect HIF1's transactivational function with the progression of malignancy.

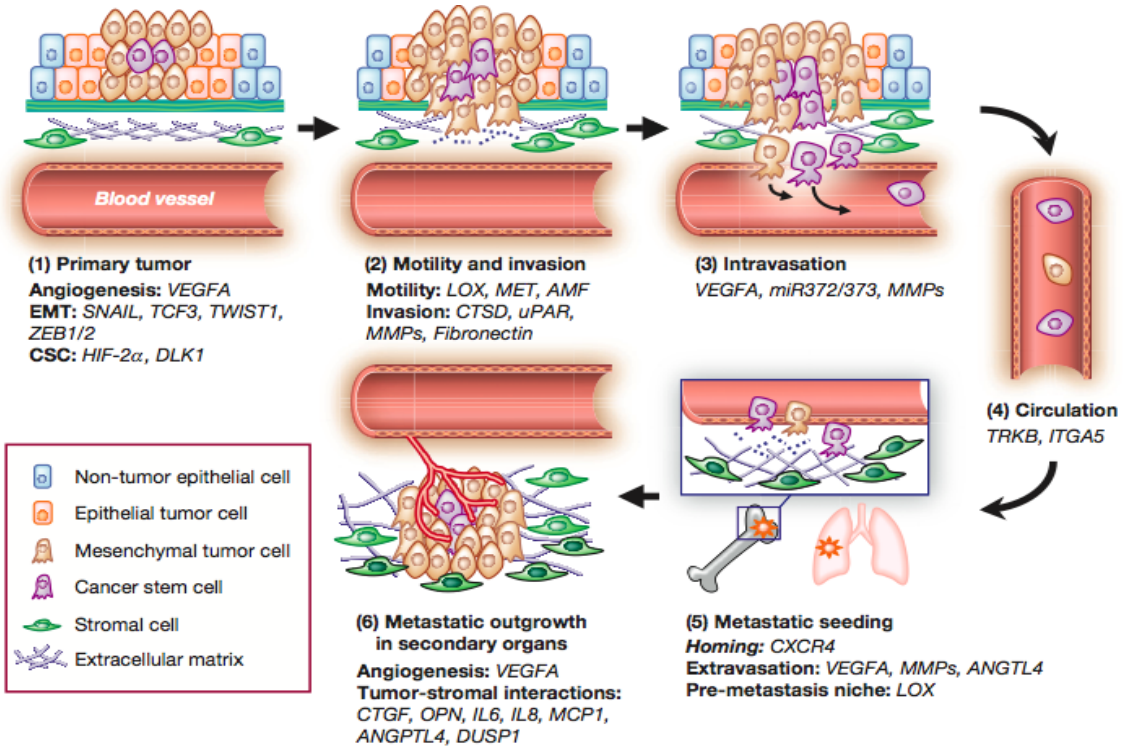

Figure 15: Role of hypoxia and hypoxia-induced factors in metastasis. Hypoxic states in the tumor microenvironment select for genetically unstable, stem cell-like and stress-resistant cancer cell populations. (1) Within the primary tumor, these cells secrete factors that induce angiogenesis, EMT and the cancer-stem cell (CSC) phenotype. (2) These changes promote cell detachment, motility and invasion. (3) Intravasation into the vasculature – or direct exfoliation into the peritoneal space, as is the case for ocarian cancers – provides a means for CTCs to disseminate throughout the body. (4) While in circulation, tumor cells face a variety of challenges such as anoikis and immune cell attack and must develop defenses against such stressors. (5) Homing signals and the establishment of premetastatic niches recruit CTCs to certain sites that are more suitable for colonization; extravasation at these predetermined locations does not necessarily translate to macrometastatic disease. (6) Angiogenesis and development of tumor-stroma interactions at secondary sites are the major determinants for micro- to macro-metastasis transformation. Factors that contribute to each of these steps and are modulated by HIF1 are italicized. Reprinted with permission from [9].

microRNA

microRNA (miRNA) are short, ~22 nucleotide RNA that, by interacting with the 3' untranslated regions (UTRs) of target mRNA, suppress protein synthesis. The functional role of these non-coding RNAs was first appreciated in 1993 with the identification of *lin-4* (Figure 16), a *Caenorhabditis elegans* gene whose expression as RNA, not protein, was found to regulate another gene, *lin-14* [275]. Less than twenty years since this remarkable discovery, over 10,000 different miRNA have been identified across a range of species, 940 in humans alone [277]. miRNA have confirmed roles in a host of physiological processes as well as pathophysiology and disease, with over 30 percent of the human genome targeted by miRNAs [278]. The rapid expansion of interest in this burgeoning field reflects miRNAs' broad involvement in all areas of biomedical research from miRNA regulation of plant biology to parasitic infections, from embryogenesis to Alzheimer's Disease, from lung ailments to regulation of circadian rhythms. As of this writing, a simple PubMed search of "microRNA" returns nearly 400 reviews focusing on miRNA – not to mention the more than 1,000 scholarly articles presenting new findings – *in the past year alone*. To be sure, miRNAs represent an area of research with great unknowns and great promise for new discovery.

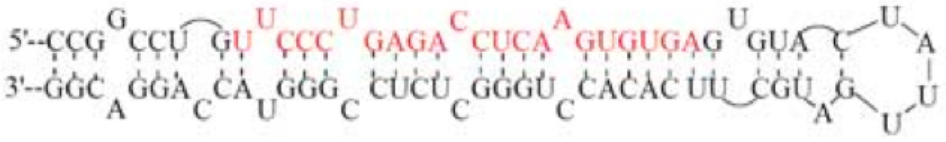

Figure 16: Precursor form of *lin-4*, the first identified microRNA [275]. This immature pri-miRNA undergoes several processing steps before it becomes the mature sequence highlighted in red. Reprinted by permission from MacMillan Publishers Ltd: [276].

microRNA synthesis

In animals, miRNA synthesis (Figure 17) begins like that of any other RNA, namely, transcription from DNA within the nucleus. The structure of the RNA transcript, however, is unique in that an approximately 60-nucleotide long hairpin is induced in the RNA by virtue of internal basepairing. Figure 16 shows a representative (*lin-4*) example of the primary precursor, termed pri-miRNA. The pri-miRNA is then cleaved by a class of RNaseIII-type endonucleases called Drosha [279]. Scission by Drosha and a regulatory subunit that contains double-stranded RNA binding domains, DGCR8, generates the pre-miRNA, an RNA duplex featuring a loop at one end and a 5' phosphate and a 3' OH group at the other, usually with a two nucleotide overhang at the 3' arm [280-283]. Exportin 5 (Exp5), a macromolecular nucleocytoplasmic trafficking protein, partners with its cofactor Ran-GTP to export the pre-miRNA from the nucleus into the cytoplasm, consuming GTP in the process [284-286]. In the cytoplasm, a second RNaseIII-type endonuclease, Dicer, associates with RNA binding unit TRBP and further cleaves the immature miRNA approximately 20 nucleotides away from the 5'/3' end to generate a ~22 nucleotide RNA duplex with two nucleotide overhangs at the 3' ends [287-294]. Completion of miRNA synthesis requires Dicer interaction with a class of proteins called Argonautes, which comprise the core of the RNA-induced silencing complex (RISC) that effects suppression of translation. Together, Dicer and Argonaute proteins select (usually) only one strand of the duplex to become biologically active. This step yields mature miRNA; however, association with RISC to form micro-ribonucleoprotein (miRNP) complexes is required for the miRNA to exert its RNA-silencing effects [276, 295].

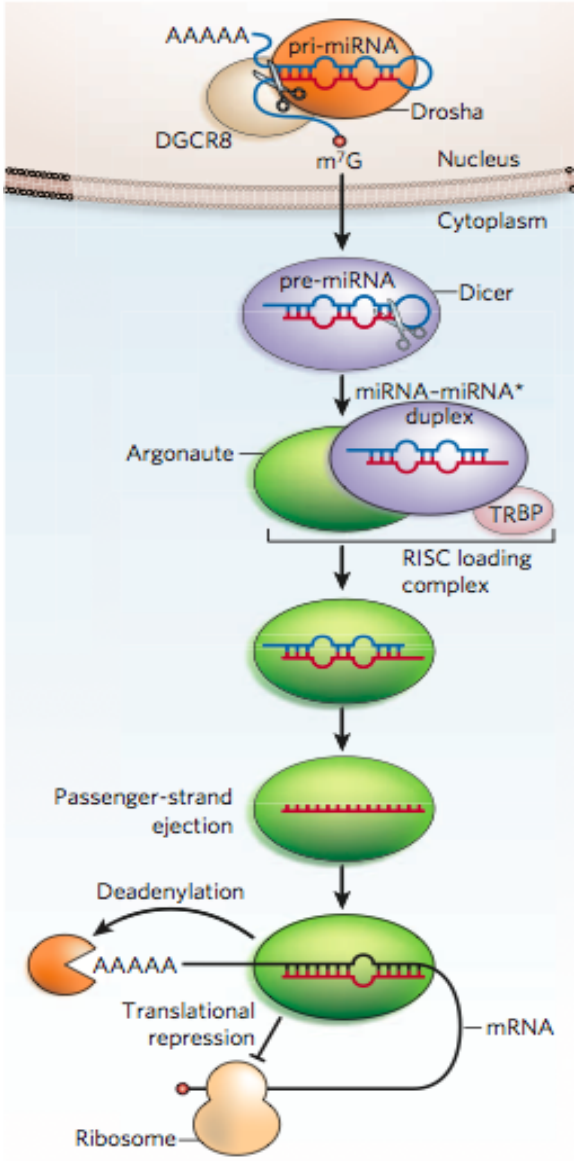

Figure 17: MicroRNA synthesis. miRNA begin as a ~60 nucleotide loop in an RNA primary transcript. Drosha and DGCR8 cleave this pri-miRNA to create the pre-miRNA. Following transfer to the cytoplasm by Exportin 5/Ran-GTP, the pre-miRNA is cleaved by Dicer, TRBP and PACT. This intermediate form is further processed by Dicer, Argonaute proteins and other elements of RISC to select the bioactive strand responsible for RNA silencing. Interaction with RISC is also required for miRNA-mediated translational repression, polyA tail removal and mRNA degradation. Reprinted by permission from MacMillan Publishers Ltd: [295].

<u>microRNA mechanisms of action</u>

miRNA-mRNA interaction

Within the RISC, the mature miRNA provides specificity for RNA silencing. In contrast to plants, in which there is nearly perfect basepairing between the miRNA and the target mRNA 3' UTR sequence, in animals there is usually some mismatch. There are, however, certain areas of interaction that require complementarity. Nucleotides 2-8 of the miRNA – the "seed" region – in particular must basepair with the 3' UTR of the target mRNA perfectly and contiguously. A second requirement is that stabilizing interactions are present at the 3' end of the miRNA as well. Finally, any mismatches or bulging must be in the middle portion or 3' end of the miRNA. The criteria for miRNA-mRNA 3' UTR interaction are highlighted in Figure 18 [296-300].

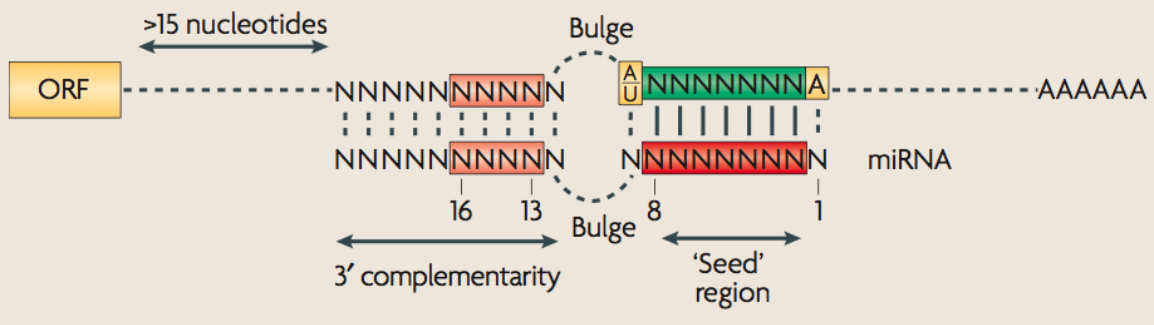

Figure 18: Criteria for miRNA-mRNA 3' UTR interaction. Association of the miRNA with the target 3' UTR requires a 15 nucleotide gap between the AUG stop codon in the open reading from (ORF) and site of miRNA binding. Studies have shown, however, that the closer the miRNA binding site is to the end of the ORF, the stronger the miRNA mRNA 3' UTR interaction Some reasonable amount of basepairing or G-U "wobble" basepairing at the 3' end of the miRNA is necessary to stabilize the interaction (shown in orange). Any bulges or mismatches must be restricted to the middle portion of the pairing. Finally, and most importantly, the "seed" region of the miRNA – nucleotides 2-8 – must demonstrate near-perfect and contiguous complementarity (shown in red and green). An A at position 1 in the miRNA or an A/U at position 9 also have favorable effects for interaction. Reprinted by permission from MacMillan Publishers Ltd: [301].

Inhibition of translation

In plants, perfect complementarity between the miRNA and the 3' UTR of the target mRNA results in endonucleolytic mRNA cleavage via an RNAi-based process [302]. In metazoans, however, the exact mechanism of RNA silencing is unknown and various processes have been observed and postulated. These include: deadenylation of the target mRNA leading to mRNA degradation; interference with ribosome or cofactor recruitment causing inhibition of translation initiation; impairment of ribosomal activity resulting in arrest or slowing of peptide elongation; and recruitment of protease to cleave of nascent peptide. By whichever mechanism miRNA exerts its RNA-silencing effects, ultimately, all of these processes (with few exceptions) result in suppression of protein expression. Figure 19 provides brief descriptions of these various modes of inhibition of protein synthesis [301].

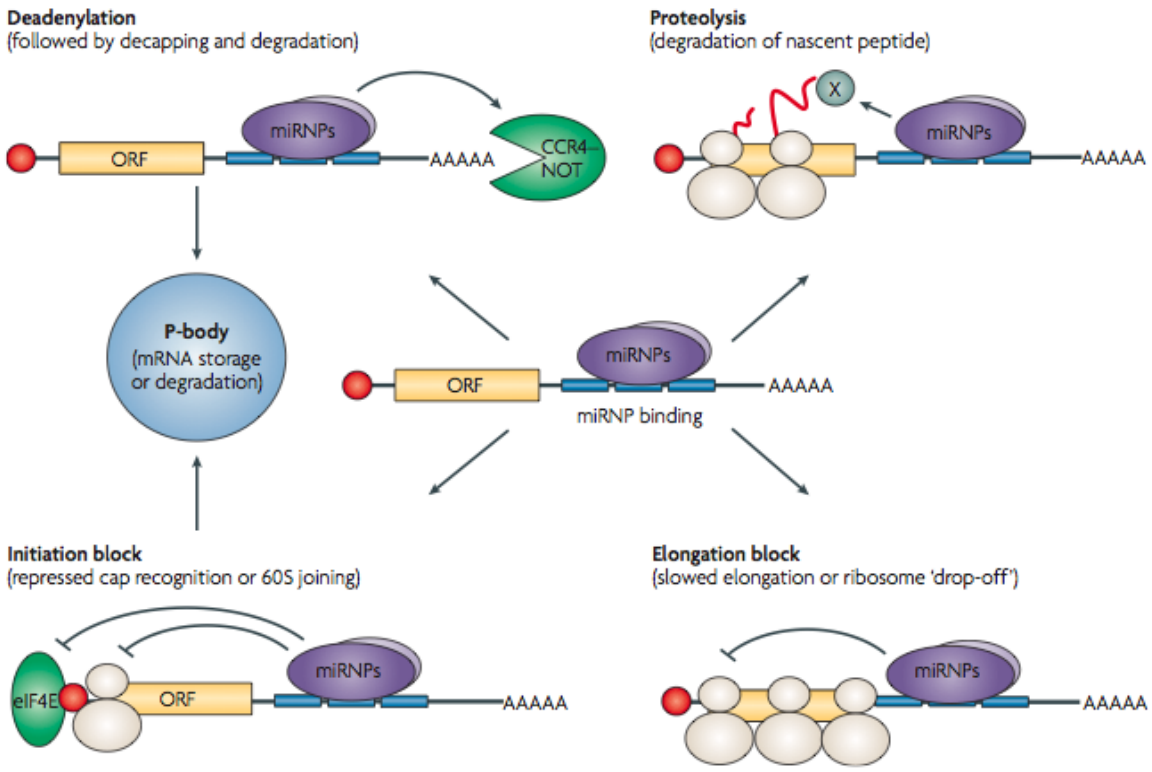

Figure 19: Mechanisms of RNA silencing by microRNA. miRNA, by associating with RISC, form micro-ribonucleuoprotein (miRNP) complexes. Upper left: miRNP can recruit CCR4-NOT deadenylation machinery to remove the polyA tail from target mRNAs, resulting in subsequent decapping, loss of mRNA stability and degradation in P-bodies [303-306]. Lower left: Alternatively, miRNP can block ribosomal subunits like the 60S ribosome or riobosome-recruiting cofactors like eIF4E from initiating translation, causing mRNA instability and P-body degradation [307-312]. Upper right: miRNP may also recruit a protease (X) that can cleave nascent peptide as it is produced, resulting in non-functional protein [313]. Bottom right: Finally, miRNP can inhibit progression of translation once is has already been initiated, either by slowing elongation or causing detachment of the ribosome [313-315]. Reprinted by permission from MacMillan Publishers Ltd: [301].

microRNA in cancer and hypoxia

As described above, miRNAs have been implicated in nearly every physiological and pathological process in the body. In cancers, miRNA expression is generally suppressed [316, 317]; in melanomas and breast and ovarian tumors, this seems to be a consequence of decreased levels of miRNA synthesis machinery such as Dicer and

Argonaute proteins, while in various cancer cell lines nuclear retention of pri-miRNAs seems to be at fault [318-321]. Aside from this global observation, most miRNAs have been studied in the context of a particular type of malignancy, as the effects of a specific miRNA in one cell line may differ drastically from its effects in another [322]. Within just one cell cancer type, however, a single miRNA, which can have multiple mRNA targets, can regulate entire biological pathways, such as the response to hypoxia, angiogenesis, and cell survival and proliferation, that shape cancer cell behavior [278]. As such, miRNAs may function as oncogenes, tumor suppressors or, in some cases, both [323], and have been found to be involved in all six of the hallmarks of cancer as defined by Hanahan and Weinberg: 1) self-sufficiency in growth signals; 2) insensitivity to growth signals; 3) evading apoptosis; 4) limitless replicative ability; 5) sustained angiogenesis; and 6) tissue invasion and metastasis (Figure 20) [219, 323]. Certainly, the role of miRNA in cancers is not to be underestimated.

In the context of hypoxia, a number of miRNAs have been found to either increase or decrease under low oxygenation conditions compared to normoxia, with the changes often depending on cell type [324, 325]. The significance of these changes in expression are as of yet generally unclear,

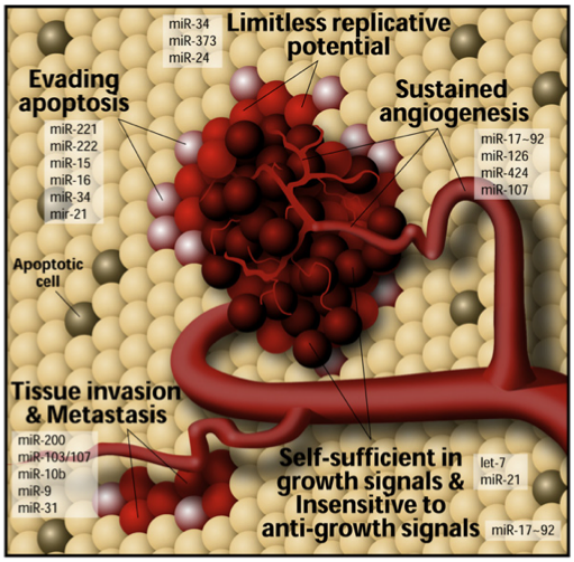

Figure 20: microRNAs implicated in the regulation of the hallmarks of cancer. Reprinted from [323] with permission.

however, and many of these miRNAs only have *in silico* targets associated with them. Still, the roles of some miRNAs, such as miR-210 and miR-424, have been elucidated and have been shown to regulate the cellular hypoxic response through modulation of HIF1α stability [326-328]. This miRNA-based "regulation of the regulator" presents an intriguing opportunity for investigations into how to minimize the broad and significant deleterious consequences of HIF1α. Indeed, just as many miRNAs have been implicated in the six hallmarks of cancer described above, so has HIF1α, and thus targeting HIF1α using miRNAs represents a novel approach to mitigating the myriads effect of HIF1α in tumor progression.

Aims of this research

EOC is a debilitating and deadly disease, causing the deaths of 15,000 women every year in the U.S. alone. The high rates of morbidity and mortality associated with EOC – the 5-year survival rate is less than 50 percent – are directly attributable to its proclivity to metastasize from the ovaries to distal sites. EOC metastasis requires robust vascular support at the primary tumor site and is thus greatly dependent on angiogenesis. Activation of angiogenesis is, in turn, contingent upon the development of and response to hypoxia in the tumor microenvironment. As such, HIF1, the master regulator of the hypoxic response in mammalian cells, is a crucial mediator of angiogenesis and metastasis. Among its many effects, selection of subpopulations of cells with a malignant and stem cell-like phenotype, stimulation of new vessel growth, priming of cell detachment, motility and invasion, and guidance of CTCs to premetastatic niches comprise the most dire consequences of HIF1 activation in the context of EOC progression. Targeting HIF1 to stem these developments is therefore the overall goal of this research.

Canonically, HIF1α is regulated at the level of protein, undergoing several post-translational modifications that reduce its stability and activity in normoxia while having the opposite effects under low oxygen conditions. This work describes two novel mechanisms of HIF1α regulation in EOCCs. The first involves dynamin 2, a mediator of endocytosis and cell motility. The data presented herein demonstrate that by virtue of its regulatory effects on iron uptake, dynamin 2 controls HIF1α protein stability. Inhibition

of dynamin 2 under normoxic conditions leads to a rapid decrease in intracellular iron stores and HIF1α polyubiquitination with a subsequent increase in stabilized HIF1α. Treatment with a form of iron that is not dependent on dynamins for endocytosis reverses this effect. In hypoxia, overexpression of dynamin 2 leads to a decrease in HIF1α protein levels.

The second novel mechanism of HIF1α regulation involves the miRNA miR-199a-1, which is contained in an intron within the dynamin 2 transcript. This work provides evidence that miR-199a-1 directly targets the HIF1α 3' UTR, causing suppression of HIF1α protein levels and expression of genes driven by HIF1α. Moreover, EOCCs overexpressing miR-199a-1 exhibit a distinct phenotype marked by defects in migratory ability. Finally, overexpression of miR-199a-1 in an IP metastatic mouse model of EOC reduced intratumoral vessel density and overall tumor burden.

Taken together, these results demonstrate the potency of targeting non-canonical pathways of regulation to affect HIF1α protein stability. Consequently, this research lays groundwork for novel anti-HIF1 strategies – and, by extension, anti-angiogenic and anti-metastatic strategies – in the treatment of EOC and other solid tumors.

CHAPTER II:

DYNAMIN 2 AND MIR-199A REGULATE HIF1α IN EPITHELIAL OVARIAN CANCER CELLS

Introduction

Epithelial ovarian cancer (EOC) is the leading cause of death among the gynecological malignancies and the fifth leading cause of cancer death among women [329]. EOC, like most solid tumors, begins as a small avascular neoplasm that cannot grow beyond ~1 mm^3 in volume because of blood supply constraints. Hypoxic areas are common in the tumor microenvironment as the increased metabolic demands of rapidly proliferating cells outpace the ability of oxygen to diffuse from capillaries into a growing tumor mass [192].

Low oxygen environments spur tumor cells to stabilize hypoxia-inducible factor 1 alpha (HIF1α), the master regulator of the cellular hypoxic response. Under hypoxia, HIF1α is able to associate with its partner HIF1β to form HIF1, a transcription factor that binds to the hypoxia response elements (HREs) of effector genes to restore normal oxygen supply to starved cells. Of particular relevance to EOC, HIF1 activates genes such as GLUTs and nearly all enzymes of the glycolytic pathway to shift cellular activity to essential processes such as metabolism at the expense of energy-consuming functions such as endocytosis [130, 131]. In addition, HIF1 increases expression of pro-angiogenic proteins such as vascular endothelial growth factor (VEGF), transforming growth factor-beta (TGF-β) and platelet-derived growth factor (PDGF) to help restore blood flow to the hypoxic tumor microenvironment [134-136] Finally, HIF1 stimulates synthesis of pro-migratory proteins like matrix metalloprotinases (MMPs), hepatocyte growth factor receptor (HGFR/MET) and lysyl oxidase (LOX) so that cells can detach, migrate and

metastasize to more fertile, resource-rich areas [11, 129, 137-139, 152, 330]. In EOC, this is of particular importance as cells that have adapted to hypoxia can disseminate from a well-vascularized primary ovarian tumor, spread through the pelvis and exfoliate directly into the peritoneal cavity to seed the gastrointestinal tract, omentum and liver. Indeed, approximately 70 percent of patients present with advanced disease including metastases at the time of initial diagnosis [331]. Thus HIF1, by inducing tumor cells to reorganize intracellular processes to become more energetically efficient, by activating angiogenesis to restore oxygen delivery and by promoting cell detachment, migration and metastasis, significantly enhances the morbidity and mortality associated with EOC.

Regulation of HIF1 is therefore a key step in the hypoxic response with profound implications for EOC growth and metastasis. Under normoxia, HIF1α is hydroxylated on two proline residues within its oxygen-dependent degradation domain (ODDD) by prolyl hydroxylases (PHD). This reaction is an oxygen-, iron-, 2-oxoglutarate and ascorbate-dependent process. Hydroxylated HIF1α is, in turn, recognized and bound by von Hippel-Lindau protein (VHL), elongin B/C, Rbx-1 and cullin-2 (Cul2), the scaffolding protein that recruits ubiquitin ligases for protein degradation by the 26S proteosome. In hypoxia, however, lower oxygen levels impair PHD hydroxylase activity and HIF1α is stabilized and transactivates HRE-containing target genes by dimerizing with the constitutively-expressed HIF1β [332].

In this study, I show that in addition to being regulated at the protein level, HIF1α is regulated by two novel mechanisms in EOCCs. First, dynamin 2 (dnm2), a GTPase involved in many endocytic processes such as tranferrin/iron uptake, regulates HIF1α by modulating intracellular levels of iron, a factor that is necessary for the rate-limiting,

PHD-hydroxylation step in HIF1α degradation under normoxia. Dnm2 levels are reduced in hypoxic EOCCs and inhibition of dnm2 in normoxia using the small molecule dynasore results in rapid decrease in intracellular iron stores and polyubiquitination of HIF1α and a corresponding increase in HIF1α protein levels. Addition of a form of iron that is not dependent on dnm2 for entry into cells reverses these effects. Conversely, overexpression of dnm2 in hypoxia results in suppression of HIF1α protein.

Second, HIF1α is regulated at the level of translation as well, by microRNA-199a-5p. MiR-199a-5p is downregulated in hypoxia and specifically targets the 3' untranslated region of HIF-1α and downregulates HIF-1α protein levels and expression of genes driven by HIF-1α. Moreover, EOC overexpressing miR-199a show a distinct phenotype with defects in cell migration. *In vivo* angiogenesis and tumor growth of EOC overexpressing miR-199a was significantly inhibited compared to control cells. Together, these studies identify what I believe are new pathways regulating HIF-1α, angiogenesis and cell metastasis in EOC.

Material and Methods

Cell Culture

A2780, MA148 and 1A9 cells were cultured in RMPI (Invitrogen) supplemented with 10% fetal bovine serum (FBS) and 100 units/ml penicillin and 100 ug/ml streptomycin (Invitrogen) and grown at 37 degrees and 5% CO_2. Hypoxia was achieved by flushing modular incubator chambers (Billups-Rothenberg) with 95% N_2, 5% CO_2 for 15 minutes to effect O_2 levels of approximately 3% in the media.

Reagents

The hypoxia mimetic desferrioxamine (DFX) was from CalBioChem and LOX inhibitor β-Aminoporprionitrile (β-APN) was from Sigma. miR-199a and scramble duplexes were synthesized by Integrated DNA Technologies. DNA vector and microRNA duplex transfections were carried out using Superfect or Hiperfect reagents, respectively (Qiagen). Control morpholino and miR-199a morpholino (sequence: CCTAACCAATGTGCAGACTACTGTA) and the transfection reagent Endoporter were purchased from Gene Tools. All transfections were performed according the manufacturers' instructions. The mutant P402A/P564A HIF1α (P to A HIF1α) was acquired from Addgene (plasmid 18955; contributed by William Kaelin [333]). The luciferase-ODD gene was also from Addgene (plasmid 18965; contributed by William

Kaelin [334]. Scrambled, HIF1α and dynamin 2 siRNA were from the RNAi Core Facility at the University of Minnesota. Dynasore and ferric ammonium citrate (FAC) were from Sigma-Aldrich. GST-dynamin 2 was a generous gift of Vijay Shah at the Mayo Clinic.

Dynamin inhibition experiments

A2780 cells were washed with HBSS, serum free media containing 1% DMSO or 80 uM dynasore was added, and cells were incubated at 37 degrees, 5% CO_2 for the indicated times before collection of cell lysate. For ferric ammonium citrate (FAC) pretreatment experiments, A2780 cells were incubated with FAC (20 uM) for 30 minutes in serum-free media, which was then replaced with DMSO- or dynasore-containing media for the given times. For FAC post-treatment experiments, DMSO or dynasore was added to the cells in serum-free media and after 30 minutes FAC (20 uM)/DMSO or FAC/dynasore was added. Cells were then incubated an additional 30 minutes or 2 hours 30 minutes before lysate collection. In calcein AM experiments, A2780 cells seeded in 96-well plates were loaded with 250 nM calcein AM as previously described [335] and fluorescence was measured on a BMG FLUOstar plate reader. Cells were then treated with 1% DMSO or 80 uM dynasore and fluorescence was measured again at 1, 2 and 3 hours. FAC was added to the appropriate wells 30 minutes after addition of DMSO/dynasore.

Custom MicroRNA microarray

Custom miRNA microarray experiments and analyses were performed as previously described [336]. Briefly, A2780 cells were grown in normoxia or hypoxia for 24 hours then submitted to our collaborator, Dr. Yan Zeng, for miRNA microarray. Three independently treated A2780 samples were analyzed. Microarray data have been deposited to the GEO database. Pearson correlation coefficients for array analysis of the same RNA samples were between 0.90 and 0.99, indicating good reproducibility.

Quantitative PCR

Total RNA was collected using Trizol Reagent (Invitrogen) with chloroform extraction, isopropanol and ethanol washes and resuspension in TE Buffer (Invitrogen). Quantitative PCR was performed according to manufacturer's instructions using the miScript Reverse Transcription Kit and the miScript SYBR Green PCR Kit (Qiagen) on a 7900HT Fast Real-Time PCR System (Applied Biosystems). All qPCR experiments were conducted in triplicate with samples from three separate experiments. Results were interpreted by the delta-delta Ct method with normalization to beta actin mRNA levels.

qPCR Primers

All primers were purchased from Integrated DNA Technologies through the BioMedical Genomics Center at the University of Minnesota, Minneapolis, MN.

miR-199a-5p: CCCAGTGTTCAGACTACCTGTTC

miR-199a-3p: ACAGTAGTCTGCACATTGGTTA

miR-199b-5p: CCCAGTGTTTAGACTATCTGTTC

Dynamin 2: forward: TCCATCGGCCAGAGCTGCCA;

reverse: TGTTGGTCCCCGTGACCCTGT

HIF1α: forward: GCTTTGCAGAATGCTCAGAGAAAGCG;

reverse: CATCCATTGATTGCCCCAGCAGTCT

VEGF: forward: TGGGTGCATTGGAGCCTTGCC;

reverse: CGCATCGCATCAGGGGCACA

LOX: forward: CCTTCCTTCACTCCAGACACTGCCC;

reverse: CTCGAGGAGGACGTGGCTCACA

EPO: forward: CATCTGCGACAGTCGAGTTCTG;

reverse: CACAACCCATCGTGACATTTTC

β-actin: forward: ACGTTGCTATCCAGGCTGTGCTAT;

reverse: CTCGGTGAGGATCTTCATGAGGTAGT

Immunoblotting

Cells were washed with PBS then lysed in RIPA buffer (150 mM NaCl, 10 mM Tris, pH 7.5, 1% NP-40, 1% deoxycholate, 0.1% SDS) supplemented with 1 mM PMSF (Fisher Scientific), 1 mM sodium orthovanadate (Sigma) and protease inhibitor cocktail (Roche). Proteins from total cell lysates were resolved by SDS-PAGE on a 10% gel, transferred to PVDF membranes (Millipore), blocked with 5% non-fat milk in PBS/Tween-20, and blotted with antibody to HIF1α or β-actin antibody and HRP secondary antibody (Santa Cruz).

Cell culture immunohistochemistry/immunofluorescence

Cells were fixed in Phemo Buffer [PIPES (0.068 M), HEPES (0.025 M), EGTA (0.015 M), MgCl2 (0.003M), DMSO (10%), pH 6.8)] supplemented with 3.7% formaldehyde, 0.05% glutaraldehyde and 0.5% Triton X-100) for 10 minutes at room temperature. After 3 washes, cells were blocked overnight with 5% BSA in TBS plus 1% Tween 20 (TBS-T). Antibody to HIF1α (BD Transduction Laboratories) was diluted in 5% BSA/TBS-T and the cells were incubated overnight. Secondary antibody, goat anti-mouse Alexafluor 647 (Invitrogen), was diluted in 5% BSA/TBS-T and applied for 2 hours. The cells were then stained with DAPI to denote nuclei (Invitrogen) overnight and mounted. Fluorescence images were captured using an Olympus FluoView 1000 BX2 Upright Confocal system. Images were acquired under the same conditions for each

experiment, and no digital manipulation of images was performed other than cropping and merging.

Reporter constructs

Dynamin 2 promoter-luciferase (dnm2 prom-luc) was created by amplifying the distal 1000 basepairs of the 5' UTR of the dynamin 2 gene from human genomic DNA to create an XhoI restriction site (primer: AAACTCGAGACTTGAGGCCAGGCGTT) and a BglII restriction site (primer: ACCAGATCTATCCGGTTCTCAGGCGACA). This amplified fragment and the PGL4.10 Luc 2 vector (Promega) were digested with XhoI and BglII (New England Biolabs) and were ligated overnight at 4 degrees Celsius with T4 DNA ligase (New England Biolabs). Dnm2 prom-luc HRE mutants were made using the QuikChange II XL Site-Directed Mutagenesis Kit (Stratagene) with the following primer sets (location of HRE mutation is highlighted).

HRE 1 MUT:

Forward: CTAAAAATACAAAATTAGCTGGGATGTGTGGCTCACACTTGTAATCCCAGC

Reverse: GCTGGGATTACAAGTGTGAGCCACACATCCCAGCTAATTTTGTATTTTTAG

HRE 2 MUT:

Forward: GCGGCGTCAAGATCGGGATGTAGCAGAAAGGGCACAGC

Reverse: GCTGTGCCCTTTCTGCTACATCCCGATCTTGACGCCGC

HRE 3 MUT:

Forward: GAAAGGGCACAGCATTTGCAAAGGATGTGAGGAGTGATTTTATTGCGTTC

Reverse: GAACGCAATAAAATCACTCCTCACATCCTTTGCAAATGCTGTGCCCTTTC

HRE 4 MUT:

Forward: CGCCAATGGGCAGAGCCAAATGTCCTTTTTCGGAAACACCCCC

Reverse: GGGGGTGTTTCCGAAAAAGGACATTTGGCTCTGCCCATTGGCG

HRE 5 MUT:

Forward: GGTGCAGCAGGCCAGTCGATGTCGGCGCGAGTGCTTTGG

Reverse: CCAAAGCACTCGCGCCGACATCGACTGGCCTGCTGCACC

Dnm2 prom-luc deletion constructs were made from the control dnm2 prom-luc construct by PCR amplification, XhoI/BglII digestion and religation into the luciferase vector with the following primer sets:

HRE 1 DEL:

Forward: AAACTCGAGACTTGAGGCCAGGCGTT

Reverse: TCTGCCGCTATTGGCTGT

HRE 2 DEL:

Forward: AAACTCGAGACTTGAGGCCAGGCGTT

Reverse: TTGCAGAGCGCATTGGGA

HRE 2 DEL:

Forward: AAACTCGAGACTTGAGGCCAGGCGTT

Reverse: AGCAGAAAGGGCACAGCA

HRE 2 DEL:

Forward: AAACTCGAGACTTGAGGCCAGGCGTT

Reverse: TGGAGTGTTAGCGGCGT

VEGF-promoter luciferase was a generous gift from the laboratory of Sabita Roy.

The luciferase-HIF1α 3' UTR construct was created by amplifying the 3' UTR of HIF1α to create an NheI restriction site (primer: ACAGCTAGCGCTTTTTCTTAATTTCATTCCTTT) and an XhoI site (primer: ACACTCGAGCCTGGTCCACAGAAGATGTTT). The PCR product was digested with NheI and XhoI (New England Biolabs) and ligated as above into NheI and XhoI-digested pCMV vector (Promega) containing a luciferase reporter segment (a generous gift of Yan Zeng). Luciferase-HIF1α mutant 3' UTR was constructed using the QuikChange II XL Site-Directed Mutagenesis Kit (Stratagene) to eliminate the ACTGG seed site of miR-199a-HIF1α 3'UTR interaction. The primers used were: forward: TTTCATTCCTTTTTTTGGACTGGCTCATTACCTAAAGCAG; reverse: CTGCTTTAGGTAATGAGCCAGTCCAAAAAAAGGAATGAAA).

Luciferase assays

Cells were grown to 70% confluence and transfected with the vectors described above along with pRL-SV40 Renilla luciferase construct (Promega) at a 10:1 ratio. Cell

extracts were prepared 24 hrs after transfection and luciferase activity was measured using the Dual-Luciferase Reporter Assay System (Promega) in a TD 20/20 Luminometer (Turner BioSystems).

Cell proliferation assays – bromodeoxyuridine incorporation

Cells were plated in 96 well plates at 20,000 cells per well (n = 48). The next day, bromodeoxyuridine (BrdU, 10 uM) (Roche) was added and plates were incubated in normoxia or hypoxia for 24 or 48 hours. The rest of the experiment (addition of anti-BrdU antibody and substrate, etc.) was performed per manufacturer's instructions.

Clonogenic assays – limiting dilution analysis

Cells were serially diluted to 512, 256, 128, 64, 32, 16, 8, 4, 2, and 1 cell per well in 48 wells for each cell type and grown long-term at 37 degrees with 5 percent CO_2. After 4 weeks, wells that had changed from the color of normal media, pink, to the color of consumed media, yellow, were counted as having clonogenic potential. Wells were examined to confirm clonogenic growth and ensure that contamination was not the source of the media color change. An average was calculated from three separate experiments. Pictures of the plates were taken with a Nikon camera.

Scratch/wound assays

Cells were seeded in 24-well plates, transfected with vehicle control or HIF1α with P to A mutations at positions 402 and 564 (P to A HIF1α), grown to 90% confluence then serum starved (2% FBS) overnight. Wounds were created with a 1 mL pipette tip and cells were allowed to migrate for 24 hours in normoxia or hypoxia. Cells were stained with DAPI and images were taken with an Arcturus PixCell II LCM system. Data was quantified from the average of 6 wells per test group.

Roche Xcelligence assays

Xcelligence experiments were performed according to published protocols from Roche. Briefly, for proliferation experiments, each well was seeded with 25,000 cells and hypoxia simulated with 500 uM DFX. Treatment with non-degradable HIF1α was achieved by transfecting cells 24 hours before seeding with vehicle- or P to A HIF1α. Measurements were taken every 10 minutes for 80 hours. In the carboplatin experiments, cells were seeded and grown overnight and drug was added the next morning at the concentrations described. Data were normalized to the time of carboplatin addition. For the migration experiments, the bottom chamber of the CIM plate (Roche) was filled with serum-containing media and the top chamber was filled with vehicle- or P to A HIF1α-transfected cells (75,000 per well) in serum-free media. For LOX inhibition assays, 300 uM β-APN was added to the top chamber. Hypoxia was simulated as above. Measurements were taken every minute for 24 hours. For attachment assays, well

surfaces were coated with laminin, fibronectin or type 1 collagen (50 ug/mL) for 24 hours prior to seeding with A2780-GFP or A2780-199 cells. Experiments proceeded as described for proliferation assays with measurements taken every 4 minutes. All experiments were run in quadruplicate.

Lentiviral vectors and cell transduction

Vectors (pCDH-CMV-MCS-EF1-copGFP) encoding either green fluorescent protein (GFP) or mir-199a and GFP were packaged into VSV-G pseudotyped viral particles with the pPACKH1 Packaging Plasmid Mix in HEK-293TN cells (System Biosciences). Lipofectamine and PLUS Reagent (Invitrogen) were also used in the packaging process, for which we followed System Biosciences' published protocols. Supernatant containing the virus was collected and A2780 cells were treated with 10 ug/ml polybrene (Chemicon) and the supernatant from either the viral GFP-treated HEK cells or the viral 199/GFP-treated cells. After 48 hours the cells were harvested and subjected to fluorescence-activated cell sorting (FACS) to collect only those cells strongly expressing GFP.

In vivo tumor models

All animal experiment protocols were approved by the IACUCs at the University of Minnesota, Minneapolis, Minnesota, USA. For tumor seeding visualization experiments, 3 million A2780-GFP or A2780-199 cells were injected intraperitoneally

(IP) into 4 week-old, female athymic mice. At seven days, one mouse from each group was sacrificed to determine the extent of tumor development. At 12 days, the rest of the mice were sacrificed and ovaries and GI were removed for imaging. Imaging was conducted using the CRi Maestro *in vivo* imaging system. For the tumor growth experiments, A2780-GFP or A2780-199 cells were injected into 20 mice per group as described above. After one week, carboplatin (CalBioChem) was delivered I.P. to half the animals (10 A2780-GFP mice and 10 A2780-199 mice) at a dose of 20 mg/kg every 4 days for 4 weeks. Animals were then sacrificed, imaged and tumors were completely removed for weighing and snap frozen for RNA work and formalin-fixed for immunohistochemistry.

Tissue immunofluorescence/immunohistochemistry

Tumors were fixed in formalin and serially sectioned and paraffin embedded by Josh Parker and colleagues in the Veterinary Population Medicine department, who also performed the hematoxylin and eosin staining procedures. Processed (deparaffinzed/antigen-retrieved) slides were blocked in 5% BSA/TBS-T overnight. Blocked sections were then incubated for 6 hours with lectin antibody conjugated to biotin (Vector Laboratories), washed and incubated with secondary antibody streptavidin-Texas Red (Vector Laboratories). DAPI (Invitrogen) was applied overnight and the slides were mounted for confocal analysis. Images were acquired as described above. Vessel density and length was measured as previously described [337]. Briefly, two sections each of five mice from each of the four experimental groups, for a total of 10 fields per

group, were imaged at 40X magnification on Olympus FluoView 1000 BX2 Upright Confocal system. Pictures were skeletonized using Adobe software and vessel ends, nodes and length were quantified. Quantification of tumor necrosis was performed in a similar manner, with 25 40X fields analyzed per group and images taken on Zeiss Axiovert 2 microscope workstation. Images were analyzed using Adobe software to outline pink (necrotic) areas and calculate a percent necrotic area based on purple (healthy) tissue.

Statistics

Statistical significance was determined using either 1-way ANOVA or the unpaired Student's t test (1-tailed), depending on the number of experimental groups analyzed.

Results

Dynamin 2 is downregulated in hypoxic EOCCs in a promoter-dependent manner

Many normal cellular functions are perturbed in hypoxic cells. Among these is endocytosis, an energy-taxing process that is downregulated in hypoxia as resources are shunted to more essential cellular reactions like glycolysis. Because dynamins are crucial to most types of endocytic processes and have a secondary role in promoting tumor cell motility, we investigated whether dnm2, the ubiquitously-expressed member of the dynamin family, is affected by low oxygen levels in EOCCs. To this end, we conducted quantitative PCR (qPCR) to measure levels of dnm2 mRNA and western blot to measure protein levels. As shown in Figures 21a and b, dnm2 transcript levels were reduced in two EOCC lines, MA148 and the well-characterized A2780, respectively. Moreover, protein levels of dnm2 were also suppressed under hypoxia in A2780 cells (Figure 21c). To further demonstrate that dnm2 was downregulated under hypoxic conditions, we used a luciferase reporter system and ligated the 1,000 basepairs of the dnm2 promoter proximal to the ATG start codon to the luciferase gene to create the dnm2 prom-luc construct. Placing luciferase expression under control of the dnm2 promoter allowed us to determine whether the changes in mRNA and protein expression observed under hypoxia were promoter-dependent. Figure 21d shows that this was indeed the case, as luciferase expression decreased significantly when A2780 cells transfected with the dnm2 prom-luc construct were exposed to hypoxia. Together, these data show that

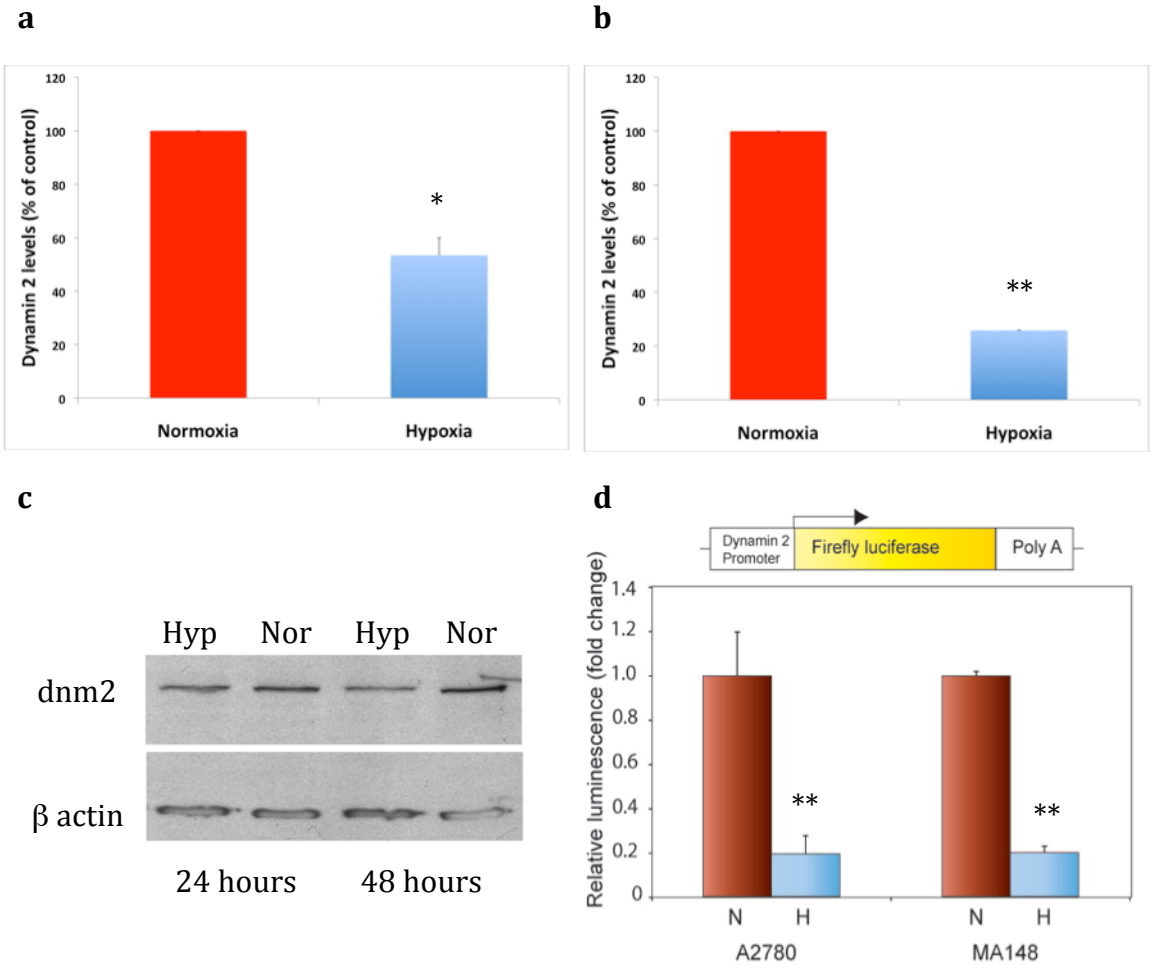

Figure 21: Dynamin 2 is downregulated in hypoxic EOCCs in a promoter-dependent manner. MA148 **(a)** and A2780 **(b)** cells were incubated in normoxia or hypoxia for 24 hours and qPCR was conducted to determine levels of dnm2 mRNA. **(c)** Western blot for dnm2 of A2780 cells incubated in normoxia or hypoxia for 24 or 48 hours. **(d)** A2780 or MA148 cells were transfected with dnm2 prom-luc, exposed to normoxia or hypoxia for 24 hours and relative luminescence was measured. A schematic of the construct used in this experiment is shown above. Red bars indicate normoxia, blue bars indicate hypoxia. Values represent mean +/- SD. *P<0.01. **P<0.001.

dynamin 2, an important mediator of endocytosis and cell motility, is downregulated in EOCCs under hypoxia.

We next wanted to interrogate the dnm2 promoter to understand why dnm2 transcription is suppressed under hypoxia. Analysis of the region of the promoter ligated to luciferase in the dnm2 prom-luc construct showed that it contains five HREs capable

of HIF1 binding (Figure 22a). Although HIF1 usually acts as a transcriptional activator, there are examples of transcriptional repression induced by binding of HIF1 to HREs [338, 339]. To determine if HIF1 might be exerting a suppressive effect on the dnm2 promoter by interacting with one or more of the five HREs, we modified each of the HREs from "CGTG" to "ATGT" to create five distinct dnm2 prom-luc mutation constructs (HRE 1-5 MUT). We then repeated the luciferase assay in A2780 cells using these constructs to determine if downregulation of luciferase signal in hypoxia would be abated. Interestingly, the findings from this study demonstrate that all five HREs within the promoter region affect dnm2 promoter activity, even under normoxic conditions (Figure 22b). Significantly, HRE 2 had a suppressive effect on dnm2 expression, as mutation of this region increased dnm2 prom-luc expression under both normoxia and hypoxia. The fact that the HRE 2 MUT construct exhibited nearly as high luciferase expression in hypoxia as the control construct in normoxia implicates this particular HRE as an important regulatory element that is involved in dnm2 inhibition in low oxygen states. On the other hand, mutation of the other HREs suppressed dnm2 prom-luc expression, implying that these regions actually are inhibitory in the context of dnm2 expression. While these changes are subtle, they are statistically significant, as denoted in the legend. As such, it is apparent that dnm2 expression, and hypoxia-driven dnm2 downregulation specifically, is HRE-dependent and involves HRE 2.

This conclusion warranted further study and the role of HIF1 in regulating HRE-mediated changes in dnm2 expression under hypoxia was of special interest to us. For this reason, we investigated whether overexpression of HIF1α in normoxia results in suppression of dnm2 prom-luc or if suppression of HIF1α in hypoxia causes an increase

a

CTCACACCTGTAATTCCAACACTTTGGGAGGCCAAGACGGGCGGATCACTTGAGGCCAGGCGT
TCGAGACCAGCCTGGCCAATATGGTGAAACCCCGTCTACTAAAAATACAAAATTAGCTGGGC
GTGGTGGCTCACACTTGTAATCCCAGCTATTCGGGAGGCTGAGGCAGGAGAATTGGTTGAAC
CGGGGAGGCGGAGGTTGCAGTGAGCCAAGATCGCGCTACTGCACTCCAGCCTGGGTGACAGA
GTGAGTACCCCGCCTCAAAAAAAAGAAAAGAAAAAAGATTCATGATCTGCTAAAGTTGAAGA
AGTGGGGGAAAACATTGGAGTGTTAGCGGCGTCAAGATCGGGCGTGAGCAGAAAGGGCACA
GCATTTGCAAAGGCGTGGAGGAGTGATTTTATTGCGTTCTATCCCTAGGAAGCAATGACTTGG
CCTCTACCATTTGCAGAGCGCATTGGGACCCTGCTCCCAGAGCTGGTTTGCAGTCTGGGAACT
GAGATGCGCTCTGGGACTTGTAGTTTTCCCCAGTGCCAGGAAACTCAAAAATCGAGACATCGG
ATCCCACCACGAGGTGTCGCCCTTGAGCGAGTACGGTGGGATCTATCCTATACTTCAGAAGGC
TGTTGCAGACATCCAACAATCACAAGGAAGAACGGGAGTTTTTCTGATTGACAGATATGGTTC
TCAATGATAGTCAAGATTCGGATGTTAAAGCCCGCCCTCTTTTGCCTGGTTGGCTGGAGCAAC
GAAGTGATATTTATATGAACCAATGGGAAATTCTTAGGGAACGAGGTAGTAGCTCAATCCCCA
ACACCATTGGTCCACATTGTCTACTGGCACGTCTGCCTGCCAATAAGATGGTGGAACTTCGCC
AATGGGCAGAGCCAACGTGCCTTTTTCGGAAACACCCCCTTCCTCTCTTGACAACTTGCTTTCT
GCCGCTATTGGCTGTTGCACAACAGTGACGGTTCTTTTGTCCAATAAGTCAGCAAGACGGTCC
CCAGGGGGAAGGTTTACTCAACCATAGGCCCGTGCCTAGTTTTTATTGGCTAGTGTATCCGAG
TGGCGGTGCAGCAGGCCAGTCGCGTGCGGCGCGAGTGCTTTGGGCGCAGCCCCCGGGGCCGG
GGCGGGAGGTCGCTCGGGTCGGGTGTCGCCTGAGAACCGGATGAGGCGGC

b

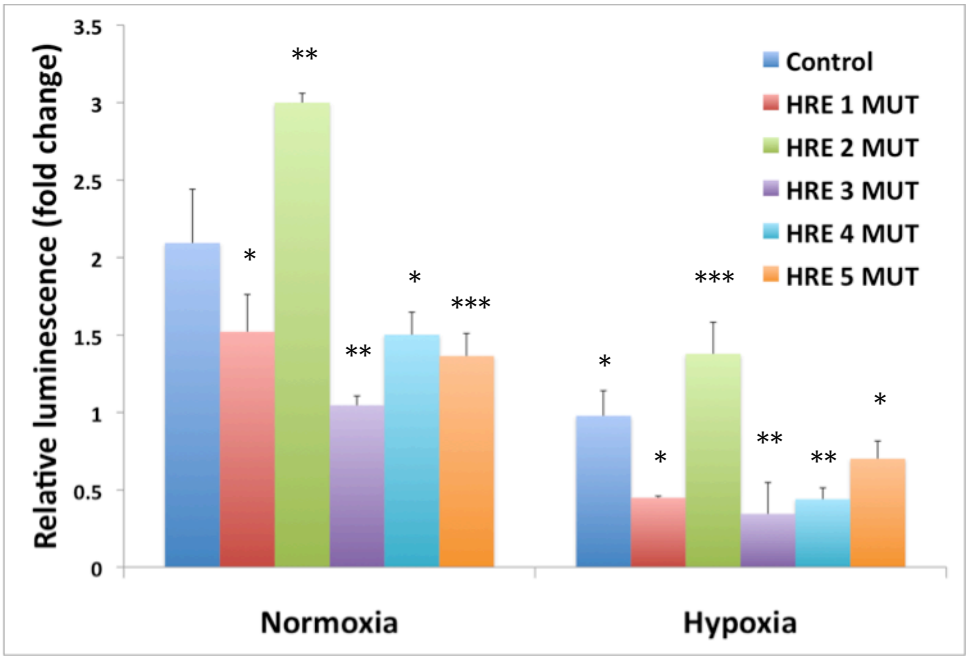

Figure 22: Downregulation of dynamin 2 in hypoxic EOCCs is regulated by hypoxia response elements within the dnm2 promoter. (a) The 1,000 basepairs of the dnm2 promoter proximal to the ATG start codon of the dnm2 gene contain five putative HRE sites (highlighted A/GCGTG sequences). **(b)** A2780 were transfected with dnm2 prom-luc or one of the five mutant forms (HRE 1-5 MUTs, bar color correlates with text color in **(a)**) in which HREs were mutated from "CGTG" to "ATGT." Relative luminescence was then calculated. Results are normalized to normoxic control. Values represent mean +/- SD. *P<0.05. **P<0.003. ***P<0.02.

in dnm2 levels. To achieve the former aim, we transfected EOCCs with a form of HIF1α that contains proline to alanine mutations at PHD-hydroxylation sites. This P to A HIF1α allows HIF1α to be stable in normoxia, allowing us to determine whether increased HIF1α levels, usually only seen under hypoxia, are responsible for suppression of dnm2. To knock down HIF1α in hypoxia, we transfected A2780 cells with an siRNA specific for HIF1α. Remarkably, overexpression of HIF1α in normoxia (Figure 23a) showed little effect on dnm2 prom-luc expression while suppression of HIF1α in hypoxia (Figure 23b) induced significant changes in dnm2 prom-luc expression, completely reversing the effects of hypoxia on dnm2 prom-luc expression, and, surprisingly, luciferase expression levels in this group actually reflect a statistically significant increase compared to normoxic, scramble siRNA-treated cells, suggesting that relief of HIF1α-induced

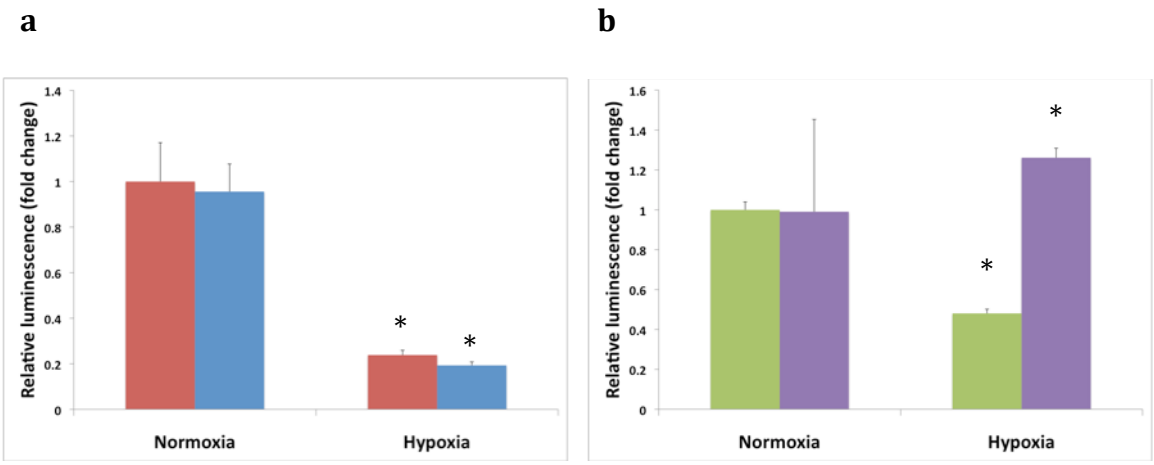

Figure 23: Downregulation of dynamin 2 in hypoxic EOCCs is regulated by HIF1α. (a) A2780 cells were transfected with non-degradable HIF1α or vehicle control, exposed to normoxia or hypoxia for 24 hours and relative luminescence measured. Red bars indicate vehicle treated cells and blue bars indicate P to A HIF1α-treated cells. **(b)** A2780 cells were transfected with scramble or HIF1α-specific siRNA, exposed to normoxia or hypoxia for 24 hours and relative luminescence measured. Green bars indicate scramble siRNA treatment and violet bars indicate HIF1α siRNA treatment. Results are normalized to normoxic control. Values represent mean +/- SD. *P<0.002.

suppression in hypoxia may remove other inhibitory elements that suppress dnm2 promoter activity in normoxia as well. Together with the results of our dnm prom-luc mutation constructs, these findings identify HIF1α as a potent negative regulator of dnm2 in hypoxia.

These HRE mutation and HIF1α overexpression/knockdown experiments did not completely explain the substantial decrease in dnm2 levels under hypoxia, especially since overexpression of HIF1α in normoxia did not result in a 5- to 10-fold drop in dnm2 levels observed in qPCR and dnm2 prom-luc luciferase assays. We therefore sought to identify regions of the promoter with particular importance for dnm2 expression. To accomplish this, we performed nested deletions of the dnm2 prom-luc construct, eliminating segments of nucleotides, each containing one HRE, from the 3' end of the dnm2 promoter. This process created four new constructs bearing 1-4 HREs each (Figure 24a). We then transfected A2780 cells with the different constructs or the control dnm prom-luc construct, exposed them to normoxia or hypoxia and measured luciferase activity. As shown in Figure 24b, deletion of the second chunk of nucleotides (construct HRE 2 DEL) resulted in a precipitous drop in luciferase expression in both oxygenation conditions. This result indicates that the eliminated area contains a sequence critical for dnm2 expression. Bioinformatic analysis of this 450-nucleotide region reveals a host of possible transcription factor binding sites, including those for HIF1α, p53 and NF-κB, all of which have been shown to be regulated by hypoxia [340, 341]. A complete list of transcription factors predicted to bind this critical region is given in Table 7. A closer look at expression of the HRE 2-4 DEL constructs (Figure 24b, inset) reveals that HRE 4 DEL-based luciferase expression actually increased, in a statistically significant manner,

a

CTCACACCTGTAATTCCAACACTTTGGGAGGCCAAGACGGGCGGATCACTTGAGGCCAGGCGT
TCGAGACCAGCCTGGCCAATATGGTGAAACCCCGTCTACTAAAAATACAAAATTAGCTGG**GC**
GTGGTGGCTCACACTTGTAATCCCAGCTATTCGGGAGGCTGAGGCAGGAGAATTGGTTGAAC
CGGGGAGGCGGAGGTTGCAGTGAGCCAAGATCGCGCTACTGCACTCCAGCCTGGGTGACAGA
GTGAGTACCCCGCCTCAAAAAAAAGAAAAGAAAAAAGATTCATGATCTGCTAAAGTTGAAGA
AGTGGGGGAAAACATTGGAGTGTTAGCGGCGTCAAGATCGG**GCGTG**AGCAGAAAGGGCACA
GCATTTGCAAAG**GCGTG**GAGGAGTGATTTTATTGCGTTCTATCCCTAGGAAGCAATGACTTGG
CCTCTACCATTTGCAGAGCGCATTGGGACCCTGCTCCCAGAGCTGGTTTGCAGTCTGGGAACT
GAGATGCGCTCTGGGACTTGTAGTTTTCCCCAGTGCCAGGAAACTCAAAAATCGAGACATCGG
ATCCCACCACGAGGTGTCGCCCTTGAGCGAGTACGGTGGGATCTATCCTATACTTCAGAAGGC
TGTTGCAGACATCCAACAATCACAAGGAAGAACGGGAGTTTTTCTGATTGACAGATATGGTTC
TCAATGATAGTCAAGATTCGGATGTTAAAGCCCGCCCTCTTTTGCCTGGTTGGCTGGAGCAAC
GAAGTGATATTTATATGAACCAATGGGAAATTCTTAGGGAACGAGGTAGTAGCTCAATCCCCA
ACACCATTGGTCCACATTGTCTACTGGCACGTCTGCCTGCCAATAAGATGGTGGAACTTCGCC
AATGGGCAGAGCCA**ACGTG**CCTTTTTCGGAAACACCCCCTTCCTCTCTTGACAACTTGCTTTCT
GCCGCTATTGGCTGTTGCACAACAGTGACGGTTCTTTTGTCCAATAAGTCAGCAAGACGGTCC
CCAGGGGGAAGGTTTACTCAACCATAGGCCCGTGCCTAGTTTTTATTGGCTAGTGTATCCGAG
TGGCGGTGCAGCAGGCCAGTC**GCGTG**CGGCGCGAGTGCTTTGGGCGCAGCCCCCGGGGCCGG
GGCGGGAGGTCGCTCGGGTCGGGTGTCGCCTGAGAACCGGATGAGGCGGC

b

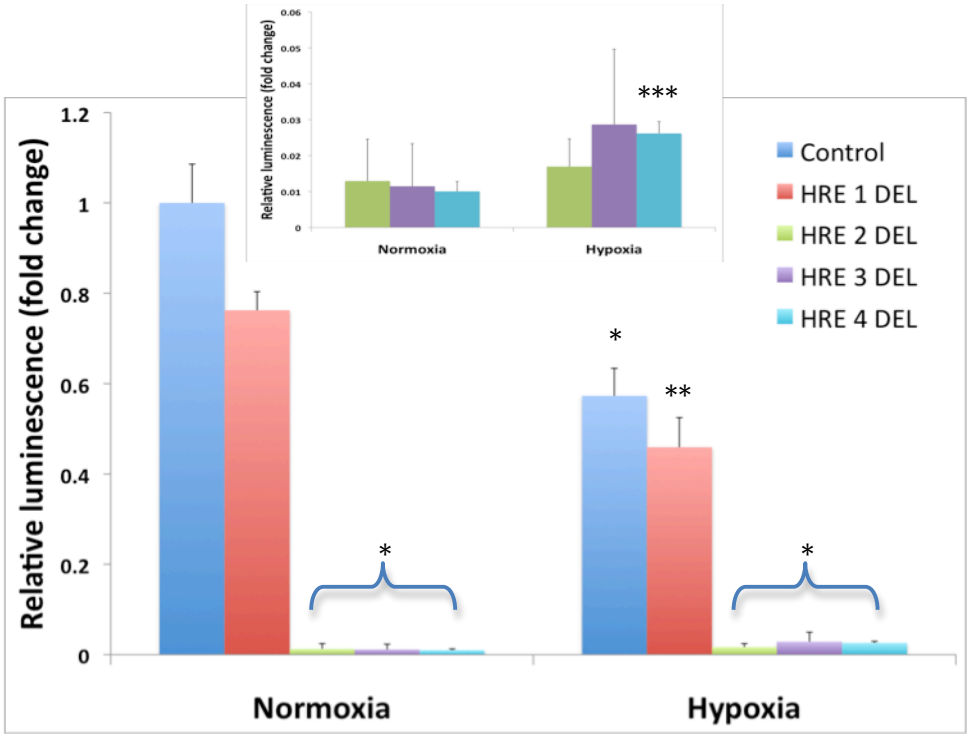

Figure 24: Deletion of a critical region within the dynamin 2 promoter abrogates expression in EOCCs. **(a)** Portions of the dnm2 promoter were deleted to create progressively smaller dnm2 prom-luc constructs. Each color represents the region deleted from the control dnm2 prom-luc construct. HREs are bolded. **(b)** A2780 were transfected with dnm2 prom-luc or one of the four deletion forms (HRE 1-4 DELs, bar color correlates with deleted region in **(a)**) and relative luminescence measured. Inset: magnification of HRE 2-4 DEL comparing normoxic and hypoxic expression. Results are normalized to normoxic control. Values represent mean +/- SD. *P<0.001. **P<0.01. ***P<0.02. P values are calculated for the appropriate normoxic or hypoxic Luc-HIF1-3' UTR control.

AP-1	Elk-1	HOXD10	p53	RXR-alpha
AP-2alphaA	ENKTF-1	HOXD9	Pax-5	Sp1
c-Ets-1	FOXP3	IRF-1	PEA3	STAT1beta
c-Ets-2	GATA-1	IRF-2	PPAR-alpha	STAT4
c-Jun	GATA-2	MEF-2A	PR A	TBP
c-Myb	GR	NF-1	PR B	TFII-I
C/EBPalpha	GR-alpha	NF-AT1	PU.1	TFIID
C/EBPbeta	GR-beta	NF-AT2	PXR-1	VDR
CTF	HIF-1	NF-kappaB	RBP-Jkappa	XBP-1
E2F	HNF-1A	NF-Y	RelA	YY1
E2F-1	HNF-3alpha	NFI/CTF		

Table 7: Transcription factors predicted to bind to the region of the dynamin 2 promoter identified as critical for expression. From the PROMO virtual laboratory and TRANSFAC database (http://alggen.lsi.upc.es).

in hypoxia compared to normoxia. Importantly, the deleted region in HRE 4 DEL contains HRE 2, which we previously identified as a crucial regulatory element required for dnm2 suppression in hypoxia. Together, these findings identify a 450-nucleotide region and HRE 2 as essential components of dnm2 regulation in normoxia and hypoxia.

Dynamin 2 regulates HIF1α stability in EOCCs via an iron-dependent mechanism

Having established that hypoxia and HIF1α regulate dnm2 expression, we wanted to determine if a reciprocal relationship exists – that is, if changes in dnm2 activity or expression induce changes in HIF1α activity or expression. We therefore used a small molecule inhibitor of dynamins, dynasore, to impair dynamin 2 activity. Inhibition of dynamin by dynasore impairs endocytosis, suppressing transferrin/iron uptake, for example, thereby reducing intracellular stores of iron, and causes a host of detachment and motility dysfunctions, highlighting the importance of dynamins in endocytic processes, cell detachment and cell motility [236, 249]. For our purposes, we treated

EOCCs with dynasore and measured HIF1α protein levels by western blot to verify the presence of any relationship between dynamin and HIF1α. To our surprise, dynasore treatment stabilized HIF1α within just 30 minutes of treatment, whereas negative control (DMSO) had no such effect (Figure 25a). Moreover, this effect was not specific for HIF1α: expression of a luciferase construct wherein reporter activity is under control of an oxygen-dependent degradation domain (ODDD) was also significantly increased by dynasore treatment compared to negative control (Figure 25b). Positive controls hypoxia, the iron chelating hypoxia mimetic, DFX, and the proteosome inhibitor, MG-132, as anticipated also all increased expression of the ODDD-luciferase construct. These findings demonstrate that inhibition of dnm2 stabilizes proteins, like HIF1α, that are regulated by hydroxylation by PHDs.

As described earlier, the PHD hydroxylation reaction requires oxygen, iron, 2-oxoglutarate and ascorbic acid. Of these four ingredients, dynamin 2 is intimately involved in regulation of one of them. Iron, which is largely dependent on transferrin for entry into a cell, is, by extension, dependent on dnm2, as transferrin uptake is a clathrin-coated endocytic process requiring dnm2's pinchase activity to release budding membrane vesicles into the cytoplasm. We therefore hypothesized that the accumulation of HIF1α under normoxic conditions upon treatment with dynasore may be the result decreased intracellular iron levels, a consequence of impairment of dnm2-dependent endocytosis. To test this, we once again treated normoxic A2780 cells with dynasore for various times. However, for this experiment we also added ferric ammonium citrate (FAC) to half the samples. FAC is an iron compound that has been shown to enter cells

a

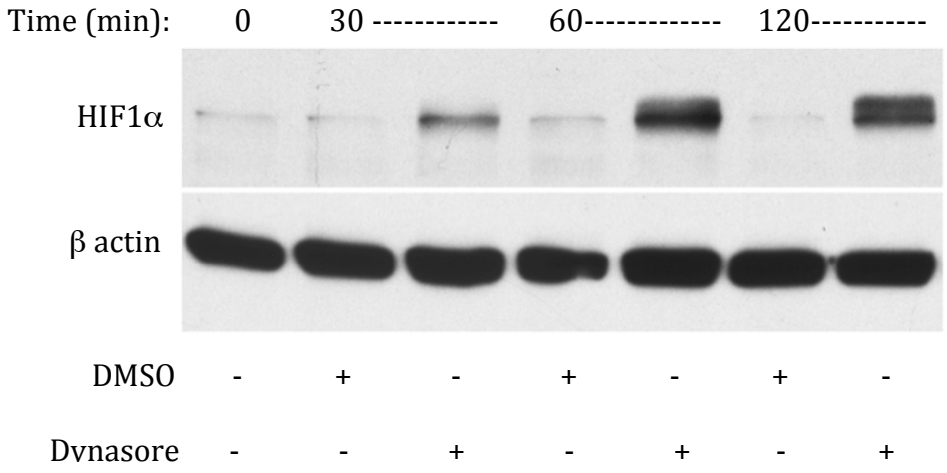

b

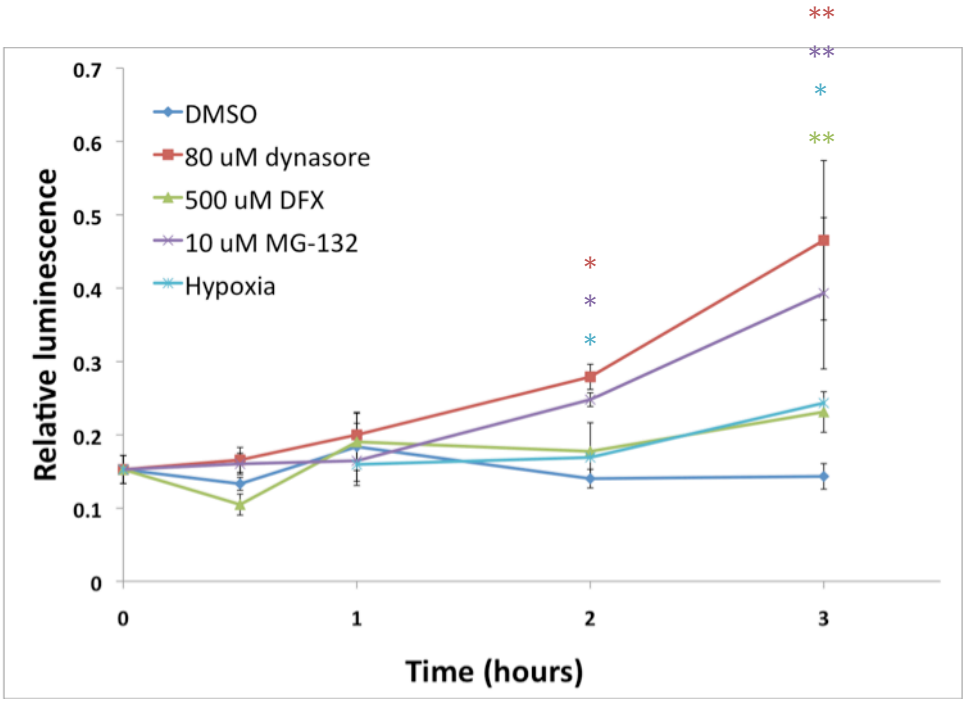

Figure 25: Impairment of dynamin 2 activity by the small molecule inhibitor dynasore stabilizes HIF1α and proteins bearing oxygen-dependent degradation domains (ODDD) in EOCCs. **(a)** A2780 cells were treated with 1% DMSO (control) or 80 uM dynasore for 30, 60 or 120 minutes and were analyzed by western blot for HIF1α. **(b)** A2780 cells were transfected with an ODDD-luciferase construct, in which luciferase expression is suppressed by PHD-based hydroxylation and subsequent degradation, and treated with 1% DMSO, dynasore, DFX, or MG-132 at the doses described or exposed to hypoxia for 1, 2 or 3 hours. Values represent mean +/- SD. *P<0.002. **P<0.05.

via transferrin- and non-transferrin-dependent mechanisms and is frequently used to "iron load" cells [342, 343]. In this way, FAC circumvents classical, dynamin-based mechanisms of endocytic iron uptake. We found that treating A2780 cells with FAC before addition of dynasore (Figure 26a) or addition of FAC after dynasore treatment had commenced (Figure 26b) both reversed dynasore-induced HIF1α accumulation substantially. These results indicate that iron is involved in the mechanisms responsible for the effects of dnm2 inhibition on HIF1α stabilization in normoxic EOCCs.

To confirm that dynasore effects a decrease in intracellular iron stores within the short time frame in which HIF1α stabilization was observed, and to verify that FAC can reverse these effects to destabilize HIF1α, we utilized the iron caging agent calcein AM. Calcein AM is a fluorescent molecule whose signal is quenched in the presence free iron. Cells incubated with calcein AM emit a fluorescent signal that decays with time. Addition of iron to the cells enhances abatement of this signal. Chelating or otherwise reducing intracellular iron stores, on the other hand, results in prolongation of the fluorescent signal. In this experiment, we loaded A2780 cells with calcein AM and treated them with DMSO or dynasore and FAC as described for the FAC post-treatment experiment (Figure 26b). Figure 27 demonstrates that dynasore treatment of A2780 cells slowed decay of calcein AM-emitted fluorescence and that addition of FAC reversed this process, accelerating quenching of the signal. These data demonstrate that dynasore, by inhibiting dnm2, is capable of causing short-term deficiencies in the intracellular labile iron pool. Combined with our previous findings that dynamin stabilizes HIF1α and other ODDD-containing proteins on a similar time scale, these experiments strongly imply that inhibition of dynamin increases HIF1α protein levels by reducing levels of intracellular

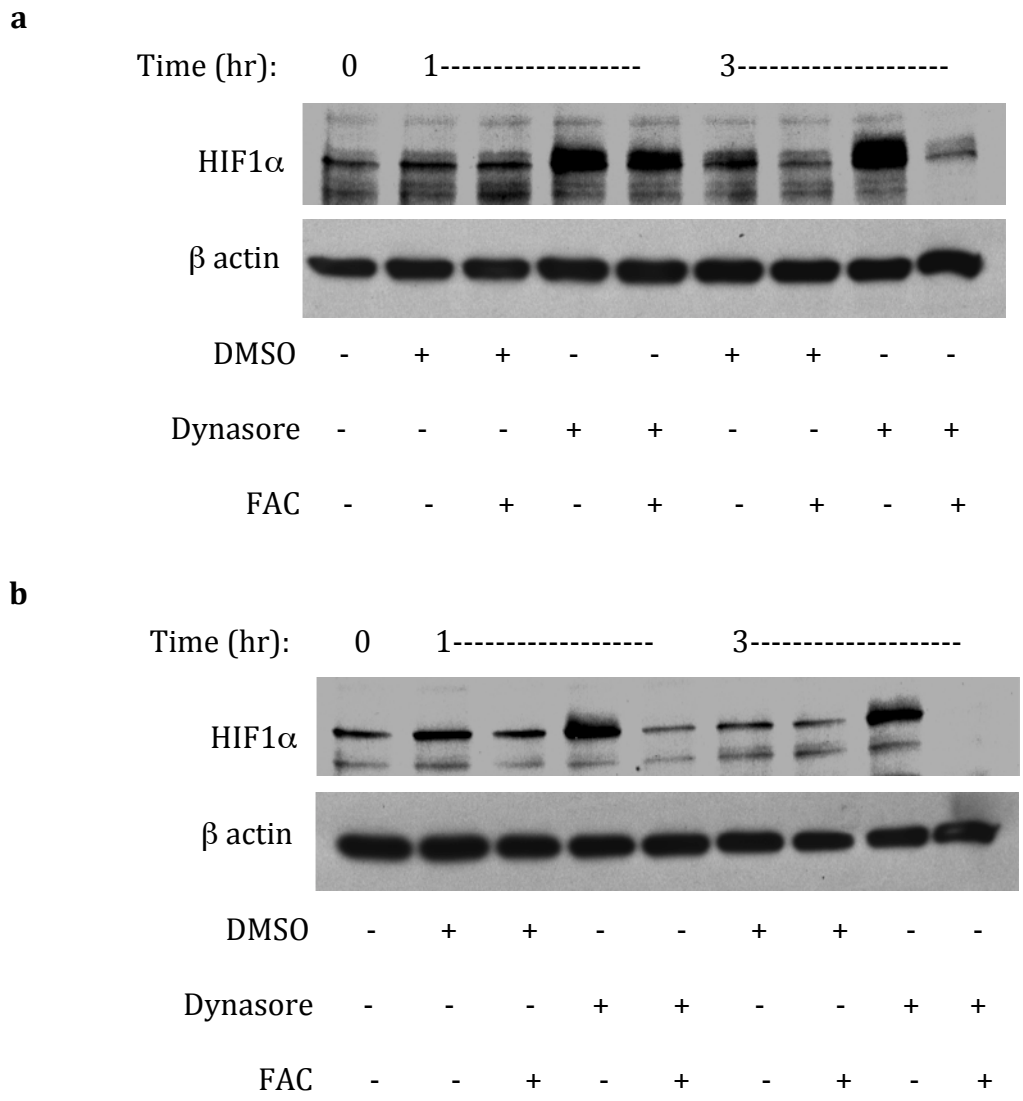

Figure 26: Dynasore-mediated stabilization of HIF1α in normoxic EOCCs is reversed by FAC treatment. (a) A2780 cells were treated with 20 uM FAC for 30 minutes prior to addition of 1% DMSO or 80 uM dynasore and then incubated for 1 or 3 hours or **(b)** were treated for 30 minutes with 1% DMSO or 80 uM dynasore before addition of FAC and then incubated for another 0.5 or 2.5 hours.

iron, a necessary component of PHD hydroxylation step in the HIF1α degradation process in normoxia.

Under normoxia and in the presence of oxygen, iron, 2-oxoglutarate and ascorbic acid, PHDs hydroxylate HIF1α, leading to its recognition and recruitment by VHL and associated scaffolding and machinery. Simultaneously, this complex recruits ubiquitin

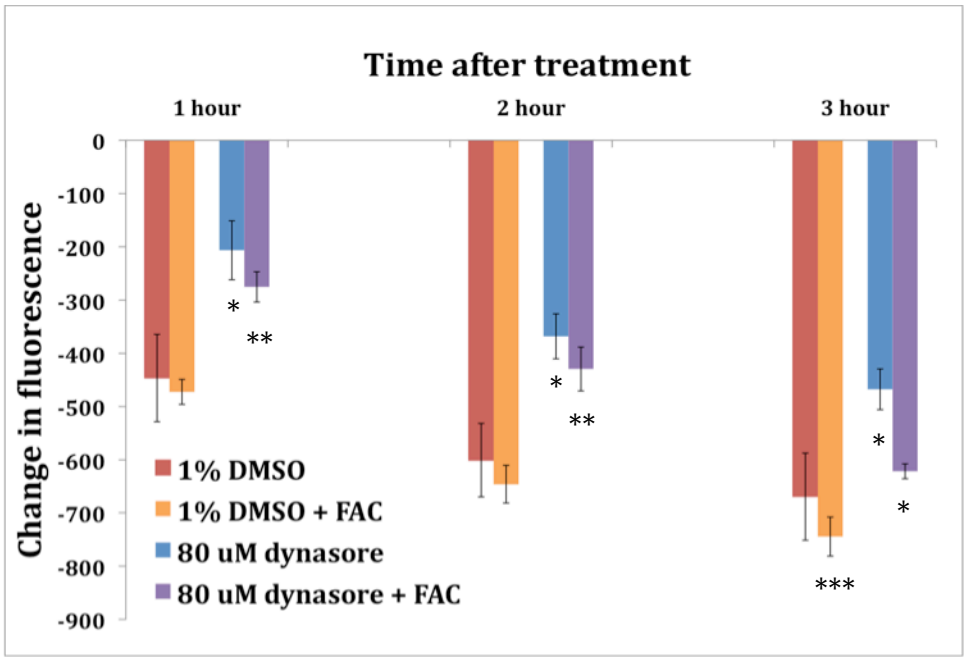

Figure 27: Inhibition of dynamin 2 by dynasore causes a rapid decrease in intracellular labile iron levels. A2780 cells were loaded with the iron-quenched fluorescent molecule calcein-AM for 30 minutes and fluorescence was measured (t = 0). Cells were then treated with 1% DMSO or 80 uM dynasore for the times indicated and fluorescence was measured again. In half the samples, FAC (20 uM) was added 30 minutes after initiation of DMSO/dynasore treatment. Y-axis shows relative units. Values represent mean +/- SD. *P<0.0001. **P<0.01. ***P<0.03.

ligases that tag hydroxylated HIF1α for degradation by the 26S proteosome. Impairment of proteosome function, by inhibitors such as MG-132, for example, leads to accumulation of polyubiqinated proteins as the final step in the degradation pathway is impeded. MG-132-treated normoxic cells, therefore, show a characteristic smear in HIF1α western blots, indicating build-up of various levels of polyubiquitinated HIF1α. If inhibition of dnm2 by dynsore impairs the PHD hydroxylation step of the HIF1α degradation pathway as we hypothesized, combined dynasore and MG-132 treatment should display no characteristic polyubiquitination smear, as steps upstream of HIF1α recruitment to the ubiquitin ligase machinery have been impaired. To test this concept,

we treated A2780 cells with DMSO or dynasore as above, but also treated half the samples with MG-132. As demonstrated in Figure 28, western blot for HIF1α of EOCCs did indeed exhibit a distinctive smear when treated with the protease inhibitor. Strikingly, this smear was all but erased in those cells also treated with dynasore. This effect was more apparent with increased treatment times. These findings support our model that HIF1α stabilization by dynasore in normoxia entails impairment of PHD-mediated hydroxylation due to inhibition of dynamin 2-dependent iron uptake.

Thus far, we have shown that inhibition of dynamin 2 activity induces HIF1α stability in normoxia. We next wanted to determine if the inverse is true, namely, if upregulation of dnm2 in hypoxia results in HIF1α downregulation. To this end, we overexpressed a GST-dynamin 2 construct in A2780 cells under hypoxia and normoxia and evaluated HIF1α expression by western blot. As shown in Figure 29, dnm2

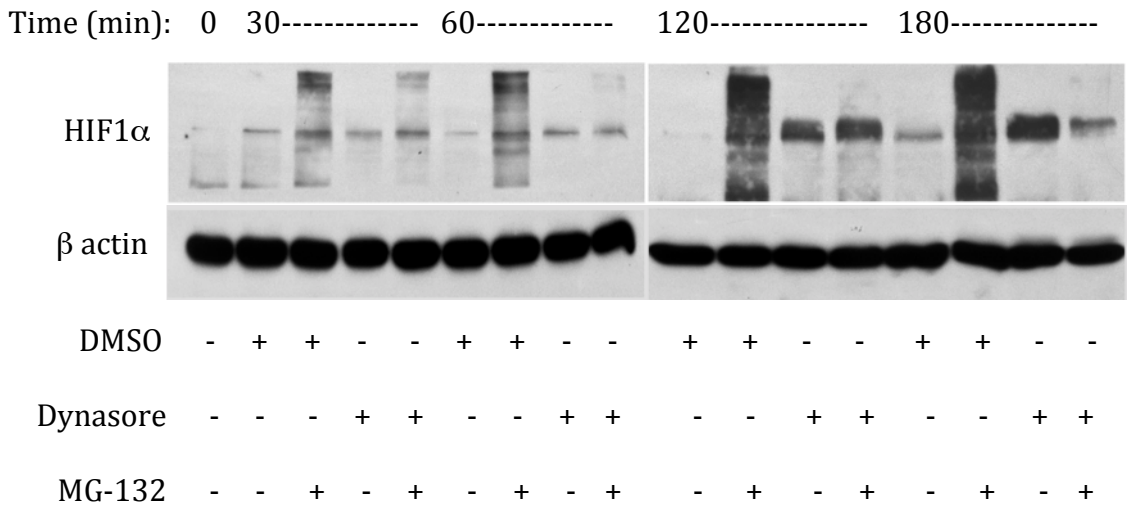

Figure 28: Inhibition of dynamin 2 by dynasore prevents polyubiquitination of HIF1α. A2780 cells were treated with 1% DMSO or 80 uM dynasore with and without the proteasome inhibitor, MG-132 (10 uM) for the times indicated and interrogated by western blot for HIF1α.

overexpression reduced levels of HIF1α in hypoxia. This finding was expected, as based on our hypothesis, dnm2 expression in hypoxia would increase intracellular iron, thereby enhancing degradation of HIF1α.

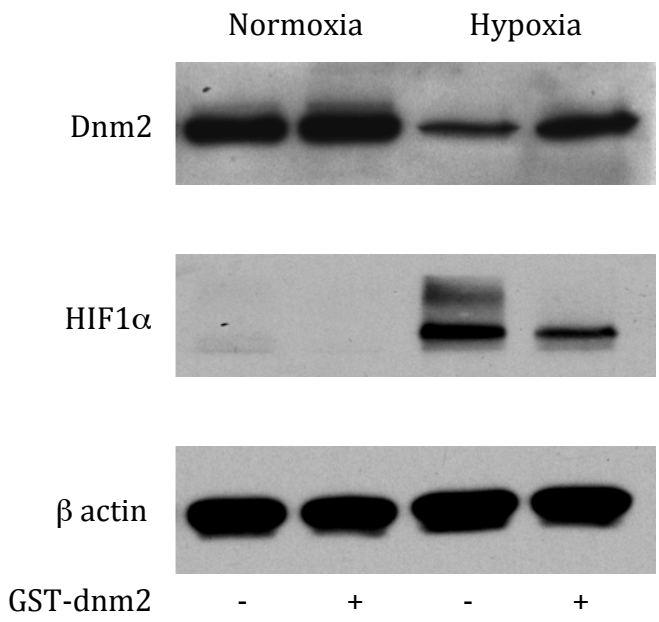

Figure 29: Overexpression of dynamin 2 in hypoxia suppresses HIF1α expression. A2780 cells were transfected with GST-dynamin 2 and exposed to normoxia or hypoxia for 24 hours. Cell lysates were then analyzed by western blot for HIF1α.

Taken together, the results of these experiments demonstrate that dynamin 2 is downregulated in hypoxic EOCCs. This relationship is mediated by HIF1α and hypoxia-response elements in the dnm2 promoter, activity of which is largely determined by an identified 450-nucleotide region and a particular HRE (HRE 2). Moreover, dynamin 2 exerts an inhibitory influence over HIF1α as well. Impairment of dnm2 activity by the small molecule inhibitor dynasore causes a rapid decrease in intracellular iron levels and HIF1α polyubiquitination with corresponding accumulation of HIF1α. Circumventing dynamin-dependent iron endocytosis to iron-load cells using ferric ammonium citrate reverses the effects of dynasore on HIF1α stabilization. Finally, overexpression of dnm2 in hypoxia results in suppression of HIF1α levels. These findings present a novel framework of mutual regulation of a hypoxia-responsive protein and one involved in endocytosis and cell motility, bearing significant implications in the context of cancer.

Hypoxia induces changes in microRNA expression in EOCCs

Having identified hypoxia as a regulator of dynamin 2, which itself exerts control over significant cancer cell processes such as endocytosis and cell motility, we wondered what other important regulatory elements involved in cancer progression may be affected by low levels oxygen in EOCCs. MicroRNAs (miRNAs), of which nearly 1,000 have already been identified in humans alone, are ~22-nucleotide inhibitors of translation and are involved in numerous biochemical processes including hypoxia and cancer progression [277, 278, 323]. During our analysis of dynamin 2 DNA, we identified two miRNAs, miR-199a-1 and miR-638, expressed in introns of the gene. We therefore sought to elucidate the potential roles of miRNA in the response of EOCCs to hypoxia. To evaluate this relationship, we first determined global changes in miRNA profiles of the well-studied EOCC line, A2780, under normoxia and hypoxia. A2780 cells were incubated in normoxia or hypoxia and RNA was submitted for miRNA microarray analysis as previously described [336]. Several of the nearly 500 human miRNA analyzed demonstrated variability in expression between normoxic and hypoxic conditions. Among these, the miR-199 family was of particular interest, as it is predicted by the University of Manchester (www.mirbase.org) and the Memorial Sloan Kettering (www.microrna.org) miRNA-mRNA bioinformatics databases to target HIF-1α, the main regulator of the hypoxic response. A representative microarray, plotted as miRNA expression in hypoxia versus expression in normoxia and denoting the levels of the three family members of miR-199 is shown in Figure 30 and as raw data in Table 8. These results have been uploaded to the NCBI GEO database (accession number GSE32313).

microRNA	Normoxia	Hypoxia
hsa-let-7a	1.916	2.689
hsa-let-7b	1.585	1.237
hsa-let-7c	1.138	1.341
hsa-let-7d	1.711	2.076
hsa-let-7e	2.231	6.556
hsa-let-7f	1.428	1.671
hsa-let-7g	0.567	0.427
hsa-miR-100	8.865	5.223
hsa-miR-101	2.789	4.366
hsa-miR-103	15.51	11.04
hsa-miR-105	0.198	0.356
hsa-miR-106a	43.42	70.16
hsa-miR-106b	7.113	6.387
hsa-miR-107	15.39	9.486
hsa-miR-10a	25.86	24.66
hsa-miR-10b	22.15	21.23
hsa-miR-124a	0.292	0.294
hsa-miR-125a	3.883	2.312
hsa-miR-125b	4.961	3.694
hsa-miR-126	0.228	0.0688
hsa-miR-128a	0.734	0.623
hsa-miR-128b	0.366	0.738
hsa-miR-130a	30.76	33.93
hsa-miR-130b	20.77	32.63
hsa-miR-135a	1.74	0.65
hsa-miR-135b	0.292	0.112
hsa-miR-136	0.0942	0.223
hsa-miR-137	4.682	3.442
hsa-miR-139	0.265	0.0381
hsa-miR-140	1.481	0.733
hsa-miR-141	0.272	0.637
hsa-miR-142-5p	0.266	0.767
hsa-miR-143	0.868	1.252
hsa-miR-144	0.377	0.324
hsa-miR-147	0.102	0.346
hsa-miR-148a	3.919	2.317
hsa-miR-148b	1.402	0.929
hsa-miR-149	1.065	0.788
hsa-miR-150	0.341	0.361
hsa-miR-151	0.764	0.685
hsa-miR-152	0.841	0.228
hsa-miR-154*	0.31	0.129
hsa-miR-154	0.312	0.467
hsa-miR-155	0.487	0.23
hsa-miR-15a	6.037	2.736
hsa-miR-15b	3.745	2.506
hsa-miR-16	15.35	9.273
hsa-miR-17-3p	2.444	2.122
hsa-miR-17-5p	46.84	47.58

microRNA	Normoxia	Hypoxia
hsa-miR-181a*	0.188	0.0413
hsa-miR-181a	0.743	0.153
hsa-miR-181b	0.345	0.452
hsa-miR-181c	1.671	0.664
hsa-miR-181d	0.565	0.684
hsa-miR-182*	0.877	0.351
hsa-miR-182	2.105	2.65
hsa-miR-183	1.329	1.318
hsa-miR-184	1.56	4.587
hsa-miR-185	1.386	2.342
hsa-miR-186	0.918	0.874
hsa-miR-188	0.622	0.749
hsa-miR-189	0.0338	0.292
hsa-miR-18a	8.428	14.93
hsa-miR-18b	11.16	6.577
hsa-miR-190	0.825	0.652
hsa-miR-191	4.595	5.359
hsa-miR-193a	0.88	0.409
hsa-miR-195	7.109	9.917
hsa-miR-196a	2.257	2.547
hsa-miR-196b	0.277	0.531
hsa-miR-198	0.603	2.512
hsa-miR-199-3p	54.32	32.46
hsa-miR-199a-5p	10.66	6.095
hsa-miR-199b	9.897	5.693
hsa-miR-19a	6.182	21.76
hsa-miR-19b	22.21	44.44
hsa-miR-202	0.833	6.165
hsa-miR-203	1.162	2.388
hsa-miR-204	0.329	0.321
hsa-miR-206	1.156	3.208
hsa-miR-20a	36.43	46.18
hsa-miR-20b	33.4	45.37
hsa-miR-21	43.51	29.5
hsa-miR-210	0.783	0.785
hsa-miR-212	0.696	0.445
hsa-miR-214	4.219	12.54
hsa-miR-216	0.22	1.004
hsa-miR-219	0.481	0.402
hsa-miR-22	3.265	5.355
hsa-miR-221	1.114	1.234
hsa-miR-222	1.588	1.424
hsa-miR-223	0.0239	0.26
hsa-miR-23a	9.985	8.581
hsa-miR-23b	13.84	12
hsa-miR-24	7.813	6.008
hsa-miR-25	2.378	2.31
hsa-miR-26a	11.78	11.95
hsa-miR-26b	3.584	2.404

microRNA	Normoxia	Hypoxia
hsa-miR-27a	2.567	1.378
hsa-miR-27b	3.449	1.46
hsa-miR-28	2.817	3.978
hsa-miR-299-5p	0.878	0.815
hsa-miR-29a	21.27	5.849
hsa-miR-29b	20.32	26.19
hsa-miR-29c	16.72	1.423
hsa-miR-301	2.319	3.188
hsa-miR-302b	0.566	0.704
hsa-miR-30a-5p	3.225	2.909
hsa-miR-30b	11.02	8.827
hsa-miR-30c	8.642	5.508
hsa-miR-30d	2.151	1.429
hsa-miR-30e-3p	0.0932	0.512
hsa-miR-30e-5p	2.064	1.29
hsa-miR-31	0.264	1.055
hsa-miR-32	0.673	0.359
hsa-miR-320	2.143	23.21
hsa-miR-326	0.367	0.236
hsa-miR-331	0.989	0.858
hsa-miR-335	1.608	3.328
hsa-miR-338	4.1	2.978
hsa-miR-342	0.979	1.375
hsa-miR-345	0.0299	0.0595
hsa-miR-34b	1.067	0.282
hsa-miR-361	3.875	2.653
hsa-miR-362	0.438	0.68
hsa-miR-363*	42.98	2.372
hsa-miR-363	6.995	8.486
hsa-miR-365	4.624	6.087
hsa-miR-369-5p	0.408	0.0508
hsa-miR-372	0.212	0.635
hsa-miR-373*	1.186	0.99
hsa-miR-374	0.636	1.374
hsa-miR-376a*	0.0989	0.181
hsa-miR-380-3p	0.156	0.13
hsa-miR-381	0.53	0.075
hsa-miR-383	0.758	0.797
hsa-miR-384	0.795	2.251
hsa-miR-409-5p	0.593	0.201
hsa-miR-410	0.503	1.424
hsa-miR-421	0.636	0.783
hsa-miR-422a	3.076	1.07
hsa-miR-422b	2.183	1.101
hsa-miR-423	0.727	0.681
hsa-miR-424	7.45	6.592
hsa-miR-425-5p	1.869	1.142
hsa-miR-429	0.517	0.324
hsa-miR-433	0.315	0.265

microRNA	Normoxia	Hypoxia
hsa-miR-448	0.258	0.203
hsa-miR-452	0.39	0.726
hsa-miR-454-3p	0.948	0.528
hsa-miR-454-5p	0.0914	0.591
hsa-miR-483	0.239	0.47
hsa-miR-484	0.744	0.647
hsa-miR-485-5p	0.498	0.521
hsa-miR-486	0.132	0.959
hsa-miR-487a	1.127	0.778
hsa-miR-487b	4.169	0.944
hsa-miR-491	0.59	0.426
hsa-miR-493-3p	1.259	0.175
hsa-miR-494	12.35	40.74
hsa-miR-495	0.527	1.155
hsa-miR-498	0.0498	0.234
hsa-miR-499	0.2	0.361
hsa-miR-500	0.827	0.819
hsa-miR-501	0.4	1.131
hsa-miR-503	0.803	0.356
hsa-miR-504	0.182	0.75
hsa-miR-505	0.351	0.343
hsa-miR-506	0.925	0.275
hsa-miR-507	0.304	0.97
hsa-miR-508	0.667	0.464
hsa-miR-510	0.532	0.38
hsa-miR-516-5p	0.856	1.438
hsa-miR-517*	0.58	1.138
hsa-miR-517a/b	0.49	0.843
hsa-miR-517c	0.45	1.007
hsa-miR-518c	2.773	1.317
hsa-miR-518c*	0.268	0.775
hsa-miR-519a	0.147	0.534
hsa-miR-519b	0.762	0.396
hsa-miR-519c	0.351	0.234
hsa-miR-519e*	0.686	1.309
hsa-miR-520a*	0.187	0.0844
hsa-miR-520d*	0.249	0.457
hsa-miR-520h	0.715	0.152
hsa-miR-521	0.486	1.785
hsa-miR-522	0.5	0.137
hsa-miR-523	1.415	0.317
hsa-miR-524*	0.251	1.14
hsa-miR-525	0.476	0.788
hsa-miR-526b	0.36	1.388
hsa-miR-526c	0.208	0.189
hsa-miR-532	0.885	0.58
hsa-miR-539	0.714	0.522
hsa-miR-542-3p	0.949	0.9
hsa-miR-545	0.202	0.179

microRNA	Normoxia	Hypoxia
hsa-miR-548a	2.076	1.025
hsa-miR-548d	0.329	0.429
hsa-miR-549	0.264	0.206
hsa-miR-553	0.547	0.386
hsa-miR-556	0.243	0.0982
hsa-miR-557	0.429	0.111
hsa-miR-558	0.039	0.374
hsa-miR-559	3.389	1.2
hsa-miR-561	3.209	10.43
hsa-miR-564	0.611	0.346
hsa-miR-565	0.565	0.169
hsa-miR-569	1.103	1.181
hsa-miR-570	0.4	0.287
hsa-miR-571	0.239	0.528
hsa-miR-572	0.0623	0.171
hsa-miR-573	0.337	0.289
hsa-miR-574	2.186	0.896
hsa-miR-575	3.28	1.041
hsa-miR-576	0.287	0.25
hsa-miR-577	0.718	0.822
hsa-miR-579	0.159	0.327
hsa-miR-580	0.478	0.248
hsa-miR-582	0.359	0.306
hsa-miR-583	0.475	0.63
hsa-miR-584	0.366	0.841
hsa-miR-585	0.0342	0.248
hsa-miR-589	0.996	0.588
hsa-miR-590	2.395	2.843
hsa-miR-594	5.77	1.05
hsa-miR-595	0.319	0.265
hsa-miR-596	0.282	0.239
hsa-miR-600	1.323	1.001
hsa-miR-601	2.795	2.86
hsa-miR-603	2.15	0.61
hsa-miR-605	0.285	0.431
hsa-miR-606	0.451	0.24
hsa-miR-607	0.758	0.286
hsa-miR-608	0.263	0.318
hsa-miR-610	0.195	0.562
hsa-miR-615	0.239	1.023
hsa-miR-616	0.248	0.407
hsa-miR-617	1.266	0.749

microRNA	Normoxia	Hypoxia
hsa-miR-620	1.158	1.274
hsa-miR-624	0.278	0.335
hsa-miR-625	10.92	8.713
hsa-miR-627	0.526	0.72
hsa-miR-628	0.728	1.08
hsa-miR-629	0.161	0.514
hsa-miR-630	0.818	0.464
hsa-miR-631	0.155	0.245
hsa-miR-633	4.051	0.339
hsa-miR-634	1.013	1.716
hsa-miR-635	0.473	0.818
hsa-miR-638	0.409	0.65
hsa-miR-642	0.0849	0.522
hsa-miR-644	0.351	0.179
hsa-miR-645	0.0226	0.826
hsa-miR-646	0.12	0.67
hsa-miR-647	0.0864	0.412
hsa-miR-649	0.476	0.222
hsa-miR-652	0.343	0.371
hsa-miR-653	0.353	0.702
hsa-miR-655	0.371	0.303
hsa-miR-656	0.0779	0.167
hsa-miR-658	0.975	0.331
hsa-miR-659	0.309	0.314
hsa-miR-660	1.602	0.844
hsa-miR-661	0.375	0.261
hsa-miR-663	0.807	0.167
hsa-miR-671	0.514	0.467
hsa-miR-7	0.64	0.224
hsa-miR-765	5.554	13.1
hsa-miR-767-5p	0.265	0.409
hsa-miR-768-3p	5.432	5.008
hsa-miR-768-5p	2.581	5.358
hsa-miR-769-3p	1.853	0.0953
hsa-miR-770-5p	0.509	0.345
hsa-miR-801	0.0227	0.15
hsa-miR-9	1.592	0.704
hsa-miR-92	1.708	1.19
hsa-miR-92b	3.534	0.554
hsa-miR-93	7.177	2.109
hsa-miR-96	0.412	1.249
hsa-miR-99a	4.152	2.605
hsa-miR-99b	2.879	1.333

Table 8: Representative microarray of human microRNA expression in A2780 EOCCs under normoxia and hypoxia. miR-199 family miRNAs are highlighted. Pearson correlation coefficients for array analysis of the same RNA samples were 0.90-0.99, indicating good reproducibility. Only miRNAs that were expressed above the threshold signal (0.01) in both normoxic and hypoxic conditions are shown.

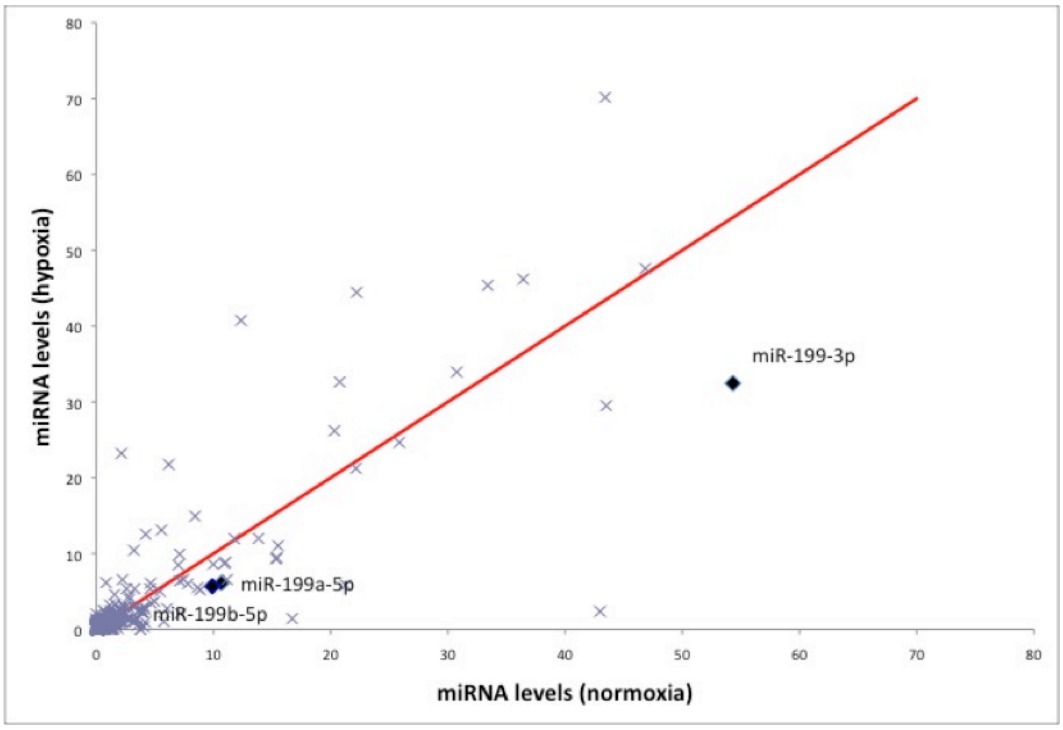

Figure 30: Representative microarray of human microRNA expression in A2780 EOCCs under normoxia and hypoxia. The three variations of miR-199a are indicated with black diamonds. MiRNA above the red line demonstrate increased expression in hypoxia whereas expression of miRNA under the red line is decreased under hypoxia.

MiR-199 is a family of miRNAs composed of six members (Figure 31a). Interestingly, all are encoded within intronic regions in the dynamin family of genes. In most miRNAs, only one arm of the Dicer-formed duplex is selected by the RISC machinery for further processing. Both the -5p and -3p arms of miR-199 members, however, are expressed in mature form. [344]. Together, by virtue of six bioactive variations, the miR-199s therefore comprise a family of miRNA with a number of potential regulatory roles. In the context of hypoxia, bioinformatics databases predict that both miR-199a-1/2-5p and 199b-5p target HIF-1α. We selected miR-199a-1-5p (Figure 31b) for further study because it is presumably found within in all cell types because of its location within the dynamin 2 gene, which is ubiquitously expressed [236].

a

hsa-miR-199b-5p
cccaguguuuagacuaucuguuc

hsa-miR-199a-1-5p
cccaguguucagacuaccuguuc

hsa-miR-199a-2-5p
cccaguguucagacuaccuguuc

hsa-miR-199a-1-3p
acaguagucugcacauugguua

hsa-miR-199a-2-3p
acaguagucugcacauugguua

hsa-miR-199b-3p
acaguagucugcacauugguua

b

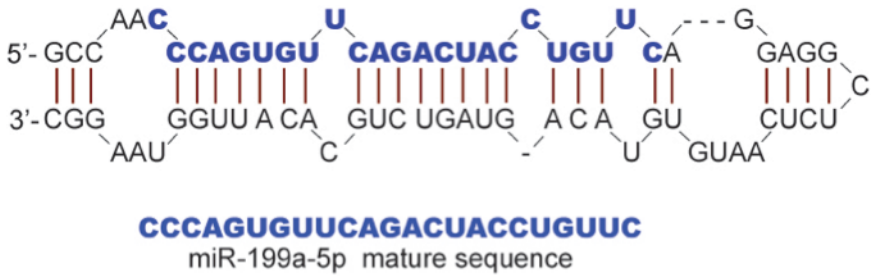

CCCAGUGUUCAGACUACCUGUUC
miR-199a-5p mature sequence

Figure 31: The miR-199 family of microRNA: miR-199a-1, miR199a-2 and miR-199b. (a) The -3p arms of all three members are identical. The -5p arms of miR-199a-1 and miR-199a-2 are identical and miR-199b differs by just two basepairs (marked in red). miR-199a-1 and miRa-2 are thus simply known as "miR-199a". The three members are located in the introns of the three different dynamin family genes. Specifically, miR-199a-1 is within dynamin 2, miR-199a-2 is within dynamin 3 and miR-199b is within dynamin 1. All six members of the family demonstrate bioactivity. miR-199-1/2-5p as well as miR-199b are predicted to target HIF1α. **(b)** The immature and mature sequences of miR-199a-1-5p. MiR-199a is expressed in the genomes of many animals, including human, mouse, rat, ehicken, zebrafish, pufferfish, xenopus and many primates. In contrast to other miR-199s, which are located within genes whose expression is restricted to neuronal tissue (miR-199b in dynamin 1) or the testes (miR-199a-2 in dynamin 3), miR-199a-1 is located within the ubiquitously expressed dynamin 2 gene.
.

The predicted interaction of miR-199a-5p with the HIF1α 3' UTR is shown in Figure 32. As described in the background section on miRNA, certain criteria should be met for a miRNA to bind with and exert regulatory control on a target mRNA. The association between miR-199a-1-5p and the HIF1α 3' UTR achieves several of these requirements: binding close to the end of the HIF1α ORF but beyond 15 nucleotides from the start of the 3' UTR; exhibiting strong "seed" region complementarity and some

a

```
3′ CUUGUCCAUCAGAUUUGUGACCC 5′ miR-199a-5p
                |:|::|||||||
5′ CAUUCCUUUUUUUGGACACUGGU 3′ HIF1-alpha 3′UTR
```

b

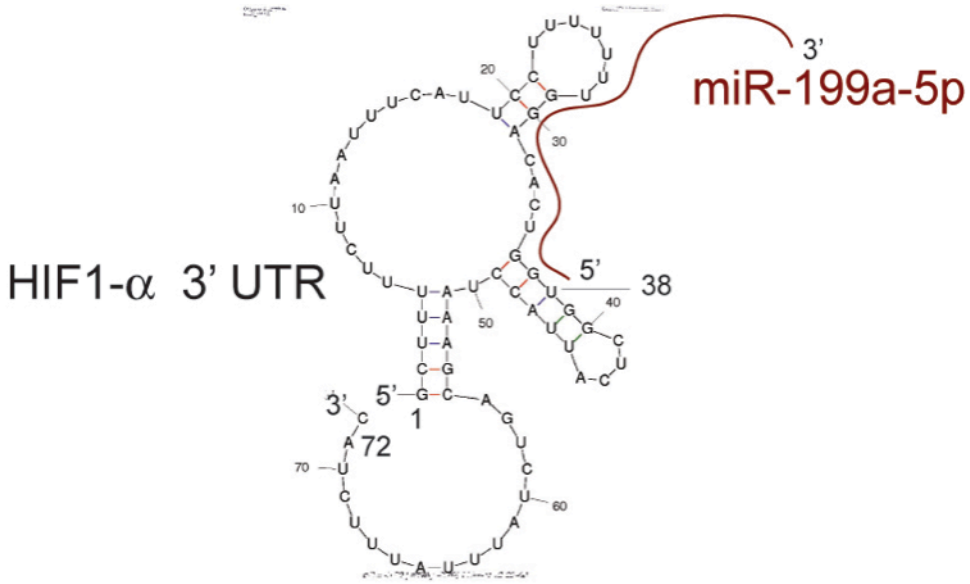

Figure 32: Predicted interaction of miR-199a-5p with the HIF1α 3' UTR. (a) This association boasts robust "seed" region complementarity as well as significant basepairing and G-U "wobble" pairing at the 3' end of the miRNA and middle portion of the interaction, respectively. **(b)** Predicted two-dimensional structure of the miR-199a-5p–HIF1α 3' UTR interaction. The start of the HIF1α 3' UTR is marked with a "1" to indicate the first 5' end nucleotide. The site of the first miR-199a-5p–HIF1α 3' UTR basepairing occurs at nucleotide 26 in the HIF1α 3' UTR.

basepairing at the 3' end of the miRNA; and bearing no significant mismatches, only G-U "wobble" basepairing, in the middle portion of the interaction. Taken together, the miRNA microarrays and bioinformatical predictions of miR-199a-5p–HIF1α 3' UTR interaction suggest that miR-199a may play an important role in the response of EOCCs to hypoxia. To confirm the findings of our array, we performed qPCR using primers specific for miR-199a-5p in three types of EOCCs, A2780, 1A9 and MA148, in both hypoxia and normoxia. As demonstrated in Figure 33, miR-199a-5p levels were

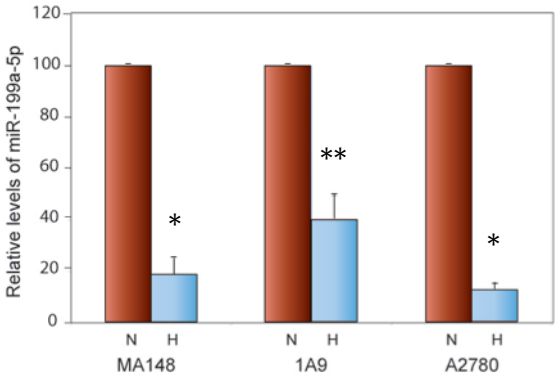

Figure 33: Expression of miR-199a-5p is decreased under hypoxia in EOCCs. MA148, 1A9 and A2780 cells were incubated in normoxia or hypoxia and qPCR for miR-199a-5p was performed. Red bars indicate normoxia and blue bars indicate hypoxia. Results are normalized to normoxic control. Values represent mean +/- SD. *P<0.01. *P<0.001.

significantly downregulated in hypoxia compared to normoxia in all three cells lines, confirming the findings of our miRNA microarray.

Because miR-199a is located in an intron within the dynamin 2 gene, expression of the miRNA is related to expression of the protein. We therefore referred to our previous findings that hypoxia exerts control over the dynamin 2 promoter. Specifically, Figure 21d demonstrates that A2780 and MA148 cells transfected with dnm2 prom-luc and exposed to hypoxia exhibited marked suppression of luciferase signal compared to normoxic cells transfected with the same construct. As such, the dnm2 promoter regulates changes in miR-199a expression in hypoxic EOCCs in a similar manner. These data confirm that miR-199a expression is downregulated in hypoxia versus normoxia and indicates that the mechanism of suppression involves the promoter of dynamin 2.

MiR-199a-5p inhibits HIF1α expression and activity in EOCCs

Because miR-199a-5p is downregulated under hypoxia and is predicted *in silico* to target HIF1α, we wanted to test whether levels of HIF1α change in hypoxia compared to normoxia in a 3' UTR-dependent manner. To accomplish this, we created another

luciferase reporter construct, this one with luciferase expression under control of the HIF1α 3' UTR. This construct, luciferase-HIF1α 3' UTR (luc-HIF1α 3' UTR), was transfected into A2780 cells which were incubated in hypoxic or normoxic conditions for varying periods of time. As shown in Figure 34, luciferase expression in these cells was suppressed in normoxia compared to hypoxia. These findings indicate that some sort of inhibitory regulation of the HIF1α 3' UTR is present under normal oxygenation but is relieved under low oxygen states. As described earlier, one of the main regulatory elements that interact with 3' UTRs and suppress protein expression are miRNAs. To demonstrate that miR-199a-5p targets the HIF1α 3' UTR directly and specifically at the site predicted bioinformatically, we created a mutant form of the luc-HIF1α 3' UTR (34) in which the area of the 3' UTR that binds the "seed" region of miR-199a-5p (see bolded sequence in Figure 32a), ACUGG, was deleted. A2780 cells were transfected with either luc-HIF1α 3' UTR or luc-HIF1α MUT 3' UTR and treated with a scramble duplex (control) or miR-199a duplex overnight and exposed to normoxia or hypoxia for 24 hours. In both conditions, relative luminescence was suppressed by miR-199a in cells transfected with luc-HIF1α 3' UTR, but not in cells transfected with the mutant form (Figure 35). In fact,

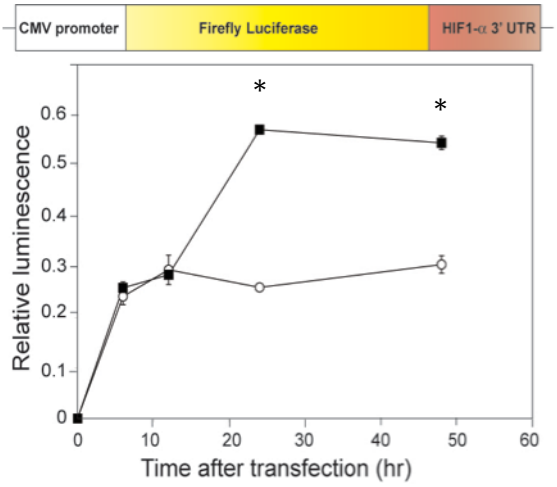

Figure 34: Expression of HIF1α is regulated by its 3' UTR under normoxia and hypoxia. A2780 cells transfected with luc-HIF1α 3' UTR were subjected to normoxic or hypoxic conditions for the times indicated and relative luminesce of the samples was measured. Open circles indicate normoxia and closed circles indicate hypoxia. A schematic of the luc-HIF1α 3' UTR construct is shown above. Values represent mean +/- SD. *P<0.005.

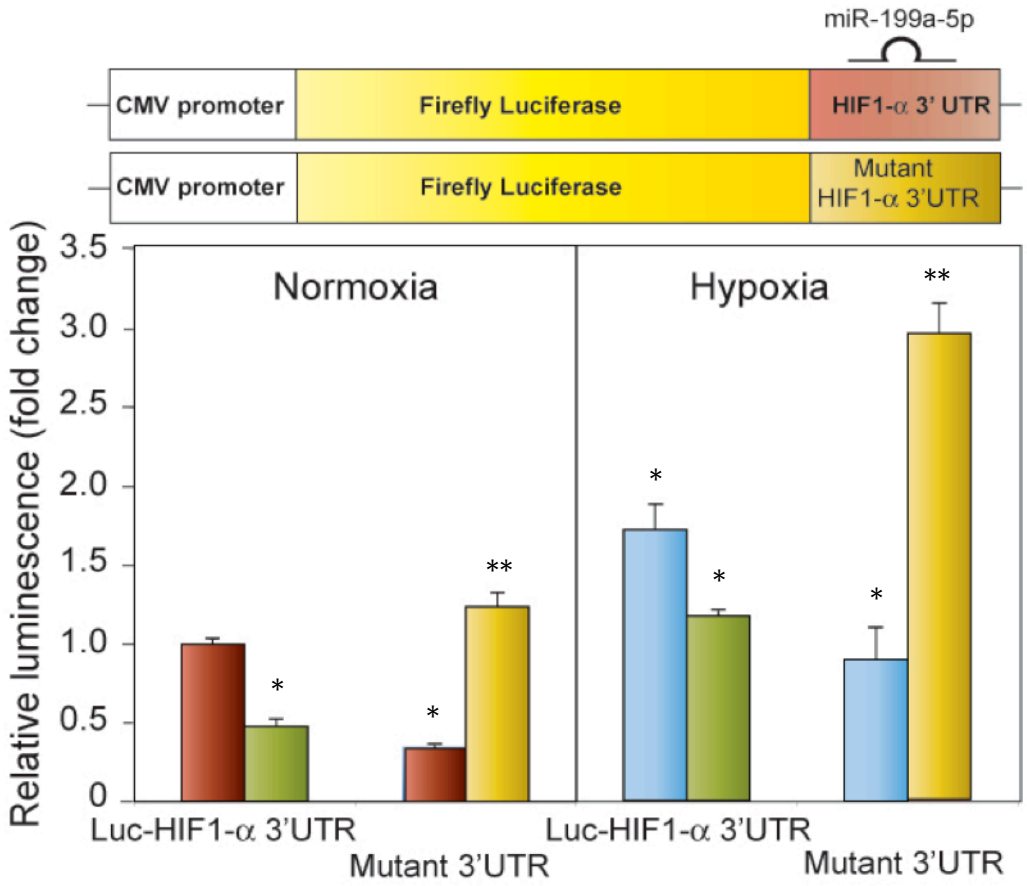

Figure 35: MiR-199a suppresses HIF1α 3' UTR-dependent protein expression in EOCCs. A2780 cells were transfected with luc-HIF1α 3' UTR or luc-HIF1α MUT 3' UTR, treated with scramble duplex or miR-199a duplex and exposed to normoxia or hypoxia. Relative luminescence of the samples was then measured. Schematics of the two constructs used in this experiment are shown above. Red and blue bars indicate scramble duplex-treated cells. Green and yellow bars indicate miR-199a treated cells. Results are normalized to normoxic control. Values represent mean +/- SD. *P<0.01. **P<0.001. P values are calculated for the appropriate normoxic or hypoxic Luc-HIF1-3' UTR control.

cells expressing luc-HIF1α MUT 3' UTR actually showed increased luminescence when treated with miR-199a. To verify that miR-199a overexpression was indeed achieved using the duplex, qPCR with primers for miR-199a-5p was performed. These data showed that 48 hour treatment with miR-199a duplex increased levels of the miRNA 20-fold under normoxia and 40-fold under hypoxia, compared to their respective controls

(Figure 36). These findings confirm that the changes observed between the scramble duplex and miR-199a groups were indeed due to an increase in miR-199a levels.

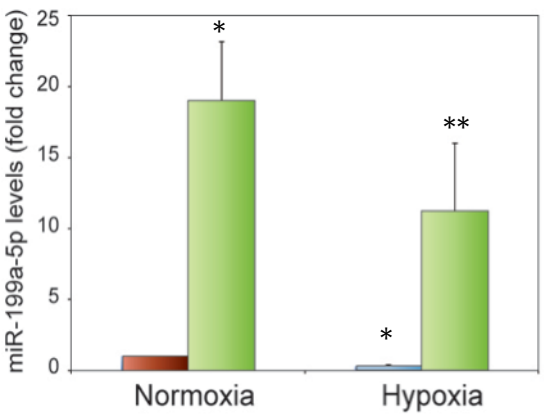

Figure 36: MiR-199a duplex increases levels of miR-199a-5p. A2780 cells were transfected with scramble or miR-199a duplex and miR-199a-5p levels were determined by qPCR. Red and blue bars indicate scramble treatment under normoxia and hypoxia, respectively, and green bars indicate miR-199a treatment. Results are normalized to normoxic control. Values represent mean +/- SD. *P<0.002. **P<0.02. P values are calculated for the appropriate normoxic or hypoxic scramble control.

Having determined the direct suppressive effect of miR-199a on HIF1α 3' UTR-based luciferase expression, we next investigated whether overexpression of the miRNA translates to changes in HIF1α mRNA and protein levels. A2780 cells were treated with scramble or miR-199a duplex overnight, exposed to normoxia or hypoxia for 24 hours and RNA and whole cell lysate were collected for qPCR and western blot, respectively. Interestingly, although mRNA levels of HIF1α did not decrease significantly with miR-199a treatment (Figure 37a), protein levels did (Figure 37b). Moreover, A2780 cells grown in culture and treated with miR-199a duplex showed slightly lower levels of cytoplasmic HIF1α in normoxia and markedly reduced nuclear accumulation of HIF1α after 24 hours of hypoxia compared to scramble-treated cells, as demonstrated by immunofluorescence (Figure 37c). The latter study also demonstrated, notably, that cells treated with miR-199a retained well-spread morphology in hypoxia whereas scramble-treated cells did not. As a complementary approach, we also determined the effects of miR-199a suppression on HIF1α mRNA and protein levels. To this end, we utilized morpholinos, synthetic nucleotide analogs that inhibit

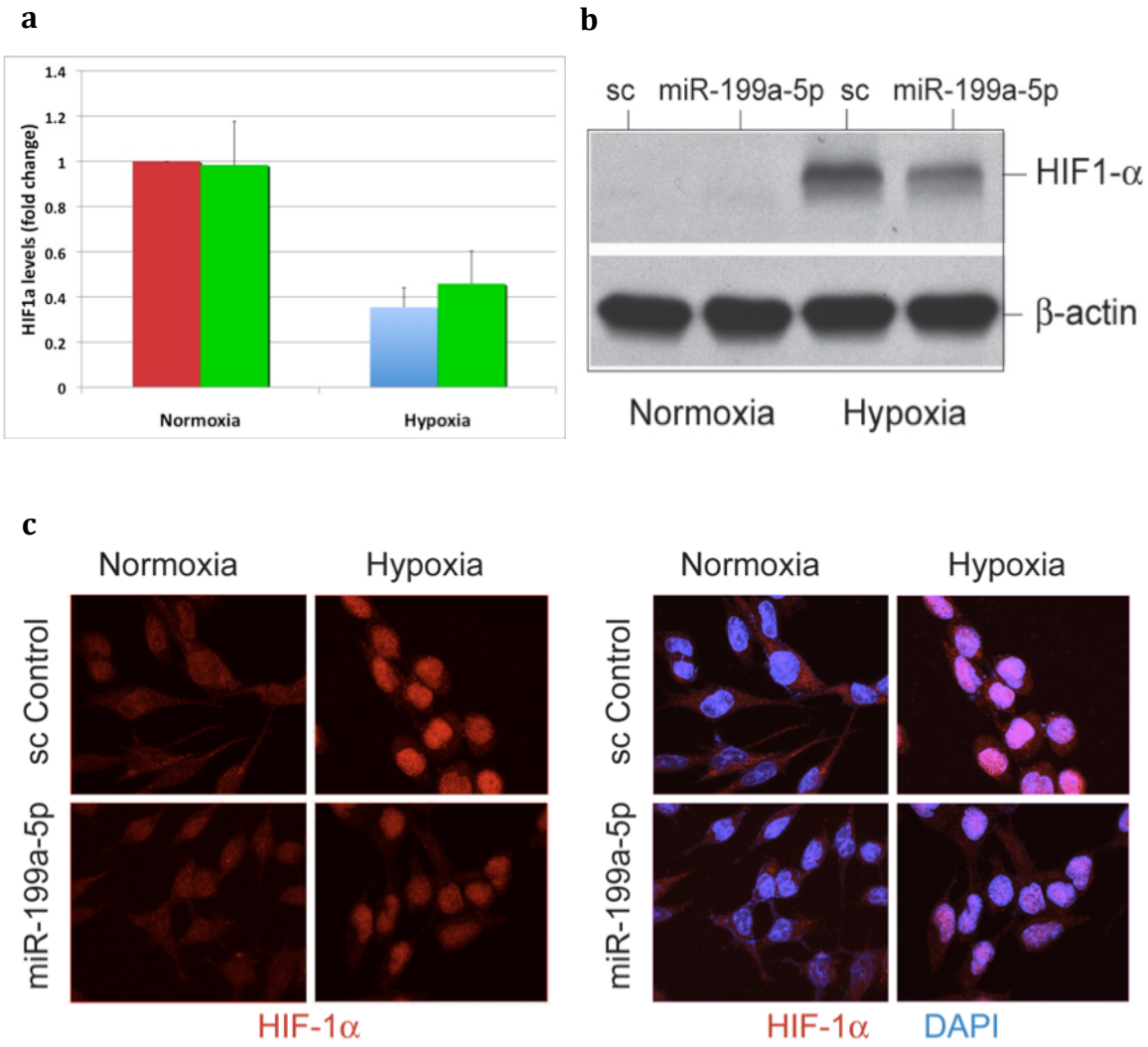

Figure 37: MiR-199a overexpression does not affect HIF1α transcript levels but suppresses HIF1α protein levels and nuclear localization in EOCCs. (a) A2780 cells were treated with scramble or miR-199a duplex overnight, exposed to normoxia or hypoxia for 24 hours for qPCR. Red and blue bars indicate scramble-treated cells in normoxia and hypoxia, respectively. Green bars indicate miR-199a-treated cells. Values represent mean +/- SD. **(b)** Western blot for HIF1α from cells treated as in **(a)**. **(c)** Cultured cells were treated as in **(a)**, fixed and stained for HIF1α (red) and nuclei (blue). Left panel shows HIF1α staining, right panel shows merged image. Abbreviations: sc, scramble.

both Drosha- and Dicer-based cleavage in the miRNA maturation process, to knockdown miR-199a. Inhibiting miR-199a expression (Figure 38a) with a morpholino specific for the miRNA led to increased levels of HIF1α transcript (Figure 38a) as well as increased

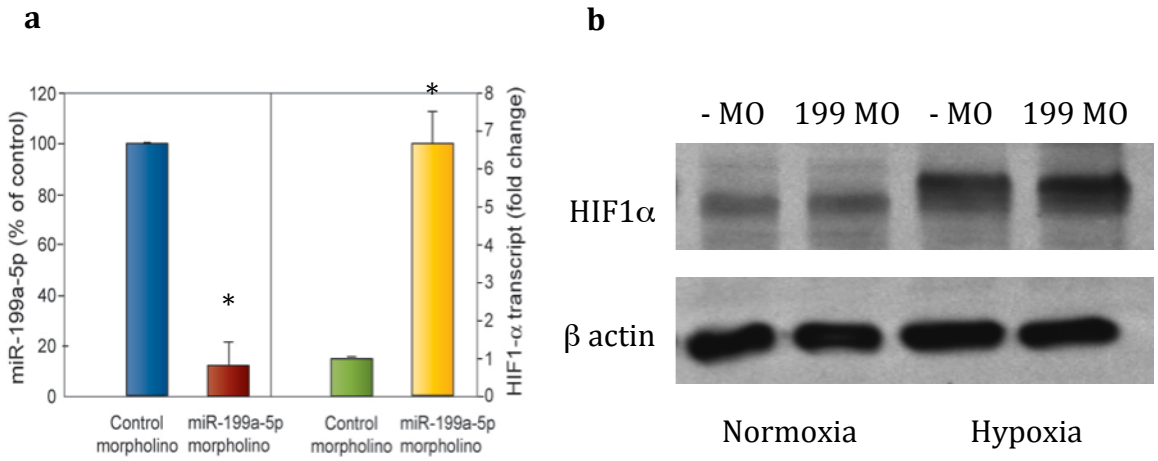

Figure 38: Knockdown of miR-199a increases HIF1α transcript and protein levels in EOCCs. A2780 cells were treated with morpholino control or miR-199a-specific morpholino. **(a)** Levels of miR-199a-5p (left) and HIF1α mRNA (right) as determined by qPCR. **(b)** Western blot for HIF1α. Values represent mean +/- SD. *P<0.01. Abbreviations: - MO, control morpholino; 199 MO, miR-199a-specific morpholino.

HIF1α protein (Figure 38b), the latter an anticipated result and the former surprising, given that miR-199a overexpression elicited no change in HIF1α mRNA levels.

We next wanted to investigate whether suppression of HIF1α protein by miR-199a has functional consequences. Because VEGF is one of the most important genes activated by HIF1, we measured levels of the pro-angiogenic molecule in EOCCs treated with miR-199a in two ways. First, we conducted qPCR on A2780 cells treated with scramble or miR-199a duplex under normoxia and hypoxia. Figure 39a shows that VEGF mRNA levels were significantly reduced in hypoxia in EOCCs overexpressing miR-199a. Second, A2780 cells were transfected with a luciferase reporter construct in which luciferase expression is under control of the HIF1α-driven VEGF promoter (VEGF prom-luc). Treatment with miR-199a duplex in hypoxia markedly reduced relative luminescence in EOCCs transfected with this luciferase reporter construct, with levels of

suppression nearly identical to those of the qPCR assay (Figure 39b). Together, these data demonstrate that miR-199a suppresses HIF1α protein levels with corresponding suppression of HIF1α target genes.

EOCCs stably expressing miR-199a exhibit impaired growth, motility and attachment

The finding that cell morphology was affected by transient miR-199a upregulation (Figure 37c) spurred us to investigate other phenotypic changes in cells overexpressing the miRNA. To this end, we first created an A2780 cell line stably expressing miR-199a so that long-term experiments could be carried out. Using GFP- and miR-199a/GFP- expressing lentiviruses (so that tumor cells could be visualized by

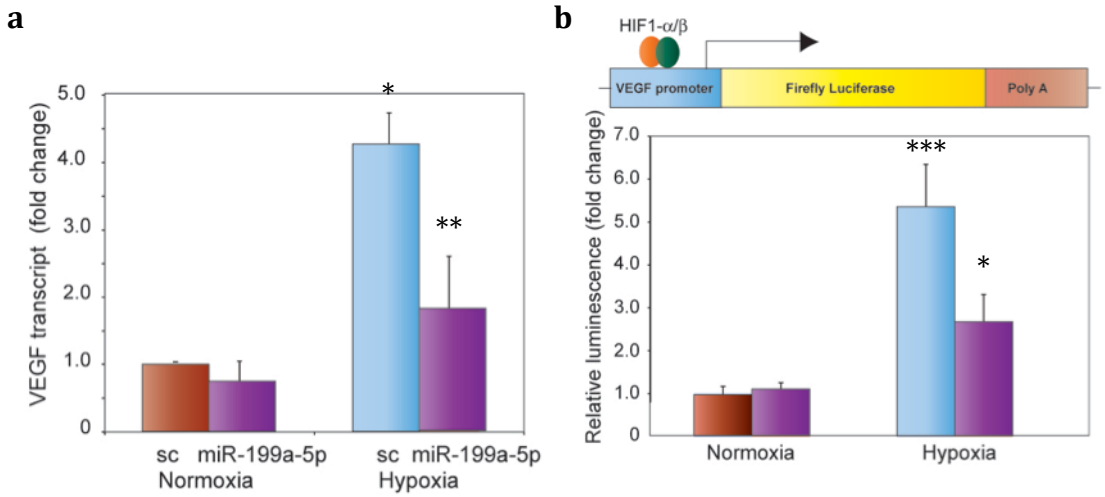

Figure 39: MiR-199a suppresses HIF1α-driven gene expression in EOCCs. (a) A2780 cells were treated with scramble or miR-199a duplex overnight and exposed to normoxia or hypoxia for 24 hours. qPCR for VEGF was then performed. **(b)** The VEGF prom-luc construct was transfected into A2780 cells and treated as in **(a)** and relative luminescence was measured. A schematic of the luciferase construct used is shown above. Red and blue bars indicate scramble-treated cells in normoxia and hypoxia, respectively. Purple bars indicate miR-199a-treated cells. Results are normalized to normoxic controls. Values represent mean +/- SD. *P<0.02. **P<0.05. ***P<0.002. P values are calculated for the appropriate normoxic or hypoxic sc control. Abbreviations: sc, scramble.

fluorescence microscopy), we generated two cell lines: A2780-GFP (control) and A2780-199. After sorting the cells by FACS to obtain enriched populations of our cells of interest (Figure 40), we incubated both groups of cells in normoxia and hypoxia and collected total RNA and whole cell lysate for qPCR and western blot, respectively. Analysis of these samples showed that miR-199a-5p levels were indeed substantially augmented in the A2780-199 group compared to the A2780-GFP group (Figure 41a). Furthermore, levels of HIF1α protein and three HIF1α-transactivated genes critical to cancer progression, VEGF, EPO and LOX, were significantly suppressed in the miR-199a overexpressing cell line compared to the control cell line (Figure 41b-e).

Having established that the A2780-199 cell line did indeed overexpress miR-199a and suppress HIF1α protein and HIF1α-driven gene expression, we next evaluated whether miR-199a affects EOC proliferation. In BrdU incorporation assays (Figure 42),

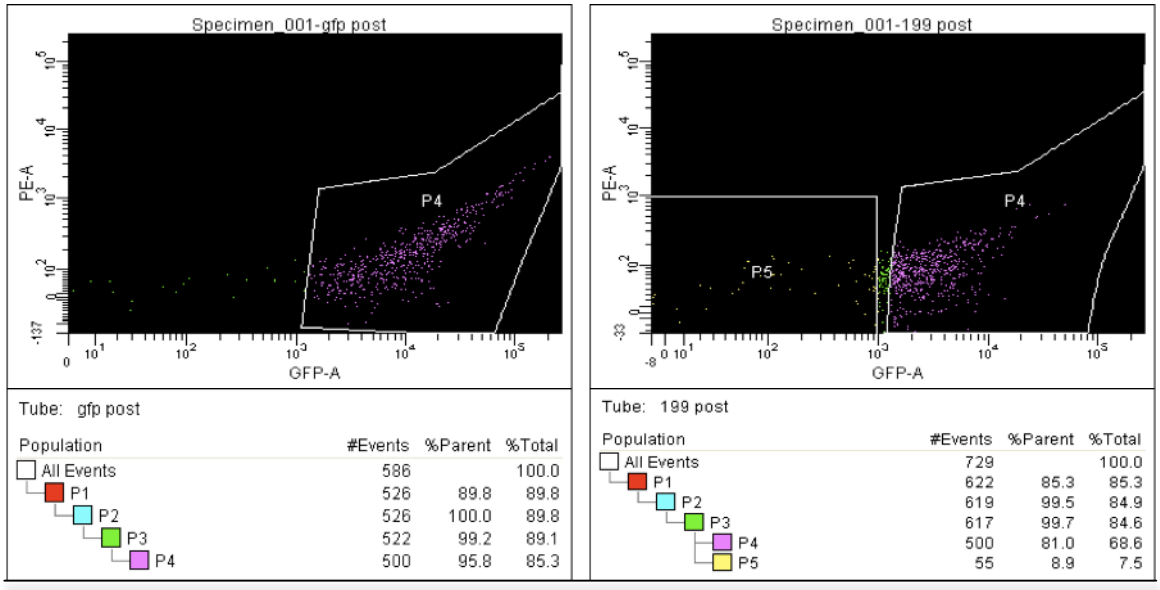

Figure 40: Fluorescence-activated cell sorting enriches A2780-GFP and A2780-199 cell populations. Post-sort analysis of GFP-based FACS of A2780-GFP cells **(a)** and A2780-199 cells **(b)**, showing transduced cell proportions of greater than 80 percent and nearly 70 percent, respectively.

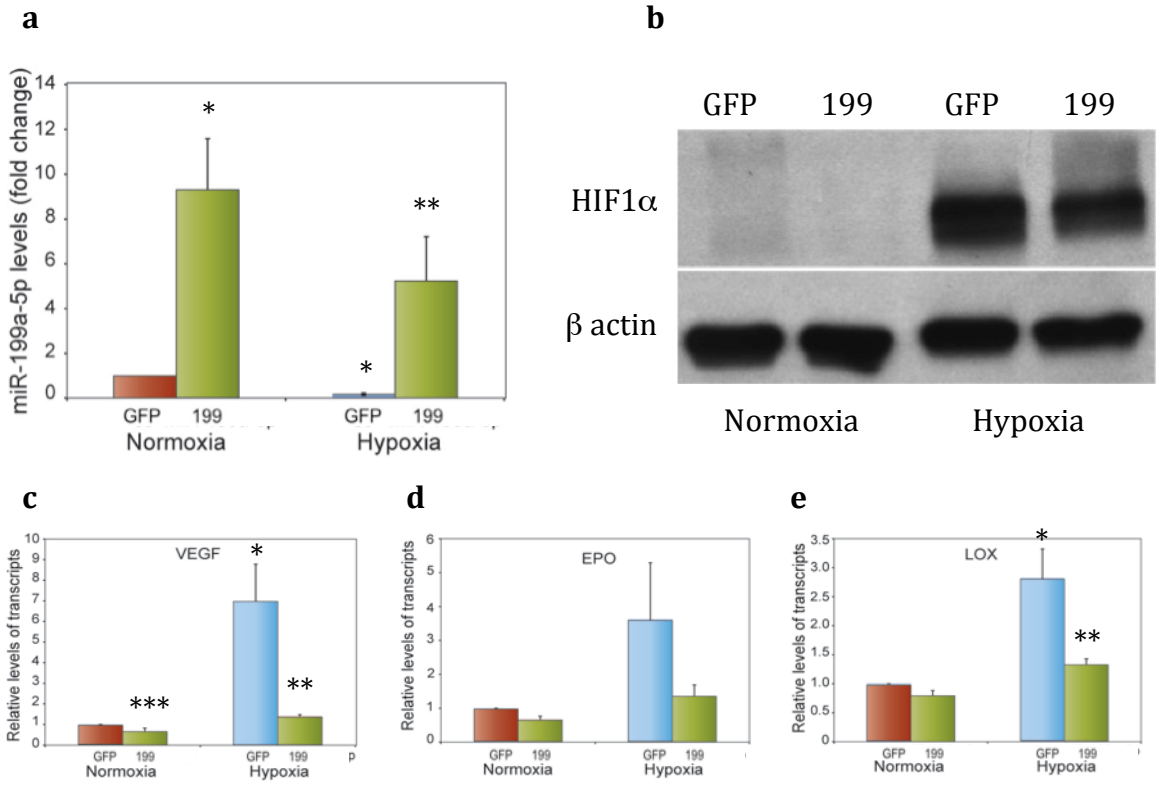

Figure 41: EOCCs stably transfected with miR-199a overexpress miR-199a-5p and suppress HIF1α expression and activity. (a) Levels of miR-199a-5p were measured in A2780-GFP and A2780-199 cells by qPCR. **(b)** Western blot for HIF1α of A2780-GFP and A2780-199 cells. qPCR of HIF1α-driven genes that activate angiogenesis (VEGF) **(c)**, increase erythropoiesis (EPO) **(d)** and promote tumor cell motility and metastasis (LOX) **(e)** in A2780-GFP and A2780-199 cells. Red and blue bars indicate A2780-GFP under normoxia and hypoxia, respectively and green bars indicate A2780-199. Results are normalized to normoxic control. Values represent mean +/- SD. *P<0.01. **P<0.02. ***P<0.05. P values are calculated for the appropriate normoxic or hypoxic GFP control.

A2780-199 cells showed small, but statistically insignificant, inhibition of proliferation compared to control cells over 24 or 48 hours in normoxia or hypoxia. These findings were mirrored by a real-time proliferation assay conducted on the Roche Xcelligence system, in which special cell culture plates determine growth rates by quantifying changes in impedance, which is outputted as "cell index," sensed by gold electrodes at the cell-plate interface. Using this novel technology, we found that A2780-199 cells

exhibited a slight, statistically significant, inhibitory effect on proliferation compared to A2780-GFP cells under normal conditions and when treated with the iron-chelating hypoxia mimetic DFX (Figure 43a). Notably, after 60 hours, the untreated A2780-199 cells continued to proliferate whereas the A2780-GFP cells had aleady achieved confluence. As an added variable, we also introduced a form of HIF1α that contains proline to alanine mutations at PHD-hydroxylation sites. This P to A HIF1α construct also lacks a 3' UTR, thus rendering it not only stable in normoxia, but invulnerable to miRNA-based inhibition as well. Transfection of cells with this construct (Figure 43b) allowed us to determine if the effects of miR-199a on growth can be reversed by the actions of its target, HIF1α. Indeed, P to A HIF1α-treated cells narrowed the growth disparity between A2780-GFP cells and A2780-199 cells under simulated hypoxia to an insignificant difference, and, strikingly, conferred untreated A2780-199 cells with a slim proliferative advantage over control cells. Together, these experiments demonstrate a small, significant inhibitory influence of miR-199a on EOC proliferation.

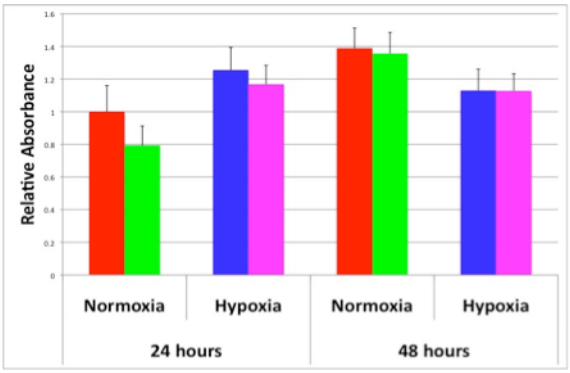

Figure 42: miR-199a has no effect on EOCC proliferation in BrdU assays. Relative absorbencies of A2780-GFP and A2780-199 cells by BrdU incorporation were measured to determine growth rate. Results are normalized to 24-hour normoxic control. Red and blue bars indicate A2780-GFP cells in normoxia and hypoxia, respectively. Green and pink bars indicate A2780-199 in normoxia and hypoxia, respectively. Values represent mean +/- SD.

We next examined whether the inhibitory effect of miR-199a on proliferation is due to suppression cancer stem cell-like populations. To this end, we performed a clonogenic assay in which 1, 2, 4, 8, 16, 32, 64, 128, 256, or 512 cells were seeded per

a

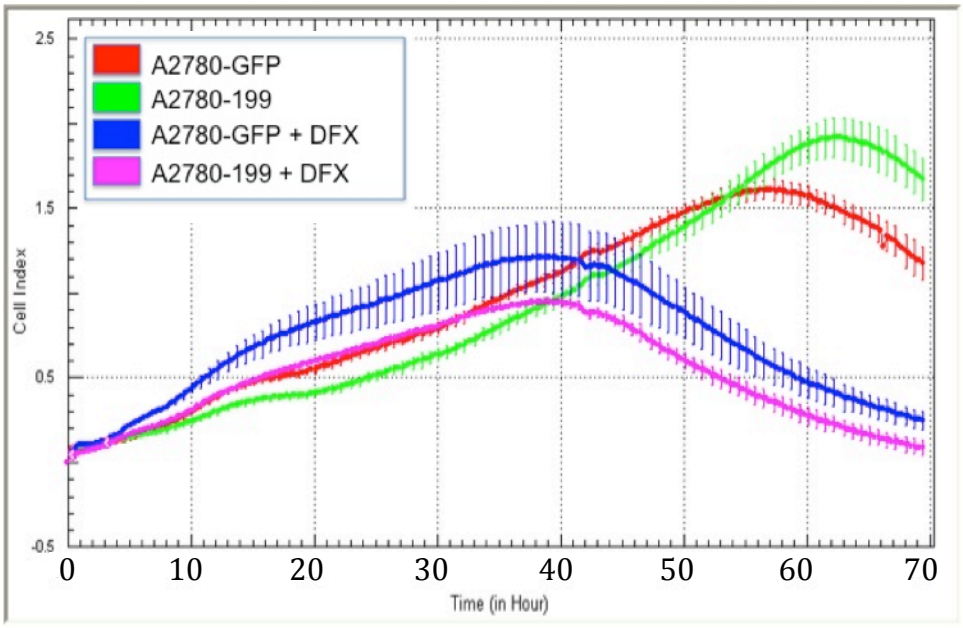

b

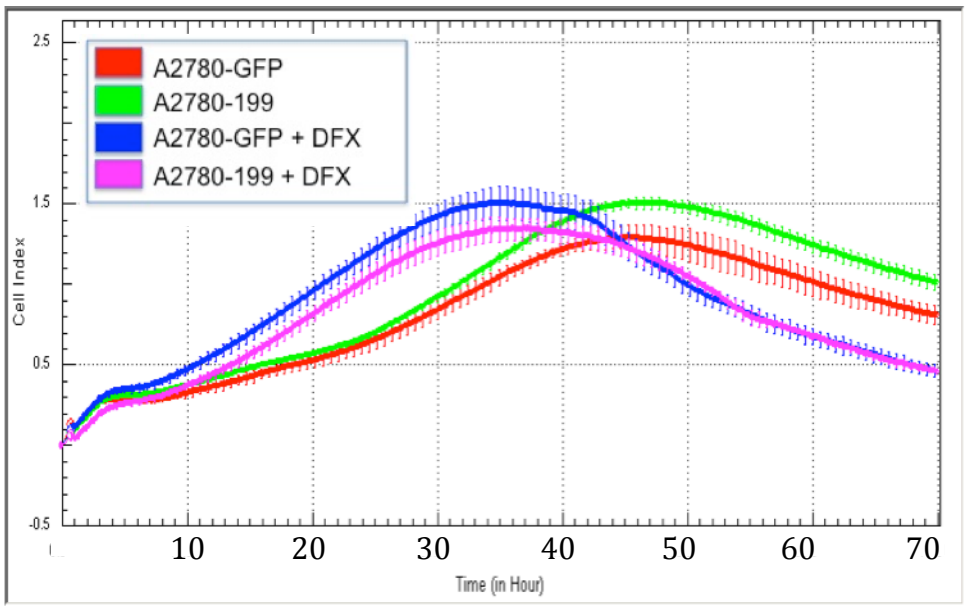

Figure 43: MiR-199a has a small effect on EOCC proliferation in Xcelligence assays. Growth rates were measured using the Roche Xcelligence system, which monitoring real-time changes in impedance, outputted as "cell index," sensed by electrodes on the cell culture surface. To approximate hypoxia, as the unit could not be placed in a hypoxia chamber, the iron-chelating hypoxia mimetic DFX (500 uM) was used. **(a)** Proliferation rates for A2780-GFP and A2780-199 with and without DFX. **(b)** Proliferation rates for A2780-GFP and A2780-199 transfected with P to A HIF1α, with and without DFX. Plot color associations are as per the legend. Values represent mean +/- SD.

wells (48 wells for each cell type) in a 96-well plate and allowed the cells to grow at normal culture conditions for 4 weeks. In both cell types, all wells containing 16 or more cells showed colony formation. As shown in Figure 44, cells seeded at 8 cells per well or less showed no significant difference in colony formation between those cells overexpressing miR-199a and control cells. These results suggest that any growth disadvantages incurred by miR-199a overexpressing EOCCs are not due to suppression of a stem cell-like phenotype.

The findings highlighted in Figure 37c, namely, the retention of well-spread cell morphology under hypoxia in A2780 cells treated with miR-199a, led us to ask if cell motility may be affected by miR-199a as well. Indeed, hypoxic states drive cell migration through HIF1α by decreasing cell-cell and cell-ECM attachment [9, 153, 162, 163]. To test this hypothesis, we conducted scratch/wound assays with A2780-GFP and A2780-199 cells in normoxia and hypoxia. As shown by the representative images in Figure 45a, A2780-199 cells exhibited impaired migratory ability compared to A2780-GFP cells under both normoxia and hypoxia, with the defect more evident in low oxygen states. Quantification of scratch/wound experiments showed a 2-fold decrease in normoxia and a nearly 3-fold decrease in hypoxia in A2780-199 migration compared to control cells (Figure 45b). Transfection with P to A HIF1α, which we hypothesized would mitigate the inhibitory effects of miR-199a overexpression on cell motility, increased migration in both cell types; however, the greatest effect was seen in A2780-199 cells, especially under hypoxia (Figure 46a). Whereas in normoxia, treatment with P to H HIF1α increased migratory distance of both A2780-GFP cells and A2780-199 cells by approximately 15 percent, in hypoxia, P to A HIF1α did not augment migration distance

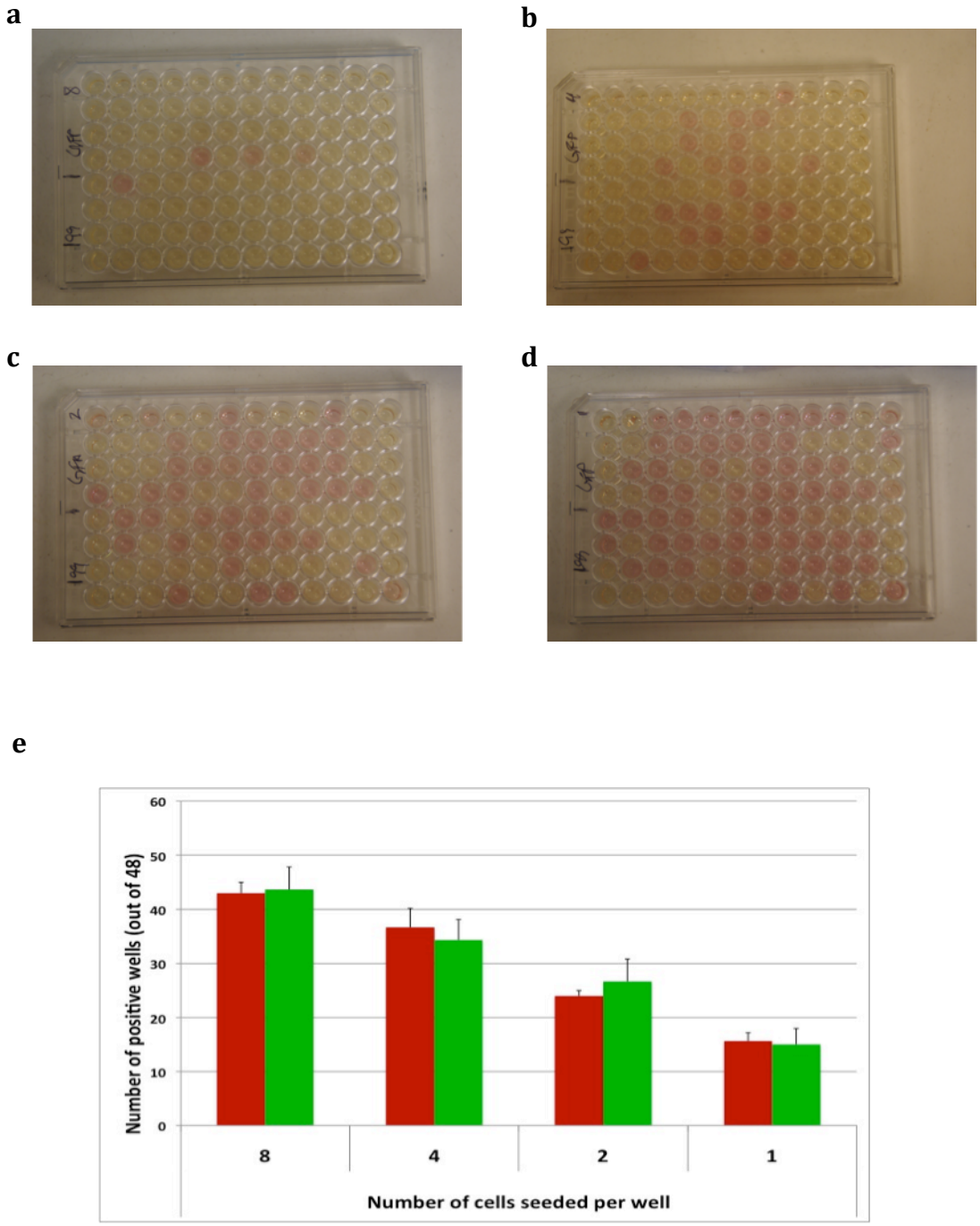

Figure 44: MiR-199a overexpression does not confer a clonogenic disadvantage to EOCCs. Representative images of clonogenic assays in which A2780-GFP cells (top rows) or A2780-199 cells (bottom rows) were seeded at 8 **(a)**, 4 **(b)**, 2 **(c)** or 1 **(d)** cells per well and grown for four weeks at normal culture conditions. Yellow wells indicate consumed media and, hence, clonogenic growth, whereas pink wells indicate no growth. **(e)** Quantification of three separate clonogenic assays conducted as in **(a-d)**. Red bars indicate A2780-GFP and green bars A2780-199. Values represent mean +/- SD.

in A2780-GFP cells while in A2780-199 cells wound closure jumped nearly 35 percent (Figure 46b).

To further investigate the role of miR-199a in EOCC migration, we again utilized the Roche Xcelligence system, in this instance to monitor, in real time, A2780-GFP and A2780-199 movement in a Boyden chamber-like system. Cells in serum-free media were added to the top chamber of a well separated from the serum-containing bottom chamber by a fine mesh comprised of gold electrodes. As cells bind and traverse the gold mesh from the serum-free to serum-containing chamber, they impart quantifiable changes in impedance that describe migration rates. As shown in Figure 47a, A2780-199 cell migration was significantly impaired compared to A2780-GFP cells in both normoxia and simulated hypoxia, which stimulated migration of A2780-GFP cells but, intriguingly, had the opposite effect on A2780-199 cells. Importantly, treatment with P to A HIF1α remarkably increased migration in both A2780-GFP (~3-fold increase) and A2780-199 (~4-fold increase) cells, nearly reversing miR-199a-induced impairment of migration under simulated hypoxia, in agreement with our scratch/wound data (Figure 47b).

These experiments demonstrate that hypoxia enhances EOCC migration, which can be inhibited under both normoxic and hypoxic conditions by miR-199a. Moreover, reconstituting A2780 cells with a form of HIF1α that is impervious to both normoxia- and miRNA-dependent degradation enhanced cell migration even in normoxia and in cells overexpressing miR-199a. Together, these findings implicate miR-199a as a potent inhibitor of HIF1α-induced EOCC migration.

Tumor cell migration is an important component of cancer metastasis and is promoted by HIF1α. Another essential step in the spread of malignant disease is the

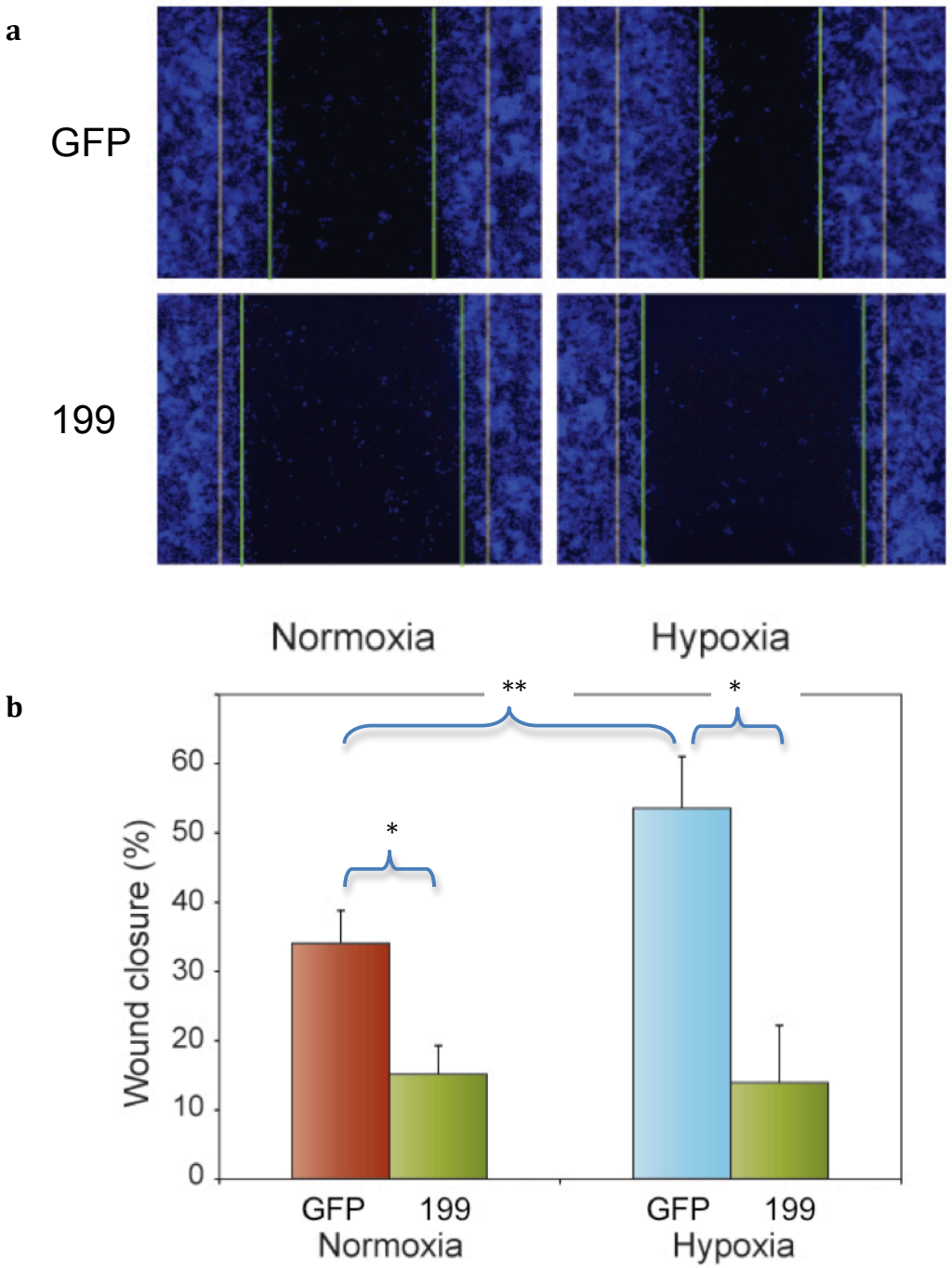

Figure 45: MiR-199a inhibits EOCC migration in normoxia and hypoxia. (a) Representative images of scratch/wound assays of A2780-GFP and A2780-199 cells exposed to normoxia and hypoxia for 24 hours, fixed and stained with DAPI. Yellow lines indicate average scratch width at t = 0. Green lines approximate extent of migration. **(b)** Quantification of scratch/wound assays described in **(a)**. Migration distances were measured from six wells per group and the average percent of wound closure was calculated. Red and blue bars indicate A2780-GFP cells in normoxia and hypoxia, respectively, and blue bars indicate A2780-199. Values represent mean +/- SD. *P< 0.01. **P<0.001.

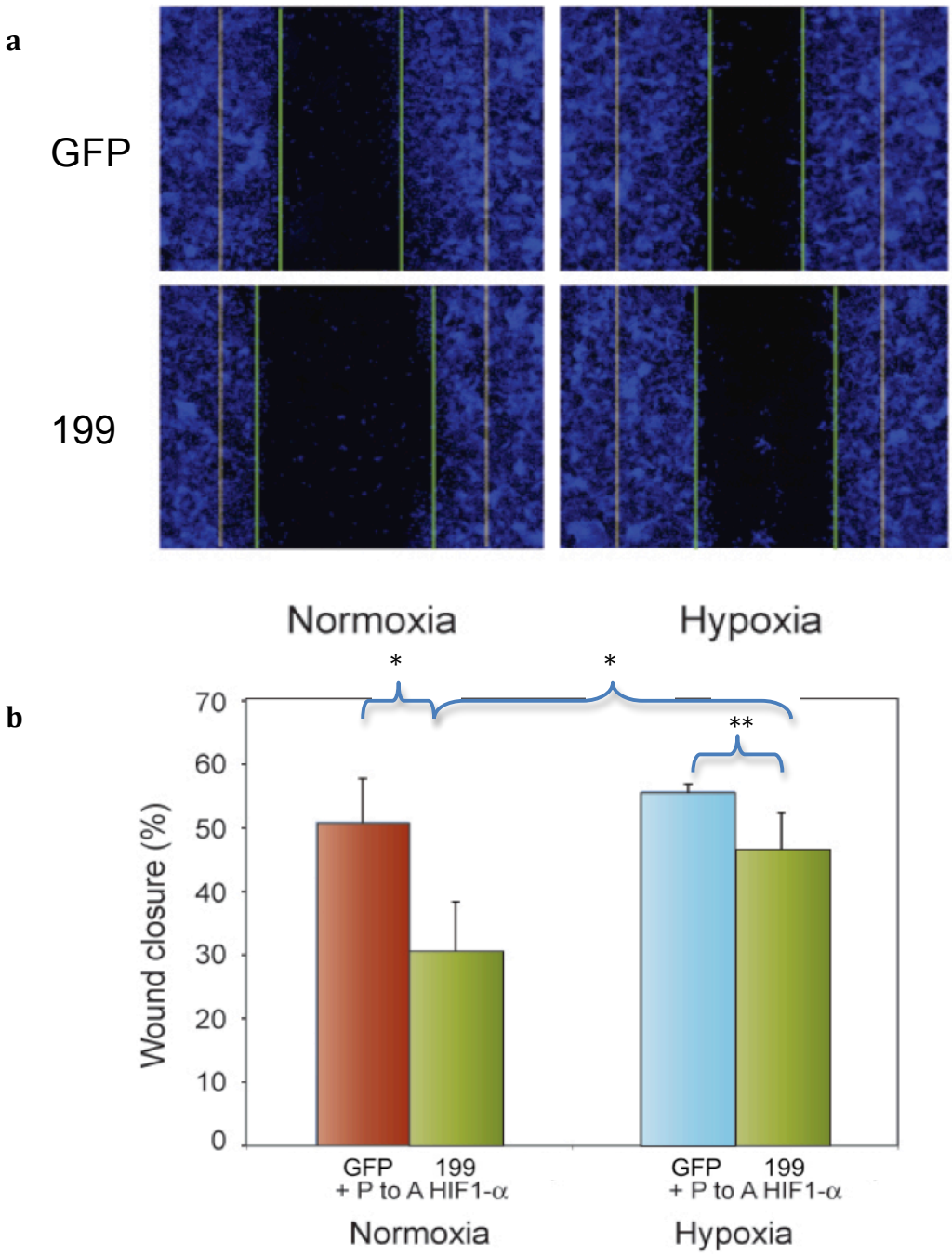

Figure 46: MiR-199a inhibition of EOCC migration in normoxia and hypoxia is reversed by a non-degradable form of HIF1α. (a) Representative images of scratch/wound assays of A2780-GFP and A2780-199 cells transfected with P to A HIF1α, exposed to normoxia and hypoxia for 24 hours, fixed and stained with DAPI. Yellow lines indicate average scratch width at t = 0. Green lines approximate extent of migration. **(b)** Quantification of scratch/wound assays described in **(a)**. Migration distances were measured from six wells per group and the average percent of wound closure was calculated accordingly. Red and blue bars indicate A2780-GFP cells in normoxia and hypoxia, respectively, and blue bars indicate A2780-199. Values represent mean +/- SD. *P<0.01. **P<0.04.

a

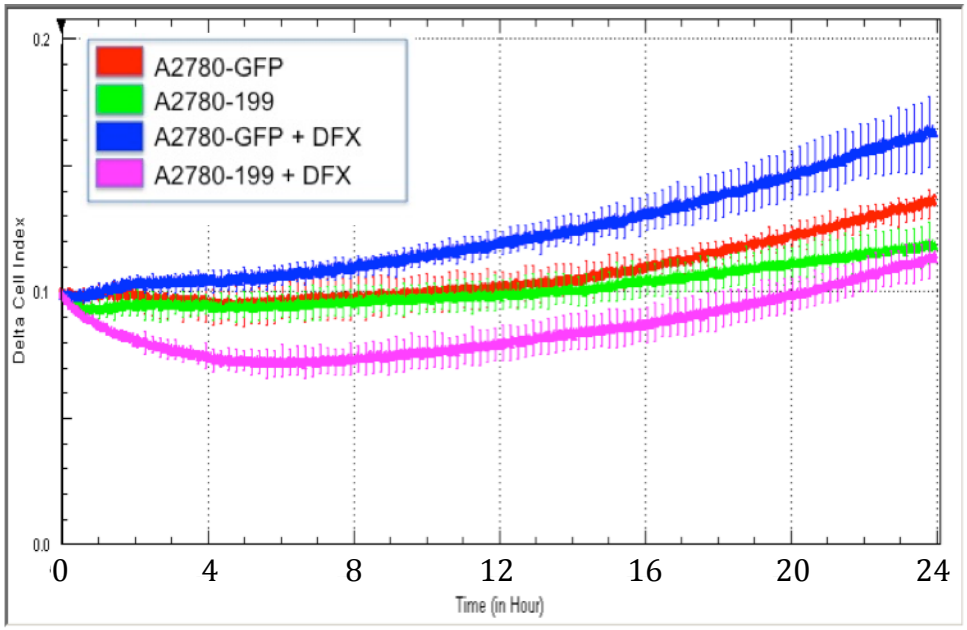

b

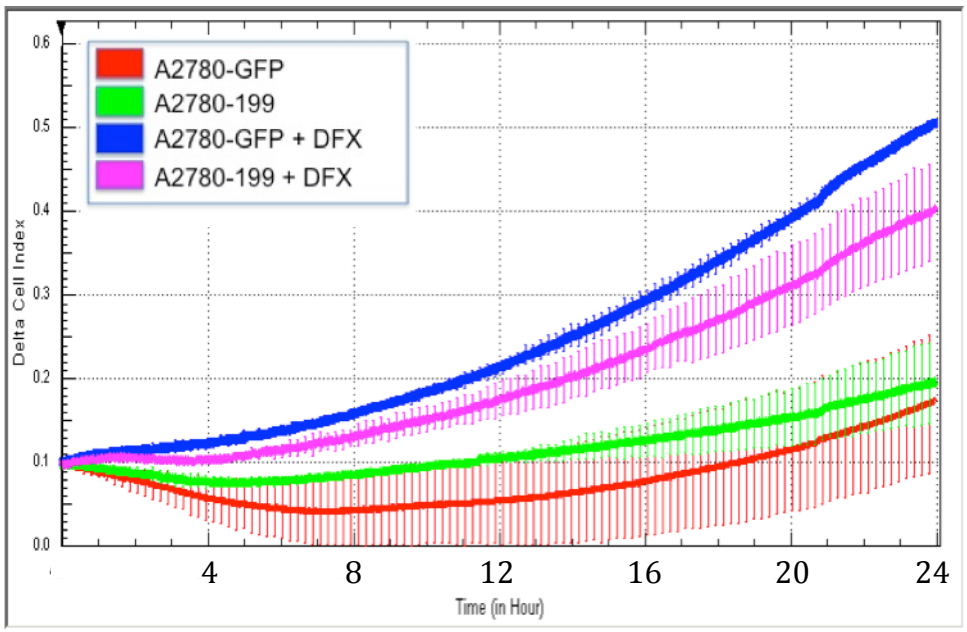

Figure 47: MiR-199a inhibits EOCC migration in hypoxia and normoxia, an effect that can be reversed by a non-degradable HIF1α. (a) The Roche Xcelligence system was used to determine real-time migration rates of A2780-GFP and A2780-199 cells. Cells were seeded into serum-free top chambers separated from serum-containing bottom chambers by a fine gold mesh capable of quantifying impedance-modulating migration across the membrane. DFX (500 uM) was used as a hypoxia mimetic. **(b)** A2780-GFP and A2780-199 cells were transfected with P to A HIF1α prior to seeding. Note the difference in scale of the axes. Plot color associations are as per the legend. Values represent mean +/- SD.

attachment of tumor cells at sites distal from the primary tumor, a process that is also HIF1α-dependent [9, 154, 156, 165]. We therefore examined the effect of miR-199a on EOC attachment to various substrates. Three different components of the ECM, laminin, fibronectin and collagen, as well as a substrate-free surface, were tested in the Roche Xcelligence system, which measures attachment in real-time as cells adhere to a gold-coated culture surface and cause quantifiable fluctuations in impedance. We found that while A2780-199 cells showed no deficiency in adhering to a fibronectin surface, attachment to a substrate-free, laminin or collagen surface was significantly impaired compared to control cells (Figure 48). These findings suggest that, even in normoxia, miR-199a may inhibit key aspects of EOC metastasis.

The defects in migration and adhesion associated with miR-199a overexpression led us to hypothesize that deficiencies in levels of LOX, a direct target of HIF1α transactivation, may be responsible. Indeed, levels of LOX, a key promoter of tumor cell metastasis, were found to be downregulated in our qPCR assays of A2780-199 cells (Figure 41e). With this in mind, we evaluated the effects of the LOX inhibitor, β-aminoproprionitrile (β-APN), on EOC migration to determine if an inhibitory effect similar to that conferred by miR-199a overexpression would be observed. Figure 49 shows that while A2780 cells treated with β-APN under normal conditions exhibited a slight, but insignificant, impairment in migration, under simulated hypoxia a striking contrast in migration emerged. These findings implicate LOX downregulation, as a consequence of HIF1α downregulation, in the mechanism underlying miR-199a-mediated inhibition of EOCC migration.

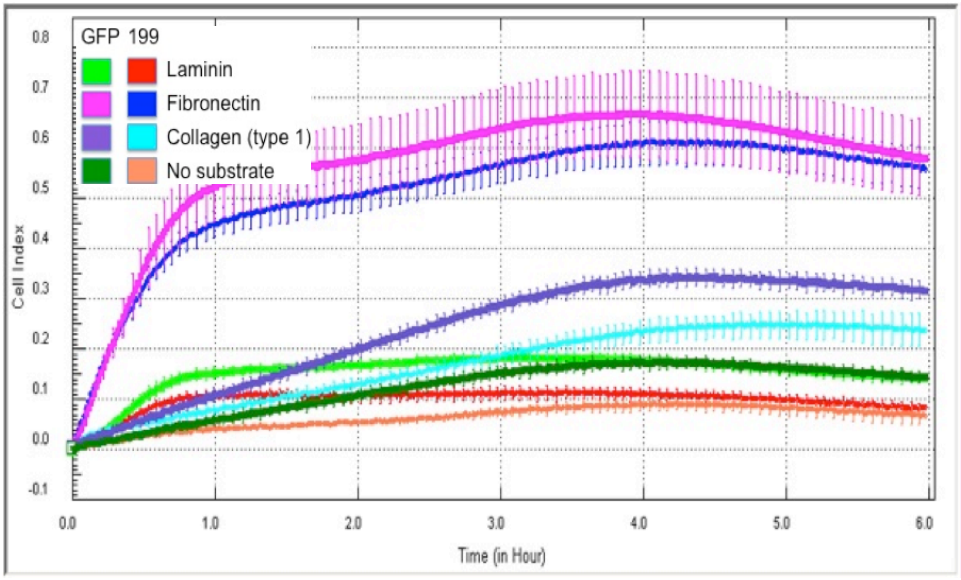

Figure 48: MiR-199a overexpression impairs EOCC attachment to ECM. The Roche Xcelligence system was used to measure EOCC attachment to various surfaces. Wells were coated with laminin, fibronectin, type 1 collagen or no substrate for 24 hours prior to being seeded with A2780-GFP or A2780-199 cells. Plot color associations are as per the legend. Values represent mean +/- SD. Courtesy of Dr. Yawu Jing.

MiR-199a inhibits tumor angiogenesis and growth in a mouse model of metastatic EOC

Our *in vitro* findings present evidence that miR-199a exerts anti-migratory effects on EOCCs through inhibition if HIF1α. We next wanted to determine if miR-199a would have similar consequences *in vivo*. To evaluate the effects of miR-199a on short-term metastatic potential of EOCCs, we injected A2780-GFP or A2780-199 cells intraperitoneally, which approximates EOCC dissemination from a primary ovarian tumor, into athymic female mice and visualized seeding of the ovaries/fallopian tubes and gastrointestinal (GI) tract using fluorescence imaging at 7 and 12 days post-injection. Significantly, animals injected with the miR-199a overexpressing line showed substantially less ovarian/fallopian seeding and GI involvement compared to those

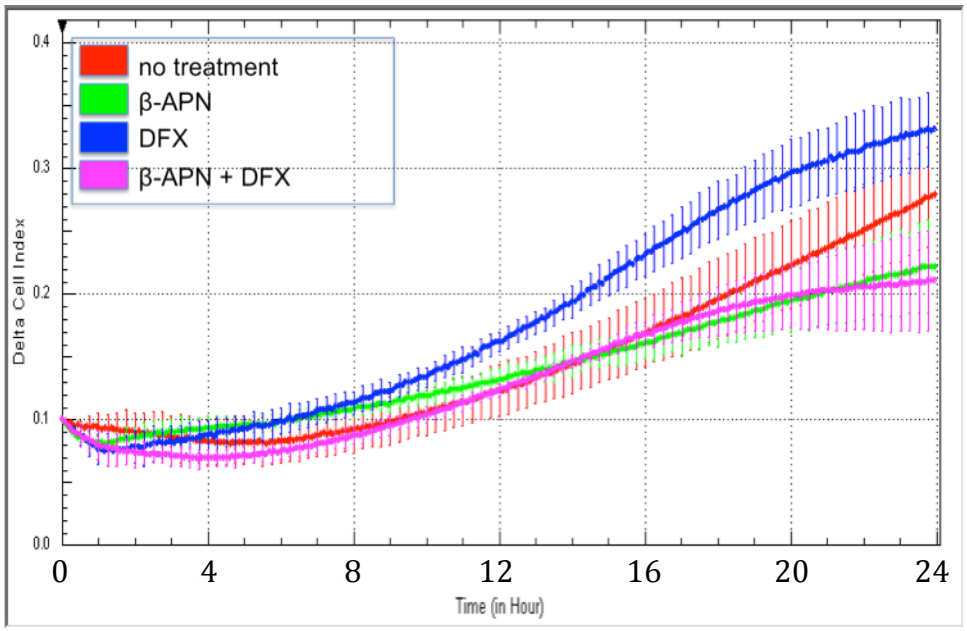

Figure 49: Inhibition of LOX causes migratory defects in EOCCs. Migration rates of A2780 cells were measured with and without the LOX inhibitor, β-APN (300 uM) under normal coniditions and simulated hypoxia (DFX, 500 uM) on the Roche Xcelligence platform. Plot color associations are as per the legend. Values represent mean +/- SD.

inoculated with control cells. While at day 7 ovarian seeding was already visible in the A2780-GFP bearing mice, no such implants were apparent in A2780-199 mice (Figure 50a, left panels). Moreover, whereas all four mice injected with A2780-GFP cells showed multiple sites of robust metastatic growths on the ovaries/fallopian tubes by day 12, only two mice injected with A2780-199 cells exhibited similar multifocal disease, and these growths were of much smaller size (Figure 50a, right panels). Examination of the GI reinforced these findings. Mice injected with A2780-GFP showed extensive metastases along the GI tract in three out of four mice (Figure 50b, top panels). In contrast, mice injected with miR-199a overexpressing A2780 cells showed minimal GI involvement (Figure 50b, bottom panels). Together, these initial *in vivo* observations demonstrate that in our IP model, miR-199a has a significant inhibitory effect on EOC seeding.

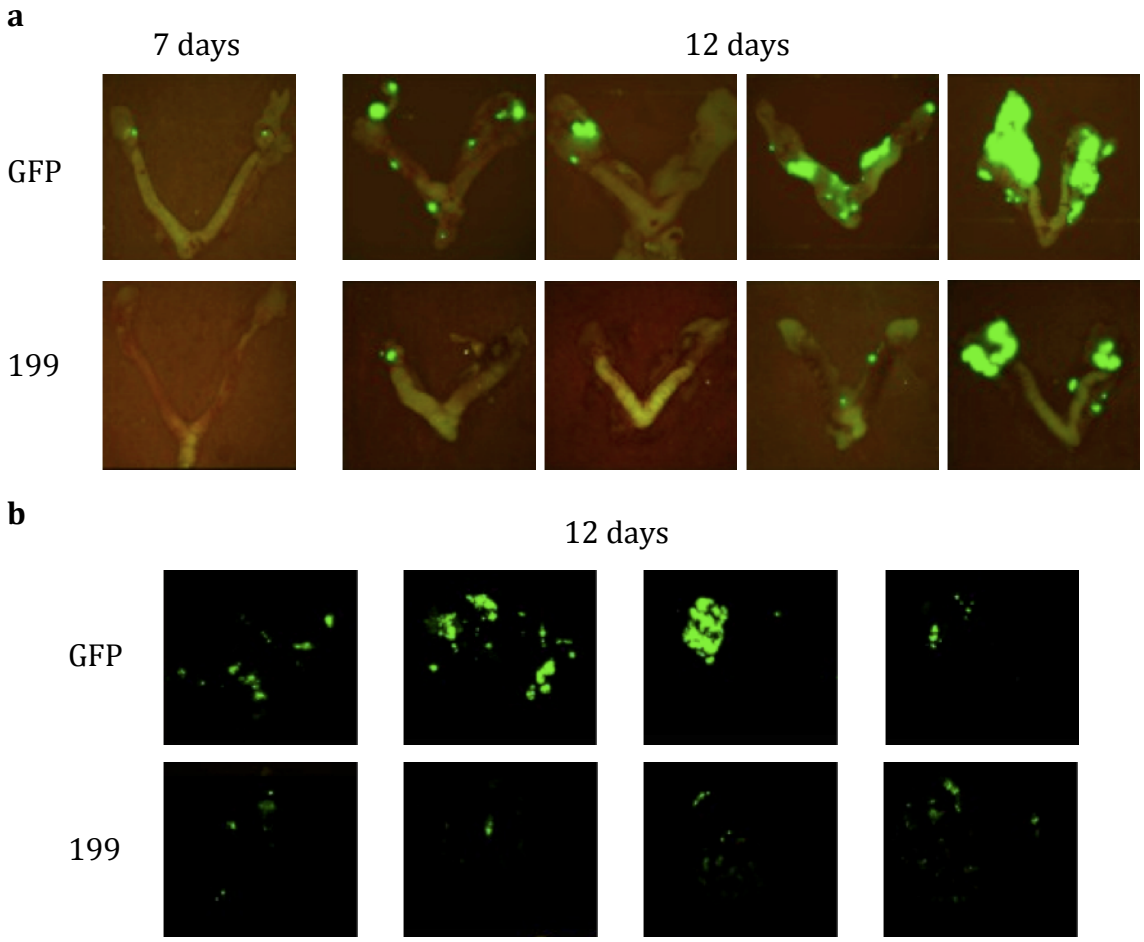

Figure 50: MiR-199a inhibits ovarian/fallopian tube and gastrointestinal seeding in a mouse model of metastatic EOC. Mice were injected intraperitoneally with A2780-GFP or A2780-199 cells and were sacrificed at the indicated time points. Ovaries/fallopian tubes **(a)** and GI tract **(b)** were then removed for fluorescence imaging.

To complement these qualitative results with quantitative *in vivo* studies, we performed a similar experiment on a larger scale with the aim of evaluating tumor angiogenesis and burden in the same metastatic model of EOC. Four groups of 10 mice were injected with either A2780-GFP or A2780-199 and then treated with carboplatin or vehicle control every four days. After four weeks, animals were sacrificed and whole-body imaged and tumors were removed, weighed and processed for histopathological

analysis. Representative images of mice from these four groups are shown in Figure 51. As is clear from these pictures, mice inoculated with A2780-GFP cells developed much larger and more disseminated tumors compared to mice injected with A2780-199 cells. Furthermore, the effect of carboplatin treatment, which was significant for A2780-GFP-injected mice, was even more pronounced in mice bearing miR-199a overexpressing tumors. Indeed, most mice in the latter group exhibited negligible levels of disease as determined by whole body imaging.

Calculation of tumor burden in each of these groups corroborated the findings evidenced by these images (Figure 52). Overexpression of miR-199a in A2780 cells cut average tumor burden nearly in half, from over 8 grams to approximately 5 grams, having the same effect as carboplatin treatment of A2780-GFP cells. Moreover, mice injected with A2780-199 cells and treated with carboplatin displayed a remarkable 3-fold reduction in average tumor burden compared to untreated control mice. To be sure, these findings demonstrate that miR-199a overexpression has significant *in vivo* consequences in addition to the important *in vitro* effects described earlier.

To better understand the anti-cancer effects of miR-199a at the level of the tumor microenvironment, we next performed histological analysis of tumor sections isolated from the four groups of mice. Staining for lectin, an endothelial marker of vasculature, allowed us to examine the role of miR-199a in tumor angiogenesis. Overall, vasculature was significantly reduced in both groups of mice injected with A2780-199 cells compared to those injected with A2780-GFP cells. Representative images highlighting this finding are shown in Figure 53 and measurement of vascular density by quantification of vessel ends, nodes and length is displayed in Figure 54. Specifically, the

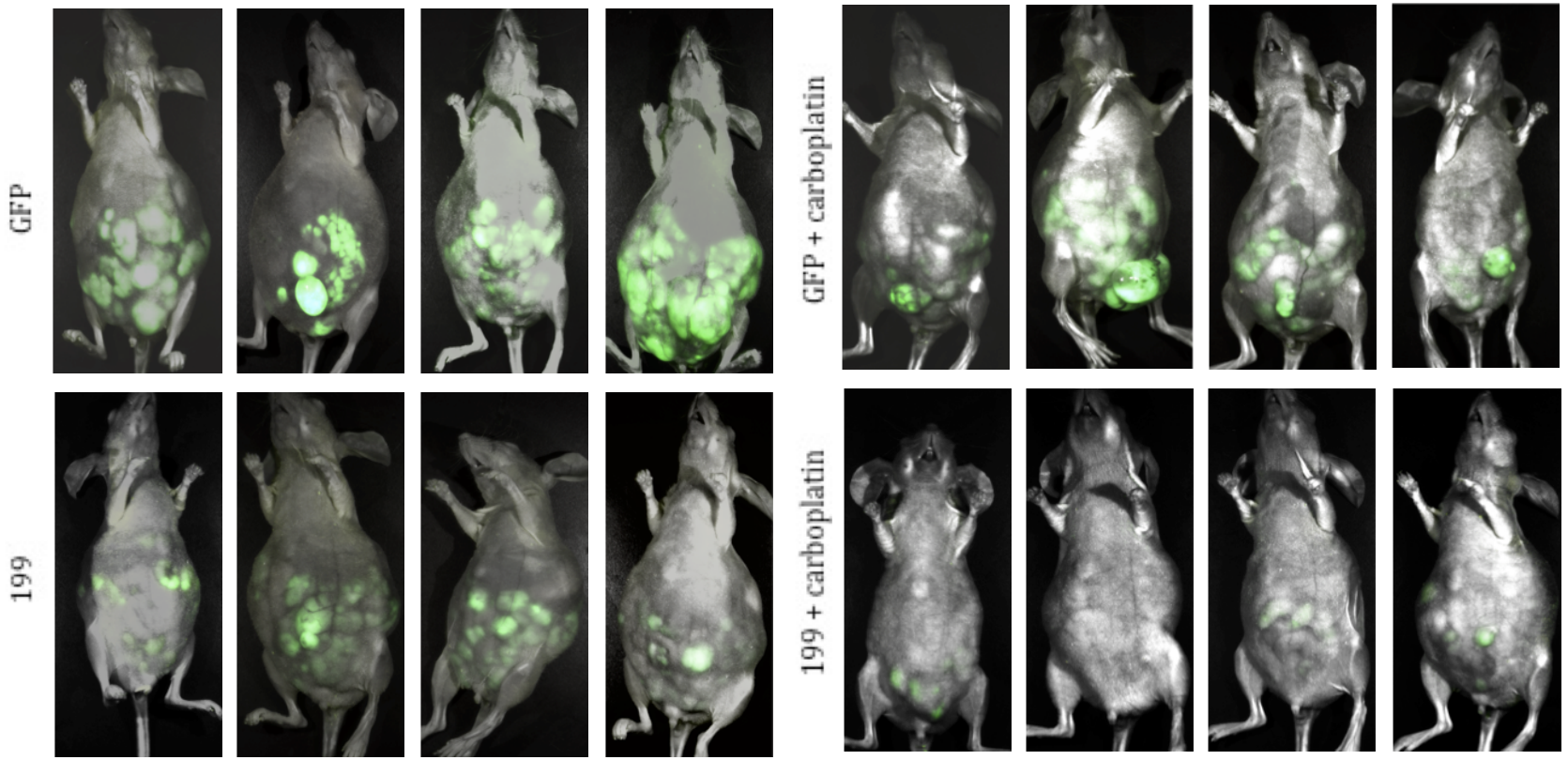

Figure 51: MiR-199a overexpression reduces tumor burden in a mouse model of metastatic EOC. Representative images of mice bearing A2780-GFP or A2780-199 tumors with and without carboplatin treatment. Athymic female mice were injected intraperitoneally with A2780-GFP cells or A2780-199 cells. Half of the mice received IP carboplatin treatment every four days while the other half received IP injections of vehicle. After four weeks, mice were sacrificed and the fluorescent tumors were visualized. Corresponding quantification of average tumor burden is shown in Figure 52.

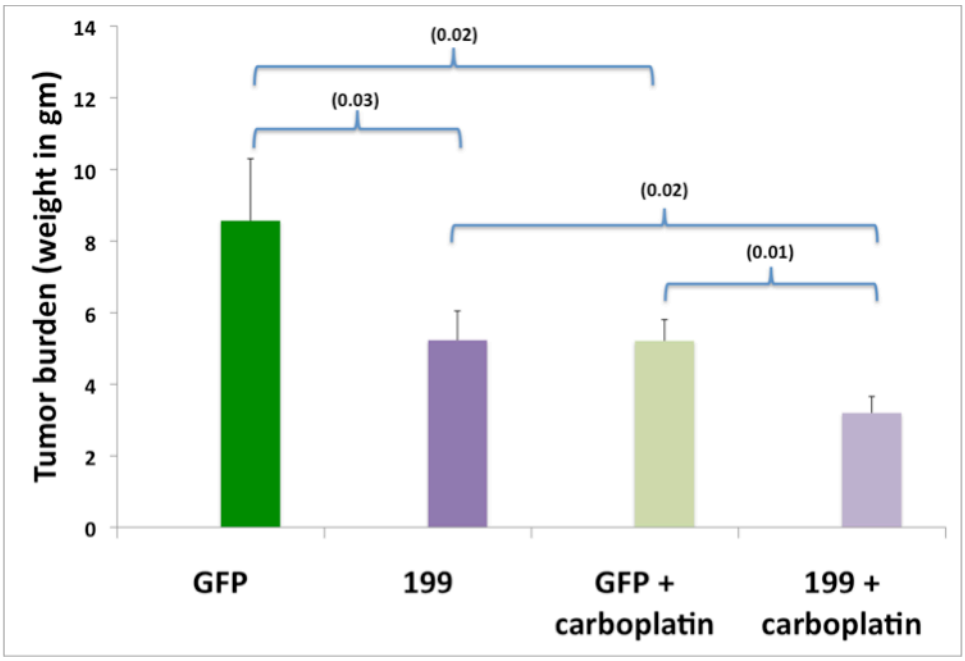

Figure 52: miR-199a overexpression reduces tumor burden in a mouse model of metastatic EOC. Quantification of tumor weight in mice bearing A2780-GFP or A2780-199 tumors with and without carboplatin treatment. Athymic female mice were injected intraperitoneally with A2780-GFP cells or A2780-199 cells. Half of the mice received IP carboplatin treatment every four days while the other half received IP injections of vehicle. After four weeks, mice were sacrificed and tumors were removing for weighing. Corresponding representative images from this study are displayed in Figure 51. Values represent mean +/- SE. P-values indicating statistical significance are in parentheses.

.

average number of vessel ends was reduced greater than 2-fold, the average number of vessel nodes was reduced greater than 3-fold and average vessel length decreased nearly 3-fold in tumors that overexpressed miR-199a compared to control tumors. By all these metrics, vasculature in A2780-199 tumors was substantially reduced compared to A2780-GFP tumors, indicating that miR-199a plays a role in inhibiting angiogenesis, perhaps through HIF1α. Of note, carboplatin treatment had minimal effects on vessel density, correlating only with a slight (but significant) drop in average number of vessel ends for A2780-GFP tumors. A2780-199 tumors, on the other hand, showed no more anti-angiogenic potential when treated with carboplatin than when untreated.

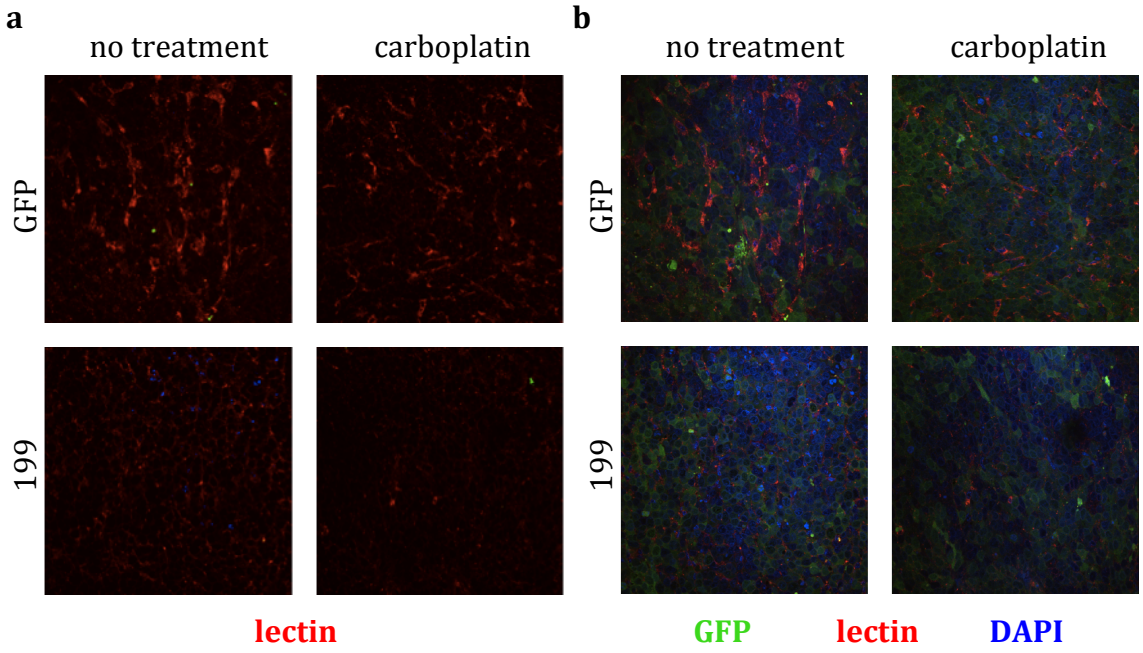

Figure 53: MiR-199a overexpression reduces intratumoral vascular density in EOC. Representative images of tumor vasculature from mice injected IP with control or miR-199a-overexpressing EOCCs with and without carboplatin treatment. Tumor sections from mice inoculated IP with A2780-GFP or A2780-199 cells were fixed and stained with lectin, an endothelial marker of vasculature, and DAPI. **(a)** Lectin-only image showing intratumoral vessels. **(b)** GFP, lectin and DAPI merge image showing A2780 cells, vessels and cell nuclei. **(c)** Skeletonization of lectin staining from **(a)**, showing method used to quantify vessel ends, nodes and length (Figure 54).

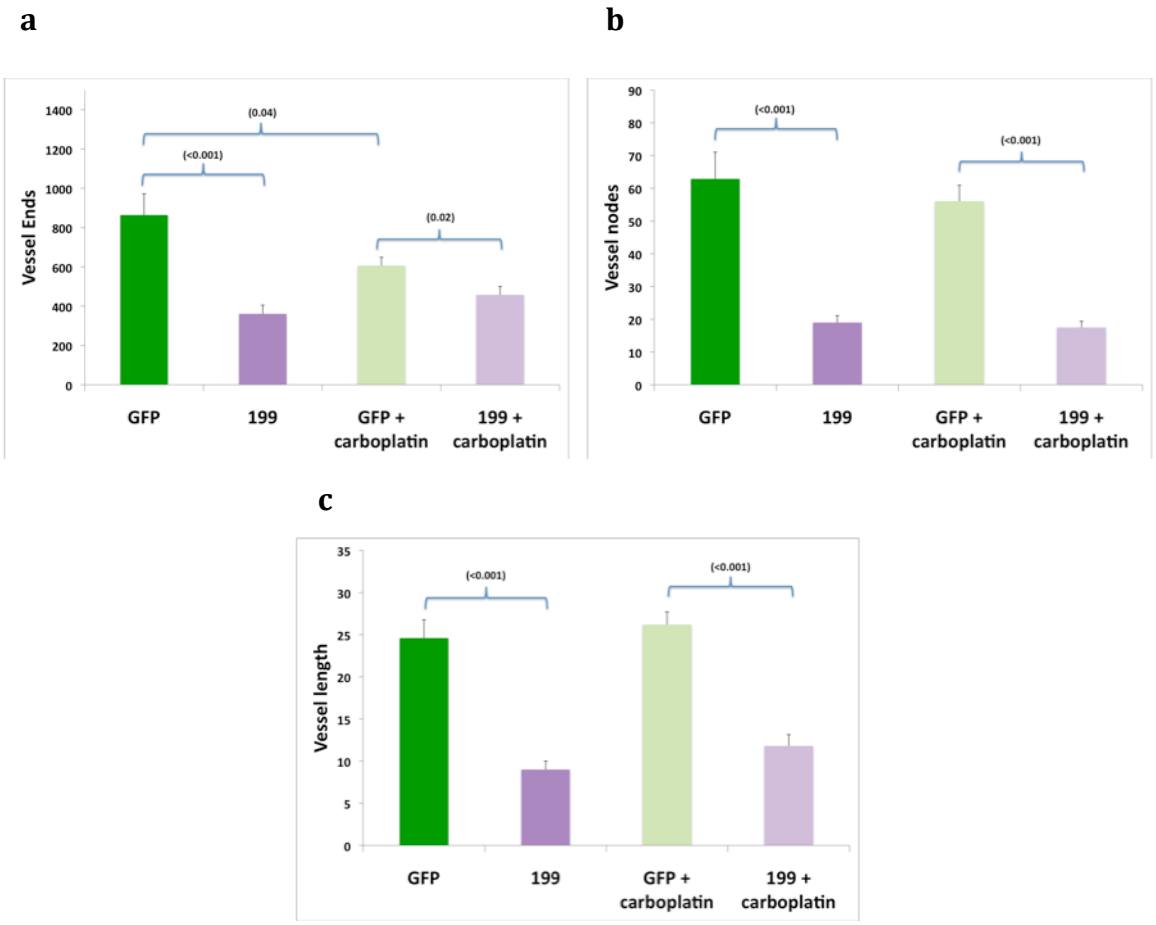

Figure 54: MiR-199a overexpression reduces intratumoral vascular density in EOC. Quantification of tumor vasculature in mice injected IP with control or miR-199a-overexpressing EOCCs with and without carboplatin treatment. Average number of vessel ends **(a)** and vessel nodes **(b)** and length of vessels **(c)** was measured based on skeletonization of lectin-stained tumor sections. Corresponding representative images from this study are displayed in Figure 53. Values represent mean +/- SE. P-values indicating statistical significance are in parentheses.

Long-term deficiencies in oxygen and nutrient supply within the tumor microenvironment, a certain consequence of impaired angiogenesis and reduced vessel density, are associated with the development of tumor necrosis [6]. As such, we examined hematoxylin-eosin stained tumor sections to determine if miR-199a overexpression induces death of cancer tissue. As evidenced by representative images

(Figure 55a) and quantification of necrotic areas (Figure 55b), A2780-199-derived tumors developed significantly larger areas of dead tissue compared to A2780-GFP-derived tumors. Whereas approximately 10 percent of control tumors exhibited the characteristic pink stain of tissue necrosis by area, nearly 40 percent of miR-199a overexpressing tumor area was necrotic (Figure 55b). Furthermore, while A2780-GFP tumors seemed to retain vascular supply to most areas, A2780-199 tumors exhibited a dearth of vasculature (Figure 55a). Carboplatin treatment increased A2780-GFP necrosis to approximately 30 percent of tumor area, but, surprisingly, treatment of mice bearing A2780-199 tumors with carboplatin did not result in any further development of tumor necrosis (Figure 55b). Nevertheless, necrotic areas in these samples appeared more confluent compared to the diffuse localization of dead tissue in the untreated A2780-199 tumors (Figure 55a). This unexpected finding suggests that the combined effect of carboplatin treatment and miR-199a overexpression in EOCCs in reducing tumor burden may be a result of multiple, distinct pathways.

The revelation that overexpression of miR-199a in EOCCs reduces tumor burden *in vivo* led us to pursue an additional *in vitro* study. In particular, we wanted to evaluate the effects of carboplatin on EOCC proliferation. We therefore used the Roche Xcelligence system and measured the rate of EOCC growth upon treatment with multiple doses of carboplatin. Figure 56 shows that the growth profiles of A2780-GFP cells and A2780-199 are markedly different with addition of carboplatin. As observed previously, even untreated EOCCs overexpressing miR-199 exhibit a growth defect. However, the contrast in proliferation rates between A2780-GFP and A2780-199 cells is even more apparent with carboplatin treatment, with the former group only showing slight

a

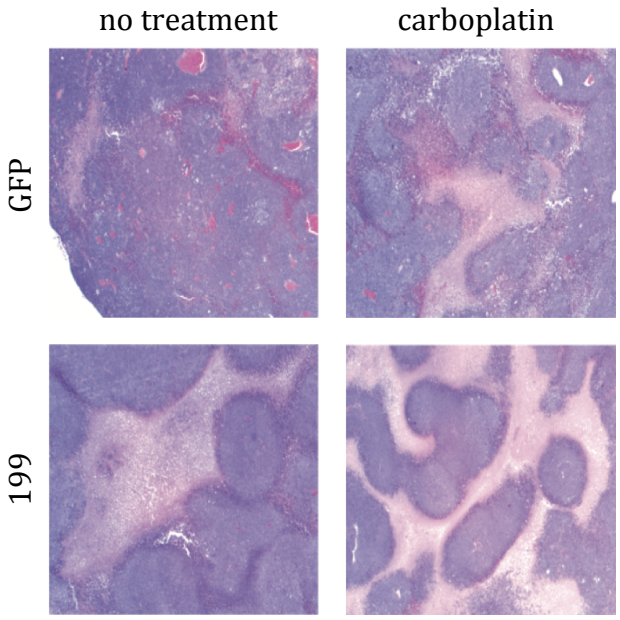

b

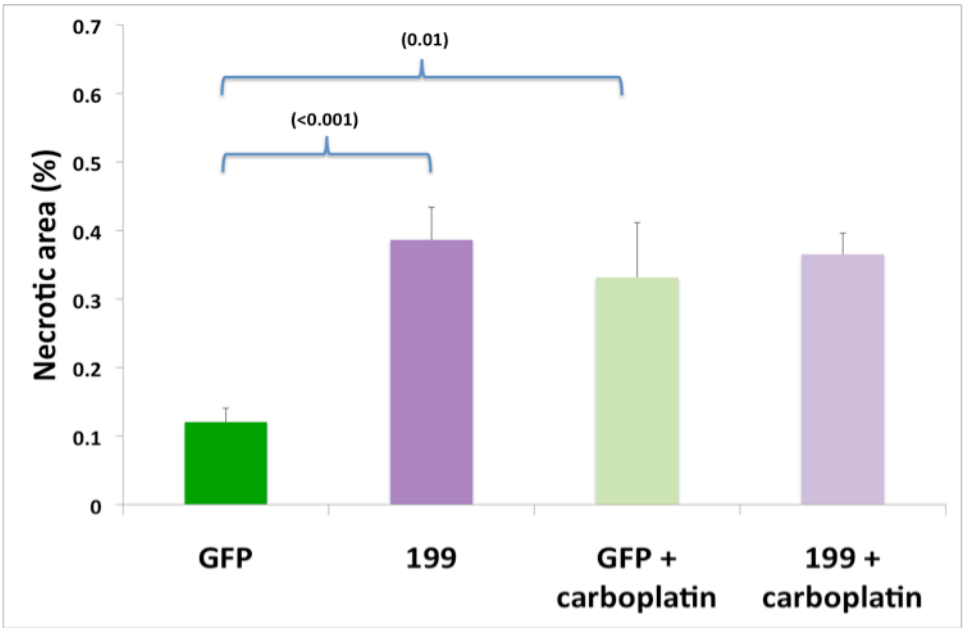

Figure 55: MiR-199a overexpression increases tumor necrosis in EOC. (a) Representative images of hematoxylin and eosin stained tumor sections from mice injected IP with control or miR-199a-overexpressing EOCCs with and without carboplatin treatment. Pink-stained areas show areas of tissue necrosis. Purple-stained areas are healthy tissue. Red areas denote vasculature. **(b)** Quantification of necrotic area as a percent of total tumor area (pink areas compared to combined pink and purple areas). Values represent mean +/- SE. P-values indicating statistical significance are in parentheses.

suppression and the latter group showing near flattening of growth curves. These data suggest miR-199a potentiates the effects of carboplatin, supporting our *in vivo* findings.

In total, our studies demonstrate that miR-199a is downregulated in hypoxic EOCCs in a dnm2 promoter-dependent manner. Moreover, miR-199a targets the HIF1α 3' UTR, inhibits HIF1α expression and suppresses transactivation of HIF1α target genes. These effects translate to phenotypic defects, with proliferation, migration and attachment being impaired in EOCCs overexpressing miR-199a. miR-199a overexpression has *in vivo* consequences as well. Mice bearing EOCs overexpressing miR-199a develop less vascularized, more necrotic and smaller tumors than control mice. Treatment with carboplatin enhances the inhibitory effect of miR-199a on tumor growth. Together, these studies highlight the importance of miRNA-mediated regulation of the hypoxic response in tumor progression.

a

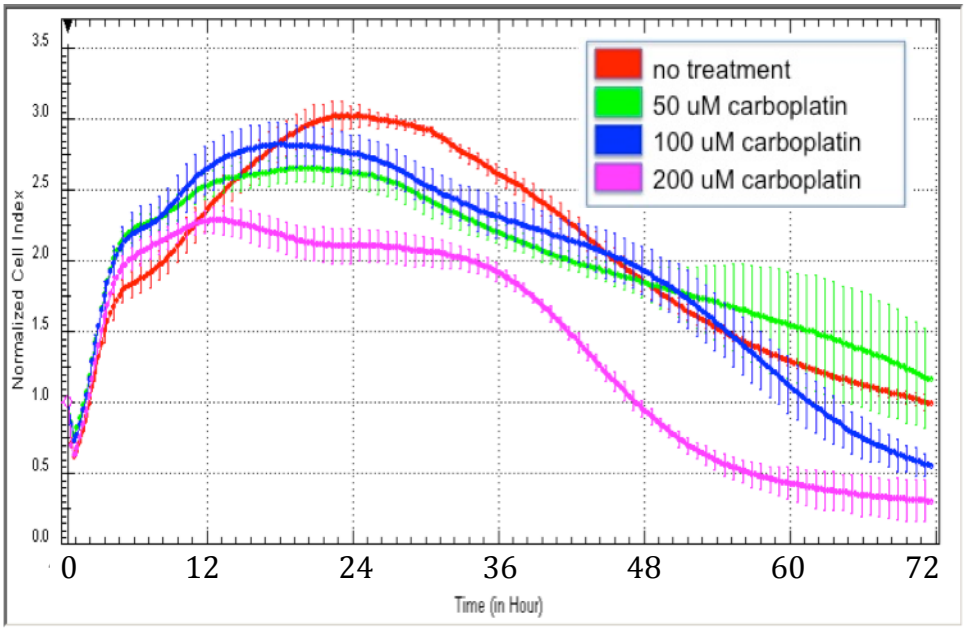

b

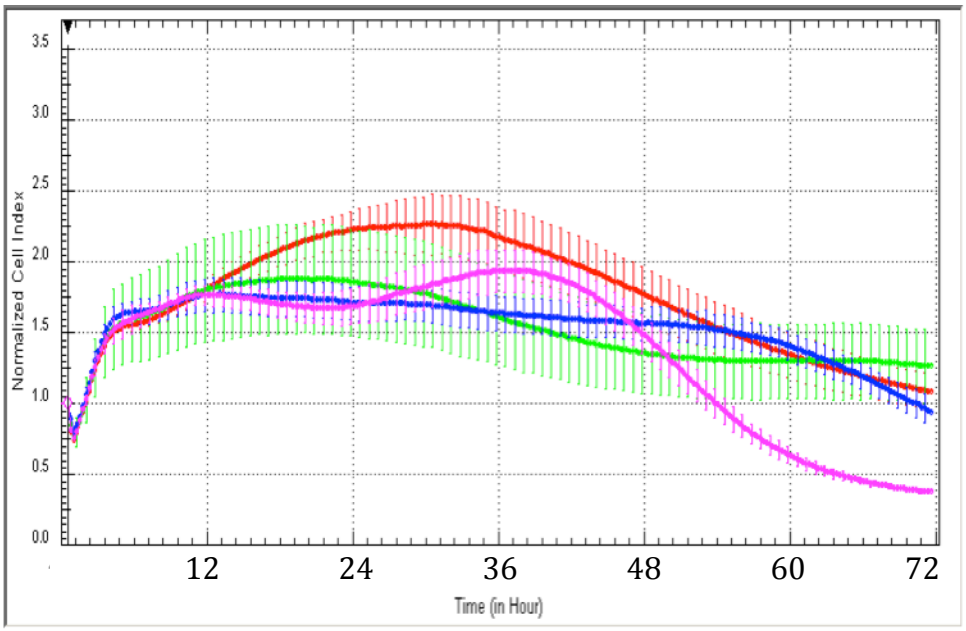

Figure 56: MiR-199a overexpression renders EOCCs more sensitive to carboplatin treatment. A2780-GFP cells **(a)** and A2780-199 **(b)** cells were treated with varying doses of carboplatin (50, 100 and 200 uM) and proliferation rates were measured on the Roche Xcelligence platform. Cells were seeded and grown overnight and drug added the next morning. Data are normalized to time of drug addition. Plot color associations are as per the legend. Values represent mean +/- SD.

Discussion

In this work, we have shown that dynamin 2 and a miRNA contained within one of its introns, miR-199a-1, are downregulated in hypoxic EOCCs, a change that is effected by elements in the dnm2 promoter (Figures 21, 22, 24, 30, 33). Of greatest importance to expression of dnm2 and miR-199a-1 is a 450-nucleotide area that we have called the "critical region" (Figure 24). Bioinformatic analysis of this area shows several putative transcription factor binding sites. Interaction of one of these transcription factors with the dnm2 promoter is likely necessary for expression of dnm2 and miR-199a-1 under all oxygenation conditions (Table 7). In hypoxic conditions, the hypoxia-response element we have labeled "HRE 2" is of great importance in regulation of dnm2/miR-199a-1 expression. Mutation or deletion of HRE 2 resulted in a significant increase in expression of dnm2/miR-199a-1 in hypoxia, indicating that the transducer of dnm 2 and miR-199a-1 suppression signals in low oxygen states, whatever it may be, requires interaction with this site (Figure 22).

An obvious candidate for this role is HIF1α, the master regulator of the hypoxic response in mammalian cells. While in most cases HIF1α acts as a transcriptional activator, it has also been shown to repress transcription by interacting with HREs [338, 339]. We evaluated the effects of HIF1α on dnm2/miR-199a-1 expression in this regard by overexpressing the transcription factor in normoxia and knocking it down in hypoxia (Figure 23). That stabilization of HIF1α in normoxia did not have as much of an effect on suppressing dnm2 expression as downregulation of HIF1α in hypoxia had on increasing

dnm2 expression suggests that HIF1α is necessary, but not sufficient, to exert the inhibitory effects on dnm2/miR-199a-1 expression observed in hypoxia. That is, additional elements are required for HIF1α-mediated regulation of dnm2/miR199a-1 in low oxygen states, but HIF1α is a crucial component of the inhibitory machinery. To establish for certain that HIF1α interacts with HRE 2 to downregulate dnm2/miR-199a-1 expression in hypoxia, chromatin immunoprecipitation assays are required. These experiments would also enable us to determine, which, if any, other factors associate with HIF1α to exert suppressive effects on the dnm2/miR-199a-1 in hypoxia.

The findings of our dnm2 promoter experiments raise a fundamental question: why do cells downregulate dnm2/miR-199a-1 in hypoxia? In the case of dynamin 2, this question exposes the dichotomous nature of dnm2 activity. As is common in hypoxic conditions, tumor cells shunt resources from non-essential processes to critical ones to maintain cell viability in the face of severe oxygen and nutrient deficits [9, 56, 69]. One cellular function in tumor cells that suffers as a result is endocytosis, an energy-consuming process that is suppressed in low oxygen states [345]. Specifically, endocytosis of growth factor/receptor complexes is inhibited by HIF1α-mediated downregulation of rabaptin-5, a necessary component of endocytic machinery that associates with dnm2, resulting in constitutive activation of survival and proliferative pathways (adding to the litany of hypoxia's tumorigenic roles) [346]. Growth factor/receptor endocytosis is directly related to the primary function of dynamins, which are responsible for the pinching-off step in clathrin-coated endocytic processes. Thus HIF1α-mediated downregulation of dnm2 in hypoxia may help explain the decrease in growth factor/receptor endocytosis observed in hypoxic tumor cells.

On the other hand, dnm2 also plays a role in cell motility by interacting with cytoskeletal elements such as actin, microtubules and focal adhesion kinases [236, 244]. Its precise function in this regard, is muddled, however, as cell movement requires both detachment and subsequent reattachment and dnm2 is involved in both of these processes. In general, due to its role in promoting E-cadherin uptake, membrane ruffling and FAK disassembly, dnm2 is thought to be pro-migratory [240]. In hypoxia, tumor cells often undergo epithelial-mesenchymal transition (EMT), a process dnm2 enhances, as they strive to escape low-resource environments and colonize areas with increased resource availability. It is counterintuitive, then, to think that tumor cells in low oxygen conditions would downregulate expression of dnm2, which would only aid this process. Certainly, it is plausible that dnm2-mediated cell motility is overshadowed by other, more significant, pro-migratory mechanisms in hypoxic tumor cells and, indeed, most canonical mechanisms of hypoxia-induced cell metastasis do not involve dnm2 [9, 211, 220].

Aside from its role in endocytosis and cell motility, we show in this work that dnm2 negatively regulates HIF1α, which could explain its downregulation in hypoxia. Inhibition of dnm2 function in normoxic EOCCs by the small molecule inhibitor, dynasore, leads to rapid accumulation of HIF1α protein (Figure 25). This remarkable result seems to involve changes in intracellular iron levels, which are largely regulated by dnm2-mediated endocytosis of transferrin/iron. Dynasore treatment decreases the intracellular labile iron pool on the order of minutes to hours, the same time scale in which HIF1α stabilization was observed (Figure 27). Moreover, saturation of cells with ferric ammonium citrate, a form of iron that can be taken up by cells in a dnm2-

independent manner, reverses both dynasore-mediated reduction in intracellular iron levels and increase in HIF1α protein levels (Figures 26 and 27). We believe that dynasore's inhibition of dnm2-mediated iron uptake impairs prolyl hydroxlase-based hydroxylation of HIF1α, as this step requires iron as a cofactor in the hydroxlyase reaction. Unfortunately, standard assays to test PHD activity directly are all cell-free procedures, which would undermine the basis of our experiments as they require cells to be intact for inhibition of endocytosis by dynasore. Still, a reduction in PHD hydroxylation would abrogate HIF1α polyubiquitination, a finding that we confirmed by western blot (Figure 28). Alternatively, overexpression of dnm2 in hypoxia, which would presumably increase iron uptake, suppressed levels of HIF1α, perhaps by stimulating PHD-based hydroxylation (Figure 29). These findings link hypoxia/HIF1α-based regulation of the dnm2 promoter, intracellular iron levels and PHD activity and HIF1α protein stability. As such, our results establish a positive feedback loop that we envision functions as follows: HIF1α stabilization in hypoxia interacts with HRE 2 in the dnm2 promoter to suppress expression of dnm2. Dnm2 downregulation results in decreased iron uptake, impairing PHD activity and further stabilizing HIF1α.

These conclusions are contrary to many of the current paradigms linking hypoxia and iron homeostasis, which posit that hypoxia increases intracellular iron levels by increasing expression of transferrin, transferrin receptor, and ferritin. These HIF1α-driven actions are presumably to increase erythropoiesis and, consequently, delivery of oxygen to starved tissues. However, the only cells directly involved in erythropoeisis are those in hematopoietic tissues. Thus increased iron uptake in hypoxic EOCCs or other non-hematopoietic cells would be of little relevance in the context of red blood cell

production. A recent study examined this issue, and found that skeletal muscle of human subjects exposed to high altitude hypoxia, contrary to expectation, actually showed decreased levels of transferrin, ferritin and intracellular labile iron compared to control subjects [347]. These developments occurred despite elevation of HIF1α mRNA and normal function of iron-response proteins, which are classically thought to increase intracellular iron levels. Furthermore, hypoxic skeletal muscle actually increased mRNA levels of the iron-exporting molecule ferroportin. Based on these findings, the authors proposed that regulation of intracellular iron levels cannot be separated from holistic iron regulation. In other words, distribution of iron to various areas of the body is based on tissue demand and the identity of the hypoxic tissue under consideration is crucial in determining whether hypoxia induces increases or decreases in intracellular iron levels [348]. Other studies have determined that levels of hepcidin, a negative regulator of iron export from the cell to plasma, decrease in hypoxia – in a HIF1-dependent manner [349-351]. In low oxygen states, then, iron transport out of the cell increases via this mechanism. These studies demonstrate that hypoxia-induced perturbations in iron homeostasis depend on cell type and can result in suppressed iron uptake and/or increased iron export and are consistent with our hypothesis that hypoxia decreases intracellular iron stores in EOCCs by downregulating dnm2.

To be sure, several additional experiments are necessary to confirm the plausibility of our model. In particular, a simple confirmation that hypoxia reduces intracellular iron levels in EOCCs is requisite. Overexpressing dnm2 in hypoxic EOCC to determine if iron levels change would also help validate our hypothesis. Other studies, such as real-time imaging studies of changes in iron and HIF1α levels upon dynasore

treatment and immunoprecipitation assays to determine polyubiquitination status of HIF1α directly in cells treated with dynasore, are also necessary. Finally, evaluating whether dnm2-based regulation of HIF1α has functional consequences, that is, affects expression of target genes such as VEGF, would underscore the importance of the dnm2-HIF1α relationship. Nevertheless, with the results presented herein, we have identified a novel mechanism of HIF1α regulation that is based on dynamin 2.

The answer to the question "why do EOCCs downregulate miR-199a-1 in hypoxia" is more straightforward. In this work, we have shown that the HIF1α 3' UTR suppresses expression of a luciferase reporter in normoxia but not after 24 hour exposure to hypoxia (Figure 34). Moreover, miR-199a-5p targets the HIF1α 3' UTR at a specific site to downregulate HIF1α expression (Figures 35 and 37). Downregulation of miR-199a in hypoxia would therefore relieve 3' UTR-based suppression of HIF1α observed in normoxia. Interestingly, while mutation of the "seed" region of interaction abolishes the suppressive effect of miR-199a-5p on the HIF1α 3' UTR, expression of luc-HIF1α MUT 3' UTR actually decreases in normoxia when treated with scramble duplex (Figure 35). This is unanticipated, as one would expect miR-199a-5p to be unable to bind normally to the HIF1α 3' UTR, thus relieving inhibition. This result may be due to activity of other miRNAs, whose interaction with this region of 3' UTR may have inadvertently been enhanced by deleting the "seed" region, as nucleotide changes in the 3' UTR affect not only RNA sequence, but secondary structure as well (Figure 32b). Indeed, two miRNAs, miR-340 and miR-410, are predicted to bind the HIF1α 3' UTR less than 15 nucleotides away (10 nucleotides away in the mutant construct) from the miR-199a-5p binding site.

Another puzzling finding from this experiment was that miR-199a treatment of EOCCs transfected with the luc-HIF1α MUT 3' UTR construct actually increased luciferase expression compared to scramble-treated cells. This finding agrees with the hypothesis presented previously, namely, that interaction of other miRNA is enhanced by deletion of the "seed" site. Treatment with miR-199a, which may still retain some affinity for the target area, as basepair associations at the 3' end of the miRNA remain intact, would interfere with other miRNAs binding to the region, thus relieving suppression and increasing luciferase expression. That luciferase expression of the miR-199a-treated hypoxic EOCCs transfected with the mutant construct exceeds expression of the scramble-treated hypoxic EOCCs transfected with the control construct may be the result of miR-199-5p and other miRNAs competing for binding in the region of "seed" site deletion, resulting in no one miRNA able to exert a significant suppressive effect.

At this juncture is it important to address the issue of miR-199a-3p. Whereas most miRNAs select only one arm of the partially processed duplex to become fully mature, miR-199a is an exception, with both the -5p and -3p arms exhibiting bioactivity. Bioinformatic analysis reveals that only the -5p arm of miR-199a targets the HIF1α 3' UTR; however, in all of our work, we have used the duplex form of the miRNA, as it is the only commercially available form, which contains both arms. It is therefore important to recognize that off-target effects, from both the -5p and -3p arms, may contribute to the effects we have observed with miR-199a overexpression.

While miR-199a overexpression resulted in decreased HIF1α protein and nuclear localization, remarkably, HIF1α mRNA levels were not affected (Figure 37a). This result implies that the mechanism of miR-199a-mediated HIF1α suppression may not involve

degradation of the HIF1α transcript, but rather suppression of translation. Alternatively, given that miR-199a knockdown by morpholino did have an effect on HIF1α mRNA levels, it is plausible that in EOCCs, miR-199a may have some baseline suppressive effect on HIF1α transcript levels, but increasing levels of the miRNA only serves to inhibit translation, not further enhance mRNA degradation (Figure 38). Downregulation of miR-199a using MO, then, may not only relieve inhibition of translation but baseline mRNA degradation as well. A similar concept may explain why the western blot in Figure 38b does not show a significant difference in HIF1α levels between control and miR-199a-specific MO in hypoxia: in low oxygen conditions, miR-199a levels are already low and further knockdown by MO may not make a tangible difference at the level of HIF1α protein stabilization.

The fact that miR-199a overexpression has functional consequences, as gauged by both qPCR of HIF1α target genes and experiments assaying cell behavior, underscores the importance of miRNA-based regulation of HIF1α in EOCCs (Figures 39, 41-49) While our proliferation experiments yielded mixed results, with BrdU and clonogenic assays (Figures 42 and 44, respectively) showing no difference between control cells and miR-199a-overexpressing cells, and Xcelligence data demonstrating that miR-199a has a suppressive effect on EOCC growth (Figure 43), the observation that VEGF and LOX transcripts are downregulated in miR-199a-overexpressing cells was corroborated by the findings of both *in vitro* and *in vivo* experiments. Scratch/wound assays and Xcelligence experiments exposed the marked migratory and attachment defects of miR-199a-overexpressing EOCCs (Figures 45, 47a, 48). Reversal of migratory impairment by reconstitution of HIF1α demonstrates that it is miR-199a's inhibitory effect on HIF1α

that translates to inhibition of EOCC migration (Figure 46 and 47b). That LOX, an enzyme that promotes tumor cell motility and metastasis by catalyzing collagen-crosslinking, is a direct target of HIF1α is therefore significant in this context [151, 154]. MiR-199a's suppressive effect on LOX (Figure 41e), likely mediated by HIF1α, may be responsible for impairment of migration and attachment. This hypothesis is supported by our finding that EOCCs treated with the LOX inhibitor β-APN showed defects in migration akin to those overexpressing miR-199a (Figure 49). Further work, including measurement of protein levels and localization of LOX in miR-199a-overexpressing cells versus control cells and experiments assaying LOX's role in EOCC adhesion to various substrates, is required to fully explain the nature of this relationship.

Inhibition of LOX by miR-199a may also explain some of our *in vivo* findings. While control cells injected IP into mice seeded the ovaries by day 7, with extensive involvement of the ovaries, fallopian tubes and gastrointestinal tract by day 12, miR-199a-overexpressing EOCCs demonstrated no such proclivity (Figure 50). LOX has been shown to aid metastasis by enhancing cell motility and attachment and by "priming" distal locations for colonization [9, 156, 262]. Downregulation of LOX by miR-199a may therefore be responsible for the differences we observed in early stage seeding of the ovaries/fallopian tubes and GI. By extension, the significant differences seen in tumor burden between mice inoculated with miR-199a-overexpressing EOCCs and those inolculated with control cells (Figures 51 and 52) may also be mediated by LOX inhibition. More plausible, however, is that the decreased tumor weight observed in miR-199a-overexpressing cells is a result of suppression of VEGF. Decreased angiogenesis presents a severe constraint to tumor growth [5, 192, 193]. As such, downregulation of

VEGF by miR-199a, likely mediated by HIF1α, is the probable reason for the significant decrease in tumor burden. This is supported by the fact that compared to control tumors, tumors overexpressing miR-199a developed significantly less vascular supply within the tumor microenvironment as determined by quantification of vessel ends, nodes and length (Figures 53 and 54). Furthermore, necrotic area in miR-199a-overexpressing tumors constituted a much larger percentage of total tumor area than in control tumors (Figure 55). Again, this is likely due to inhibition of angiogenesis. Indeed, H and E stained sections comparing necrotic areas of control and miR-199a-overexpressing tumors showed a robust blood supply in the former and a dearth of blood supply in the former. Careful examination of the images from miR-199a-overexpressing tumors shows that necrotic areas developed in areas with the least vascular density and viable areas formed near perfect circles around vessels, supporting that idea that inhibition of VEGF is at least partly the cause of increased necrosis and decreased tumor weight observed in miR-199a-overexpressing tumors.

By adding carboplatin treatment to our experiments, we introduced an element of clinical relevance to our model. While having no significant effect of angiogenesis (Figures 53 and 54), combined miR-199a and carboplatin treatment seemed to have an additive effect on EOCC proliferation *in vitro* (Figure 56) and tumor burden *in vivo* (Figures 51 and 52). Interestingly, while tumor weight was reduced with combined miR-199a overexpression and carboplatin compared to either alone, tumor necrosis did not increase in miR-199a-overexpressing tumors treated with carboplatin. This finding indicates that in the combination treatment group, any further inhibition of tumor growth beyond what miR-199a achieved is due to induction of apoptosis, which, in fact, has been

identified as the main mechanism of platinum-based tumor cell death [352, 353]. As such, combination treatment employing miR-199a overexpression and carboplatin may activate two distinct pathways to effect tumor reduction and may potentially overcome any resistances EOCCs develop to either treatment alone.

MiR-199a has been investigated in the context of EOC in other studies. In particular, Chen et al identified IKKβ as a target of miR-199a in EOCCs [354]. While this group demonstrated that inhibition of miR-199a increased levels of IKKβ, we were unable to show, inversely, that miR-199a overexpression suppresses levels of IKKβ (unpublished data). Another group identified miR-199a as a regulator of TWIST is EOCCs, with implications for stem-cell like behavior. We are currently investigating the relationship between our miR-199a-overexpressing cell line, A2780-199, and CD44, the marker identified by this group as important in demonstrating TWIST function in EOCCs. The role of miR-199a in other contexts has also been the subject of numerous other studies. miR-199a is involved in testicular cancer [355], osteosarcoma [356], hepatocellular carcinoma [357, 358], and gastric cancer [359], and, importantly, has been shown to target HIF1α in cardiac myocytes [360]. Certainly, miR-199a seems to be a significant factor both normal physiology and the progression of maligancies.

One of the overarching aims of this research is to develop novel therapies for the treatment of EOC. While miRNA therapies are relatively new, several methods of delivery, the biggest hurdle in miRNA-based approaches, are being studied. Recent successes utilizing viruses [361], conjugated collagens [362] and nanoparticles [363, 364] as vehicles for delivery in animal models highlight the great potential of miRNAs as therapeutic molecules.

In total, the findings presented within this dissertation establish two reciprocal negative regulatory pathways that constitute a positive feedback loop for HIF1α stabilization in hypoxia. The two novel pathways of HIF1α regulation are described in Figure 57 and a schematic summarizing our proposed model is shown in Figure 58.

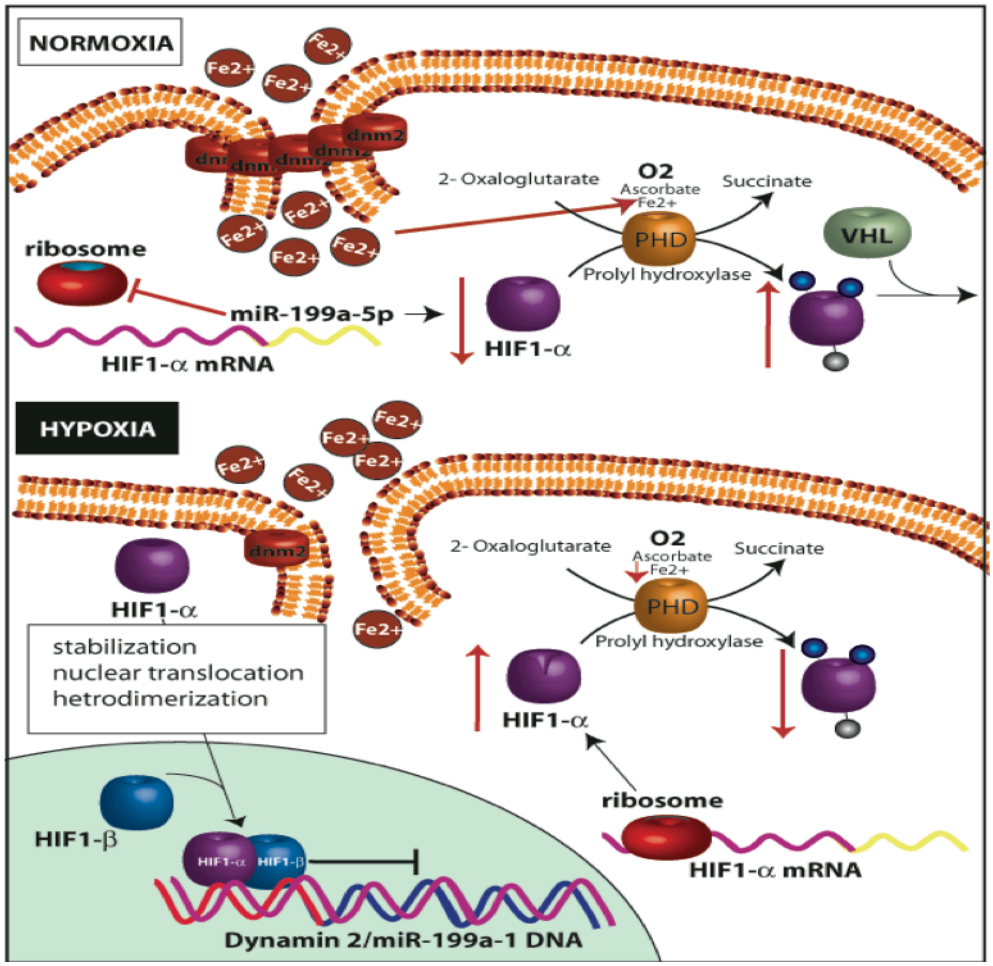

Figure 57: Proposed non-canonical pathways of HIF1α regulation in EOC. In normoxia, miR-199a binds the HIF1α 3' UTR and dnm2-mediated endocytosis allows iron uptake. Together, these processes result in suppressed levels of stabilized HIF1α protein, as miR-199a impairs HIF1α synthesis by inhibiting translation and dnm2 enhances HIF1α degradation by facilitating PHD-based hydroxylation. In hypoxia, however, HIF1α, stabilized by low levels of oxygen, downregulates both dnm2 and miR-199a at the level of transcription. Lowered levels of miR-199a in hypoxia relieve inhibition of HIF1α translation and lowered levels of dnm2 reduce iron uptake, which results in decreased PHD activity. Thus in hypoxia, the inhibitory effects of miR-199a and dnm2 on HIF1α protein synthesis and stability, respectively, are abrogated and levels of stabilized HIF1α are further increased.

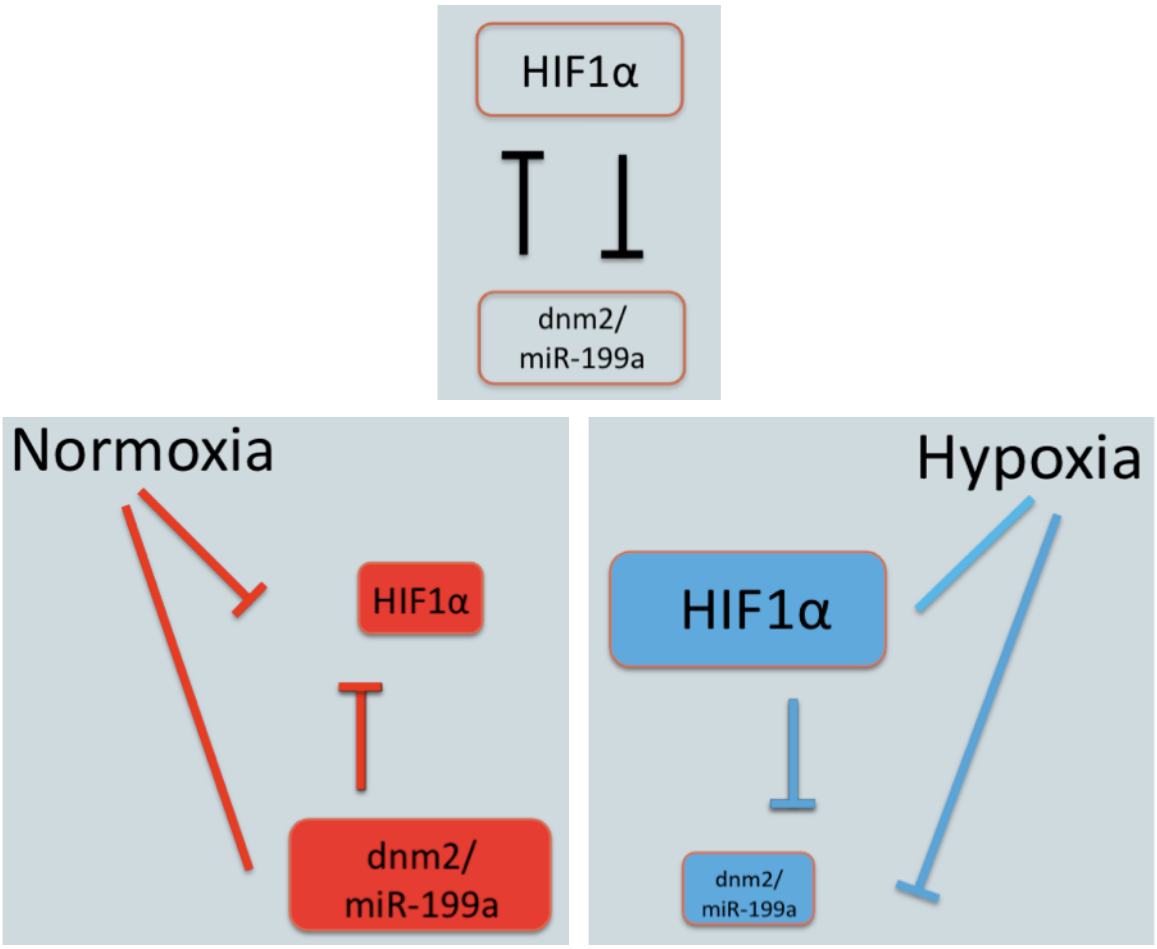

Figure 58: Schematic of proposed non-canonical pathways of HIF1α regulation in EOC. Top: HIF1α and dnm2/miR-199a exhibit reciprocal negative regulation. **Bottom left:** In normoxia, HIF1α levels are low whereas dnm2 and miR-199a levels are normal. Dnm2 and miR-199a expression in normoxia compounds the effects of oxygen on decreasing levels of stabilized HIF1α, leading to decreased HIF1α synthesis and increased HIF1α degradation. **Bottom right:** In contrast, in hypoxia, HIF1α is stabilized and dnm2 and miR-199a levels are decreased, leading to a further increase in levels of stabilized HIF1α.

CHAPTER III:

CONCLUSIONS AND FUTURE DIRECTIONS

Epithelial ovarian cancer is a deadly disease causing significant morbidity and mortality. The lethal nature of EOC is largely dependent on angiogenesis and metastasis [8-11]. Both of these processes are driven by the development low oxygen conditions in the tumor microenvironment, an inevitable consequence of rapid EOCC proliferation [5-7]. In reaction to these low oxygen states, EOCCs activate HIF1α, the master regulator of the hypoxic response [133]. HIF1α, in turn, activates a plethora of genes that allow EOCs to survive and thrive despite experiencing a number of different stressors such as hypoxia, activate angiogenesis and promote metastasis [11, 132]. As such, HIF1α plays a critical role in furthering EOC malignancy [9, 211].

In this work we have shown that beyond the classical model of HIF1α regulation, which postulates that HIF1α regulation occurs at the level of protein stabilization in response to changes in oxygenation, HIF1α expression is also controlled by dynamin 2 in an iron-dependent fashion and by the miRNA miR-199a at the level of translation. These findings have important implications for the treatment of EOCs and other solid tumors that demonstrate angiogenic and metastatic characteristics.

Dynamin 2 and miR-199a-1 are downregulated in hypoxia

Dynamin 2 is a crucial mediator of endocytosis and cell motility, two processes with great relevance in tumor cell biology [236]. We found that transcript and protein levels of dnm2 are downregulated in low oxygen states in EOCCs in a promoter-dependent manner. Moreover, we identified a critical region of the dnm2 promoter that is necessary for its expression under all oxygenation conditions and a hypoxia-responsive

region, HRE 2, that determines dnm2 downregulation in hypoxia. Because miR-199a-1 is located in an intron within the dnm2 gene, expression of the miRNA is controlled by the dnm2 promoter. As such, levels of miR-199a-1, which, like dnm2, decrease in hypoxia, are similarly dependent on the important regions identified within the dnm2 promoter. We also found that HIF1α suppression in hypoxia relieves inhibition of the dnm2 promoter, indicating that dnm2/miR-199a-1 is regulated directly by HIF1α. However, the finding that overexpression of HIF1α in normoxia does not suppress the dnm2 promoter suggests that other factors, in addition to HIF1α, are required for proper control of dnm2/miR-199a-1 expression in hypoxia. Additional experiments, such as a chromatin-immunoprecipitation assay, would confirm the relationship between HIF1α and the dnm2 promoter. These experiments are ongoing and should provide a definitive explanation of the role of hypoxia in determining levels of dnm2 and miR-199a-1 in EOCCs.

Inhibition of dynamin 2 stabilizes HIF1α

We next determined that inhibition of dnm2 by the small molecule dynasore results in rapid stabilization of HIF1α in normoxic EOCCs. This process seems to be dependent on fluctuations in intracellular iron levels, as dynasore treatment induces a significant and rapid drop in the intracellular iron pool. Moreover, both dynasore-mediated reduction in iron level and increase in HIF1α stability can be reversed by loading cells with a form of iron whose uptake is dnm2-independent. This finding suggests that by inhibiting dnm2, dynasore prevents iron uptake leading to an increase in HIF1α protein levels. Because the PHD hydroxylation step of HIF1α regulation is iron-

dependent, we studied whether polyubiquitination of HIF1α, a step downstream of PHD-based hydroxylation, is impaired in dynasore treated EOCCs. Indeed, treatment with the dynamin inhibitor substantially decreased HIF1α polyubiquitination. Together these findings suggest that by inhibiting dnm2 activity, dynasore reduces iron uptake. Reduced intracellular iron levels, in turn, impair PHD hydroxylation of HIF1α, thereby stabilizing the protein. We are currently performing a number of experiments to validate this model. In particular, we are studying how dynasore affects intracellular iron levels and HIF1α stability using real-time imaging methods. Moreover, we are investigating the polyubiquitination status of HIF1α in dynasore-treated EOCCs directly by immunopreciptation. Finally, to understand whether a positive feedback loop exists in which HIF1α downregulates dnm2 expression in hypoxia to further stabilize itself, we are measuring levels of the intracellular iron pool in hypoxic states and with dynasore treatment.

MiR-199a inhibits HIF1α expression and activity

Using a luciferase construct in which expression of the reporter is under control of the HIF1α 3' UTR, we showed that miR-199a directly targets an *in silico* predicted site within the HIF1α 3' UTR to inhibit luciferase expression. Moreover, deletion of the "seed" site in the HIF1α 3' UTR abrogates miR-199a-mediated inhibition of luciferase expression. That miR-199a inhibits protein levels and nuclear localization of HIF1α, and,

importantly, genes transactivated by HIF1α such as VEGF and LOX, underscores the important implications of this miRNA-based mechanism of HIF1α regulation [9].

miR-199a confers EOCCs with proliferative, migratory and attachment defects

These implications were further confirmed by observations that EOCCs overexpressing miR-199a exhibit a phenotype with impaired proliferation, migration and attachment. As these are all critical processes in the progression of EOC, miR-199a demonstrates an important anti-cancer effect as measured by these metrics. Reconstitution of HIF1α in miR-199a-overexpressing EOCCs reverses the defects in proliferation and migration, confirming that miR-199a's effects on these processes are indeed mediated through changes in HIF1α expression. We are currently studying the role of LOX, a HIF1α-driven promoter of cell motility and attachment, in miR-199a-induced inhibition of migration and attachment. Indeed, inhibition of LOX using β-APN showed an impaired migration profile similar to that of miR-199a-overexpressing EOCCs. LOX has been implicated in metastasis of a number of cancers and thus miR-199a-mediated inhibition of LOX would present an important finding in the context of EOC progression [154, 157, 158, 161].

miR-199a reduces tumor angiogenesis and burden and increases tumor necrosis

To further demonstrate the anti-cancer potency of miR-199a, we used a mouse model of metastatic EOC to evaluate the *in vivo* effects of the miRNA. Significantly,

EOC seeding of the ovaries, fallopian tubes and gastrointestinal tract was impaired in mice injected with miR-199a-overexpressing EOCCs compared to mice injected with control cells. Moreover, tumor angiogenesis and burden in mice inoculated with EOCs overexpressing miR-199a was substantially reduced compared control mice. Treatment with carboplatin further enhanced miR-199a-mediated suppression of tumor growth, a finding that was mirrored *in vitro* in studies of carboplatin treatment in conjunction with miR-199a overexpression. Importantly, miR-199a-overexpressing tumors showed significantly larger percentages of necrotic areas than control tumors.

Long-term prospects

The findings presented in this work lay important groundwork for future investigations into treatments of EOC. While many current anti-cancer therapies address tumor proliferation and growth, angiogenesis or metastasis, few target all three together. We have shown that miR-199a is able to inhibit all three of deleterious characteristics of EOCs both *in vitro* and in a mouse model of metastatic EOC, an effect that seems to be largely driven by suppression of HIF1α. Targeting this critical molecule, which has been implicated in nearly every facet of EOC progression [93] and correlates with poor clinical outcomes [89, 90], is therefore an attractive strategy to treat EOCs. Our finding that dnm2 is also intimately involved in HIF1α regulation via management of intracellular iron levels presents another dimension to such anti-HIF1α approaches. We therefore believe that miR-199a- and dnm2-based treatments of EOC may have great therapeutic potential and warrant further study.

CHAPTER III:

BIBLIOGRAPHY

Bibliography

References are listed in the order cited in the text.

1. *American Cancer Society*. 2010 August 21, 2011]; Available from: www.cancer.org.
2. Jemal, A., et al., *Cancer statistics, 2010.* CA Cancer J Clin, 2010. **60**(5): p. 277-300.
3. Merino, M.J. and G. Jaffe, *Age contrast in ovarian pathology.* Cancer, 1993. **71**(2 Suppl): p. 537-44.
4. Colombo, N., M. Peiretti, and M. Castiglione, *Non-epithelial ovarian cancer: ESMO clinical recommendations for diagnosis, treatment and follow-up.* Ann Oncol, 2009. **20 Suppl 4**: p. 24-6.
5. Folkman, J., *What is the evidence that tumors are angiogenesis dependent?* J Natl Cancer Inst, 1990. **82**(1): p. 4-6.
6. Folkman, J., *Tumor angiogenesis: therapeutic implications.* N Engl J Med, 1971. **285**(21): p. 1182-6.
7. Teoh, D.G. and A.A. Secord, *Antiangiogenic therapies in epithelial ovarian cancer.* Cancer Control, 2011. **18**(1): p. 31-43.
8. Galanis, A., et al., *Reactive oxygen species and HIF-1 signalling in cancer.* Cancer Lett, 2008. **266**(1): p. 12-20.
9. Lu, X. and Y. Kang, *Hypoxia and hypoxia-inducible factors: master regulators of metastasis.* Clin Cancer Res, 2010. **16**(24): p. 5928-35.
10. Cassavaugh, J. and K.M. Lounsbury, *Hypoxia-mediated biological control.* J Cell Biochem, 2011. **112**(3): p. 735-44.
11. Ke, Q. and M. Costa, *Hypoxia-inducible factor-1 (HIF-1).* Mol Pharmacol, 2006. **70**(5): p. 1469-80.
12. Spannuth, W.A., A.K. Sood, and R.L. Coleman, *Angiogenesis as a strategic target for ovarian cancer therapy.* Nat Clin Pract Oncol, 2008. **5**(4): p. 194-204.
13. Lu, Z., et al., *Intraperitoneal therapy for peritoneal cancer.* Future Oncol, 2010. **6**(10): p. 1625-41.
14. Feki, A., et al., *Dissemination of intraperitoneal ovarian cancer: Discussion of mechanisms and demonstration of lymphatic spreading in ovarian cancer model.* Crit Rev Oncol Hematol, 2009. **72**(1): p. 1-9.
15. Naora, H. and D.J. Montell, *Ovarian cancer metastasis: integrating insights from disparate model organisms.* Nat Rev Cancer, 2005. **5**(5): p. 355-66.
16. Jemal, A., et al., *Cancer statistics, 2009.* CA Cancer J Clin, 2009. **59**(4): p. 225-49.
17. Pignata, S., et al., *Chemotherapy in epithelial ovarian cancer.* Cancer Lett, 2011. **303**(2): p. 73-83.

18. Heintz, A.P., et al., *Carcinoma of the ovary. FIGO 26th Annual Report on the Results of Treatment in Gynecological Cancer.* Int J Gynaecol Obstet, 2006. **95 Suppl 1**: p. S161-92.
19. Lutz, A.M., et al., *Early diagnosis of ovarian carcinoma: is a solution in sight?* Radiology, 2011. **259**(2): p. 329-45.
20. Leblanc, E., et al., *Surgical staging of early invasive epithelial ovarian tumors.* Semin Surg Oncol, 2000. **19**(1): p. 36-41.
21. Markman, M., et al., *Phase III trial of standard-dose intravenous cisplatin plus paclitaxel versus moderately high-dose carboplatin followed by intravenous paclitaxel and intraperitoneal cisplatin in small-volume stage III ovarian carcinoma: an intergroup study of the Gynecologic Oncology Group, Southwestern Oncology Group, and Eastern Cooperative Oncology Group.* J Clin Oncol, 2001. **19**(4): p. 1001-7.
22. Rothenberg, M.L., et al., *Combined intraperitoneal and intravenous chemotherapy for women with optimally debulked ovarian cancer: results from an intergroup phase II trial.* J Clin Oncol, 2003. **21**(7): p. 1313-9.
23. Armstrong, D.K., et al., *Intraperitoneal cisplatin and paclitaxel in ovarian cancer.* N Engl J Med, 2006. **354**(1): p. 34-43.
24. Vasey, P.A., et al., *Phase III randomized trial of docetaxel-carboplatin versus paclitaxel-carboplatin as first-line chemotherapy for ovarian carcinoma.* J Natl Cancer Inst, 2004. **96**(22): p. 1682-91.
25. Pignata, S., et al., *Pegylated liposomal doxorubicin combined with carboplatin: a rational treatment choice for advanced ovarian cancer.* Crit Rev Oncol Hematol, 2010. **73**(1): p. 23-30.
26. Katsumata, N., et al., *Dose-dense paclitaxel once a week in combination with carboplatin every 3 weeks for advanced ovarian cancer: a phase 3, open-label, randomised controlled trial.* Lancet, 2009. **374**(9698): p. 1331-8.
27. Burger, R.A., Brady, M.F., Bookman, M.A., Walker, J.L., Homesley, H.D., Fowler J.D., Monk, B.J., Greer, B.E., Boente, M., Liang, S.X., *Phase III trial of bevacizumab (BEV) in the primary treatment of advanced epithelial ovarian cancer (EOC), primary peritoneal cancer (PPC), or fallopian tube cancer (FTC): a gynecologic oncology group study.* J. Clin. Oncol., 2010. **28**(18s).
28. Perren, T., Swart, A.M., Fisterer, J.P. et al., , *ICON7: a phase III randomized gyaecologic cancer onter group trial of concurrent bevacizumab and chemotherapy followed by maintenence bevacizumab, versus chemotherapy alone in women with newly diagnosed epithelial ovarian cancer (EOC), primary peritoneal cancer (PPC) or fallopian tube cancer (FTC).* Ann Oncol, 2010. **21**(8).
29. Ellis, L.M. and D.J. Hicklin, *VEGF-targeted therapy: mechanisms of anti-tumour activity.* Nat Rev Cancer, 2008. **8**(8): p. 579-91.
30. Raspollini, M.R., et al., *Correlation of epidermal growth factor receptor expression with tumor microdensity vessels and with vascular endothelial growth factor expression in ovarian carcinoma.* Int J Surg Pathol, 2005. **13**(2): p. 135-42.

31. Grzankowski, K.S. and M. Carney, *Quality of life in ovarian cancer.* Cancer Control, 2011. **18**(1): p. 52-8.
32. Del Carmen, M.G., *Primary epithelial ovarian cancer: diagnosis and management*, in *Education Book of the American Society of Clinical Oncology*2006, American Society of Clinical Oncology: Alexandria, VA.
33. Goff, B.A., et al., *Development of an ovarian cancer symptom index: possibilities for earlier detection.* Cancer, 2007. **109**(2): p. 221-7.
34. Kenemans, P., et al., *CA 125 in gynecological pathology--a review.* Eur J Obstet Gynecol Reprod Biol, 1993. **49**(1-2): p. 115-24.
35. Cannistra, S.A., *Cancer of the ovary.* N Engl J Med, 2004. **351**(24): p. 2519-29.
36. Vuento, M.H., et al., *Significance of a single CA 125 assay combined with ultrasound in the early detection of ovarian and endometrial cancer.* Gynecol Oncol, 1997. **64**(1): p. 141-6.
37. Meyer, T. and G.J. Rustin, *Role of tumour markers in monitoring epithelial ovarian cancer.* Br J Cancer, 2000. **82**(9): p. 1535-8.
38. Buys, S.S., et al., *Effect of screening on ovarian cancer mortality: the Prostate, Lung, Colorectal and Ovarian (PLCO) Cancer Screening Randomized Controlled Trial.* JAMA, 2011. **305**(22): p. 2295-303.
39. Ramirez, I., H.S. Chon, and S.M. Apte, *The role of surgery in the management of epithelial ovarian cancer.* Cancer Control, 2011. **18**(1): p. 22-30.
40. Harter, P., et al., *Prognostic factors for complete debulking in first- and second-line ovarian cancer.* Int J Gynecol Cancer, 2009. **19 Suppl 2**: p. S14-7.
41. Guastalla, J.P., 3rd and V. Dieras, *The taxanes: toxicity and quality of life considerations in advanced ovarian cancer.* Br J Cancer, 2003. **89 Suppl 3**: p. S16-22.
42. Bodurka-Bevers, D., et al., *Depression, anxiety, and quality of life in patients with epithelial ovarian cancer.* Gynecol Oncol, 2000. **78**(3 Pt 1): p. 302-8.
43. Koldjeski, D., et al., *The ovarian cancer journey of families the first postdiagnostic year.* Cancer Nurs, 2007. **30**(3): p. 232-42.
44. Jackson, J.M., et al., *Social support among women who died of ovarian cancer.* Support Care Cancer, 2007. **15**(5): p. 547-56.
45. Sherwood, P.R., et al., *A house of cards: the impact of treatment costs on women with breast and ovarian cancer.* Cancer Nurs, 2008. **31**(6): p. 470-7.
46. Lee, K.A., R.A. Roth, and J.J. LaPres, *Hypoxia, drug therapy and toxicity.* Pharmacol Ther, 2007. **113**(2): p. 229-46.
47. Brahimi-Horn, C. and J. Pouyssegur, *The role of the hypoxia-inducible factor in tumor metabolism growth and invasion.* Bull Cancer, 2006. **93**(8): p. E73-80.
48. Zhang, Y., et al., *Recent advances in tumor hypoxia: tumor progression, molecular mechanisms, and therapeutic implications.* Med Sci Monit, 2007. **13**(10): p. RA175-80.
49. Martinez-Poveda, B., et al., *Non-invasive monitoring of hypoxia-inducible factor activation by optical imaging during antiangiogenic treatment in a xenograft model of ovarian carcinoma.* Int J Oncol, 2011. **39**(3): p. 543-52.

50. Vaupel, P., F. Kallinowski, and P. Okunieff, *Blood flow, oxygen and nutrient supply, and metabolic microenvironment of human tumors: a review.* Cancer Res, 1989. **49**(23): p. 6449-65.
51. Nordsmark, M., et al., *Hypoxia in human soft tissue sarcomas: adverse impact on survival and no association with p53 mutations.* Br J Cancer, 2001. **84**(8): p. 1070-5.
52. Hockel, M., et al., *Association between tumor hypoxia and malignant progression in advanced cancer of the uterine cervix.* Cancer Res, 1996. **56**(19): p. 4509-15.
53. Knocke, T.H., et al., *Intratumoral pO2-measurements as predictive assay in the treatment of carcinoma of the uterine cervix.* Radiother Oncol, 1999. **53**(2): p. 99-104.
54. Nordsmark, M. and J. Overgaard, *Tumor hypoxia is independent of hemoglobin and prognostic for loco-regional tumor control after primary radiotherapy in advanced head and neck cancer.* Acta Oncol, 2004. **43**(4): p. 396-403.
55. Rudat, V., et al., *Repeatability and prognostic impact of the pretreatment pO(2) histography in patients with advanced head and neck cancer.* Radiother Oncol, 2000. **57**(1): p. 31-7.
56. Vaupel, P. and A. Mayer, *Hypoxia in cancer: significance and impact on clinical outcome.* Cancer Metastasis Rev, 2007. **26**(2): p. 225-39.
57. Kiaer, T. and K.D. Kristensen, *Intracompartmental pressure, PO2, PCO2 and blood flow in the human skeletal muscle.* Arch Orthop Trauma Surg, 1988. **107**(2): p. 114-6.
58. Deong, T.Q., Kim, S.G., *Quantitative MR Measurements of Interstitial Oxygen Tensionin intact rat brain; hyperoxia and hypercapnia.* Proc Int Soc Magn Reson Med, 2000. **8**: p. 440.
59. Vaupel, P., *Tumor microenvironmental physiology and its implications for radiation oncology.* Semin Radiat Oncol, 2004. **14**(3): p. 198-206.
60. Yue, X. and R.J. Tomanek, *Stimulation of coronary vasculogenesis/angiogenesis by hypoxia in cultured embryonic hearts.* Dev Dyn, 1999. **216**(1): p. 28-36.
61. Shinkai, T., et al., *The role of oxygen tension in the regulation of embryonic lung development.* J Pediatr Surg, 2005. **40**(1): p. 32-5.
62. Lee, Y.M., et al., *Determination of hypoxic region by hypoxia marker in developing mouse embryos in vivo: a possible signal for vessel development.* Dev Dyn, 2001. **220**(2): p. 175-86.
63. van Tuyl, M., et al., *Role of oxygen and vascular development in epithelial branching morphogenesis of the developing mouse lung.* Am J Physiol Lung Cell Mol Physiol, 2005. **288**(1): p. L167-78.
64. Brooks, G.A., Fahey, T.D., White, T.P., Baldwin, K.M., *Exercise Physiology: Human Bioenergetics and Its Applications, Third Edition.* Third ed2000, Mountain View, CA: Mayfield Publishing Company.
65. Helmlinger, G., et al., *Interstitial pH and pO2 gradients in solid tumors in vivo: high-resolution measurements reveal a lack of correlation.* Nat Med, 1997. **3**(2): p. 177-82.

66. Coleman, C.N., J.B. Mitchell, and K. Camphausen, *Tumor hypoxia: chicken, egg, or a piece of the farm?* J Clin Oncol, 2002. **20**(3): p. 610-5.
67. Kunz, M., et al., *Activation of c-Jun NH2-terminal kinase/stress-activated protein kinase (JNK/SAPK) is critical for hypoxia-induced apoptosis of human malignant melanoma.* Cell Growth Differ, 2001. **12**(3): p. 137-45.
68. Harris, A.L., *Hypoxia--a key regulatory factor in tumour growth.* Nat Rev Cancer, 2002. **2**(1): p. 38-47.
69. Semenza, G.L., *Hypoxia, clonal selection, and the role of HIF-1 in tumor progression.* Crit Rev Biochem Mol Biol, 2000. **35**(2): p. 71-103.
70. Seimiya, H., et al., *Hypoxia up-regulates telomerase activity via mitogen-activated protein kinase signaling in human solid tumor cells.* Biochem Biophys Res Commun, 1999. **260**(2): p. 365-70.
71. Shimoda, L.A., et al., *HIF-1 regulates hypoxic induction of NHE1 expression and alkalinization of intracellular pH in pulmonary arterial myocytes.* Am J Physiol Lung Cell Mol Physiol, 2006. **291**(5): p. L941-9.
72. Wykoff, C.C., et al., *Hypoxia-inducible expression of tumor-associated carbonic anhydrases.* Cancer Res, 2000. **60**(24): p. 7075-83.
73. Chiche, J., M.C. Brahimi-Horn, and J. Pouyssegur, *Tumour hypoxia induces a metabolic shift causing acidosis: a common feature in cancer.* J Cell Mol Med, 2010. **14**(4): p. 771-94.
74. Jain, R.K., *Normalization of tumor vasculature: an emerging concept in antiangiogenic therapy.* Science, 2005. **307**(5706): p. 58-62.
75. Vaupel, P., O. Thews, and M. Hoeckel, *Treatment resistance of solid tumors: role of hypoxia and anemia.* Med Oncol, 2001. **18**(4): p. 243-59.
76. Al-Waili, N.S., et al., *Hyperbaric oxygen and malignancies: a potential role in radiotherapy, chemotherapy, tumor surgery and phototherapy.* Med Sci Monit, 2005. **11**(9): p. RA279-89.
77. Kondo, A., et al., *Hypoxia-induced enrichment and mutagenesis of cells that have lost DNA mismatch repair.* Cancer Res, 2001. **61**(20): p. 7603-7.
78. Hockel, M. and P. Vaupel, *Tumor hypoxia: definitions and current clinical, biologic, and molecular aspects.* J Natl Cancer Inst, 2001. **93**(4): p. 266-76.
79. Graeber, T.G., et al., *Hypoxia-mediated selection of cells with diminished apoptotic potential in solid tumours.* Nature, 1996. **379**(6560): p. 88-91.
80. Kim, C.Y., et al., *Selection of human cervical epithelial cells that possess reduced apoptotic potential to low-oxygen conditions.* Cancer Res, 1997. **57**(19): p. 4200-4.
81. Holmquist, L., T. Lofstedt, and S. Pahlman, *Effect of hypoxia on the tumor phenotype: the neuroblastoma and breast cancer models.* Adv Exp Med Biol, 2006. **587**: p. 179-93.
82. Hill, R.P., D.T. Marie-Egyptienne, and D.W. Hedley, *Cancer stem cells, hypoxia and metastasis.* Semin Radiat Oncol, 2009. **19**(2): p. 106-11.
83. Pennacchietti, S., et al., *Hypoxia promotes invasive growth by transcriptional activation of the met protooncogene.* Cancer Cell, 2003. **3**(4): p. 347-61.

84. Chang, Q., et al., *Hypoxia predicts aggressive growth and spontaneous metastasis formation from orthotopically grown primary xenografts of human pancreatic cancer.* Cancer Res, 2011. **71**(8): p. 3110-20.
85. Yotnda, P., D. Wu, and A.M. Swanson, *Hypoxic tumors and their effect on immune cells and cancer therapy.* Methods Mol Biol, 2010. **651**: p. 1-29.
86. Littlewood, T.J., *The impact of hemoglobin levels on treatment outcomes in patients with cancer.* Semin Oncol, 2001. **28**(2 Suppl 8): p. 49-53.
87. Littlewood, T.J., et al., *Effects of epoetin alfa on hematologic parameters and quality of life in cancer patients receiving nonplatinum chemotherapy: results of a randomized, double-blind, placebo-controlled trial.* J Clin Oncol, 2001. **19**(11): p. 2865-74.
88. Overgaard, J., *Clinical evaluation of nitroimidazoles as modifiers of hypoxia in solid tumors.* Oncol Res, 1994. **6**(10-11): p. 509-18.
89. Nordsmark, M., et al., *Prognostic value of tumor oxygenation in 397 head and neck tumors after primary radiation therapy. An international multi-center study.* Radiother Oncol, 2005. **77**(1): p. 18-24.
90. Vaupel, P. and M. Hockel, *[Hypoxia in cervical cancer: pathogenesis, characterization, and biological/clinical consequences].* Zentralbl Gynakol, 2001. **123**(4): p. 192-7.
91. Vaupel, P., S. Briest, and M. Hockel, *Hypoxia in breast cancer: pathogenesis, characterization and biological/therapeutic implications.* Wien Med Wochenschr, 2002. **152**(13-14): p. 334-42.
92. Wilson, W.R. and M.P. Hay, *Targeting hypoxia in cancer therapy.* Nat Rev Cancer, 2011. **11**(6): p. 393-410.
93. Semenza, G.L., *Hypoxia-inducible factor 1: master regulator of O2 homeostasis.* Curr Opin Genet Dev, 1998. **8**(5): p. 588-94.
94. Wang, G.L., et al., *Hypoxia-inducible factor 1 is a basic-helix-loop-helix-PAS heterodimer regulated by cellular O2 tension.* Proc Natl Acad Sci U S A, 1995. **92**(12): p. 5510-4.
95. Semenza, G.L., *Hydroxylation of HIF-1: oxygen sensing at the molecular level.* Physiology (Bethesda), 2004. **19**: p. 176-82.
96. Lando, D., et al., *Asparagine hydroxylation of the HIF transactivation domain a hypoxic switch.* Science, 2002. **295**(5556): p. 858-61.
97. Wang, G.L. and G.L. Semenza, *General involvement of hypoxia-inducible factor 1 in transcriptional response to hypoxia.* Proc Natl Acad Sci U S A, 1993. **90**(9): p. 4304-8.
98. Li, H., H.P. Ko, and J.P. Whitlock, *Induction of phosphoglycerate kinase 1 gene expression by hypoxia. Roles of Arnt and HIF1alpha.* J Biol Chem, 1996. **271**(35): p. 21262-7.
99. Laughner, E., et al., *HER2 (neu) signaling increases the rate of hypoxia-inducible factor 1alpha (HIF-1alpha) synthesis: novel mechanism for HIF-1-mediated vascular endothelial growth factor expression.* Mol Cell Biol, 2001. **21**(12): p. 3995-4004.

100. Fukuda, R., et al., *Insulin-like growth factor 1 induces hypoxia-inducible factor 1-mediated vascular endothelial growth factor expression, which is dependent on MAP kinase and phosphatidylinositol 3-kinase signaling in colon cancer cells.* J Biol Chem, 2002. **277**(41): p. 38205-11.
101. Akeno, N., et al., *Induction of vascular endothelial growth factor by IGF-I in osteoblast-like cells is mediated by the PI3K signaling pathway through the hypoxia-inducible factor-2alpha.* Endocrinology, 2002. **143**(2): p. 420-5.
102. Kallio, P.J., et al., *Activation of hypoxia-inducible factor 1alpha: posttranscriptional regulation and conformational change by recruitment of the Arnt transcription factor.* Proc Natl Acad Sci U S A, 1997. **94**(11): p. 5667-72.
103. Wiesener, M.S., et al., *Induction of endothelial PAS domain protein-1 by hypoxia: characterization and comparison with hypoxia-inducible factor-1alpha.* Blood, 1998. **92**(7): p. 2260-8.
104. Srinivas, V., et al., *Characterization of an oxygen/redox-dependent degradation domain of hypoxia-inducible factor alpha (HIF-alpha) proteins.* Biochem Biophys Res Commun, 1999. **260**(2): p. 557-61.
105. Masson, N. and P.J. Ratcliffe, *HIF prolyl and asparaginyl hydroxylases in the biological response to intracellular O(2) levels.* J Cell Sci, 2003. **116**(Pt 15): p. 3041-9.
106. Masson, N., et al., *Independent function of two destruction domains in hypoxia-inducible factor-alpha chains activated by prolyl hydroxylation.* EMBO J, 2001. **20**(18): p. 5197-206.
107. Huang, J., et al., *Sequence determinants in hypoxia-inducible factor-1alpha for hydroxylation by the prolyl hydroxylases PHD1, PHD2, and PHD3.* J Biol Chem, 2002. **277**(42): p. 39792-800.
108. Berra, E., et al., *HIF prolyl-hydroxylase 2 is the key oxygen sensor setting low steady-state levels of HIF-1alpha in normoxia.* EMBO J, 2003. **22**(16): p. 4082-90.
109. Schofield, C.J. and Z. Zhang, *Structural and mechanistic studies on 2-oxoglutarate-dependent oxygenases and related enzymes.* Curr Opin Struct Biol, 1999. **9**(6): p. 722-31.
110. Ivan, M. and W.G. Kaelin, Jr., *The von Hippel-Lindau tumor suppressor protein.* Curr Opin Genet Dev, 2001. **11**(1): p. 27-34.
111. Kamura, T., et al., *Activation of HIF1alpha ubiquitination by a reconstituted von Hippel-Lindau (VHL) tumor suppressor complex.* Proc Natl Acad Sci U S A, 2000. **97**(19): p. 10430-5.
112. Salceda, S. and J. Caro, *Hypoxia-inducible factor 1alpha (HIF-1alpha) protein is rapidly degraded by the ubiquitin-proteasome system under normoxic conditions. Its stabilization by hypoxia depends on redox-induced changes.* J Biol Chem, 1997. **272**(36): p. 22642-7.
113. Jeong, J.W., et al., *Regulation and destabilization of HIF-1alpha by ARD1-mediated acetylation.* Cell, 2002. **111**(5): p. 709-20.

114. Kong, X., et al., *Histone deacetylase inhibitors induce VHL and ubiquitin-independent proteasomal degradation of hypoxia-inducible factor 1alpha.* Mol Cell Biol, 2006. **26**(6): p. 2019-28.
115. Arnesen, T., et al., *Interaction between HIF-1 alpha (ODD) and hARD1 does not induce acetylation and destabilization of HIF-1 alpha.* FEBS Lett, 2005. **579**(28): p. 6428-32.
116. Bilton, R., et al., *Arrest-defective-1 protein, an acetyltransferase, does not alter stability of hypoxia-inducible factor (HIF)-1alpha and is not induced by hypoxia or HIF.* J Biol Chem, 2005. **280**(35): p. 31132-40.
117. Fisher, T.S., et al., *Analysis of ARD1 function in hypoxia response using retroviral RNA interference.* J Biol Chem, 2005. **280**(18): p. 17749-57.
118. Bilton, R., et al., *ARDent about acetylation and deacetylation in hypoxia signalling.* Trends Cell Biol, 2006. **16**(12): p. 616-21.
119. Lee, M.N., et al., *Roles of arrest-defective protein 1(225) and hypoxia-inducible factor 1alpha in tumor growth and metastasis.* J Natl Cancer Inst, 2010. **102**(6): p. 426-42.
120. Hewitson, K.S., et al., *Hypoxia-inducible factor (HIF) asparagine hydroxylase is identical to factor inhibiting HIF (FIH) and is related to the cupin structural family.* J Biol Chem, 2002. **277**(29): p. 26351-5.
121. Sang, N., et al., *Carboxyl-terminal transactivation activity of hypoxia-inducible factor 1 alpha is governed by a von Hippel-Lindau protein-independent, hydroxylation-regulated association with p300/CBP.* Mol Cell Biol, 2002. **22**(9): p. 2984-92.
122. Lando, D., et al., *FIH-1 is an asparaginyl hydroxylase enzyme that regulates the transcriptional activity of hypoxia-inducible factor.* Genes Dev, 2002. **16**(12): p. 1466-71.
123. Suzuki, H., A. Tomida, and T. Tsuruo, *Dephosphorylated hypoxia-inducible factor 1alpha as a mediator of p53-dependent apoptosis during hypoxia.* Oncogene, 2001. **20**(41): p. 5779-88.
124. Richard, D.E., et al., *p42/p44 mitogen-activated protein kinases phosphorylate hypoxia-inducible factor 1alpha (HIF-1alpha) and enhance the transcriptional activity of HIF-1.* J Biol Chem, 1999. **274**(46): p. 32631-7.
125. Yasinska, I.M. and V.V. Sumbayev, *S-nitrosation of Cys-800 of HIF-1alpha protein activates its interaction with p300 and stimulates its transcriptional activity.* FEBS Lett, 2003. **549**(1-3): p. 105-9.
126. Brahimi-Horn, C., N. Mazure, and J. Pouyssegur, *Signalling via the hypoxia-inducible factor-1alpha requires multiple posttranslational modifications.* Cell Signal, 2005. **17**(1): p. 1-9.
127. Feldser, D., et al., *Reciprocal positive regulation of hypoxia-inducible factor 1alpha and insulin-like growth factor 2.* Cancer Res, 1999. **59**(16): p. 3915-8.
128. Krishnamachary, B., et al., *Regulation of colon carcinoma cell invasion by hypoxia-inducible factor 1.* Cancer Res, 2003. **63**(5): p. 1138-43.
129. Semenza, G.L., *Targeting HIF-1 for cancer therapy.* Nat Rev Cancer, 2003. **3**(10): p. 721-32.

130. Wenger, R.H., *Cellular adaptation to hypoxia: O2-sensing protein hydroxylases, hypoxia-inducible transcription factors, and O2-regulated gene expression.* FASEB J, 2002. **16**(10): p. 1151-62.
131. Chen, C., et al., *Regulation of glut1 mRNA by hypoxia-inducible factor-1. Interaction between H-ras and hypoxia.* J Biol Chem, 2001. **276**(12): p. 9519-25.
132. Lu, H., R.A. Forbes, and A. Verma, *Hypoxia-inducible factor 1 activation by aerobic glycolysis implicates the Warburg effect in carcinogenesis.* J Biol Chem, 2002. **277**(26): p. 23111-5.
133. Giordano, F.J. and R.S. Johnson, *Angiogenesis: the role of the microenvironment in flipping the switch.* Curr Opin Genet Dev, 2001. **11**(1): p. 35-40.
134. Levy, A.P., et al., *Transcriptional regulation of the rat vascular endothelial growth factor gene by hypoxia.* J Biol Chem, 1995. **270**(22): p. 13333-40.
135. Scheid, A., et al., *Physiologically low oxygen concentrations in fetal skin regulate hypoxia-inducible factor 1 and transforming growth factor-beta3.* FASEB J, 2002. **16**(3): p. 411-3.
136. Kelly, B.D., et al., *Cell type-specific regulation of angiogenic growth factor gene expression and induction of angiogenesis in nonischemic tissue by a constitutively active form of hypoxia-inducible factor 1.* Circ Res, 2003. **93**(11): p. 1074-81.
137. Ben-Yosef, Y., et al., *Regulation of endothelial matrix metalloproteinase-2 by hypoxia/reoxygenation.* Circ Res, 2002. **90**(7): p. 784-91.
138. Kietzmann, T., U. Roth, and K. Jungermann, *Induction of the plasminogen activator inhibitor-1 gene expression by mild hypoxia via a hypoxia response element binding the hypoxia-inducible factor-1 in rat hepatocytes.* Blood, 1999. **94**(12): p. 4177-85.
139. Takahashi, Y., et al., *Hypoxic induction of prolyl 4-hydroxylase alpha (I) in cultured cells.* J Biol Chem, 2000. **275**(19): p. 14139-46.
140. Zheng, X., et al., *Interaction with factor inhibiting HIF-1 defines an additional mode of cross-coupling between the Notch and hypoxia signaling pathways.* Proc Natl Acad Sci U S A, 2008. **105**(9): p. 3368-73.
141. Qiang, L., et al., *HIF-1alpha is critical for hypoxia-mediated maintenance of glioblastoma stem cells by activating Notch signaling pathway.* Cell Death Differ, 2011.
142. Melillo, G., et al., *A hypoxia-responsive element mediates a novel pathway of activation of the inducible nitric oxide synthase promoter.* J Exp Med, 1995. **182**(6): p. 1683-93.
143. Lee, P.J., et al., *Hypoxia-inducible factor-1 mediates transcriptional activation of the heme oxygenase-1 gene in response to hypoxia.* J Biol Chem, 1997. **272**(9): p. 5375-81.
144. Nguyen, S.V. and W.C. Claycomb, *Hypoxia regulates the expression of the adrenomedullin and HIF-1 genes in cultured HL-1 cardiomyocytes.* Biochem Biophys Res Commun, 1999. **265**(2): p. 382-6.

145. Eckhart, A.D., et al., *Characterization of the alpha1B-adrenergic receptor gene promoter region and hypoxia regulatory elements in vascular smooth muscle.* Proc Natl Acad Sci U S A, 1997. **94**(17): p. 9487-92.
146. Semenza, G.L., et al., *Hypoxia-inducible nuclear factors bind to an enhancer element located 3' to the human erythropoietin gene.* Proc Natl Acad Sci U S A, 1991. **88**(13): p. 5680-4.
147. Rolfs, A., et al., *Oxygen-regulated transferrin expression is mediated by hypoxia-inducible factor-1.* J Biol Chem, 1997. **272**(32): p. 20055-62.
148. Bianchi, L., L. Tacchini, and G. Cairo, *HIF-1-mediated activation of transferrin receptor gene transcription by iron chelation.* Nucleic Acids Res, 1999. **27**(21): p. 4223-7.
149. Lok, C.N. and P. Ponka, *Identification of a hypoxia response element in the transferrin receptor gene.* J Biol Chem, 1999. **274**(34): p. 24147-52.
150. Tacchini, L., et al., *Transferrin receptor induction by hypoxia. HIF-1-mediated transcriptional activation and cell-specific post-transcriptional regulation.* J Biol Chem, 1999. **274**(34): p. 24142-6.
151. Csiszar, K., *Lysyl oxidases: a novel multifunctional amine oxidase family.* Prog Nucleic Acid Res Mol Biol, 2001. **70**: p. 1-32.
152. Schietke, R., et al., *The lysyl oxidases LOX and LOXL2 are necessary and sufficient to repress E-cadherin in hypoxia: insights into cellular transformation processes mediated by HIF-1.* J Biol Chem, 2010. **285**(9): p. 6658-69.
153. Peinado, H., et al., *A molecular role for lysyl oxidase-like 2 enzyme in snail regulation and tumor progression.* EMBO J, 2005. **24**(19): p. 3446-58.
154. Erler, J.T., et al., *Lysyl oxidase is essential for hypoxia-induced metastasis.* Nature, 2006. **440**(7088): p. 1222-6.
155. Imai, T., et al., *Hypoxia attenuates the expression of E-cadherin via up-regulation of SNAIL in ovarian carcinoma cells.* Am J Pathol, 2003. **163**(4): p. 1437-47.
156. Erler, J.T. and A.J. Giaccia, *Lysyl oxidase mediates hypoxic control of metastasis.* Cancer Res, 2006. **66**(21): p. 10238-41.
157. Kagan, H.M. and W. Li, *Lysyl oxidase: properties, specificity, and biological roles inside and outside of the cell.* J Cell Biochem, 2003. **88**(4): p. 660-72.
158. Kirschmann, D.A., et al., *A molecular role for lysyl oxidase in breast cancer invasion.* Cancer Res, 2002. **62**(15): p. 4478-83.
159. Bondareva, A., et al., *The lysyl oxidase inhibitor, beta-aminopropionitrile, diminishes the metastatic colonization potential of circulating breast cancer cells.* PLoS One, 2009. **4**(5): p. e5620.
160. Chang, H.Y., et al., *Robustness, scalability, and integration of a wound-response gene expression signature in predicting breast cancer survival.* Proc Natl Acad Sci U S A, 2005. **102**(10): p. 3738-43.
161. Chen, Y., et al., *Identification of hypoxia-regulated proteins in head and neck cancer by proteomic and tissue array profiling.* Cancer Res, 2004. **64**(20): p. 7302-10.

162. Yang, M.H., et al., *Direct regulation of TWIST by HIF-1alpha promotes metastasis.* Nat Cell Biol, 2008. **10**(3): p. 295-305.
163. Krishnamachary, B., et al., *Hypoxia-inducible factor-1-dependent repression of E-cadherin in von Hippel-Lindau tumor suppressor-null renal cell carcinoma mediated by TCF3, ZFHX1A, and ZFHX1B.* Cancer Res, 2006. **66**(5): p. 2725-31.
164. Funasaka, T. and A. Raz, *The role of autocrine motility factor in tumor and tumor microenvironment.* Cancer Metastasis Rev, 2007. **26**(3-4): p. 725-35.
165. Muller, A., et al., *Involvement of chemokine receptors in breast cancer metastasis.* Nature, 2001. **410**(6824): p. 50-6.
166. Erler, J.T., et al., *Hypoxia-induced lysyl oxidase is a critical mediator of bone marrow cell recruitment to form the premetastatic niche.* Cancer Cell, 2009. **15**(1): p. 35-44.
167. Covello, K.L., et al., *HIF-2alpha regulates Oct-4: effects of hypoxia on stem cell function, embryonic development, and tumor growth.* Genes Dev, 2006. **20**(5): p. 557-70.
168. Barnhart, B.C. and M.C. Simon, *Metastasis and stem cell pathways.* Cancer Metastasis Rev, 2007. **26**(2): p. 261-71.
169. Lofstedt, T., et al., *Induction of ID2 expression by hypoxia-inducible factor-1: a role in dedifferentiation of hypoxic neuroblastoma cells.* J Biol Chem, 2004. **279**(38): p. 39223-31.
170. Koshiji, M., et al., *HIF-1alpha induces genetic instability by transcriptionally downregulating MutSalpha expression.* Mol Cell, 2005. **17**(6): p. 793-803.
171. Bindra, R.S., M.E. Crosby, and P.M. Glazer, *Regulation of DNA repair in hypoxic cancer cells.* Cancer Metastasis Rev, 2007. **26**(2): p. 249-60.
172. Moeller, B.J., R.A. Richardson, and M.W. Dewhirst, *Hypoxia and radiotherapy: opportunities for improved outcomes in cancer treatment.* Cancer Metastasis Rev, 2007. **26**(2): p. 241-8.
173. Comerford, K.M., et al., *Hypoxia-inducible factor-1-dependent regulation of the multidrug resistance (MDR1) gene.* Cancer Res, 2002. **62**(12): p. 3387-94.
174. Krishnamurthy, P., et al., *The stem cell marker Bcrp/ABCG2 enhances hypoxic cell survival through interactions with heme.* J Biol Chem, 2004. **279**(23): p. 24218-25.
175. Semenza, G.L., *Evaluation of HIF-1 inhibitors as anticancer agents.* Drug Discov Today, 2007. **12**(19-20): p. 853-9.
176. Ema, M., et al., *A novel bHLH-PAS factor with close sequence similarity to hypoxia-inducible factor 1alpha regulates the VEGF expression and is potentially involved in lung and vascular development.* Proc Natl Acad Sci U S A, 1997. **94**(9): p. 4273-8.
177. Tian, H., S.L. McKnight, and D.W. Russell, *Endothelial PAS domain protein 1 (EPAS1), a transcription factor selectively expressed in endothelial cells.* Genes Dev, 1997. **11**(1): p. 72-82.
178. Fraisl, P., et al., *Regulation of angiogenesis by oxygen and metabolism.* Dev Cell, 2009. **16**(2): p. 167-79.

179. Carroll, V.A. and M. Ashcroft, *Targeting the molecular basis for tumour hypoxia.* Expert Rev Mol Med, 2005. **7**(6): p. 1-16.
180. Carroll, V.A. and M. Ashcroft, *Role of hypoxia-inducible factor (HIF)-1alpha versus HIF-2alpha in the regulation of HIF target genes in response to hypoxia, insulin-like growth factor-I, or loss of von Hippel-Lindau function: implications for targeting the HIF pathway.* Cancer Res, 2006. **66**(12): p. 6264-70.
181. Maynard, M.A., et al., *Human HIF-3alpha4 is a dominant-negative regulator of HIF-1 and is down-regulated in renal cell carcinoma.* FASEB J, 2005. **19**(11): p. 1396-406.
182. Maynard, M.A., et al., *Dominant-negative HIF-3 alpha 4 suppresses VHL-null renal cell carcinoma progression.* Cell Cycle, 2007. **6**(22): p. 2810-6.
183. Makino, Y., et al., *Inhibitory PAS domain protein (IPAS) is a hypoxia-inducible splicing variant of the hypoxia-inducible factor-3alpha locus.* J Biol Chem, 2002. **277**(36): p. 32405-8.
184. Makino, Y., et al., *Inhibitory PAS domain protein is a negative regulator of hypoxia-inducible gene expression.* Nature, 2001. **414**(6863): p. 550-4.
185. Maynard, M.A., et al., *Multiple splice variants of the human HIF-3 alpha locus are targets of the von Hippel-Lindau E3 ubiquitin ligase complex.* J Biol Chem, 2003. **278**(13): p. 11032-40.
186. Carmeliet, P. and R.K. Jain, *Molecular mechanisms and clinical applications of angiogenesis.* Nature, 2011. **473**(7347): p. 298-307.
187. Hanahan, D. and J. Folkman, *Patterns and emerging mechanisms of the angiogenic switch during tumorigenesis.* Cell, 1996. **86**(3): p. 353-64.
188. Engerman, R.L., D. Pfaffenbach, and M.D. Davis, *Cell turnover of capillaries.* Lab Invest, 1967. **17**(6): p. 738-43.
189. Hobson, B. and J. Denekamp, *Endothelial proliferation in tumours and normal tissues: continuous labelling studies.* Br J Cancer, 1984. **49**(4): p. 405-13.
190. Holash, J., et al., *Vessel cooption, regression, and growth in tumors mediated by angiopoietins and VEGF.* Science, 1999. **284**(5422): p. 1994-8.
191. Pettersson, A., et al., *Heterogeneity of the angiogenic response induced in different normal adult tissues by vascular permeability factor/vascular endothelial growth factor.* Lab Invest, 2000. **80**(1): p. 99-115.
192. Bergers, G. and L.E. Benjamin, *Tumorigenesis and the angiogenic switch.* Nat Rev Cancer, 2003. **3**(6): p. 401-10.
193. Ferrara, N., *VEGF-A: a critical regulator of blood vessel growth.* Eur Cytokine Netw, 2009. **20**(4): p. 158-63.
194. Nagy, J.A., A.M. Dvorak, and H.F. Dvorak, *VEGF-A and the induction of pathological angiogenesis.* Annu Rev Pathol, 2007. **2**: p. 251-75.
195. Neufeld, G. and O. Kessler, *The semaphorins: versatile regulators of tumour progression and tumour angiogenesis.* Nat Rev Cancer, 2008. **8**(8): p. 632-45.
196. Carmeliet, P., *Angiogenesis in health and disease.* Nat Med, 2003. **9**(6): p. 653-60.
197. Phng, L.K. and H. Gerhardt, *Angiogenesis: a team effort coordinated by notch.* Dev Cell, 2009. **16**(2): p. 196-208.

198. Ferrara, N. and T. Davis-Smyth, *The biology of vascular endothelial growth factor.* Endocr Rev, 1997. **18**(1): p. 4-25.
199. Chung, A.S., J. Lee, and N. Ferrara, *Targeting the tumour vasculature: insights from physiological angiogenesis.* Nat Rev Cancer, 2010. **10**(7): p. 505-14.
200. Phng, L.K., et al., *Nrarp coordinates endothelial Notch and Wnt signaling to control vessel density in angiogenesis.* Dev Cell, 2009. **16**(1): p. 70-82.
201. Bergers, G., et al., *Matrix metalloproteinase-9 triggers the angiogenic switch during carcinogenesis.* Nat Cell Biol, 2000. **2**(10): p. 737-44.
202. Bergers, G. and D. Hanahan, *Modes of resistance to anti-angiogenic therapy.* Nat Rev Cancer, 2008. **8**(8): p. 592-603.
203. Ramakrishnan, S., et al., *Angiogenesis in normal and neoplastic ovaries.* Angiogenesis, 2005. **8**(2): p. 169-82.
204. Sudhakar, A., *"The matrix reloaded: new insights from type IV collagen derived endogenous angiogenesis inhibitors and their mechanisms of action".* Journal of Bioequivalence and Bioavailability, 2009. **1**(2).
205. Holland, J.F., *Cancer medicine*. 5th ed2000, Hamilton, Ontario ; New York: B.C. Decker. 2546 p.
206. Folberg, R., M.J. Hendrix, and A.J. Maniotis, *Vasculogenic mimicry and tumor angiogenesis.* Am J Pathol, 2000. **156**(2): p. 361-81.
207. McDonald, D.M., L. Munn, and R.K. Jain, *Vasculogenic mimicry: how convincing, how novel, and how significant?* Am J Pathol, 2000. **156**(2): p. 383-8.
208. Stockmann, C., et al., *Deletion of vascular endothelial growth factor in myeloid cells accelerates tumorigenesis.* Nature, 2008. **456**(7223): p. 814-8.
209. Jubb, A.M. and A.L. Harris, *Biomarkers to predict the clinical efficacy of bevacizumab in cancer.* Lancet Oncol, 2010. **11**(12): p. 1172-83.
210. Millar, A., *Limitations of combination anti-angiogenesis and chemotherapy.* Nat Rev Cancer, 2003. **1**(2): p. 727-739.
211. Gupta, G.P. and J. Massague, *Cancer metastasis: building a framework.* Cell, 2006. **127**(4): p. 679-95.
212. Downward, J., *Targeting RAS signalling pathways in cancer therapy.* Nat Rev Cancer, 2003. **3**(1): p. 11-22.
213. Hernando, E., et al., *Rb inactivation promotes genomic instability by uncoupling cell cycle progression from mitotic control.* Nature, 2004. **430**(7001): p. 797-802.
214. Puc, J. and R. Parsons, *PTEN loss inhibits CHK1 to cause double stranded-DNA breaks in cells.* Cell Cycle, 2005. **4**(7): p. 927-9.
215. O'Hagan, R.C., et al., *Telomere dysfunction provokes regional amplification and deletion in cancer genomes.* Cancer Cell, 2002. **2**(2): p. 149-55.
216. Varambally, S., et al., *The polycomb group protein EZH2 is involved in progression of prostate cancer.* Nature, 2002. **419**(6907): p. 624-9.
217. Beachy, P.A., S.S. Karhadkar, and D.M. Berman, *Tissue repair and stem cell renewal in carcinogenesis.* Nature, 2004. **432**(7015): p. 324-31.
218. Radtke, F. and H. Clevers, *Self-renewal and cancer of the gut: two sides of a coin.* Science, 2005. **307**(5717): p. 1904-9.

219. Hanahan, D. and R.A. Weinberg, *The hallmarks of cancer.* Cell, 2000. **100**(1): p. 57-70.
220. Finger, E.C. and A.J. Giaccia, *Hypoxia, inflammation, and the tumor microenvironment in metastatic disease.* Cancer Metastasis Rev, 2010. **29**(2): p. 285-93.
221. Cavallaro, U. and G. Christofori, *Cell adhesion and signalling by cadherins and Ig-CAMs in cancer.* Nat Rev Cancer, 2004. **4**(2): p. 118-32.
222. Birchmeier, W. and J. Behrens, *Cadherin expression in carcinomas: role in the formation of cell junctions and the prevention of invasiveness.* Biochim Biophys Acta, 1994. **1198**(1): p. 11-26.
223. Yilmaz, M. and G. Christofori, *EMT, the cytoskeleton, and cancer cell invasion.* Cancer Metastasis Rev, 2009. **28**(1-2): p. 15-33.
224. Hazan, R.B., et al., *Cadherin switch in tumor progression.* Ann N Y Acad Sci, 2004. **1014**: p. 155-63.
225. Yang, Z., et al., *Up-regulation of gastric cancer cell invasion by Twist is accompanied by N-cadherin and fibronectin expression.* Biochem Biophys Res Commun, 2007. **358**(3): p. 925-30.
226. Niu, R.F., et al., *Up-regulation of Twist induces angiogenesis and correlates with metastasis in hepatocellular carcinoma.* J Exp Clin Cancer Res, 2007. **26**(3): p. 385-94.
227. Barbera, M.J., et al., *Regulation of Snail transcription during epithelial to mesenchymal transition of tumor cells.* Oncogene, 2004. **23**(44): p. 7345-54.
228. Beviglia, L. and R.H. Kramer, *HGF induces FAK activation and integrin-mediated adhesion in MTLn3 breast carcinoma cells.* Int J Cancer, 1999. **83**(5): p. 640-9.
229. Guan, J.L., *Integrin signaling through FAK in the regulation of mammary stem cells and breast cancer.* IUBMB Life, 2010. **62**(4): p. 268-76.
230. Bellovin, D.I., et al., *Altered localization of p120 catenin during epithelial to mesenchymal transition of colon carcinoma is prognostic for aggressive disease.* Cancer Res, 2005. **65**(23): p. 10938-45.
231. Cozzolino, M., et al., *p120 Catenin is required for growth factor-dependent cell motility and scattering in epithelial cells.* Mol Biol Cell, 2003. **14**(5): p. 1964-77.
232. Etienne-Manneville, S. and A. Hall, *Rho GTPases in cell biology.* Nature, 2002. **420**(6916): p. 629-35.
233. Sahai, E. and C.J. Marshall, *RHO-GTPases and cancer.* Nat Rev Cancer, 2002. **2**(2): p. 133-42.
234. Buccione, R., J.D. Orth, and M.A. McNiven, *Foot and mouth: podosomes, invadopodia and circular dorsal ruffles.* Nat Rev Mol Cell Biol, 2004. **5**(8): p. 647-57.
235. Coutts, A.S., et al., *Hypoxia-driven cell motility reflects the interplay between JMY and HIF-1alpha.* Oncogene, 2011.
236. Kruchten, A.E. and M.A. McNiven, *Dynamin as a mover and pincher during cell migration and invasion.* J Cell Sci, 2006. **119**(Pt 9): p. 1683-90.

237. Barylko, B., et al., *Synergistic activation of dynamin GTPase by Grb2 and phosphoinositides.* J Biol Chem, 1998. **273**(6): p. 3791-7.
238. Muhlberg, A.B., D.E. Warnock, and S.L. Schmid, *Domain structure and intramolecular regulation of dynamin GTPase.* EMBO J, 1997. **16**(22): p. 6676-83.
239. Kessels, M.M., et al., *Mammalian Abp1, a signal-responsive F-actin-binding protein, links the actin cytoskeleton to endocytosis via the GTPase dynamin.* J Cell Biol, 2001. **153**(2): p. 351-66.
240. McNiven, M.A., et al., *Regulated interactions between dynamin and the actin-binding protein cortactin modulate cell shape.* J Cell Biol, 2000. **151**(1): p. 187-98.
241. Zamanian, J.L. and R.B. Kelly, *Intersectin 1L guanine nucleotide exchange activity is regulated by adjacent src homology 3 domains that are also involved in endocytosis.* Mol Biol Cell, 2003. **14**(4): p. 1624-37.
242. Ringstad, N., Y. Nemoto, and P. De Camilli, *The SH3p4/Sh3p8/SH3p13 protein family: binding partners for synaptojanin and dynamin via a Grb2-like Src homology 3 domain.* Proc Natl Acad Sci U S A, 1997. **94**(16): p. 8569-74.
243. Gout, I., et al., *The GTPase dynamin binds to and is activated by a subset of SH3 domains.* Cell, 1993. **75**(1): p. 25-36.
244. Schmid, S.L., M.A. McNiven, and P. De Camilli, *Dynamin and its partners: a progress report.* Curr Opin Cell Biol, 1998. **10**(4): p. 504-12.
245. Chiasson, C.M., et al., *p120-catenin inhibits VE-cadherin internalization through a Rho-independent mechanism.* Mol Biol Cell, 2009. **20**(7): p. 1970-80.
246. Pirraglia, C., J. Walters, and M.M. Myat, *Pak1 control of E-cadherin endocytosis regulates salivary gland lumen size and shape.* Development, 2010. **137**(24): p. 4177-89.
247. Georgiou, M., et al., *Cdc42, Par6, and aPKC regulate Arp2/3-mediated endocytosis to control local adherens junction stability.* Curr Biol, 2008. **18**(21): p. 1631-8.
248. Leibfried, A., et al., *Drosophila Cip4 and WASp define a branch of the Cdc42-Par6-aPKC pathway regulating E-cadherin endocytosis.* Curr Biol, 2008. **18**(21): p. 1639-48.
249. Kirchhausen, T., E. Macia, and H.E. Pelish, *Use of dynasore, the small molecule inhibitor of dynamin, in the regulation of endocytosis.* Methods Enzymol, 2008. **438**: p. 77-93.
250. Kumari, S., S. Mg, and S. Mayor, *Endocytosis unplugged: multiple ways to enter the cell.* Cell Res, 2010. **20**(3): p. 256-75.
251. Machesky, L., Jurdic, P., Hinz, B., *Grab, stick, pull and digest: the functional diversity of actin-associated matrix-adhesion structures.* Embo Reports, 2008. **9**: p. 139-143.
252. Kessels, M.M. and B. Qualmann, *Extending the court for cortactin: from the cortex to the Golgi.* Nat Cell Biol, 2005. **7**(5): p. 448-9.

253. Orimo, A., et al., *Stromal fibroblasts present in invasive human breast carcinomas promote tumor growth and angiogenesis through elevated SDF-1/CXCL12 secretion.* Cell, 2005. **121**(3): p. 335-48.
254. Condeelis, J. and J.W. Pollard, *Macrophages: obligate partners for tumor cell migration, invasion, and metastasis.* Cell, 2006. **124**(2): p. 263-6.
255. Nash, G.F., et al., *Platelets and cancer.* Lancet Oncol, 2002. **3**(7): p. 425-30.
256. Douma, S., et al., *Suppression of anoikis and induction of metastasis by the neurotrophic receptor TrkB.* Nature, 2004. **430**(7003): p. 1034-9.
257. Martens, L.K., et al., *Hypoxia-inducible factor-1 (HIF-1) is a transcriptional activator of the TrkB neurotrophin receptor gene.* J Biol Chem, 2007. **282**(19): p. 14379-88.
258. Rohwer, N., et al., *Hypoxia-inducible factor 1alpha mediates anoikis resistance via suppression of alpha5 integrin.* Cancer Res, 2008. **68**(24): p. 10113-20.
259. Weis, S.M. and D.A. Cheresh, *Pathophysiological consequences of VEGF-induced vascular permeability.* Nature, 2005. **437**(7058): p. 497-504.
260. Criscuoli, M.L., M. Nguyen, and B.P. Eliceiri, *Tumor metastasis but not tumor growth is dependent on Src-mediated vascular permeability.* Blood, 2005. **105**(4): p. 1508-14.
261. Paget, S., *The Distribution of Secondary Growths in Cancer of the Breast.* Lancet, 1889. **133**(3421): p. 571-573.
262. Fidler, I.J., *The pathogenesis of cancer metastasis: the 'seed and soil' hypothesis revisited.* Nat Rev Cancer, 2003. **3**(6): p. 453-8.
263. Tarin, D., et al., *Mechanisms of human tumor metastasis studied in patients with peritoneovenous shunts.* Cancer Res, 1984. **44**(8): p. 3584-92.
264. Brown, D.M. and E. Ruoslahti, *Metadherin, a cell surface protein in breast tumors that mediates lung metastasis.* Cancer Cell, 2004. **5**(4): p. 365-74.
265. Staller, P., et al., *Chemokine receptor CXCR4 downregulated by von Hippel-Lindau tumour suppressor pVHL.* Nature, 2003. **425**(6955): p. 307-11.
266. Schioppa, T., et al., *Regulation of the chemokine receptor CXCR4 by hypoxia.* J Exp Med, 2003. **198**(9): p. 1391-402.
267. Lu, X., et al., *In vivo dynamics and distinct functions of hypoxia in primary tumor growth and organotropic metastasis of breast cancer.* Cancer Res, 2010. **70**(10): p. 3905-14.
268. Liu, Y.L., et al., *Regulation of the chemokine receptor CXCR4 and metastasis by hypoxia-inducible factor in non small cell lung cancer cell lines.* Cancer Biol Ther, 2006. **5**(10): p. 1320-6.
269. Kaplan, R.N., et al., *VEGFR1-positive haematopoietic bone marrow progenitors initiate the pre-metastatic niche.* Nature, 2005. **438**(7069): p. 820-7.
270. Hiratsuka, S., et al., *MMP9 induction by vascular endothelial growth factor receptor-1 is involved in lung-specific metastasis.* Cancer Cell, 2002. **2**(4): p. 289-300.
271. Gao, D., et al., *Endothelial progenitor cells control the angiogenic switch in mouse lung metastasis.* Science, 2008. **319**(5860): p. 195-8.

272. Pantel, K. and R.H. Brakenhoff, *Dissecting the metastatic cascade.* Nat Rev Cancer, 2004. **4**(6): p. 448-56.
273. Chambers, A.F., A.C. Groom, and I.C. MacDonald, *Dissemination and growth of cancer cells in metastatic sites.* Nat Rev Cancer, 2002. **2**(8): p. 563-72.
274. Solakoglu, O., et al., *Heterogeneous proliferative potential of occult metastatic cells in bone marrow of patients with solid epithelial tumors.* Proc Natl Acad Sci U S A, 2002. **99**(4): p. 2246-51.
275. Lee, R.C., R.L. Feinbaum, and V. Ambros, *The C. elegans heterochronic gene lin-4 encodes small RNAs with antisense complementarity to lin-14.* Cell, 1993. **75**(5): p. 843-54.
276. Zeng, Y., *Principles of micro-RNA production and maturation.* Oncogene, 2006. **25**(46): p. 6156-62.
277. Sayed, D. and M. Abdellatif, *MicroRNAs in development and disease.* Physiol Rev, 2011. **91**(3): p. 827-87.
278. Croce, C.M., *Causes and consequences of microRNA dysregulation in cancer.* Nat Rev Genet, 2009. **10**(10): p. 704-14.
279. Lee, Y., et al., *The nuclear RNase III Drosha initiates microRNA processing.* Nature, 2003. **425**(6956): p. 415-9.
280. Denli, A.M., et al., *Processing of primary microRNAs by the Microprocessor complex.* Nature, 2004. **432**(7014): p. 231-5.
281. Gregory, R.I., et al., *The Microprocessor complex mediates the genesis of microRNAs.* Nature, 2004. **432**(7014): p. 235-40.
282. Han, J., et al., *The Drosha-DGCR8 complex in primary microRNA processing.* Genes Dev, 2004. **18**(24): p. 3016-27.
283. Landthaler, M., A. Yalcin, and T. Tuschl, *The human DiGeorge syndrome critical region gene 8 and Its D. melanogaster homolog are required for miRNA biogenesis.* Curr Biol, 2004. **14**(23): p. 2162-7.
284. Bohnsack, M.T., K. Czaplinski, and D. Gorlich, *Exportin 5 is a RanGTP-dependent dsRNA-binding protein that mediates nuclear export of pre-miRNAs.* RNA, 2004. **10**(2): p. 185-91.
285. Lund, E., et al., *Nuclear export of microRNA precursors.* Science, 2004. **303**(5654): p. 95-8.
286. Yi, R., et al., *Exportin-5 mediates the nuclear export of pre-microRNAs and short hairpin RNAs.* Genes Dev, 2003. **17**(24): p. 3011-6.
287. Chendrimada, T.P., et al., *TRBP recruits the Dicer complex to Ago2 for microRNA processing and gene silencing.* Nature, 2005. **436**(7051): p. 740-4.
288. Forstemann, K., et al., *Normal microRNA maturation and germ-line stem cell maintenance requires Loquacious, a double-stranded RNA-binding domain protein.* PLoS Biol, 2005. **3**(7): p. e236.
289. Gregory, R.I., et al., *Human RISC couples microRNA biogenesis and posttranscriptional gene silencing.* Cell, 2005. **123**(4): p. 631-40.
290. Haase, A.D., et al., *TRBP, a regulator of cellular PKR and HIV-1 virus expression, interacts with Dicer and functions in RNA silencing.* EMBO Rep, 2005. **6**(10): p. 961-7.

291. Jiang, F., et al., *Dicer-1 and R3D1-L catalyze microRNA maturation in Drosophila.* Genes Dev, 2005. **19**(14): p. 1674-9.
292. Maniataki, E. and Z. Mourelatos, *A human, ATP-independent, RISC assembly machine fueled by pre-miRNA.* Genes Dev, 2005. **19**(24): p. 2979-90.
293. Saito, K., et al., *Processing of pre-microRNAs by the Dicer-1-Loquacious complex in Drosophila cells.* PLoS Biol, 2005. **3**(7): p. e235.
294. Lee, Y., et al., *The role of PACT in the RNA silencing pathway.* EMBO J, 2006. **25**(3): p. 522-32.
295. Jinek, M. and J.A. Doudna, *A three-dimensional view of the molecular machinery of RNA interference.* Nature, 2009. **457**(7228): p. 405-12.
296. Doench, J.G. and P.A. Sharp, *Specificity of microRNA target selection in translational repression.* Genes Dev, 2004. **18**(5): p. 504-11.
297. Brennecke, J., et al., *Principles of microRNA-target recognition.* PLoS Biol, 2005. **3**(3): p. e85.
298. Lewis, B.P., C.B. Burge, and D.P. Bartel, *Conserved seed pairing, often flanked by adenosines, indicates that thousands of human genes are microRNA targets.* Cell, 2005. **120**(1): p. 15-20.
299. Grimson, A., et al., *MicroRNA targeting specificity in mammals: determinants beyond seed pairing.* Mol Cell, 2007. **27**(1): p. 91-105.
300. Nielsen, C.B., et al., *Determinants of targeting by endogenous and exogenous microRNAs and siRNAs.* RNA, 2007. **13**(11): p. 1894-910.
301. Filipowicz, W., S.N. Bhattacharyya, and N. Sonenberg, *Mechanisms of post-transcriptional regulation by microRNAs: are the answers in sight?* Nat Rev Genet, 2008. **9**(2): p. 102-14.
302. Jones-Rhoades, M.W., D.P. Bartel, and B. Bartel, *MicroRNAS and their regulatory roles in plants.* Annu Rev Plant Biol, 2006. **57**: p. 19-53.
303. Wu, L., J. Fan, and J.G. Belasco, *MicroRNAs direct rapid deadenylation of mRNA.* Proc Natl Acad Sci U S A, 2006. **103**(11): p. 4034-9.
304. Behm-Ansmant, I., et al., *mRNA degradation by miRNAs and GW182 requires both CCR4:NOT deadenylase and DCP1:DCP2 decapping complexes.* Genes Dev, 2006. **20**(14): p. 1885-98.
305. Giraldez, A.J., et al., *Zebrafish MiR-430 promotes deadenylation and clearance of maternal mRNAs.* Science, 2006. **312**(5770): p. 75-9.
306. Eulalio, A., et al., *Target-specific requirements for enhancers of decapping in miRNA-mediated gene silencing.* Genes Dev, 2007. **21**(20): p. 2558-70.
307. Pillai, R.S., et al., *Inhibition of translational initiation by Let-7 MicroRNA in human cells.* Science, 2005. **309**(5740): p. 1573-6.
308. Thermann, R. and M.W. Hentze, *Drosophila miR2 induces pseudo-polysomes and inhibits translation initiation.* Nature, 2007. **447**(7146): p. 875-8.
309. Mathonnet, G., et al., *MicroRNA inhibition of translation initiation in vitro by targeting the cap-binding complex eIF4F.* Science, 2007. **317**(5845): p. 1764-7.

310. Wakiyama, M., et al., *Let-7 microRNA-mediated mRNA deadenylation and translational repression in a mammalian cell-free system.* Genes Dev, 2007. **21**(15): p. 1857-62.
311. Chendrimada, T.P., et al., *MicroRNA silencing through RISC recruitment of eIF6.* Nature, 2007. **447**(7146): p. 823-8.
312. Humphreys, D.T., et al., *MicroRNAs control translation initiation by inhibiting eukaryotic initiation factor 4E/cap and poly(A) tail function.* Proc Natl Acad Sci U S A, 2005. **102**(47): p. 16961-6.
313. Nottrott, S., M.J. Simard, and J.D. Richter, *Human let-7a miRNA blocks protein production on actively translating polyribosomes.* Nat Struct Mol Biol, 2006. **13**(12): p. 1108-14.
314. Petersen, C.P., et al., *Short RNAs repress translation after initiation in mammalian cells.* Mol Cell, 2006. **21**(4): p. 533-42.
315. Maroney, P.A., et al., *Evidence that microRNAs are associated with translating messenger RNAs in human cells.* Nat Struct Mol Biol, 2006. **13**(12): p. 1102-7.
316. Volinia, S., et al., *A microRNA expression signature of human solid tumors defines cancer gene targets.* Proc Natl Acad Sci U S A, 2006. **103**(7): p. 2257-61.
317. Lu, J., et al., *MicroRNA expression profiles classify human cancers.* Nature, 2005. **435**(7043): p. 834-8.
318. Zhang, L., et al., *microRNAs exhibit high frequency genomic alterations in human cancer.* Proc Natl Acad Sci U S A, 2006. **103**(24): p. 9136-41.
319. Kim, M.S., et al., *Somatic mutations and losses of expression of microRNA regulation-related genes AGO2 and TNRC6A in gastric and colorectal cancers.* J Pathol, 2010. **221**(2): p. 139-46.
320. Lee, E.J., et al., *Systematic evaluation of microRNA processing patterns in tissues, cell lines, and tumors.* RNA, 2008. **14**(1): p. 35-42.
321. Melo, S.A., et al., *A genetic defect in exportin-5 traps precursor microRNAs in the nucleus of cancer cells.* Cancer Cell, 2010. **18**(4): p. 303-15.
322. van Kouwenhove, M., M. Kedde, and R. Agami, *MicroRNA regulation by RNA-binding proteins and its implications for cancer.* Nat Rev Cancer, 2011. **11**(9): p. 644-56.
323. Nana-Sinkam, S.P. and C.M. Croce, *MicroRNAs as therapeutic targets in cancer.* Transl Res, 2011. **157**(4): p. 216-25.
324. Guimbellot, J.S., et al., *Correlation of microRNA levels during hypoxia with predicted target mRNAs through genome-wide microarray analysis.* BMC Med Genomics, 2009. **2**: p. 15.
325. Kulshreshtha, R., et al., *Regulation of microRNA expression: the hypoxic component.* Cell Cycle, 2007. **6**(12): p. 1426-31.
326. Ghosh, G., et al., *Hypoxia-induced microRNA-424 expression in human endothelial cells regulates HIF-alpha isoforms and promotes angiogenesis.* J Clin Invest, 2010. **120**(11): p. 4141-54.

327. Kelly, T.J., et al., *A hypoxia-induced positive feedback loop promotes hypoxia-inducible factor 1alpha stability through miR-210 suppression of glycerol-3-phosphate dehydrogenase 1-like.* Mol Cell Biol, 2011. **31**(13): p. 2696-706.
328. Puissegur, M.P., et al., *miR-210 is overexpressed in late stages of lung cancer and mediates mitochondrial alterations associated with modulation of HIF-1 activity.* Cell Death Differ, 2011. **18**(3): p. 465-78.
329. Jemal, A., et al., *Cancer statistics, 2007.* CA Cancer J Clin, 2007. **57**(1): p. 43-66.
330. Brahimi-Horn, M.C., J. Chiche, and J. Pouyssegur, *Hypoxia and cancer.* J Mol Med (Berl), 2007. **85**(12): p. 1301-7.
331. Jemal, A., et al., *Cancer statistics, 2004.* CA Cancer J Clin, 2004. **54**(1): p. 8-29.
332. Liao, D. and R.S. Johnson, *Hypoxia: a key regulator of angiogenesis in cancer.* Cancer Metastasis Rev, 2007. **26**(2): p. 281-90.
333. Yan, Q., et al., *The hypoxia-inducible factor 2alpha N-terminal and C-terminal transactivation domains cooperate to promote renal tumorigenesis in vivo.* Mol Cell Biol, 2007. **27**(6): p. 2092-102.
334. Safran, M., et al., *Mouse model for noninvasive imaging of HIF prolyl hydroxylase activity: assessment of an oral agent that stimulates erythropoietin production.* Proceedings of the National Academy of Sciences of the United States of America, 2006. **103**(1): p. 105-10.
335. Epsztejn, S., et al., *Fluorescence analysis of the labile iron pool of mammalian cells.* Anal Biochem, 1997. **248**(1): p. 31-40.
336. Kalscheuer, S., et al., *Differential expression of microRNAs in early-stage neoplastic transformation in the lungs of F344 rats chronically treated with the tobacco carcinogen 4-(methylnitrosamino)-1-(3-pyridyl)-1-butanone.* Carcinogenesis, 2008. **29**(12): p. 2394-9.
337. Wild, R., et al., *Quantitative assessment of angiogenesis and tumor vessel architecture by computer-assisted digital image analysis: effects of VEGF-toxin conjugate on tumor microvessel density.* Microvasc Res, 2000. **59**(3): p. 368-76.
338. Chen, K.F., et al., *Transcriptional repression of human cad gene by hypoxia inducible factor-1alpha.* Nucleic Acids Res, 2005. **33**(16): p. 5190-8.
339. Eltzschig, H.K., et al., *HIF-1-dependent repression of equilibrative nucleoside transporter (ENT) in hypoxia.* J Exp Med, 2005. **202**(11): p. 1493-505.
340. Hammond, E.M. and A.J. Giaccia, *Hypoxia-inducible factor-1 and p53: friends, acquaintances, or strangers?* Clin Cancer Res, 2006. **12**(17): p. 5007-9.
341. Rius, J., et al., *NF-kappaB links innate immunity to the hypoxic response through transcriptional regulation of HIF-1alpha.* Nature, 2008. **453**(7196): p. 807-11.
342. Richardson, D. and E. Baker, *Two mechanisms of iron uptake from transferrin by melanoma cells. The effect of desferrioxamine and ferric ammonium citrate.* J Biol Chem, 1992. **267**(20): p. 13972-9.
343. Goralska, M., et al., *The effect of ascorbic acid and ferric ammonium citrate on iron uptake and storage in lens epithelial cells.* Exp Eye Res, 1998. **66**(6): p. 687-97.

344. Landgraf, P., et al., *A mammalian microRNA expression atlas based on small RNA library sequencing.* Cell, 2007. **129**(7): p. 1401-14.
345. Wang, Y. and M. Ohh, *Oxygen-mediated endocytosis in cancer.* J Cell Mol Med, 2010. **14**(3): p. 496-503.
346. Wang, Y., et al., *Regulation of endocytosis via the oxygen-sensing pathway.* Nat Med, 2009. **15**(3): p. 319-24.
347. Robach, P., et al., *Strong iron demand during hypoxia-induced erythropoiesis is associated with down-regulation of iron-related proteins and myoglobin in human skeletal muscle.* Blood, 2007. **109**(11): p. 4724-31.
348. Chepelev, N.L. and W.G. Willmore, *Regulation of iron pathways in response to hypoxia.* Free Radic Biol Med, 2011. **50**(6): p. 645-66.
349. Nicolas, G., et al., *Severe iron deficiency anemia in transgenic mice expressing liver hepcidin.* Proceedings of the National Academy of Sciences of the United States of America, 2002. **99**(7): p. 4596-601.
350. Peyssonnaux, C., et al., *Regulation of iron homeostasis by the hypoxia-inducible transcription factors (HIFs).* The Journal of clinical investigation, 2007. **117**(7): p. 1926-32.
351. Yoon, D., et al., *Hypoxia-inducible factor-1 deficiency results in dysregulated erythropoiesis signaling and iron homeostasis in mouse development.* The Journal of biological chemistry, 2006. **281**(35): p. 25703-11.
352. Gonzalez, V.M., et al., *Is cisplatin-induced cell death always produced by apoptosis?* Mol Pharmacol, 2001. **59**(4): p. 657-63.
353. Eastman, A., *The mechanism of action of cisplatin: From adducts to apoptosis.*, in *Cisplatin. Chemistry and Biochemistry of a Leading Anticancer Drug*, B. Lippert, Editor 1999, Wiley: Basel, Switzerland. p. 111-134.
354. Chen, R., et al., *Regulation of IKKbeta by miR-199a affects NF-kappaB activity in ovarian cancer cells.* Oncogene, 2008. **27**(34): p. 4712-23.
355. Cheung, H.H., et al., *Methylation of an intronic region regulates miR-199a in testicular tumor malignancy.* Oncogene, 2011. **30**(31): p. 3404-15.
356. Duan, Z., et al., *MicroRNA-199a-3p is downregulated in human osteosarcoma and regulates cell proliferation and migration.* Mol Cancer Ther, 2011. **10**(8): p. 1337-45.
357. Hou, J., et al., *Identification of miRNomes in human liver and hepatocellular carcinoma reveals miR-199a/b-3p as therapeutic target for hepatocellular carcinoma.* Cancer Cell, 2011. **19**(2): p. 232-43.
358. Jia, X.Q., et al., *Lentivirus-Mediated Overexpression of MicroRNA-199a Inhibits Cell Proliferation of Human Hepatocellular Carcinoma.* Cell Biochem Biophys, 2011.
359. Song, G., et al., *miR-199a regulates the tumor suppressor mitogen-activated protein kinase kinase kinase 11 in gastric cancer.* Biol Pharm Bull, 2010. **33**(11): p. 1822-7.
360. Rane, S., et al., *Downregulation of miR-199a derepresses hypoxia-inducible factor-1alpha and Sirtuin 1 and recapitulates hypoxia preconditioning in cardiac myocytes.* Circ Res, 2009. **104**(7): p. 879-86.

361. Kota, J., et al., *Therapeutic microRNA delivery suppresses tumorigenesis in a murine liver cancer model.* Cell, 2009. **137**(6): p. 1005-17.
362. Takeshita, F., et al., *Systemic delivery of synthetic microRNA-16 inhibits the growth of metastatic prostate tumors via downregulation of multiple cell-cycle genes.* Mol Ther, 2010. **18**(1): p. 181-7.
363. Anand, S., et al., *MicroRNA-132-mediated loss of p120RasGAP activates the endothelium to facilitate pathological angiogenesis.* Nat Med, 2010. **16**(8): p. 909-14.
364. Chen, Y., et al., *Nanoparticles modified with tumor-targeting scFv deliver siRNA and miRNA for cancer therapy.* Mol Ther, 2010. **18**(9): p. 1650-6.

CHAPTER IV:

APPENDIX

Appendix I: Rights and Permissions

Permissions were sought and received for all images reproduced in this work. Confirmation receipts of permissions are available upon request.